Effects of Cyclodextrins on the Kinetics of Emulsion Polymerisation

---

A thesis submitted in partial fulfilment of the requirements

for the degree of

Doctor of Philosophy in Chemistry

University of Canterbury

Omar El-Hadad

2009

بِسۡمِ ٱللَّهِ ٱلرَّحۡمَٰنِ ٱلرَّحِيمِ

وَجَٰهِدُوا فِي ٱللَّهِ حَقَّ جِهَادِهِۦ

In the name of Allah, Most Gracious, Most Merciful.

And strive in God's cause as you ought to strive, (with sincerity and under discipline).

Holy Quran, Surat Al-Hajj (The Pilgrimage) (22:78)

Abstract

Cyclodextrins (CD) are semi-natural oligosaccharides composed of a number of D-glucose units. They are produced from renewable resources, and have been found to be of catalytic effect for the emulsion polymerization of many monomers. Using monomers whose emulsion polymerization kinetics have been thoroughly studied, this research analyses the effect of CD on the entry and exit rate coefficients for the emulsion polymerization of styrene, and the entry and termination rate coefficients for the emulsion polymerization of MMA.

Throughout the course of the work, CD was found to have a positive impact on the polymerization rate of styrene in a polystyrene latex stabilized with a cationic surfactant. Furthermore, the exit rate coefficient for this latex was found, via γ-relaxation experiments, to increase in proportion to the styrene solubility in water, exactly as predicted by theory. Of itself this would lead to a decrease in reaction rate. That there is still an overall increase in the reaction rate in the presence of CD is because of a quite strong effect on entry rate coefficients. Again, this is consistent with the prevailing theory for entry, that of Maxwell and Morrison, which says that increased aqueous phase solubility of monomer will lead to faster entry.

Intriguingly, experiments done on a polystyrene latex stabilized with an anionic surfactant showed a different effect for CD: γ-relaxation experiments found very little effect of CD on exit rate, and chemically initiated experiments found the same for overall rate. This is consistent with CD having little effect on aqueous phase styrene solubility, which in fact is what direct measurements via UV-visible spectroscopy indicated. It is speculated that the anionic surfactant was successfully competing with styrene to occupy the CD cavities. On the other hand, measurements suggested that styrene successfully competes with cationic surfactant, which is consistent with kinetic results.

Experiments of the above nature were then carried out with methyl methacrylate (MMA), a more water soluble monomer than styrene and one with emulsion polymerisation kinetics of a different nature (so-called pseudo-bulk). γ-relaxation experiments found no

effect of CD on termination rate coefficients, exactly as one would expect given that termination is an intra-particle reaction whereas CD exists in the aqueous phase. However the same experiments also revealed an unexpected effect of CD on entry: the thermal entry rate coefficient was found to increase markedly in the presence of CD. It seems likely that this unusual effect stems from interaction of products of γ radiolysis with CD.

Results for chemically-initiated polymerization of MMA were inconclusive. Under some conditions there was actually retardation in the presence of CD, which is actually consistent with measurements of MMA solubility in water, which suggested a slightly negative effect of CD. However it is hard to explain such a phenomenon. Further, under other conditions it was found that CD either had no effect on chemically-initiated rate or could even increase it slightly. The only safe conclusion at this stage is that CD has no major effect on MMA kinetics, which arguably is consistent with MMA being relatively water soluble: intuitively one would expect that CD is most useful (‘catalytic’) for the EP of monomers of low solubility.

Acknowledgement

All praise is to God, the Creator, the Sustainer, who gave me the chance to work throughout this research and write this thesis, hoping that it can present something new in the world of science and chemical technologies.

I would then to thank my supervisor, Associate Professor Gregory T. Russell, to whom I cannot really be thankful enough. In addition to his academic duty as my supervisor, he was also an older brother, a very caring and helpful friend. His efforts with me have resulted in some new discoveries, which are being presented in this thesis.

This is also a good chance to give my thanks and appreciation to Dr. Abdul-Fattah Asfour, my M.A.Sc supervisor, the first person to introduce me to the real world of science and research. I think without what he taught me I wouldn't have been able to make my way through this PhD.

Next I would like to thank the person who invited me to apply to study at this university and offered me a scholarship, Mr. Adrian Carpinter from the Scholarships Office. I am also thankful to Professor Bryce Williamson and Dr. Peter Gostomski, the Heads of Chemistry and of Chemical and Process Engineeringrespectively, who were very helpful to me.

In the Chemistry Department I have to thank the colleagues who introduced me to the polymer chemistry lab, Bryce Jackson and Briar Schwalger-Smith. It is good also to mention Kim van Berkel, who has been very helpful and has answered my emailed questions about a lot of technical problems faced throughout this project. Other students in the research team include Greg Smith and Majed Al-Ghamdi. Special thanks to Dr. Marie Squire for proof reading almost all this thesis, and Dr. Matthew Polson for help with solubility experiments.

Technical problems have always been attended to by the departmental technicians. They include (in the electronics workshop) Sandy Ferguson, Steven Graham and Roger Merryweather, and (in the mechanical workshop) Wayne Mackay, Nick Oliver, Danny Leonard and Russell Gillard. Very important also was Robert McGregor, the glass technician who was helpful with most of the glassware problems. Thanks also to all other technicians in the department who were helpful to my work.

Outside the department I have to thank Mike Flaws in the Mechanical Engineering department, and Manfred Ingerfeld from the School of Biological Sceicnes, who were both helpful in work done by TEM.

In Sydney, Dr. Hank de Bruyn was very helpful with the work done at the γ-radiation facilities. In addition to him, a lot of people in the Australian Institute of Nuclear Science and Engineering were very helpful to this project. These include Dr. Dennis Mather, managing director of AINSE, and Rhiannon Still. In addition to them there was good help from the researchers on site, most importantly Dr. Dimitri Alexiev, Dr. Li Mo, Lindsay Bignell, and the glass technician David Stutters.

Finally, I would like to thank my wife, Noha Abu Karam, whose support during the term of this work will always be remembered and appreciated, and my parents, who were very encouraging, especially during times of stress and worry.

Table of contents

Chapter I
Introduction

Polymerization is one of the most widely used human inventions all through history. It is defined as reacting a number of molecules, of one or more chemicals, to arrange them all in one chain, or a group of chains forming a three dimensional network. Following the concept of naming an era after the material mostly used during that era, our era can be called the "plastic age".[1] Needless to say, polymers are present in nearly everything around us, from cell phones to aeroplanes. But although huge amounts of polymers are produced every year, still relatively little is known about the reaction mechanisms. Many polymers have only been produced through trial and error. This involves trying over and over again until satisfactory results are obtained, and certainly chemists who do research in such a field require good knowledge, some luck and perhaps even magical powers.

Every polymer can be produced through one (or more than one) polymerization technique. Polymerization can occur in either step growth or chain growth processes.

Step growth polymerization is a process through which chains grow through the addition of other multifunctional polymer molecules, that is, a growing chain can be added to another growing chain.

In chain growth polymerization, on the other hand, only the unsaturated molecule can be added to the growing chain. Molecules are added one by one, so no chain can be added directly to another chain, except in the case of the combination reaction in termination.

Chain growth polymerization can be further broken down into a number of processes; these include free-radical, coordination, cationic and anionic polymerization.[2]

Free radical polymerization has a few means of realization, including bulk, suspension, dispersion, precipitation, emulsion and inverse emulsion polymerization.[3]

1.1 Reactions of Free Radical Polymerization

In all radical polymerization including emulsion polymerization, there are three main reactions through which the polymerization process takes place.

1.1.1 Initiation

a. By chemical initiator: Initiation is the transformation of a number of monomer molecules from the stable molecular form to the free radical form; in two ways it can take place, the addition of the initiator to the reaction medium, and using γ-rays.

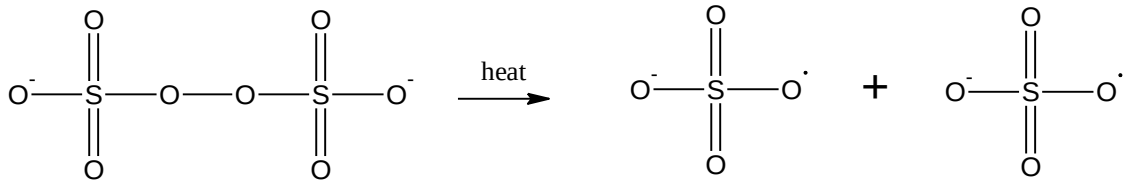

Scheme 1.1. Initiator decomposition reaction for potassium persulphate

Scheme 1.1 shows the decomposition of potassium peroxodisulphate ($K_2S_2O_8$, also known as potassium persulphate or KPS) to give two free radicals. For the reaction to take place at a practical rate, it has to be carried out at a relatively high temperature, around 50 ^{o}C or higher.

Throughout the work done in this thesis, two initiators have been used with styrene polymerization reactions: KPS and 2,2'-Azobis(2-methylpropionamidine)dihydrochloride, which has the commercial name V-50, KPS alone was used with methyl methacrylate polymerization reactions. Scheme 1.2 shows the structure of V-50.[4]

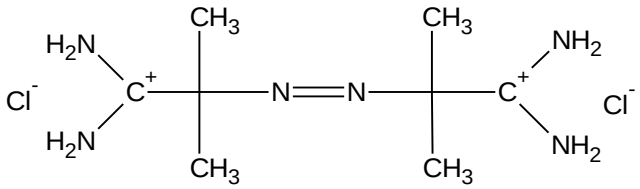

Scheme 1.2. Structure of 2,2'-Azobis(2-methylpropionamidine)dihydrochloride (V-50)

Taking the example of KPS, and labelling the $^{\cdot}SO_4^-$ free radical as $R^{\bullet}$, the monomer which is styrene in the current example can be initiated as per the reaction shown in Scheme 1.3.

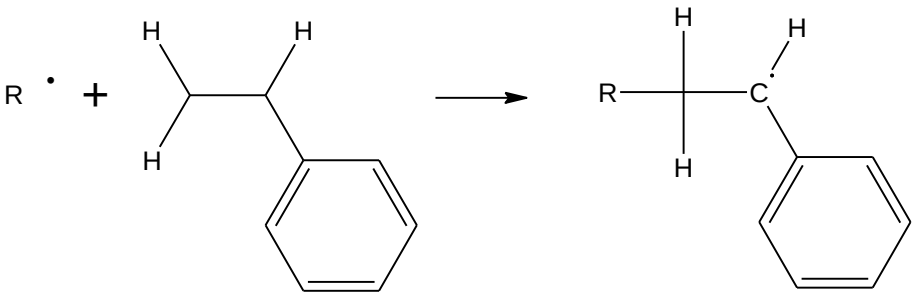

Scheme 1.3. Primary radical addition

b. By γ-rays: The source from which γ-rays are emitted is the nuclei of some metal isotopes, as these nuclei move down from an excited state to a lower energy state.[5] In some cases this happens through the *β*-decay, which can be explained as the emission of a negatron or a positron from the nuclei.[6] This is the case of ^{60}Co, the source of γ-rays used during the course of this work.

1.1.2 Propagation

After the monomer molecule has been initiated, it is now in a state in which it can receive more styrene molecules, the reaction known as propagation. And then the polymer chain starts to form and grow, through successive additions of monomer molecules, as is shown Scheme 1.4.

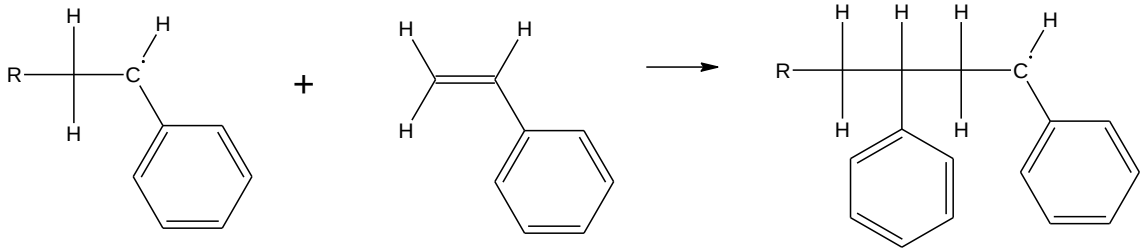

Scheme 1.4. Propagation reaction

This reaction represents the addition of one styrene molecule to an initiated free radical, and the reaction continues and more monomer molecules continue to be added to the growing chain. Propagation is arguably the most important of the three free radical reactions, as it represents the step in which the polymer molecule grows and expands until it reaches the required length.

1.1.3 Termination

The termination of the propagation reaction occurs when the free radicals on two growing polymer chains interact with each other, reaction occurs and the two free radicals are sacrificed, producing one or two polymer chain(s) to which no more monomer molecules can be added. Termination takes place following one of two mechanisms:

(a) Combination

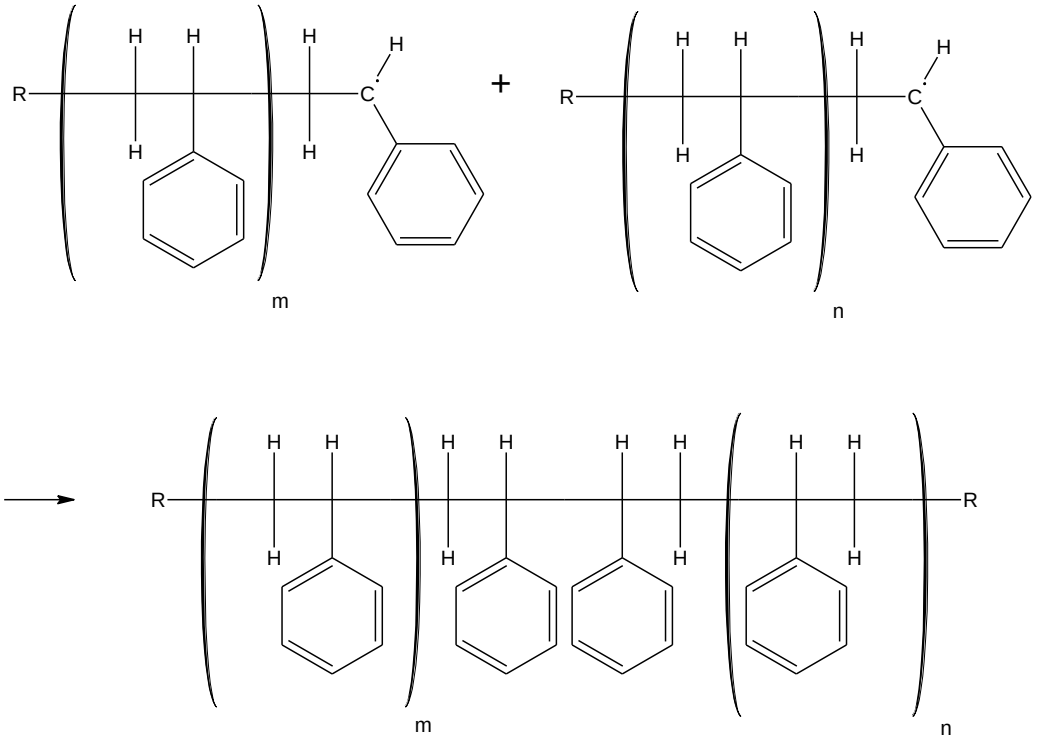

Scheme 1.5. Termination by combination

Combination reactions take place when the two free radical sites on the two growing polymer chains react together to form one polymer chain whose degree of polymerization (DP) is equal to the DP of both chains together, according to the reaction in Scheme 1.5.

(b) Disproportionation:

When the termination takes place by the disproportionation technique, the two free radical growing chains react together to give two molecules, each of them having the same DP as the reacting molecule, and with a double bond on one of them, as shown by Scheme 1.6.

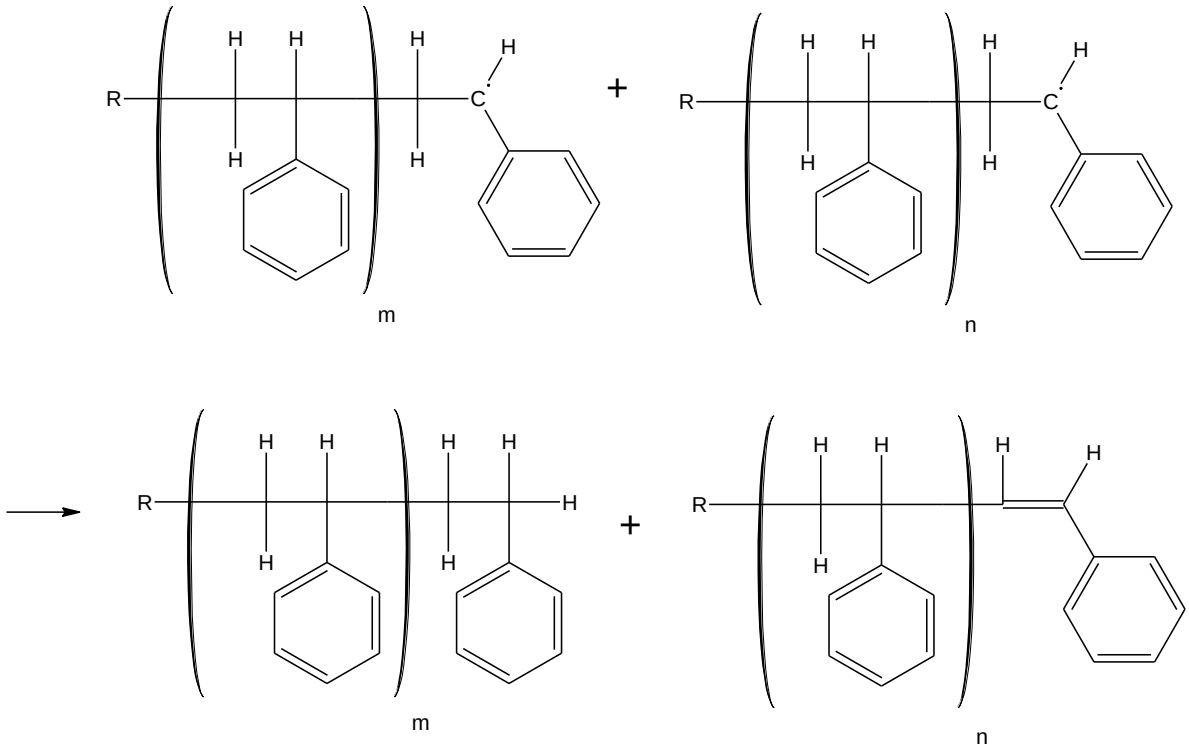

Scheme 1.6. Termination by disproportionation

1.2 Intervals of emulsion polymerization

Emulsion polymerization, figure 1.1 can be divided into three different intervals,[7] as shown in Figure 1.2.[3]

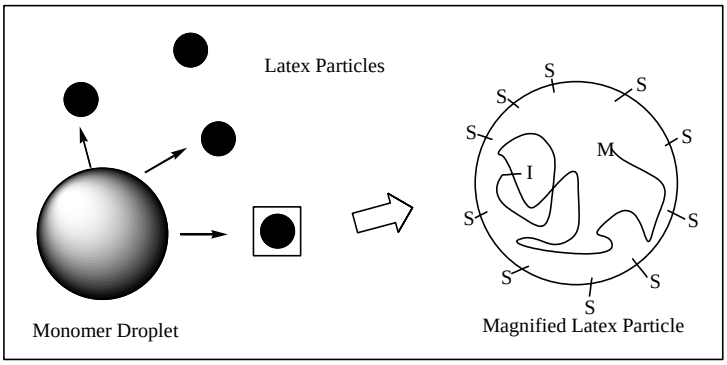

Figure 1.1. Magnified view of Emulsion Polymerisation

1.2.1 **Interval I**, also called "nucleation period", represents the first steps of reaction. At the beginning, the reaction medium contains the monomer, water, surfactant, and some electrolytes for pH control. During this interval, small polymer particles start to form. This happens through the consumption of the initiator (in case of chemically seeded

experiments), or the use of γ-rays. Particle formation takes place only during interval I, and it should be noted that all measures should be taken to prevent particle formation from happening during interval II, as this may "contaminate" the results obtained for kinetic measurements for interval II experiments.

1.2.2 **Interval II** is the interval during which most kinetic measurements done in this research project took place. During interval II, particle growth takes place, and monomer droplets are still present in the reaction medium. This interval has two specific characteristics, there should be no particle formation (if there is, it is called secondary nucleation), and the monomer molecules keep moving towards the particles already formed during interval I. Monomer concentration within the particles C_P, remains at a constant value C_P^{SAT} , which is the saturated concentration of the monomer within the polymer particles. Particles keep growing during interval II.

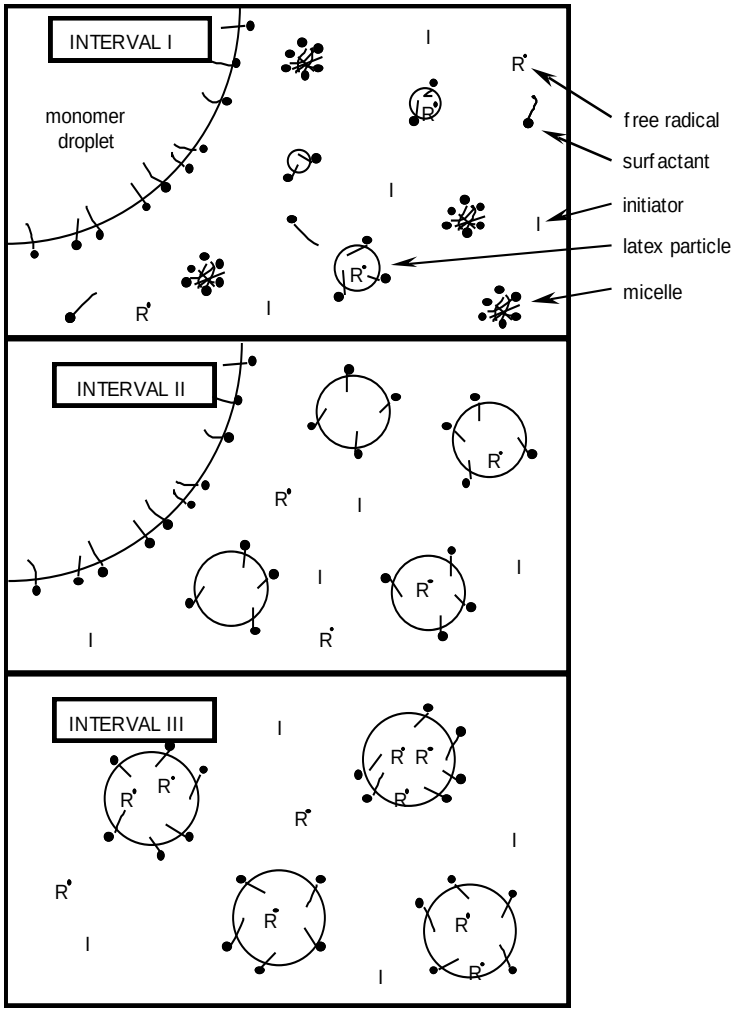

Figure 1.2. Intervals of Emulsion Polymerisation.[3]

The reason why most kinetic measurements took place during interval II is that, during interval I, any kinetic study trying to analyze entry and exit rates of free radicals to and from the particles (or any other factors affecting particle growth) will be affected by the nucleation process.[3] During interval III, the concentration of the monomer within the swollen particles keeps changing, adding an additional unknown variable to the equations, while in interval II this concentration is at its maximum (saturated) value. The absence of secondary nucleation during interval II can be confirmed through particle size analysis for the latex after the end of the experiment.

The kinetic experiments done throughout this work were all started by "seeding" the emulsion medium with particles already prepared before (also called *ab initio* experiments). So they were practically started during interval II. The "seeding" has another benefit, which is that it makes N_c, which is the number of particles per unit volume of the aqueous phase, constant and known.
With a high enough N_c (usually higher than 10^{16} particles/L), the seed particles efficiently capture any free radicals moving in the reaction medium.[8]

Following this procedure, conversion can be calculated through the following equation, whose mathematical derivation has already been presented earlier:[3]

$$\frac{dx}{dt} = \frac{k_p C_P \bar{n} N_c}{n_M{}^0 N_A} \equiv A\bar{n} \qquad (1.1)$$

Where:

x : fractional conversion of monomer to polymer, and is equal to $\frac{\text{mass of monomer converted to polymer}}{\text{mass of monomer originally present}}$

t : time

k_p : propagation rate coefficient

C_P monomer concentration within the latex particles

$\bar{n}$ average number of free radicals per latex particle

N_c number of latex particles per unit volume of aqueous phase

$n_M{}^0$ amount of added monomer to the latex per unit volume of the aqueous phase

N_A Avogadro number

Conversion can be calculated through a number of different techniques, these include gravimetry, densitometry, chromatography, microalorimetry, and spectroscopic methods.[3] The technique that was used throughout this work was dilatometry. More details about dilatometry are available in section 2.4.

1.2.3 **Interval III** starts when monomer droplets are consumed. This means the monomer concentration within the latex particles starts to decrease ($C_P < C_P^{SAT}$), and keeps decreasing until all monomer is consumed. Another important characteristic of interval III is that the rate of reaction often decreases, because of the continuous decrease in C_P. N_c remains constant during this reaction, and no monomer droplets are present as they have all been consumed during interval II[3]. Exact understanding for the kinetic processes and mechanisms during interval III is still incomplete, since Norrish and Smith[9] noticed that, during the bulk polymerization of methyl methacrylate (MMA), the order of the polymerization reaction kept increasing with the increased chain length of the products. This increase in rate was found to start in interval II and continue throughout interval III. According to equation (1.1), this can be directly linked to an increase in the value of $\bar{n}$. This effect is called "gel effect" or "Trommsdorff-Norrish effect", and results in an increased contraction of the latex particles swollen with monomer.

1.2.4 **The aim of this work** is to find the effect of cyclodextrins on the rate of emulsion polymerization during interval II, particularly for the emulsion polymerization of styrene and MMA. More details about cyclodextrins will be mentioned in section 1.7. This was done by virtually starting the kinetic measurements for the reaction in interval II, to avoid the entire difficulties and complications related to interval I (such complications are discussed later via the Harkins theory). The idea of starting the reaction in interval II is simple. First of all a seed latex is made as follows, styrene or MMA were reacted in water, with the surfactant and initiator, at 92 ^{o}C for 24 hours. During this time, all the monomer will be converted into polymer and a huge number of latex particles are formed, the latex preparation includes all three intervals. This latex is then dialyzed to remove any extra surfactant. The latex particle size can be measured with several techniques, and by knowing the particle size and all required physical properties of the latex, and then the required amount of the latex can be used, with the addition of monomer, surfactant and initiator, the reaction can be started. Through this, all the conditions at the beginning of the reaction are known, the "seeds" are present in a mixture with the added monomer, so

the kinetic measurements are all taken through interval II, until C_P starts to be less than C_P^{SAT}, where interval III starts.

Another method to be used is to start the reaction with a small amount of monomer, which is less than what is required for C_P to be equal to C_P^{SAT}. This technique makes it possible to run the whole reaction in interval III conditions. This technique was not used during this project.

1.3 The Harkins Theory of emulsion polymerization

Historically, polymerization of unsaturated organic compounds was reported to be successful in 1838.[10] At that time, only bulk liquid monomers were noticed to transform to a very viscous or solid phase, due to reaction with a catalyst or exposure to heat. A common catalyst during that period was sodium metal, which made the production of the earliest polymers successful. Sodium made them low quality material, mainly because of the impossibility to separate the sodium metal residues from the produced polymer. Complaints came mainly after the use of the low quality product in the battlefield of the First World War.

This problem led to the idea of running the polymerization in an aqueous medium, to avoid all complications of catalyzed bulk polimerization. Another reason to start the polymerization process in the aqueous medium was that, naturally within plants, all rubbers are found in the form of latices, so the conclusion was that polymerization which happens within the plant takes place in an aqueous medium.[10] As a result the earliest processes for emulsion polymerization were started industrially.

The high demand for rubber during the Second World War made polystyrene and polybutadiene highly required materials, and this led to the implementation of more advanced emulsion polymerization techniques, founded mainly on trial and error. There have been some early theories which explain emulsion polymerization, but the one which was later proven to be the closest to the true case was the theory of Harkins.[11,12,13]

Although this theory describes what happens in emulsion polymerization in a qualitative way, it is the basis on which all more advanced theories are based.[14] According to the theory, the emulsion polymerization process proceeds as follows:

1. The main role of monomer droplets is to act as a "storehouse"[13] for monomer. From this storehouse, all monomer molecules diffuse into the water to either polymer latex particles or detergent micelles.

2. In the case where surfactant is present within the system, then the polymerization starts by the formation of very small nuclei within the micelles. As the micelles are small, and so the monomer present within these micelles is much smaller, then the nucleation happens in this extremely small amount of monomer dissolved within the micelles. As the particles form, then principal loci of polymerization become the micelles and the particles already formed within. The particles absorb the monomer from the surrounding media, which are the micelles and the aqueous phase. After some time, the particles grow in size and become bigger than the micelles originally present.

3. If surfactant is not present within the system, then the nucleation starts within the aqueous phase, and keeps progressing in the same way mentioned earlier. It is important to note that this nucleation happens in the aqueous phase whether surfactant is present or not (so called surfactant free nucleation), but its importance decreases as the amount of surfactant in the system increases.

4. With the continuous growth of the particles, surfactant gets adsorbed around the particles, thanks to the increase in their surface area. Micelles containing monomer keep being absorbed by the particles, which keep growing because of the continuous adsorption of "micellar monomer" and its addition to the absorbed monomer already present within the particles.

5. With the continuous increase of the particle surface area, the surfactant adsorption increases until no more micelles are present in the medium.

6. With the disappearance of the surfactant phase from the medium, nucleation stops. Now the reaction is pure interval II or III, depending on the amount of monomer remaining. Essentially all the remaining polymerization takes place within the particles.

7. Continuous absorbance of the monomer within the polymer particles leads to the disappearance of the monomer phase from the medium. At this stage the medium contains only water and particles.

The Harkins theory though has a problem, mostly because of its qualitative nature. It is clear that the theory assumes an "ideal" case of emulsion polymerization.[15] In this case the monomer's solubility in water is so small that it can be considered negligible and the polymer is soluble in its monomer. The reason behind such an assumption was the polymerization of both styrene and butadiene can be considered "ideal". But actually, most other monomers do not follow such assumptions, because of one or more of the following:[15]

a) Monomer type and solubility: some monomers cannot be polymerized by emulsion systems, this is because of the chemistry of the monomer molecule which results in "inhibiting chain transfer". examples are α-methylstyrene, vinylmesitylene, trimethyl benzene and allyl acetate.[15] In other cases, the extremely low solubility of the monomer makes its emulsion polymerization very slow if possible at all. An example is lauryl acrylate,[16] and this was one of the motives to use cyclodextrin to polymerize such water insoluble monomers.

b) Different types of initiators and their solubilities: a commonly known source of free radicals is metal alkyls, but they are also a good example of free radical producing chemicals which cannot be used as initiators in emulsion polymerization, simply because they hydrolyze in water.[15] Initiators having very low solubility in water, i.e. azobisisobutyronitrile, also known as AIBN, are not suitable for use in emulsion polymerization during interval I and interval II, where they can move towards the monomer droplets present and start the initiation process within these droplets, resulting in obtaining coagulum. However, AIBN

can be used in interval III emulsion polymerization where no monomer droplets are present.[17] Coagulum is undesirable either in laboratory scale experiments or industrially. In laboratory experiments it renders accurately analyzing the kinetic results impossible, because of the formation of new particles of unknown number or characteristics during the process. Industrially it is also undesirable because the reactor would require extensive cleaning in case coagulum is formed on a large scale.[18]

c) Different types of surfactants: some surfactants, most commonly anionic surfactants, tend to form a coagulum. This should be avoided in emulsion polymerization, because it interferes with the kinetics[3] and the coagulum is industrially considered an impurity,[15] which should be removed in cases a pure product is required.

d) Presence of inhibitors or retarders: any inhibitor which was not removed before the polymerization process started can have a major slowing down effect on the reaction kinetics.[19]

e) Presence of any secondary components (like soluble electrolytes): such electrolytes can either have a positive or a negative effect on the reaction kinetics. The best situation is if such electrolytes are present in the amounts giving the best pH to avoid coagulation. Change of concentration of such compounds can affect the pH, resulting in the formation of coagulum.

f) Phase ratio: although according to Harkins theory increasing the amount of monomer in the system should not have an effect on the polymerization process, practically it results in obtaining larger particles. To avoid that, a larger amount of surfactant should be used.[15]

g) Continuous addition of surfactant, initiator, or monomer.

h) Particle size control: as previously mentioned in f), increasing the monomer amount while keeping the surfactant amount constant results in bigger particles.

Such deviation from Harkins theory gives an advantage of controlling the particle size of the produced latex particles.

i) Seeding, as already described.

It is clear from the above list and the possibility that any one (or more) of the factors mentioned affects the process, that emulsion polymerization generally does not happen exactly as per the Harkins theory. However, this theory has to be mentioned as it forms the basis on which more modern kinetic theories are based.

Before discussing the kinetic theories of emulsion polymerization, it is appropriate to mention the advantages of emulsion polymerization over other polymerization techniques, which can be listed as follows:[3,15,20]

1. in many applications, like paints and surface coatings, the latex itself is in the most suitable form by which the polymer can be used,
2. with most commonly produced emulsion polymerization polymers, high conversion is achieved with high rates of polymerization,
3. there is no need to run the polymerization process at very high temperatures, as it is run in an aqueous phase. However, in cases of monomers like vinyl chloride, high pressure and temperature are required because of the gaseous nature of vinyl chloride at standard temperature and pressure.
4. as water is the medium, it gives an environmental advantage regarding the waste of the process, a mass transfer advantage because of its low viscosity and good heat transfer, and a financial advantage because it eliminates the cost of using other organic solvents, which are all more expensive than water,
5. removing the product from the reaction medium is relatively easy if required, and it happens through simple coagulation and drying process,
6. emulsion polymerization products are used in many applications, like paper coating and coatings (styrene-butadiene copolymers), synthetic rubber (butadiene-styrene copolymers), and many other applications.
7. because of the easy control over the process, like particle size control which was discussed earlier, products of emulsion polymerization can be made with many different properties, according to the requirements of the end user.

1.4 Kinetic Theories of Emulsion Polymerization

1.4.1 The Smith-Ewart model[21]

The Smith-Ewart model is considered the first quantitative basis on which more advanced theories have been based. Since its publication it has been kept under continuous refinement and improvement. The theory is a quantitative modeling to the Harkins qualitative conclusions. The theory provides two main equations, one for the calculation of the total particle number of polymers in the emulsion, and the other for the average number of free radicals per particle.

The theory follows the Harkins assumption that the nucleation happens at the surfactant micelles, and later these nuclei become the particles at which the rest of the reaction takes place. The theory goes along the same assumptions that there is no nucleation (and so polymerization) in the aqueous phase or at the monomer droplets. The model is divided into two parts:

1. There are three cases for the distribution of free radicals within the medium, and for every case the model gives a general equation for the overall rate of polymerization within each particle, and the average polymerizing lifetime of a free radical. Case 1 discusses the kinetics when the number of free radicals per particle is small compared to unity, and the rate of reaction can be presented by the following equation:

$$\frac{\mathrm{d}C_p}{\mathrm{d}t} = k_\mathrm{p} C_\mathrm{p} N_\mathrm{c} \bar{n}\,, \qquad \bar{n} = \frac{\rho V_\mathrm{s}}{k N_\mathrm{c} A_\mathrm{P}} \tag{1.2a}$$

where ρ is the pseudo first order rate coefficient for radical entry into a latex particle, k is the pseudo first order rate coefficient for radical exit from a latex particle, V_s is the volume of the swollen latex particle and A_P is the interfacial area of the latex particle.

Case 2 focuses on the situation where the number of free radicals per particle is approximately 0.5, the only difference with case 1 is that the average number of radicals within the latex particle:

$$\bar{n} = 0.5 \tag{1.2b}$$

When $\bar{n}$ is smaller than or equal to 0.5, the system is called zero-one system.More details about zero-one systems will be presented in section 1.4.2.

Case 3 is about the kinetics of the system when the number of free radicals per particle is large compared with unity, and here $\bar{n}$ can be calculated as:

$$\bar{n} = \sqrt{\frac{\rho V_s}{2k_t N_c}} \tag{1.2c}$$

where k_t is the pseudo second order rate coefficient for radical termination within a latex particle.

2. Calculating the average particle number within the system, referred to as N_c, and this was found to be

$$N_c = y\left(\frac{\rho_i}{\mu}\right)^{2/5}(a_s E)^{3/5} \tag{1.3}$$

Where ρ_i is the rate of initiation, μ is the volumetric growth rate, a_s is the specific surface area of the surfactant and E is the concentration of the surfactant, and y is a constant whose value falls between 0.37 and 0.53.

From this it can be seen that the model's target is to calculate the steady state rate of polymerization after the nucleation process is over, which can be calculated from the interparticle kinetics (part 1) and number of particles (part 2). The model also focuses on interval II and III, as all the equations are to be used after the nucleation part is over.

The kinetics of emulsion polymerization is affected by a number of factors, which include the rates of initiation, propagation and termination. In turn, the rates of entry and exit, and the number fraction of particles containing n radicals, N_n, can all be summarized in the following equation:[3]

$$\frac{\mathrm{d}N_n}{\mathrm{d}t} = \rho N_{n-1} - [\rho + nk + n(n-1)c]N_n + (n+1)kN_{n+1} + (n+2)(n+1)cN_{n+2} \quad (1.4)$$

where c is the pseudo first-order termination rate coefficient.

The average number of free radicals within one particle,$\bar{n}$, can be calculated from the following equation:

$$\bar{n} = \sum_{n=1}^{\infty} nN_n$$

In fact, only case 2 was deeply studied by Smith and Ewart, and generally it is known as the Smith-Ewart theory. Mathematical treatments for the two other cases were later done by other researchers**Error! Bookmark not defined.**. Another noticeable feature of this work is the use of symbols. The entry and exit rate constants through this thesis and many books previously written[2,3] are referred to as ρ and k, while in the original work of Smith and Ewart, the symbols ρ' and k_0 are used for the same rate constants. Currently, more than sixty years after Smith and Ewart published their theory, their model is still the starting point for fitting emulsion polymerization data.

The work done by Smith and Ewart, had some imperfections, and so some improvements to the model were made by Gardon,[22,23] who made a new prediction for the particle size distribution. As an example for one other imperfection, Ugelstad and Mørk [24] noticed that the work of Smith and Ewart is not applicable when studying the kinetics of the emulsion polymerization of PVC. To go around this problem they introduced some modifications to the theory and this made it applicable for the case of PVC, and other monomers having very low solubility in their polymers. Introducing such modifications resulted in the appearance of a new unknown parameter. Finally, Ugelstad and Hansen[25] provided the solution for the unknown parameter, and so the complete solution for the new Smith-Ewart based theory became available.

1.4.2 The simple zero-one system

A system can be defined to be "zero-one" if it fulfills the condition of instantaneous termination, $c >> \rho, k$, where c is the pseudo first order rate coefficient for termination within the particles. From this definition it can be seen that every latex particle in such a system either has zero or one free radical. "zero-one" means that the average number of free radicals per latex particle, $\bar{n}$, can not exceed 0.5, as this maximum value is based on the assumption that half the particles contain no free radical, the other half contains one free radical. Because of the assumption of instantaneous termination, the termination rate will not be considered in the kinetic calculations for this system. With the exclusion of the termination rate, rate coefficients for other growth events can be determined in a more reliable manner. This situation is referred to in the Smith-Ewart theory by "Case 1". "Case 2" deals with the limiting value of $\bar{n} = 0.5$, which happens if $c >> \rho >> k$.
The mathematical treatment starts by considering all particles having either zero or one free radical, and normalizing the number fraction to 1, so

$$N_0 + N_1 = 1$$

and

$$\bar{n} = \frac{N_1}{N_0 + N_1}$$

so the above equation can be simplified into $\bar{n} = N_1$. Substituting into the general Smith-Ewart equation (1.4):

$$\frac{\mathrm{d}N_0}{\mathrm{d}t} = -\rho N_0 + (\rho + k)N_1 \tag{1.5}$$

$$\frac{\mathrm{d}N_1}{\mathrm{d}t} = \rho N_0 - (\rho + k)N_1 \tag{1.6}$$

Equations (1.5) and (1.6) are based on the assumption that the particle may either contain one free radical or no radical at all. The equations also do not have particle formation

terms, and so to be able to use these equations, the total number of particles must remain constant, and so secondary nucleation must be totally avoided, otherwise the solution of the equations may not be accurate. The solution for equations (1.5) and (1.6) is:[3]

$$N_1 = \frac{\rho}{2\rho+k} + \left(\bar{n}_0 - \frac{\rho}{2\rho+k}\right) e^{-(2\rho+k)t} \tag{1.7}$$

$\bar{n}_0$is the value of $\bar{n}$ at t = 0. If polymerization starts at t = 0, then $\bar{n}_0$ = 0, but this is not always the situation, as will be discussed in chapter III and V.

The steady state solution for equation (1.7), at $t = \infty$, is:

$$N_{1,ss} = \bar{n}_{ss} = \frac{\rho}{2\rho+k} \tag{1.8}$$

1.4.3 The simple pseudo-bulk system

In a pseudo-bulk systems $\bar{n}$ > 0.5, and termination cannot be neglected, as it is the rate-determining event. It is clear from the name of the equation that it likens the kinetics of this emulsion polymerization system to the kinetics of the bulk system.

The system equation is also obtained from the Smith-Ewart general equation (1.4), by multiplying each $\mathrm{d}N_n/\mathrm{d}t$ by *n*, and then summing over all *n*, so

$$\frac{\mathrm{d}\bar{n}}{\mathrm{d}t} = \rho - k\bar{n} - 2c(\overline{n^2} - \bar{n}) \tag{1.9}$$

where,

$$\overline{n^2} = \frac{\sum_{n=0}^{\infty} n^2 N_n}{\sum_{n=0}^{\infty} N_n}$$

is the second moment of the N_n. As $\overline{n^2} = \bar{n}^2 + \bar{n}$. Then equation (1.9) can be written as:

$$\frac{\mathrm{d}\bar{n}}{\mathrm{d}t} = \rho - k\bar{n} - 2c\bar{n}^2 \tag{1.10}$$

The assumption of $\overline{n^2} = \bar{n}^2 + \bar{n}$ is valid if N_n follows a Poisson distribution.[26] When $\bar{n}$ is large, N_n is certainly expected to conform to such a distribution.[27] It can also be the case for some $\bar{n} < 0.5$.

1.5 Model for Entry

The original models for the mechanism of emulsion polymerization were all based on the work of Harkins[13], and the Smith-Ewart theory[21], however every one of these models specified a different rate-determining step. For example the Smith-Ewart model assumes that all radicals coming from the initiator go to react with monomer present within latex particles. But more studies[28,29,30] have shown that this assumption is simply wrong. The proof was simple, the rate of entry in many cases was found to be much less than its value as predicted from the rate of initiation.

Theories of entry were either classified as one of the following:

1. "The diffusion of monomer and radicals to the reacting centres or sites":[31] this approach considered the emulsion polymerization reactions to be diffusion controlled. The approach has some problems; the main problem being that the model results did not totally agree with the experimental results of many experiments.

2. "Coagulation as a kinetic process":[32] the coagulation process was considered the rate-determining step, and the rate constant for it can be calculated from DLVO theory,[33] but it was found that ρ remains constant in some styrene emulsion polymerization systems even if the ionic strength is changed, and so the theory was found to be invalid, because it quite obviously predicts otherwise.

3. "Kinetics of emulsifier adsorption":[34] the adsorption of the surfactant from the particle surface was found to be the rate-determining step, but it was found

that ρ was not affected by increasing the surface coverage of the particles in a rate 1:4.[3]

The main work[35] which has shown the invalidity of these theories was presented as evidence to show the amount of problems facing research at that time. And to solve these problems and many others, Maxwell and Morrison[36] presented their entry model, based on the ideas of Priest,[37] which were concluded after his study on emulsion polymerization of non-micellar systems. It was found that it was unlikely for the free radical to be transferred from the aqueous phase directly to the particle. Based on this suggestion, the model's mechanism assumes that, in order for the free radical to be able to move from the aqueous phase to the monomer, a critical degree of polymerization, *z*, has to be reached. At this degree of polymerization, the "*z*-mer free radical" becomes surface-active with lower water solubility, and so it must go to the particle to be able to continue the polymerization reaction, so entry is its only fate.

The reaction starts by the decomposition of the initiator:

$$\mathrm{I{-}I} \xrightarrow{k_\mathrm{d}} 2\mathrm{I}^{\bullet} \tag{1.11}$$

where k_d is the first order rate coefficient for initiator decomposition. The initiator free radical ($\mathrm{I}^{\bullet}$) starts to react with monomer molecules suspended in the aqueous phase:

$$\mathrm{I}^{\bullet} + \mathrm{M} \xrightarrow{k_\mathrm{pi}} \mathrm{IM}^{\bullet} \tag{1.12}$$

where k_pi is the second order rate coefficient for aqueous phase propagation between initiator free radical and monomer. To avoid the complication of requiring to know exactly the value of k_pi, it is commonly acceptable to use the initiator efficiency in the calculations, so that:

$$\left.\frac{\mathrm{d}[\mathrm{IM}^{\bullet}]}{\mathrm{d}t}\right|_{\text{initiation}} \quad 2fk_\mathrm{d}[\mathrm{I}] \tag{1.13}$$

The factor 2 is used only if the two molecules produced from the initiator decomposition are free radicals which can initiate polymerization. *f* is the initiator efficiency, which is defined as the fraction of the free radicals produced from equation (1.12) which reacts with monomer molecules. *f* usually has a value between 0.2 and 0.7.[3]

The free radical produced in equation 1.12 will then go for subsequent propagation:

$$IM_i^{\bullet} + M \xrightarrow{k^i_{p,aq}} IM_{i+1}^{\bullet} \qquad (1.14)$$

$k^i_{p,aq}$ is the rate coefficient for aqueous phase propagation of the free radical whose degree of polymerization is *i*, and *i* must be equal to *z* before this free radical can penetrate into one of the particles, so

$$IM_z^{\bullet} + \text{latex particle} \xrightarrow{\rho} \text{entry} \qquad (1.15)$$

Finally, if the free radical $IM_i^{\bullet}$ reacted with any other free radical present in the aqueous phase, $T^{\bullet}$, then

$$IM_i^{\bullet} + T^{\bullet} \xrightarrow{i<z,\ 2k_{t,aq}} \text{inert products} \qquad (1.16)$$

where $k_{t,aq}$ is the second order rate coefficient for termination between free radicals in the aqueous phase.

The rate equations for the reactions written above are:

$$\frac{d[I^{\bullet}]}{dt} = 2fk_d[I] - k_{pi}[I^{\bullet}]C_W - k_{t,aq}[I^{\bullet}][T^{\bullet}] \qquad (1.17)$$

where [I], $[I^{\bullet}]$, C_w and $[T^{\bullet}]$, are the concentrations of the initiator, initiator free radicals, monomer and total radical concentration in the aqueous medium, respectively.

$$\frac{d[IM^{\bullet}]}{dt} = k_{pi}[I^{\bullet}]C_W - k^1_{p,aq}[IM^{\bullet}]C_W - 2k_{t,aq}[IM^{\bullet}][T^{\bullet}] \qquad (1.18)$$

where [T$^{\bullet}$] is the total free radical concentration in the water phase.

$$\frac{\mathrm{d}[\mathrm{IM}_i^{\bullet}]}{\mathrm{d}t} = k_{\mathrm{p,aq}}^{i-1}[\mathrm{IM}_{i-1}^{\bullet}]C_{\mathrm{W}} - k_{\mathrm{p,aq}}^{i}[\mathrm{IM}_i^{\bullet}]C_{\mathrm{W}} - 2k_{\mathrm{t,aq}}[\mathrm{IM}_i^{\bullet}][\mathrm{T}^{\bullet}] \tag{1.19}$$

$$\frac{\mathrm{d}[\mathrm{IM}_z^{\bullet}]}{\mathrm{d}t} = k_{\mathrm{p,aq}}^{z-1}[\mathrm{IM}_{z-1}^{\bullet}]C_{\mathrm{W}} - \rho\frac{N_{\mathrm{c}}}{N_{\mathrm{A}}} \tag{1.20}$$

Comparing the values of all the reaction rate constants shows that all rate constants can be considered negligible compared to k_{pi},[38,39] and the rate of both reactions (1.11) and (1.12) will be determined by the rate of decomposition of the monomer, $2fk_{\mathrm{d}}$.

The rate of formation of all aqueous phase free radicals can be calculated as:

$$\frac{\mathrm{d}[\mathrm{T}^{\bullet}]}{\mathrm{d}t} = 2fk_{\mathrm{d}}[\mathrm{I}] - 2k_{\mathrm{t,aq}}[\mathrm{T}^{\bullet}]^2 \tag{1.21}$$

At steady state, the concentrations of the concentrations of all free radical components present in the aqueous phase can be calculated by:

$$[\mathrm{IM}_i^{\bullet}] = \frac{2fk_{\mathrm{d}}[\mathrm{I}]}{k_{\mathrm{p,aq}}^{1}C_{\mathrm{W}} + 2k_{\mathrm{t,aq}}[\mathrm{T}^{\bullet}]},\ i = 1 \tag{1.22}$$

$$[\mathrm{IM}_i^{\bullet}] = \frac{k_{\mathrm{p,aq}}^{i-1}C_{\mathrm{W}}[\mathrm{IM}_{i-1}^{\bullet}]}{k_{\mathrm{p,aq}}^{i}C_{\mathrm{W}} + 2k_{\mathrm{t,aq}}[\mathrm{T}^{\bullet}]},\ 1 < i < z-1 \tag{1.23}$$

$$[\mathrm{T}^{\bullet}] = \sum_{i=1}^{z-1}[\mathrm{IM}_i^{\bullet}] \tag{1.24}$$

Equations (1.22) — (1.24) can be solved iteratively to yield [$\mathrm{IM}_{z\text{-}1}^{\bullet}$], which is the only unknown on the right hand side of equation (1.20), as all other variables can be found experimentally, with the assumption that $k_{\mathrm{p,aq}}^{i}$ is chain length independent.

From equation (1.21), the total aqueous phase free radical concentration can be calculated as:

$$[\mathrm{T}^{\bullet}] \approx \sqrt{\frac{2fk_{\mathrm{d}}[\mathrm{I}]}{k_{\mathrm{t,aq}}}} \tag{1.25}$$

Finally, the first order rate coefficient for entry can be calculated by:

$$\rho_{\mathrm{initiator}} = \frac{N_{\mathrm{A}}}{N_{\mathrm{c}}} k_{\mathrm{p,aq}}^{z-1} C_{\mathrm{W}} [\mathrm{IM}_{z-1}{}^{\bullet}] \tag{1.26}$$

To calculate the value of $[\mathrm{IM}_{z\text{-}1}{}^{\bullet}]$, equation (1.22) can be written as:

$$[\mathrm{IM}_{z-1}{}^{\bullet}] = \frac{k_{\mathrm{p,aq}}^{i-1} C_{\mathrm{W}}}{k_{\mathrm{p,aq}}^{i} C_{\mathrm{W}} + 2k_{\mathrm{t,aq}}[\mathrm{T}^{\bullet}]} [\mathrm{IM}_{i-1}{}^{\bullet}], \qquad 2 \le i \le z-1, \tag{1.27}$$

Substituting equation (1.22), (1.23) into (1.27) leads to:

$$[\mathrm{IM}_{z-1}{}^{\bullet}] \approx \left(\frac{k_{\mathrm{p,aq}}^{i-1} C_{\mathrm{W}}}{k_{\mathrm{p,aq}}^{i} C_{\mathrm{W}} + 2k_{\mathrm{t,aq}}[\mathrm{T}^{\bullet}]} \right)^{z-2} [\mathrm{IM}^{\bullet}]$$

$$[\mathrm{IM}_{z-1}{}^{\bullet}] = \frac{2fk_{\mathrm{d}}[\mathrm{I}]}{k_{\mathrm{p,aq}}^{1} C_{\mathrm{W}}} \left(\frac{k_{\mathrm{p,aq}}^{i-1} C_{\mathrm{W}}}{k_{\mathrm{p,aq}}^{i} C_{\mathrm{W}} + 2k_{\mathrm{t,aq}}[\mathrm{T}^{\bullet}]} \right)^{z-1} \tag{1.28}$$

And by substituting equation (1.25) into equation (1.26), $\rho_{\mathrm{initiator}}$ can be calculated as:

$$\rho_{\mathrm{initiator}} = \frac{2fk_{\mathrm{d}}[\mathrm{I}]N_{\mathrm{A}}}{N_{\mathrm{c}}} \left(\frac{k_{\mathrm{p,aq}}^{i-1} C_{\mathrm{W}}}{k_{\mathrm{p,aq}}^{i} C_{\mathrm{W}} + 2k_{\mathrm{t,aq}}[\mathrm{T}^{\bullet}]} \right)^{z-1} \tag{1.29}$$

Substituting equation (1.25) into (1.29) leads to:

$$\rho_{\mathrm{initiator}} = \frac{2fk_{\mathrm{d}}[\mathrm{I}]N_{\mathrm{A}}}{N_{\mathrm{c}}} \left(\frac{2\sqrt{k_{\mathrm{d}}[\mathrm{I}]k_{\mathrm{t,aq}}}}{k_{\mathrm{p,aq}} C_{\mathrm{W}}} + 1 \right)^{1-z} \tag{1.30}$$

When $z = 1$, a free radical which can penetrate the particle will definitely enter the particle. But when $z \geq 2$, there is a probability that the free radical can terminate in water before $i = z$, and so the 100% success of entry will not be possible, as a result, the entry efficiency factor, F, was introduced.[36]

An initiator efficiency of 100% can be calculated as:

$$\rho_{\text{initiator } 100\%} = \frac{2fk_{\text{d}}[\text{I}]N_{\text{A}}}{N_{\text{c}}} \tag{1.31}$$

So the entry efficiency, *F*, can be calculated from:

$$F = \frac{\rho_{\text{initiator}}}{\rho_{\text{initiator100\%}}} = \left(\frac{2\sqrt{fk_{\text{d}}[\text{I}]k_{\text{t,aq}}}}{k_{\text{p,aq}}C_{\text{W}}} + 1\right)^{1-z} \tag{1.32}$$

1.6 Model for Exit

1.5.1 Desorption of monomeric radicals

As with the work done for entry model, which ignored the effect of exit on the entry process, the model presented here for exit ignores any effect for the radicals produced from the initiator decomposition.

For monomeric desorption, the diffusion of the monomer molecule from the particle is the rate determining step.[40] To calculate it, the equations for adsorption and desorption of the free radical to and from the particle are given as:

$$\text{M}^{\bullet} + \text{particle} \underset{k_{\text{dM}}}{\overset{k_{\text{ads}}}{\rightleftharpoons}} (\text{particle} - \text{M}^{\bullet}) \tag{1.33}$$

where k_{ads} is the second order rate coefficient for adsorption of species to particle surface, and k_{dM} is the first order rate coefficient for desorption of monomeric radical from particles to aqueous phase.

Following this, k_{ads} can be calculated from the Smoluchowski equation,[41] in the form:

$$k_{\text{ads}} = 4\pi D_{\text{W}} N_{\text{A}} r_{\text{S}} \tag{1.34}$$

where r_s is the swollen particle radius and D_W is the diffusion coefficient of a monomeric free-radical into the aqueous phase. It is assumed that the desorbing species is also a monomeric radical, following the basis that if $i > 1$, then the oligomer has no solubility in water. At equilibrium the rates of adsorption and desorption have to be equal, so:

$$k_{ads} C_W = k_{dM} V_s C_P N_A \tag{1.35}$$

Assuming that both inter-particle diffusion and intra-particle diffusion are both rate-determining,[40,42] then k_{dM} can be calculated from the equation:

$$k_{dM} = \frac{3 D_{mon} D_W}{\left(\frac{C_P}{C_W} D_{mon} + D_W\right) {r_s}^2} \tag{1.36}$$

where D_{mon} is the diffusion coefficient of the monomeric radical inside the particle. In most cases[3] C_P exceeds C_W significantly, so D_W can be ignored, and equation (1.36) takes the form:

$$k_{dM} = \frac{3 D_W}{{r_s}^2} \frac{C_W}{C_P} \tag{1.37}$$

Equations (1.35) and (1.37) give two different methods to calculate k_{dM}.

1.5.2 Desorption and exit rate coefficient

In a zero-one system, if $N_0 + N_1 = 1$ and $\bar{n} = N_1$, then the relationship between k_{dM} and k can be discussed. Equations (1.5) and (1.6) can be written as:

$$\frac{d\bar{n}}{dt} = \rho(1 - 2\bar{n}) - k\bar{n} \tag{1.38}$$

To write the equations more accurately, it is good to divide the group of particles containing one radical and whose number fraction is N_1, into two sub groups: ${N_1}^m$ is the number fraction of particles containing one monomeric radical, and ${N_1}^P$ is the number fraction of particles containing one non-monomeric radical. As the initiator free radicals are all in the aqueous phase and have no solubility in the monomer phase and the particles,

so all the monomeric free radicals were transferred from the aqueous phase to the particles. The total number of particles can be normalized as:

$$N_0 + N_1^{\mathrm{m}} + N_1^{\mathrm{P}} = 1$$

Following that there are two cases for termination, either no aqueous phase termination or complete aqueous phase termination. In case of no aqueous phase termination, all radicals which exit the particles have to re-enter. So the following events take place within the particles:

1. Propagation, from the reaction between a monomeric radical and a monomer molecule
2. Transfer to monomer, a polymeric radical terminates its propagation leaving one monomeric free radical
3. Entry, into a particle containing one free radial which will definitely result in instantaneous termination,
4. Entry into a particle containing no free radical
5. Exit, which is only possible for monomeric radicals.

Based on the assumption of no aqueous phase termination, then rate of re-entry will be equal to rate of desorption, $k_{\mathrm{dM}} N_1^{\mathrm{m}}$, and equations (1.5) and (1.6) can be re-written as:

$$\frac{\mathrm{d}N_0}{\mathrm{d}t} = \rho\left(N_0 + N_1^{\mathrm{m}} + N_1^{\mathrm{P}}\right) + k_{\mathrm{dM}} N_1^{\mathrm{m}} \tag{1.39}$$

$$\frac{\mathrm{d}N_1^{\mathrm{m}}}{\mathrm{d}t} = \rho_{\mathrm{re-entry}}\, N_0 - \rho N_1^{\mathrm{m}} - k_{\mathrm{dM}} N_1^{\mathrm{m}} + k_{\mathrm{tr}} C_{\mathrm{P}} N_1^{\mathrm{P}} - k_{\mathrm{p}}^1 C_{\mathrm{P}} N_1^{\mathrm{m}} \tag{1.40}$$

$$\frac{\mathrm{d}N_1^{\mathrm{P}}}{\mathrm{d}t} = \rho N_0 - \rho N_1^{\mathrm{P}} - k_{\mathrm{dM}} N_1^{\mathrm{m}} - k_{\mathrm{tr}} C_{\mathrm{P}} N_1^{\mathrm{P}} + k_{\mathrm{p}}^1 C_{\mathrm{P}} N_1^{\mathrm{m}} \tag{1.41}$$

where k_{tr} is the second order rate coefficient for transfer. Entry takes place because of the initiator, re-entry and the presence of continuous generation of free radicals within the system even without the presence of initiator. Entry because of the latter reason specifically is called “thermal entry”, so

$$\rho = \rho_{\text{thermal}} + \rho_{\text{initiator}} + k_{\text{dM}} N_1^{\text{m}}$$

and equation (1.41) can be re-written as:

$$\frac{\mathrm{d}N_1^{\text{P}}}{\mathrm{d}t} = \left(\rho_{\text{thermal}} + \rho_{\text{initiator}}\right)N_0 - \rho N_1^{\text{P}} - k_{\text{tr}} C_{\text{P}} N_1^{\text{P}} + k_{\text{p}}^1 C_{\text{P}} N_1^{\text{m}} \tag{1.42}$$

At steady state, only a very small fraction of the radicals within the particles are monomeric, so $\bar{n} = N_1^P$, and $k_{\text{dM}}\,\bar{n} \gg \rho$, and the rate equation can be in the form:

$$\frac{\mathrm{d}\bar{n}}{\mathrm{d}t} = \left(\rho_{\text{thermal}} + \rho_{\text{initiator}}\right)(1 - 2\bar{n}) - \frac{2k_{\text{tr}}\,C_{\text{P}}\,k_{\text{dM}}\,\bar{n}}{k_{\text{dM}}\,\bar{n} + k_{\text{p}}^1 C_{\text{P}}}\,\bar{n} \tag{1.43}$$

comparing equations (1.38) and (1.43) provides the following equation for the overall exit rate coefficient:

$$k = \frac{2k_{\text{tr}} C_{\text{P}} k_{\text{dM}} \bar{n}}{k_{\text{dM}} \bar{n} + k_{\text{p}}^1 C_{\text{P}}} \tag{1.44}$$

For the second case, that of complete aqueous phase termination, equation (1.38) can be written as:

$$\frac{\mathrm{d}\bar{n}}{\mathrm{d}t} = (\rho_{\text{thermal}} + \rho_{\text{initiator}})(1 - 2\bar{n}) - k_{\text{ct}}\bar{n} \tag{1.45}$$

where k_{ct} is the first order rate coefficient for exit. At the conditions of complete aqueous phase termination, k_{ct} is calculated through:

$$k_{\text{ct}} = \frac{k_{\text{tr}} C_{\text{P}} k_{\text{dM}}}{k_{\text{dM}} + k_{\text{p}}^1 C_{\text{P}}} \tag{1.46}$$

Comparing equations (1.38) and (1.45) shows that in the case of complete aqueous phase termination $k = k_{\text{ct}}$.

It is easily noticed from equations (1.29), (1.37) and (1.46) that there is a big number of factors which can affect the values of the entry and exit rate coefficients. It is then

preferred to work with limits of the expressions mentioned above; the limits should be physically true, and easy to use for analyzing data.

Limit 1: Complete aqueous phase termination

In this limit, the desorbed free radical will terminate by reacting with another aqueous phase free radical. The aqueous phase free radical can be another desorbed free radical (homo- termination) or an initiator derived free radical (hetero-termination).

- **Limit 1a:** homo-termination is the only fate for the desorbed free radical. The rate equation is:

$$\frac{\mathrm{d}\bar{n}}{\mathrm{d}t} = (\rho_{\text{thermal}} + \rho_{\text{initiator}})(1 - 2\bar{n}) - k_{\text{ct}}\bar{n} \tag{1.45}$$

  An expression for k_{ct} is already given in equation (1.46)

- **Limit 1b:** hetero-termination is the only possible end for the desorbed free radical, but not for the initiator derived free radical as it also has a possibility for entry.

$$\frac{\mathrm{d}\bar{n}}{\mathrm{d}t} = (\rho_{\text{thermal}} + \rho_{\text{initiator}})(1 - 2\bar{n}) - 2k_{\text{ct}}\bar{n} + 2k_{\text{ct}}\bar{n}^2 \tag{1.47}$$

  The term $2k_{\text{ct}}\bar{n}^2$ is for the entry that was going to happen by the initiator derived free radical if it was not terminated with the desorbed free radical.

- **Limit 1c:** the initiator efficiency is very low, and most initiator free radicals terminate within other initiator free radicals, but a minor amount of initiator free radicals terminate with desorbed free radicals, and all the desorbed free radicals terminate by hetero-termination. Using equation (1.47) for heterogeneous termination, the term for the entry of the initiator derived free radical which did not happen will not be included in the equation, and equation (1.45) is the most accurate approximation for this limit.

The zero-one system is best approximated by Limits 1a and 1c.

Limit 2: Negligible aqueous phase termination

The desorbed free radical can re-enter another particle then re-escape, or it can propagate then terminate within the particle. At these conditions $P_e k_{ads} N_c / N_A \ll k_{t,aq}[T^\bullet]$, where P_e is the probability that the adsorbed free radical propagates without taking place in any other event. Equation (1.42) is the true representation for this case, though it has two limits.

- **Limit 2a:** The exited free radical is highly likely to re-enter another particle where it propagates and so its exit becomes impossible, or it terminates if the particle already has another propagating free radical. Because of the negligible aqueous phase termination, the limit is taken as if the two particles, the one from which the radical exited and the one at which the radical propagates or terminates, have no barrier between them, and so $k_{dM} \ll k_p^1 C_P$ and the free radical loss is considered second order in $\bar{n}$, and equation (1.42) becomes:

$$\frac{d\bar{n}}{dt} = (\rho_{thermal} + \rho_{initiator})(1 - 2\bar{n}) - 2k_{cr}\bar{n}^2, k_{cr} = \frac{k_{tr}\, k_{dM}}{k_p^1} \quad (1.48)$$

- **Limit 2b:** if the free radical has a frequency for propagation much lower than its exit rate coefficient, the radical keeps entering and exiting until it enters a particle already having a free radical, where it will terminate instantaneously. The only fate for the free radical is to terminate, and consequently the loss is first order, and termination results in the loss of two radicals. Keeping the situation that $k_{dM} \ll k_p^1 C_P$, equation (1.42) becomes:

$$\frac{d\bar{n}}{dt} = (\rho_{thermal} + \rho_{initiator})(1 - 2\bar{n}) - 2k_{cr} C_P \bar{n} \quad (1.49)$$

Limit 3: Rapid re-entry and re-escape, rate-determining event is intra-particle termination

The first assumption in this system is that the termination of short radicals is the rate-determining step. The free radical undergoes exit, re-entry and re-exit, and termination

here is not instantaneous. The system here has monomeric radicals, moving very rapidly in the aqueous phase and freely entering and exiting to and from the particles. The system behaves like a bulk system, so it is called "pseudo-bulk".

In this case, exit occurs frequently, but it is not rate-determining, so following the assumption that ρ, $c \ll k$, equation (1.10) can be re-written as:

$$\frac{\mathrm{d}\bar{n}}{\mathrm{d}t} = \rho - 2c\bar{n}^2 \tag{1.50}$$

The limit does not explicitly include the chain length effect on the termination rate, or the "gel effect", which will be discussed in details in chapters V and VI.

1.7 Cyclodextrins in emulsion polymerization

The most important natural polymers of glucose are cellulose and starch. Cellulose has its monomer D-glucose units connected through β (1→4) linkages, while starch has α (1→4) linkages. Hydrolysis of any of these two polymers with acids, enzymes, heating, or any other method leads to a mixture of oligomers, namely "dextrins". A special case of this chain splitting reaction is when the starch is degraded by glucosyltransferase enzyme, some of the oligomers formed take the form of a cyclic product. As a result, cyclodextrins (CDs) are formed.[43]

The three "parent cyclodextrins" are the oldest discovered and most well known CDs, the α-CD molecule is a ring formed of 6 glucose units, β-CD is formed of 7 and γ-CD is formed of 8. Historically CDs were first referred to in 1891 as a result of digesting starch with *Bacillus amylobacter*. α-CD and β-CD were first separated and distinguished in 1911, while γ-CD was first discovered in 1948. The mass production of CDs was not recommended at that period because of a mistakenly drawn conclusion by one of the leading researchers of CDs[43], resulting in the consideration of CDs as toxic materials when inhaled. More competent toxicological studies have shown that CDs are not poisonous[43].

Because of the non-poisonous, semi-natural nature of CDs on one hand, and the advancements of genetic engineering on the other hand, more enzymes were discovered that make the production of highly pure CDs possible. In 1970, the cost of 1 kg of β-CD was US$ 2000; it was considered a rare chemical. Today the bulk price of 1 kg of β-CD is US$ 5, and the yearly production is around 10,000 tonnes.[44]

In addition to the parent CDs, δ-CD and ε-CD were discovered in 1957, and higher derivatives were discovered later,[43] nevertheless most research currently done on CDs still focuses on the parent CDs.

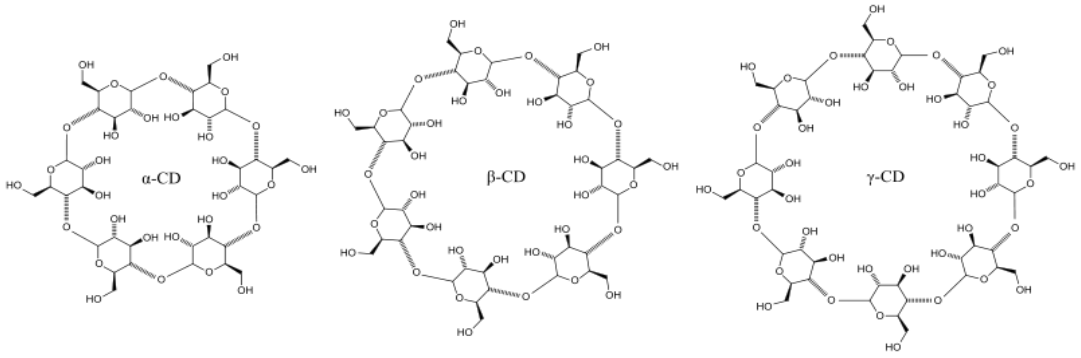

Figure 1.3. Structure of α-, β- and γ-CDs.

1.7.1 Structural features and physical properties of cyclodextrins

Figure 1.4[43] shows the main reason for the importance of CDs. At the centre of every molecule there is a cavity, lined with the hydrogen bonded to carbon atoms number 3 and 5 of the glucose unit.[45] X-ray crystallography has shown that CD molecules have a truncated cone structure with a cavity in the middle.[46] With the H atoms surrounding the

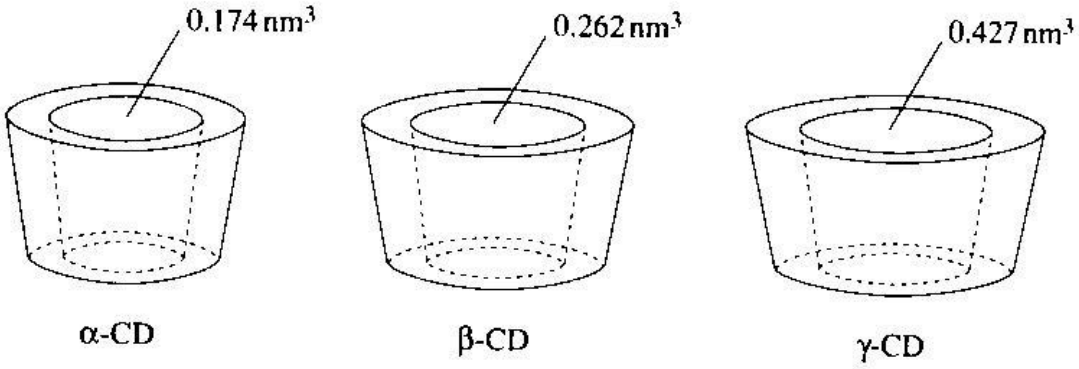

Figure 1.4. cavity sizes for parent CDs. [45]

cavity,[47] and because of the glucosidic oxygen atoms having their lone pairs facing the internal side of the CD molecule[45], the CD molecules have a hydrophobic cavity. On the external side of the CD molecule, the opposite takes place, because of the presence of many hydroxyl groups, the exterior of the CD molecule is hydrophilic.

Figure 1.4[45] shows the cavity sizes of the three parent CDs. It is clear that with such cavities monomers of many types can easily be included into the CDs to form complexes. The inclusion selectivity does not only depend on the size, but also on the structure, conformation, and hydration[45]. One example about this is the use of α-CD to form insoluble complexes with fatty acids, a property which is very desirable for some medical blood tests. Forming such complexes cannot be achieved with β-CD or γ-CD because of their bigger cavities. As per the cavity diameters for the parent CDs, α-CD cavity internal diameter is 0.57 nm, for β-CD it is 0.78 nm, and for γ-CD it is 0.95 nm.[47]

As seen in the schematic illustration for the inclusion process, Figure 1.5, [45] the water present within the CD cavity can be replaced by the hydrophobic compound. Consequently, the solubility of the guest in water will change. If the guest is soluble in water then no change is expected, but if its concentration increases above a specific level then CD precipitates, sometimes this level is at a low concentration. Whether this means a complex has been formed or not is debatable. In other cases, the CD solubility increases with the presence of other water-miscible compounds. Again this is not a definite sign of complex formation. [45]

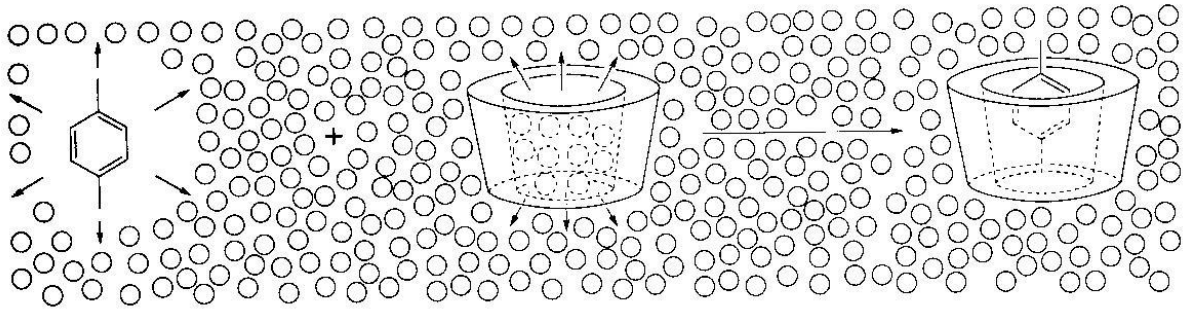

Figure 1.5. inclusion of *p*-xylene by a CD. [43]

But the most important case, the one directly applicable to the work done in this thesis, is when the guest has a low solubility in water and the capability of forming a CD complex.

In this case the solubility of the guest compound will be a function of the CD concentration, as shown in Figure 1.6.[43] In Figure 1.6, [Dissolved Guest] refers to the total concentration of both the guest compound which includes the amount dissolved in water and the amount included within the CD cavities, and S_0 is the solubility of the guest without CD. If the complex has a high solubility then the solubility of the guest compound can be represented by one of the A curves. A_L represents compounds which have a linear increase of solubility with increased amount of CD in water, expressing unchanged stoichiometry between guest compound and CD. A_P represents positive derivation from linearity, the host-guest stoichiometry which was 1:1 for example at low CD concentration becomes 2:3. On the other hand, A_N represents and negative derivation from linearity, which can be because of changed stoichiometry or because of changed solute-solvent interaction. [45]

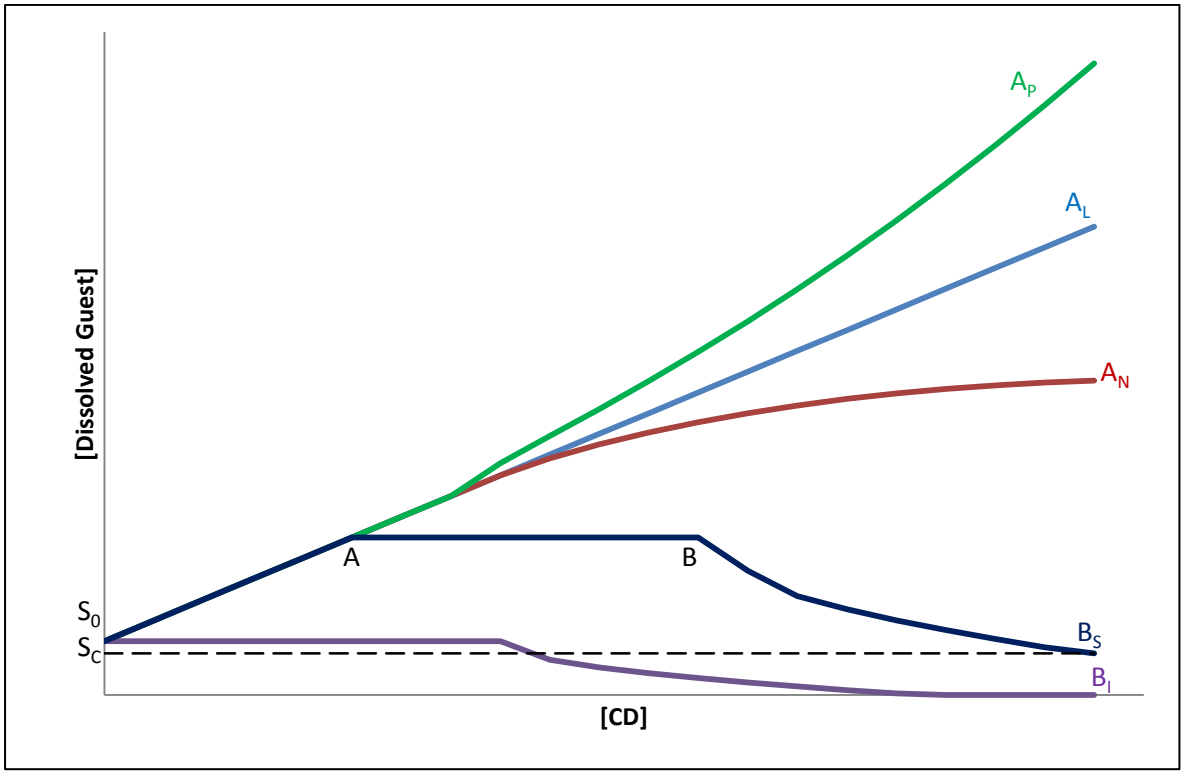

Figure 1.6. Solubility of guest compounds as a function of CD concentration, see text for meaning of symbols.[43]

On the other hand, if a poorly soluble complex is formed, the solubility is represented by the curve B_S, and the solubility limit of the complex is S_C. But if the complex formed is

insoluble in water, while the guest molecule has a low solubility, then the solubility is represented by the curve B_I.

1.7.2 Cyclodextrins, phase transport catalysis and emulsion polymerization

Because of their capabilities of increasing the solubility of hydrophobic compounds in water, CDs can be used as "phase transport catalysts".[48] The term was used with CD as early as 1984, in a paper which has shown that the rate of a nucleophilic displacement reaction increased with higher concentration of CD in the reaction medium.[49] Use of CDs as phase transport catalysts is understandable following the Harkins theory; an increase in the solubility of the monomer in the water will increase the reaction rate, because of increasing the concentration of the reactants within the water phase. Following the Smith-Ewart model, equation (1.30) shows that the entry rate increases with increasing C_W, which results in an increase in the overall reaction rate. This will be discussed more thoroughly in chapter IV and VI.

The first patent for emulsion and solution polymerization using CDs was done on 1996 by Lau, although in the patent there is a reference to an earlier trial by Kuieda *et al*. on 1984, to include CD in the free radical polymerization of some methacrylic esters. The work done by Lau[16] has shown the advantages of using CD in the emulsion polymerization of two types of monomers:

1. monomers having low water solubility like styrene and MMA, and stated that the method is also applicable for monomers with water solubility lower than 200 mM.
2. essentially water insoluble monomers, or monomers with extremely low water solubility, like lauryl acrylate and butyl acrylate, the patent has also shown the possibility of the emulsion polymerization of such highly hydrophobic monomers, which is very hard, and in some cases even impossible without CDs.

For the monomers with low water solubility, some studies have been done before. As a new field, most of the research done is qualitative in nature. The topic of kinetics of emulsion polymerization with CD has not been thoroughly studied yet, though there are a number of publications about this topic.

Storsberg and Ritter,[50] found that the use of an equimolar amount of monomer and CD with styrene and MMA improves the reaction kinetics, turning the reaction to be even faster than the polymerization in an organic solvent. This result shows that CD can give the emulsion polymerization in water some of the characteristics of solution polymerization (it was found later that what was happening was actually solution polymerization and not emulsion polymerization). In addition to such conclusions, ^{1}H NMR has shown that the CD protons 3 and 5 have been both raised to a higher field, indicating the position of the styrene molecule was found to be within the cavity of the CD. This confirms the assumptions made before, that the CD cavity is the place at which the guest molecules are present.

But Ritter[50] also found that emulsion polymerization kinetics do not agree with the increase of reaction rate which he found with the use of CD. This can be explained to be because of using equimolar amounts of styrene and MMA with CD, which makes it hard to describe this process as pure emulsion polymerization. For the 1:1 MMA/CD complex, reaction kinetics is found to be that of solution polymerization. It was later found[51] that, even for styrene, which has lower water solubility, the 1:1 styrene/CD complex kinetics are solution polymerization kinetics. Note that in the present project, the maximum CD concentration within the emulsion was always less than 5% of monomer weight. This ensured the absence of any solution/emulsion interference within the kinetics of this project.

In another study, more focusing on the nucleation process, Ritter *et al.*[52] found that the polydispersity index (PDI) is lower with the presence of CD, because of the use of semi-continuous reaction instead of the usual batch reactor. The use of CD with the preparation of the latex had a good impact on the colloidal stability of the polymer particles, making the formation of coagulum less probable. Overall, the latices prepared with CD were more stable, another advantage of using CD. It is not clearly stated whether this case was solution or emulsion polymerization, but Ritter's note of high CD/monomer ratio suggests it was solution polymerization work.

Hu[53] has analyzed the CD effect from a different point of view, simply by using the monomer from which CD is formed. Glucose was found to increase the rate of polymerization of styrene. Although glucose was not as effective as CD, both

experiments were done in the absence of surfactant. Other research[54] has shown that where surfactant is present, the CD effect is minor and sometimes even negligible. This is because the surfactant becomes the guest filling the CD cavity, which reduces its effect and the effect of the CD. Research done with MMA[55] without surfactant has shown a direct relationship between an increase in the CD concentration and an increase in reaction rate. Because of the advantage resulting from a lack of surfactants, emulsion polymerization with CD is described as "a green way to polymer synthesis".[56] Work done by Hu was only emulsion polymerization work.

Work by Ritter[57] involved the polymerization of styrene included using reversible addition-fragmentation chain transfer (RAFT) polymerization with CD. RAFT reagents are used to control the molecular weight distribution of the polymer, thus giving lower PDI. It was concluded that the use of CD/RAFT system gives a better control on PDI than when CD is used by itself.

Where monomers have no water solubility, the use of CD is necessary, sometimes even essential, for emulsion polymerization of such monomers to take place. After the patent of Lau16, Rimmer and Tattersall[58] worked on the emulsion polymerization of dodecyl and octadecyl methacrylates. Without CD, more than 50% of the used monomer turned into coagulum, but when CD was used the result was stable latices. The same authors have also noticed, in another project[59] dealing with the polymerization of butyl methacrylate with CD, that when CD is used in small amounts (up to 10% per weight of the monomer), it has a negligible effect on the rate of polymerization.

Madison and Long[60] have done similar work with tert-butyl methacrylate, cyclohexyl methacrylate and 2-ethylhexyl methacrylate. Monomer : CD ratio was 0.72 : 1 on a molar basis, such a ratio gives an indication that the higher the hydrophobicity of the monomer, the higher the ratio of CD to monomer required to make the polymerization possible. Moreover, this work has shown the possibility of recovering the CD used in the reaction, which gives an answer to the question whether the CD acts mainly as a catalyst, or does it interfere in the reaction. If ≈ 5% residual CD was present within the product mixture at a high concentration, the glass transition temperature increased, giving CD plasticizer properties. Also, the effect of CD on PDI was mentioned in that project.

Ritter and Glöckner[61] reported the possibility of the copolymerization of two hydrophobic monomers, butyl and isobornyl acrylates. Similarly, the copolymerization of styrene with stearyl acrylate was successful with CD present in the mixture.[62] CD was also shown to help in the copolymerization of MMA with 6-oxo-1,6-dihydropyrimidin-3-ium-4-olates. The aim was to prepare a polymer containing mesoionic groups on the main chain, through an emulsion polymerization process.[63]

CD can also affect the rate of the polymerization in another way, as was the case with the emulsion polymerization of 4-vinylbenzaldehyde, in which the CD was found to retard the reaction, because of the position of the vinyl group within the CD cavity. The retarding effect can be used in such cases to avoid uncontrolled polymerization of such monomers.[64]

As with to the case mentioned for using RAFT with CD in the polymerization of monomers having low water solubility, RAFT and CD can also be used with hydrophobic monomers such as butyl methacrylate. The RAFT technique was successfully used in that case, with lower PDI for the polymer produced. In that process, a water insoluble RAFT reagent was used and CD helped in making both the RAFT and monomer soluble in water[65].

1.8 Statement of aims for this study

The literature review presented above regarding the use of CD in emulsion polymerization, shows that although the presence of CD has been shown to affect the reaction rate of emulsion polymerization of many monomers, no studies have been done to determine the effect of CD on the different processes included within the emulsion polymerization.

An earlier study by van Berkel[66] has thoroughly studied the entry process, and has given a detailed analysis on the effect of initiator concentration and latex charge on both entry and exit. The study show the effect on ρ, k and c using both KPS and V-50 in case of styrene, and only KPS in case of MMA.

The current study is an expansion to the van Berkel study, following the same approach, another parameter which is expected to affect entry, exit and termination rates has been studied here. This parameter is the CD concentration within the emulsion.

The current study was done on systems which were studied well without CD. This is just to have a clear idea on the exact mechanistic effect of CD, by comparing the work done with CD and without CD. Having the effect of CD on ρ, k and c with systems which have already been studied well will open the door for a mechanistic approach for the emulsion polymerization of water insoluble monomers.

1.9 Thesis outline

Chapter I focuses on emulsion polymerization, work previously done, models currently used with the emulsion polymerization kinetics, and finally the use of CD in emulsion polymerization.

Work done in the current project will be discussed starting from chapter II, which focuses on the experimental techniques used throughout the course of this project. This includes general discussion on the procedures used for preparation of latex from raw materials until they become useable in seeded emulsion polymerization experiments. Chapter II will also discuss also the techniques used to get the properties of the latices, and the solubility of monomer in water in presence of CD and surfactant.

Chapter III covers the effect of CD on the emulsion polymerization of styrene, a monomer having low water solubility, which is styrene. The aim of calculations and work of chapter III is on obtaining some of the important kinetic parameters of two polystyrene latices used in this work, and the focus is on the thermally initiated and the γ- rays initiated polymerization experiments and the effect of the presence of CD on both thermal entry and exit rate coefficients of both latices used.

Chapter IV is based on the results obtained and conclusions reached in chapter III, and it focuses on the effect of CD on chemically initiated emulsion polymerization experiments.

Data calculated in chapter III will be shown to play a major role in chapter IV calculations. Chapter IV will also show that in emulsion polymerization, CD can have a positive, negative, or negligible impact on the polymerization kinetics, depending on the conditions of the reaction medium.

Chapter V discusses the effect of CD on the emulsion polymerization of MMA, a monomer having higher water solubility. By finding the important kinetic parameters for the emulsion polymerization of MMA, the effect of CD on the chemically initiated emulsion polymerization of MMA can be further analyzed. Chapter V focuses on the thermally initiated and the γ- rays initiated polymerization experiments, and the aim is to calculate the entry and termination rate parameters.

Chapter VI is based on the results shown in chapter V, and discusses the effect of CD on MMA chemically initiated seeded emulsion polymerization experiments.

1.10 A note about the structure of the thesis

One of the aims of research is to find scientific facts or reach scientific conclusions, then make such facts or conclusions accessible to other people working in the same field. And as the work done during the course of this project discussed and answered questions which were never answered before, such results should be published in academic journals. Every chapter of this thesis is planned to be published as a research paper. Consequently, the experimental part for example might be repeated from chapter to chapter, with minor differences according to the experiments which are discussed within every chapter.

References

(1) Miller, D., *Archaeological Dialogues*, **2007**, 14 :1:23–27

(2) Campbell, I.M., *introduction to synthetic polymers*, **1994**, Oxford University Press.

(3) Gilbert, Robert G., *Emulsion polymerisation, a mechanistic approach*, **1995**, Academic Press, London.

(4) Dougherty, T., *J. Am. Chem. Soc.*, **1961**, 83, 4849

(5) Lieser, K., *Nuclear and Radiochemistry Fundamentals and Applications*, **1996**, VCH Verlagsgesellschaft, Germany

(6) McKay, H., *Principles of Radiochemistry*, **1971**, Butterworth & Co Ltd, London

(7) Gardon, J.L., *Br. Polym. J.*, **1970**, 2,1

(8) Lovell P.A., *Batch and semi-batch processes*, in Lovell P.A., and El-Aasser M.S. (editors), *Emulsion polymerization and emulsion polymers*, **1997**, John Wiley and sons, New York.

(9) Norrish R.G.W., Smith R.R., *Nature*, **1942**, 150, 336

(10) Blackley D.C., *Emulsion polymerization theory and practice*, **1975**, Applied science publishers ltd, London

(11) W.D. Harkins, *J. Chem. Phys.*, **1945**, 13,381

(12) W.D. Harkins, *J. Chem. Phys.*, **1946**, 14,47

(13) W.D. Harkins, *J. Chem. Phys.*, **1947**, 69, 1428

(14) Finn Knut Hansen, *historic overview*,in A.M. van Herk (editor),*Chemistry and technology of emulsion polymerization*, **2005**, Blackwell Publishing

(15) Mark, H.F., *Encyclopedia of polymer science and technology*, Duck, E.W., *Emulsion polymerisation*, vol. 5, **1966**, John Wiley, New York

(16) Lau, W., US Patent Number 5521266.

(17) Sudol E.D., El-Aasser M.S., Vanderhoff, J.W., *J. Pol. Sci.*, **1986**, 24, 3515

(18) Lovell, P.A., *Batch and Semi-Batch Processes*, in Lovell P.A., and El-Aasser M.S. (editors), *Emulsion polymerization and emulsion polymers*, **1997**, John Wiley and sons, New York.

(19) Stickler, M. and Meyerhoff, G., *Makromol. Chem.*, **1978**, 179, 2729.

(20) Klein, A. and Daniels, E., *Formulation Components*, in Lovell P.A., and El-Aasser M.S. (editors), *Emulsion polymerization and emulsion polymers*, **1997**, John Wiley and sons, New York.

(21) W.V. Smith and R.H. Ewart, *J. Chem. Phys.*, **1948**, 16,592

(22) Gardon, J.L., *J. Polym. Sci., Part A: Polym. Chem.*, **1968**, 6, 623

(23) Gardon, J.L., *J. Polym. Sci., Part A: Polym. Chem.*, **1968**, 6, 2859

(24) Ugelstad, J. and Mørk, P., *Br. Polym. J.*, **1970**, 2, 31

(25) Ugelstad, J. and Hansen, F.K., *Rubber Chem. Technol.*, **1976**, 49, 536.

(26) Bevington, P. and Robinson, D., *Data Reduction and Error Analysis*, **2003**, McGraw-Hill Higher Education, New York

(27) Taylor, L.D., *Probability and Mathematical Statistics*, **1974**, Harper & Row, New York

(28) Hawkett, B., Napper, D. and Gilbert, R., *J. Chem. Soc., Faraday Trans. 1*, **1980**, 76, 1323.

(29) Ballard, M., Napper, D., and Gilbert R., *J. Polym. Sci., Polym. Chem. Ed.*, **1984**, 22, 3225.

(30) Halnan, B., Napper, D. and Gilbert, R., *J. Chem. Soc., Faraday Trans. 1*, **1984**, 80, 2851

(31) Van der Hoff, J., *The mechanism of emulsion polymerization*, in Ham, G. (Editor), *Vinyl Polymerization*, **1969**, Vol 1., Part 2.

(32) Ottewill, R., *The stability and instability of polymer latices*, in Piirma, I.(Editor), *Emulsion Polymerization*, **1982**, Academic Press, New York.

(33) Hunter, R.J., *Foundations of Colloid Science Volume I*, **1987**, Oxford University Press, New York.

(34) Yeliseyeva, I., *Polymerization of Polar Monomers*, in Piirma, I.(Editor), *Emulsion Polymerization*, **1982**, Academic Press, New York.

(35) Adams, M., Trau, M., Gilbert, R., Napper, D. and Sangster, D., *Aust. J. Chem.*, **1988**, 41, 1799

(36) Maxwell, I., Morrison, B., Napper, D. and Gilbert, R., *Macromolecules*, **1991**, 24, 1629.

(37) Priest, W., *J. Phys. Chem.*, **1952**, 56, 1077.

(38) McAskill, N. and Sangster, D., *Aust. J. Chem.*, **1979**, 32, 2611

(39) McAskill, N. and Sangster, D., *Aust. J. Chem.*, **1984**, 37, 2137

(40) Ugelstad, J., Hansen, F., *Rubber Chem. Technol.*, **1976**, 49, 536

(41) de Paula, J. and Atkins, P., *Atkins' Physical Chemistry ninth edition*, **2010**, Oxford University Press, New York.

(42) Harada, M., Nomura, M., Eguchi, W., Nagata, S., *J. Chem. Eng. Jpn.*, **1971**, 4, 54

(43)Szejtli, J. and Osa, T., *Volume 3: Cyclodextrins*, in Lehn, J. *at al.* (Editor), *Comprehensive Supramolecular Chemistry*, **1996**, Pergamon, UK

(44) Loftsson, T. and Duchêne, D., *Int. J. Pharm.*, **2007**, 329, 1

(45)Helena D., *Molecules with Holes-Cyclodextrins*, in Helena D. (editor), *Cyclodextrins and their complexes*, **2006**, Wiley-VCH, Weinheim

(46)Makoto M. and Monflier E., *Cyclodextin Catalysis*, in Helena D. (editor), *Cyclodextrins and their complexes*, **2006**, Wiley-VCH, Weinheim

(47) Szejtli, J., *Chem. Rev.*, **1998**, 98, 1743

(48) Lau, W., *Macromol. Symp.*, **2002**, 182, 283.

(49) Trifinov, A., Nikiforov, T., *J. Mol. Catal.*, **1984**, 24, 15.

(50) Ritter, R. and Storsberg, J., *Macromol. Rapid Commun.*, **2000**, 21, 236.

(51) Ritter, H., Steffens, C. and Storsberg, J., *e-polymers*, **2005**, 34, 1.

(52) Ritter, H., Storsberg, J., van Aert, H. and Roost, C., *Macromolecules*, **2003**, 36, 50.

(53) Hu, J., Li, S., Wang, D. and Liu, B., *Polym. Int.*, **2004**, 53, 1003

(54) Hu, J., Li, S. and Liu, B, *J. Polym. Mater.*, **2005**, 22, 213.

(55) Hu, J., Li, S., Wang, D., Li, H., Liu, B. and Liao, X., *Polymer*, **2004**, 45, 1511.

(56) Hu., J., Huang, R., Cao, S. and Hua, Y., *e-polymers*, **2008**, 171.

(57) Ritter, H., Köllisch, H. and Barner-Kowollik, C., *Macromol. Rapid Commun.*, **2006**, 27, 848.

(58) Rimmer, S. and Tattersall, P., *Polymer*, **1999**, 40, 5729

(59) Rimmer, S. and Tattersall, P., *Polymer*, **1999**, 40, 6673

(60) Madison, P., and Long, T., *Biomacromolecules*, **2000**, 1, 615

(61) Ritter, H., Glöckner, P., *Macromol. Rapid Commun.*, **1999**, 20, 602

(62) Leyrer, J. and Mächtle, *Macromol. Chem. Phys.*, **2000**, 201, 1235

(63) Ritter, H., Theis, A., *Macromol. Chem. Phys.*, **2003**, 204, 1297

(64) Ritter, H., Heinenberg, M., *Macromol. Chem. Phys.*, **2003**, 204, 1297

(65) Zhang, F., Ni, P., Xiong, Q., Yu, Z., *J. Polym. Sci., Part A: Polym. Chem.*, **2005**, 43, 2931.

(66) van Berkel, K., *Entry and the Kinetics of Emulsion polymerization*, a PhD thesis, University of Canterbury, 2004.

Chapter II
Experimental Techniques

During the course of this project, a wide variety of techniques has been used in order to carry out the required experimental analysis. These experiments required the use of different chemicals and equipment to provide a wide range of conditions.

2.1 Chemicals

The two monomers used in this project were styrene and methyl methacrylate (MMA). Styrene was obtained from Nuplex Industries. It came containing the inhibitor hydroquinone, and a purity of 99.92%, as measured in this work through gas chromatography. MMA of 99% purity was purchased from Merck Schuchardt OHG, also containing hydroquinone.

Inhibitor was removed from both styrene and MMA by passing the monomers through a column containing basic activated aluminium oxide, from Sigma-Aldrich. Because of the high impact of the monomer purity on the experimental results,[1] styrene was further distilled under vacuum. Gas chromatography showed that the purity of the purified styrene was found to be 99.99%, while that of MMA was 100%.

Two initiators were used, the anionic initiator used was potassium persulphate $K_2S_2O_8$, (KPS) (BDH, A.R. grade),; and the cationic initiator used was, 2,2'-azobis(2-methylpropionamidine)dichloride, $[=NC(CH_3)_2C(=NH)NH_2]_2 \cdot 2HCl$, (Aldrich, 97%), available commercially with the name V-50. Both initiators were re-crystallized before usage, KPS was recrystallized from water, and V-50 was recrystalized from water/acetone (1:1 by weight). The anionic surfactant used was sodium dihexyl sulphosuccinate (AMA-80), used as an 80% solution in water and isopropanol (BDH), and the cationic surfactant was dodecyltrimethyl ammonium bromide (DTAB) (Aldrich, A.R. Grade).

During measurements of the monomer solubility within the particles, C_P^{SAT}, the inhibitor used was 2,6 di-tert,butylphenol, 99%. Another inhibitor used was hydroquinone (BDH, B.P. Grade) which was used at the end of kinetic experiments to measure the conversion by gravimetry.

The only cyclodextrin used in this research was methyl-β-cyclodextrin (Sigma-Aldrich and Aldrich, both A.R. grade), as β-CD is the key product of commercial production of CD,[2] is the cheapest and so the first CD choice in industrial applications, mainly because of its lower solubility compared to α-CD and γ-CD. β-CD derivatives are used because of their higher solubility,[3,4] the β-CD derivative mainly produced is methyl-β-cyclodextrin.[2] Throughout the rest of this thesis, methyl- β-cyclodextrin will be referred to as CD.

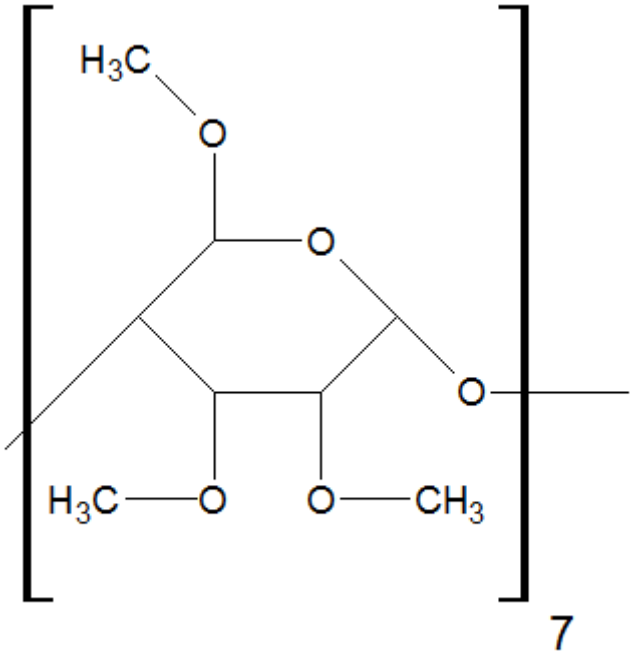

Scheme 2.1. Structure of methyl-β-cyclodextrin, the only CD used throughout the course of this work.

2.2 Seed latices

The seed latex preparation is the first step on the path of conducting kinetic measurements using dilatometry. Full details about the preparation and chemical components used for every latex used are presented in the respective chapter. An overall description follows.

2.2.1 Preparation of the latex

Chemicals required for the preparation of the latex are added to the reactor. These include milli-Q water, surfactant, and buffer, which was only used with the anionic polystyrene and poly methyl methacrylate (PMMA) latices. The components are mixed together and the reaction medium temperature is kept at 92 ^{o}C. During this time, the reaction medium is kept under nitrogen atmosphere, in order to minimize the presence of oxygen in the medium before adding the monomer.

When the required temperature is reached, the monomer, previously purified, is added to the reaction medium, and reactants left until thermal equilibrium is reached, and the initiator is then added in the form of an aqueous solution. Nitrogen gas flow over the reaction medium is stopped in order to avoid the evaporation of water at the high temperature, and then the reaction medium is fully closed to avoid any contamination with oxygen gas from the air.

The reactor, Figures 2.1 and 2.2, is a borosilicate glass walled 1L cylinder, with a length of 18 cm and a diameter of 10.5 cm. The top and bottom of the reactor are made of stainless steel, and glass fiber reinforced Teflon gaskets were placed between the glass walls and the stainless steel top and base. The top of the reactor has two inlets, one for nitrogen gas, and the other for the monomer and solutions fed into the reactor. An electric motor is placed above the reactor, connected to a stainless steel rod, which is connected to the stirring impeller.

The reactor temperature is controlled through a jacket surrounding the reactor. Hot water flows within the jacket, and the water temperature is controlled through a water recirculation unit, which can heat the water flowing in the jacket, and is connected to tap water to cool down the reaction medium in the event that the exothermic effect of the polymerization causes a sudden increase in temperature. The recirculation unit is controlled through two temperature probes; one is in the reactor and the other in the jacket. Both give signals to an electric control unit, which then opens or closes the stream for hot or cold water, according to the immediate requirement.
The reactor was made with three impellers to be used with it: flat blade, pitched blade,

and marine type propeller. Because of the nature of the emulsion, where the particles are suspended within the liquid medium, the pitched blade impeller was chosen as the best impeller for this exercise,[5] and it was used for all latices synthesized during this project.

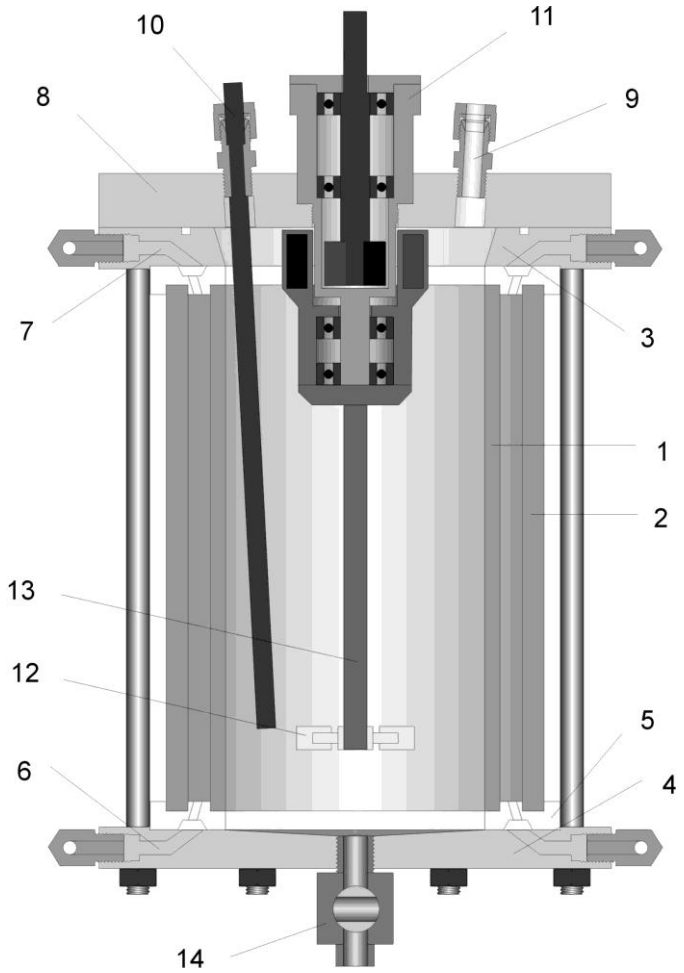

Figure 2.1. Latex synthesis reactor. 1&2: borosilicate glass cylinders, 3&4: stainless steel top and bottom plates, 5: Teflon spacer, 6&7: entry and exit of hot or cold water to control temperature, 8: stainless steel reactor head, 9: nitrogen inlet, 10: reactants inlet, 11: magnetic coupling connected to electric motor, 12: stirring impeller, 13: stirring shaft, 14: valve for emptying the reactor.[6]

The reaction lasts for 24 hours, during which the three reaction intervals take place (for more information about intervals check section 1.2). At the end of this period, the reaction products are filtered through glass wool, to remove any coagulum formed during the reaction. A full description of the reactor has previously been written[6] and it should be consulted for further details.

Figure 2.2. The reactor in its position, the figure shows the water entry and exit used to control the reactor temperature and the reactor connection to its control unit.

2.2.2 Purification of the latex

Kinetic experiments are very sensitive to any change in the concentration of any of the components. The latex must first be purified as the chemicals used in its preparation may have an impact on kinetic studies. The best example here is surfactant. Although it is desired in the preparation of a latex, as the first particles form within the micelles, an excess concentration of surfactant may result in secondary nucleation in subsequent experiments. Additionally, any remaining initiator molecules that did not react with the monomer should be removed, as these molecules may remain and affect the subsequent kinetic measurements, giving reaction rates which are higher than the rates resulting only from the added initiator.

The best technique found to suit these requirements is dialysis. The latex was filtered through glass wool, into a dialysis tube. The filled dialysis tube was placed in a 5 L beaker, containing milli-Q water. The conductivity of the milli-Q water was measured

using an electric conductivity meter. The latex components (like the buffer, unreacted initiator, surfactant, unreacted monomer, aqueous phase oligomers) can move from the latex to the milli-Q water. Latex particles are too big to go through the dialysis tube pores. The process of measuring water conductivity and changing the water was done every 24 hours, except for the first week of the dialysis when it was done twice a day. The conductivity of water keeps decreasing over a period of about 4 weeks. The dialysis of latex was done until the measurement of conductivity gave constant low numbers (a number close enough to the conductivity of milli-Q water) for about one week.

2.3 Determination of the physical properties of the seed latices

Before starting to use the latex in kinetic experiments, some of its physical properties have to be measured. The precise determination of properties is essential, as a minor mistake in the value of any of the physical properties may negatively affect the accuracy of the rate determination and the calculation of $\bar{n}$ to a major extent.

2.3.1 Solids ratio within the latex

Although it is a simple step, the knowledge of the amount of polymer emulsified within the latex is the first step for any calculations. It is important as the value of the solids ratio is required for the calculation of most other parameters required to determine the rate parameters, like C_P^{SAT}, conversion, N_c and $\bar{n}$.

Solids ratio was determined through gravimetry, where a latex sample of known weight is heated until it is dry. This calculation follows the assumption that all solids other than the polymer particles have been removed through the dialysis. Such solids include surfactant, buffer and unreacted initiator. The length of the dialysis period, which was about five weeks for every latex, makes this assumption close enough to be considered true.

2.3.2 Latex average particle diameter

Knowing precisely the average particle diameter is important in identifying the dependence of various parameters on size. As seen in the discussion of the Smith-Ewart model, and in equations calculating the polymerization rate like equation (1.1), the

determination of an accurate value of N_c is very important to calculate $\bar{n}$. Determining $\bar{n}$ accurately is essential, in order to calculate the rate coefficients, ρ, k and c, for all different processes within emulsion polymerization.

Another important parameter related to the different particle diameters is the particle size distribution (PSD). Calculations used throughout this thesis assume that all particles have the same diameter, an assumption which can not be perfect. Nevertheless, the PSD for all latices used throughout this work show they are all very close to monodisperse. The importance of monodispersity comes from the consideration that ρ, k and c are dependent on particle volume.[7]

Particle diameters for the latices were measured with the following three techniques:

a. **Transmission Electron Microscopy.** This is a widely used technique for determination of the size of any particle which can tolerate a high electron flux. Two Transmission Electron Microscopy (TEM) machines were used. One is a Hitachi H600 TEM, which can work at a potential up to 100 kV. Later it was replaced by a Phillips CM200 TEM, which can work up to the higher potential of 200 kV.

   Sample preparation for TEM was done through the use of TEM grids which have been previously coated with a layer of poly(vinyl butaryl) (commercially known as Pioloform®). Depositing the latex particle directly on the plastic film resulted in highly dense samples, making it difficult to see particles clearly. Therefore the latex was diluted with milli-Q water, 1 g latex diluted to around 150 g emulsion. On another coated grid, particles of known particle size were deposited. Both grids are left overnight to dry before being inspected. PMMA deforms under electron beam, so particles were coated with a carbon layer prior to inspection by TEM. TEM images for particles deposited on both grids were taken. Although the TEM determination of size can be taken directly from the images, the instrument must be calibrated for high accuracy. It was found during the course of this work that, if TEM is to be used without calibration, errors can be as high as 15%, (though the error usually was in the range of 4% to 5%).

Images obtained from TEM were analyzed using Image-Pro Plus. Both average particle diameter and PSD were calculated through counting the particles on every image, measuring the diameter as seen on the computer screen, then scaling the number up or down, according to the calibration process. Around 500 particles were measured for every latex. Sample calibration was done using around 40 standard particles.

In all calculations, the number average particle diameter was used. This was calculated from the equation

$$r_{\mathrm{u}} = \frac{\Sigma_{\mathrm{all}\ r}\, r\, n(r)}{\Sigma_{\mathrm{all}\ r}\, n(r)} \tag{2.1}$$

where r is the latex unswollen particle radius and $n(r)$ is the number of particles with radius r. In practice the use of this equation requires defining intervals of finite size Δr. Typically these were 1 nm. There is some discussion about whether it is more appropriate to use the volume-average radius for particle size as the correct mean for calculating N_{c}. This makes little difference where the latex is highly monodisperse, as was mostly the case in this work.

Polydispersity index (PDI) was calculated from the equation

$$\mathrm{PDI} = \frac{\Sigma\left(r_{\mathrm{i}}{}^{2} n_{\mathrm{i}}\right)}{\Sigma\left(r_{\mathrm{i}} n_{\mathrm{i}}\right)} \tag{2.2}$$

This is in analogy with polydispersity index for molar mass distributions. Again, there is some debate as to the most appropriate index of polydispersity for PSD, but the above makes clear the definition used in this work.

Figure 2.3 shows a typical TEM image for latex AN02, the cationic latex used during the course of this project.

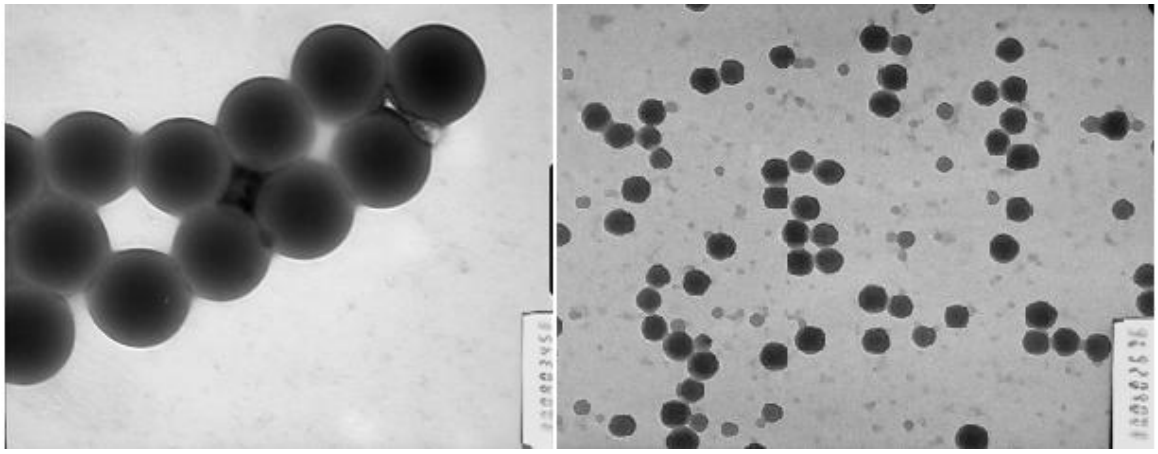

(a) (b)

Figure 2.3. Typical TEM images illustrating the determination of particle size. (a) Image of latex particles with known diameter of 234 nm. (b) Image of latex particles (AN02 in this case) of unknown size taken during same TEM session. By measuring the relative sizes of particles in both images (done using image analysis software), the unknown latex particle size can be accurately determined.

b. Particle Size Distribution Analyzer. Two anionic latices used during the course of this work, including one anionic polystyrene latex and one anionic poly(MMA) latex, were both analyzed by Polymer Laboratories Particle Size Distribution Analyzer (PL-PSDA). The PSDA used in this project is located in the chemistry department, University of Sydney, and it uses "high resolution packed column hydrodynamic chromatography (HDC)".[8] HDC has a few advantages over other techniques: it is fast, equipment is not very expensive, and there is no need for high skill or laborious efforts as in the case of analysis of TEM images.[9]

HDC is a sub-category of size-exclusion chromatography, a technique which was not used with emulsions earlier. The first trials used with the invention of the HDC technique were to separate polystyrene particles from a latex using cation exchange resin particles, and larger particles were found to exit before smaller ones[9]. This formed the basis by which PSDA works.

A major disadvantage for the PL-PSDA used in the course of this work is that it had a tendency to be fouled when it was used to analyze any cationic latex. This is because the lining through which the latex particles pass and get

chromatographically separated cannot desorb the cationic components present within the latex. Therfore, it was only possible to size anionic latices.

The average obtained through the PSDA is the volume average particle diameter. For comparison between diameters obtained through different techniques, this number was normalized to the number average particle diameter.

c. **Dynamic Light Scattering** The dynamic light scattering equipment used in the course of this project utilizes Photon Correlation Spectroscopy. Equipment used was a Malvern Instruments High Performance Particle Sizer (HPPS), which uses a laser beam of 632.8 nm, and its measurement was done at a backscattering angle of 173^{o}. The HPPS equipment is located at the Chemistry Department, University of Sydney.

Dynamic light scattering depends on the fact that particles having a bigger size move slower than those having a smaller size. If these particles are targeted by a vertically polarized laser beam, then the intensity of the scattered light will be equal in all directions.[10] By moving the particles within a fluid medium of known viscosity at a known temperature, and with continuous measurement of the speed of the particle (through the measurement of the intensity of light scattered), the z-average particle diameter can be measured.[10] The z-average particle diameter is the intensity weighted mean hydrodynamic size of the whole group of particles measured by dynamic light scattering.[10]

It is obvious from this procedure that HPPS results may not be highly accurate, especially when polydispersity is very high, or in the case of a mixture of very big particles and very small particles mixed together (like a mixture of particles whose diameter is 2500 nm and others whose diameter is 20 nm). In this case the big particle may overshadow the smaller particles. Although the polydispersity of all latices synthesized during this project was low, HPPS results were just used as an indication of how accurate other techniques are, and were not used by themselves, except when stated.

2.3.3 Intra-particle monomer concentration

C_P^{SAT} is very important property of the latex, which is required in the calculation of conversion and so in the analysis of kinetic data. It is defined as the maximum concentration of monomer within the swollen latex particle.

To describe the monomer concentration within the polymer particle, it can be said that most monomers which can be polymerized through emulsion polymerization have some solubility with the polymer. So in the reaction medium three phases exit together, the monomer, and aqueous phase, and the polymer. From thermodynamics it is expected there will be equilibrium between these three phases. This is reached by mixing the reaction components together, resulting in the monomer moving towards the particles. Polymer particles start to swell, and the particles volume keeps increasing until it can take no more monomer, and the particles are saturated. The concentration of the monomer within the polymer particle is C_P^{SAT}. The value of C_P^{SAT} depends on the thermodynamic balance between the particle's surface energy, and the free energy of solution of monomer within the polymer. As mentioned in chapter I, the moment $C_P < C_P^{SAT}$ is the beginning of interval III, which gives another reason for the need of an exact value for C_P^{SAT}.

A problem with C_P^{SAT} is that it is affected by the particle size and surface characteristics of every latex. So, every latex had its C_P^{SAT} measured individually, through the use of two methods:

a. Static swelling[7,11,12]is the technique which has been used to determine C_P^{SAT} for all the latices made throughout the course of this work. In this method, a seeded emulsion polymerization system is prepared (as described in section 2.4). The dilatometer is filled with latex, monomer and water. To prevent any auto initiation of polymerization, a small amount of 2,6 di-tert,butylphenol was added. The amount of monomer used is chosen to be enough to saturate both water and polymer particles, in addition to excess monomer of about 1 g. The sample is stirred overnight and then the mixture was heated to 50 ^oC (the same temperature at which all kinetic experiments were run). Stirring at this temperature continue for about one hour, to guarantee thermal equilibrium within the emulsion mixture, and to be sure that all particles have been saturated with the monomer. Stirring is

stopped, and heating is continued. After about one hour the aqueous phase and the monomer are separated into two layers, and a narrow capillary tube is inserted at the top of the glass vessel in which the reaction takes place. A very thin polyethylene hose (external diameter about 1 mm) is then passed through the glass capillary then inserted into the emulsion mixture. Water is injected to the mixture very slowly, so the monomer phase ascends within the glass capillary. The hose is then taken out, and a mark is made on the external side of the glass capillary at the top and bottom of the monomer layer. The length of the monomer layer is measured using a vernier caliper. Knowing the internal diameter of the capillary used, and the length of the monomer layer, the mass of excess monomer can be calculated via its density.

The mass of monomer in the latex particles m_P can be calculated as the total mass of monomer added at the beginning m_M^0, minus the sum of the excess monomer m_M^{excess}, and the monomer dissolved in water.

$$m_P = m_M^0 - m_M^{excess} - C_W{}^{sat} V_W M_0$$

$C_W{}^{SAT}$ is the saturation concentration of monomer in the water in mol/L, V_W is the volume of the aqueous phase, M_0 is the molecular weight of the monomer.

Knowing the mass of monomer which is present in the swollen particles, the concentration can be calculated by dividing the total mass of monomer present in the particles by the total volume of swollen particles:

$$C_P{}^{SAT} = \frac{m_P/M_0}{\frac{m_P}{d_M} + \frac{m_{particles}}{d_P}} \qquad (2.3)$$

$m_{particles}$ is the total mass of particles added with the seed latex at the beginning of the experiment, d_M is the density of monomer and d_P is the density of polymer. Equation (2.3) assumes ideal mixing of monomer and polymer in the particle.

There is one minor disadvantage of this method, which is that it assumes volume

additivity, and so any changes of volume happening because of the mixing are neglected. By having a deeper look at the monomers used in this project, it is found that both of them have low solubility in water (details about solubilities of styrene and MMA in water are in chapter IV and VI), moreover no data is available for the density of the monomer when dissolved within the polymer. That makes the volume additivity assumption inevitable.

Note also that C_P^{SAT} is independent of CD concentration in the aqueous phase. Previous work done on CD usage in emulsion polymerization did not mention any change of monomer solubility in the particles with the addition of CD. Knowing that CD role is only played in the water phase, and that CD is not involved in the inter-particle monomer presence, CD was not used in any of the C_P^{SAT} determination experiments.

The kinetic method is another technique used for determination of C_P^{SAT}. Based on equation (1.1), it is clear that the rate of the reaction (expressed as dx/dt) is proportional to the value of C_P. During interval II C_P is constant, and so the rate of the reaction will remain constant, and as for many emulsion polymerization systems other variables like $\bar{n}$, N_c and k_p remain constant during interval II.

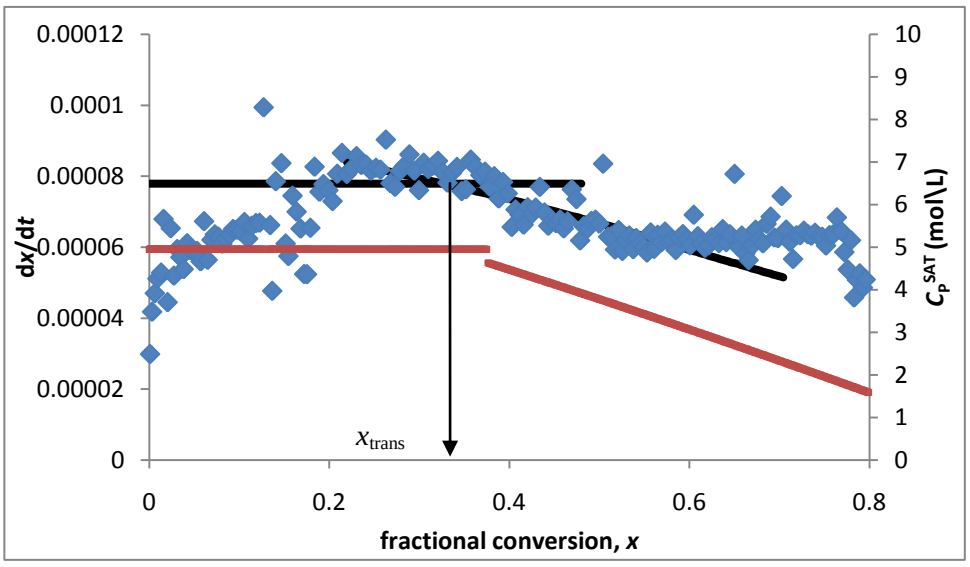

(a)

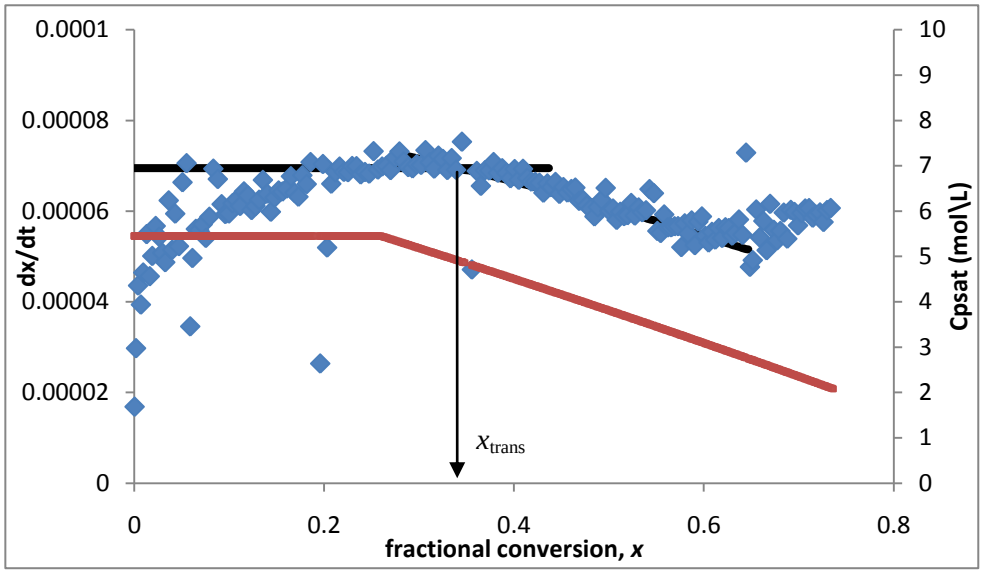

(b)

Figure 2.4. Showing experimentally measured rate of polymerization (blue dots and black lines) and calculated C_P (red lines, using C_P^{SAT} from static swelling experiments with the same latex) experiments (a) SNT27 and (b) SNT28 with latex AN01. The point where the rate begins to decline, as indicated by x_{trans}, may be used to estimate C_P^{SAT}: this is the so-called kinetic method. It is evident that (a) yields C_P^{SAT} less than the static method, while (b) yields it greater. This shows the unreliability of the kinetic method, which should only be used as a crosscheck of the more accurate values from the static swelling method.

The situation changes when interval III starts: C_P starts decreasing, so dx/dt will also decrease. The instant at which the system moves from interval II to interval III can be considered a transition point, at the point the value of Cp will start to depend on the conversion x_{trans}, and C_P^{SAT} can be calculated as follows:[7]

$$C_P^{SAT} = (1 - x_{trans}) \frac{m_P/M_0}{\frac{m_P}{d_M} + \frac{m_{particles}}{d_P} + x_{trans} m_M^0 \left(\frac{1}{d_p} - \frac{1}{d_M}\right)} \quad (2.4)$$

The similarity between equation (2.3) and (2.4) is clear, and so any assumptions of volume additivity mentioned in the static swelling method are also inevitable in the kinetic method.

Another disadvantage of this of this method is that it assumes $\bar{n}$ is constant

throughout interval II. While this can be the case with systems like styrene, this technique cannot be used with systems like MMA, where the value of $\bar{n}$ keeps increasing over the range of interval II because of the Trommsdorff-Norrish effect, which will make identifying x_{trans} a real problem.

Figure 2.4 shows a major disadvantage of this method, as the exact point of x_{trans} is not easily identified from the graph, having a series of dots like the one shown in the graph makes it very hard to precisely indentify x_{trans}. Moreover, a comparison between figures 2.1a and 2.1b shows that C_P^{SAT} resulting from this method fall within a range from the value of the value of C_P^{SAT} as found through experiments. It is clear that any unpredictable change for any of the parameters affecting the experiment can have a major impact on the value of C_P^{SAT} resulting from this method. Although the method has been tried with some polystyrene experimental data, the values used for C_P^{SAT} for all experiments in this work were only those obtained from the static swelling method.

2.4 Dilatometry

Throughout the course of this work, the technique mostly used was dilatometry. Dilatometry is based on the fact that the density of the monomer is usually less than that of the polymer. Consequently, during an emulsion polymerization, the total volume of the system will keep decreasing as the reaction proceeds. Monitoring this change in volume is the rationale behind dilatometry.[13] A dilatometer has to have accurate temperature control and correct data measurement.[14] With such requirements, in order to obtain accurate dilatometric measurements a number of factors have to be very precisely known, such as the exact volume of monomer, polymer and total volume at the beginning of the reaction and at any moment during it, the temperature of the reactor, and density-temperature relationship for monomer, polymer and water.[14] To reduce the number of variables required, all experiments were run at the same temperature, and temperature control was used in all experiments, as will be shown shortly.

Dilatometry has a few advantages over other techniques. As an on-line technique, it can be followed while the experiment is taking place. This is a very good advantage, as it is easy to notice when there is a leak, and so the leakage problem could be fixed at the

earliest step of the experiment before the polymerization starts. Having the capability of seeing the results on the computer screen while the experiment is running was also helpful to determine whether there was any mistake during the preparation of the experiment, in case the initiator was not added for example or the stirring was not turned on at the beginning. Correcting such mistakes would be certainly good for the experiment.

During the course of this work, two dilatometers have been used. One of them (Figure 2.5) was used for experiments which involved the use of chemical initiator or thermal initiation, which all took place at the University of Canterbury. Another dilatometer was used with γ-radiolysis experiments, which all took place at the Australian Nuclear Science and Technology Organization (ANSTO) at Lucas Heights, Sydney. Both pieces of equipment were used together to run more than 600 dilatometry experiments done during the course of this work.

2.4.1 Dilatometry experiments: preparation

Before every kinetic experiment, the reactants have all to be mixed together in the dilatometer reaction vessel. In order to start in interval II, the seed latex, which has already been prepared and dialyzed, has to be added to the reaction vessel. Monomer and surfactant are also added, and the glass dilatometer vessel is filled with water, except for about 3 cm^3 near the top which are left empty at this stage, in order to accommodate for the thermal expansion of the aqueous medium and the addition of the initiator, which is added in the form of an aqueous solution.

Four dilatometer vessels (figure 2.5) were used during the course of this work. The volume of the void where the reaction takes place is in the range of 57-60 cm^3. In addition to these, four other dilatometer vessels were used for the experiments done at ANSTO. Both types have the same characteristics except that the ANSTO vessels are smaller, 27-36 cm^3, so that they can be inserted within the narrow space of the ^{60}Co unit as will be explained. All vessels are made out of two parts:

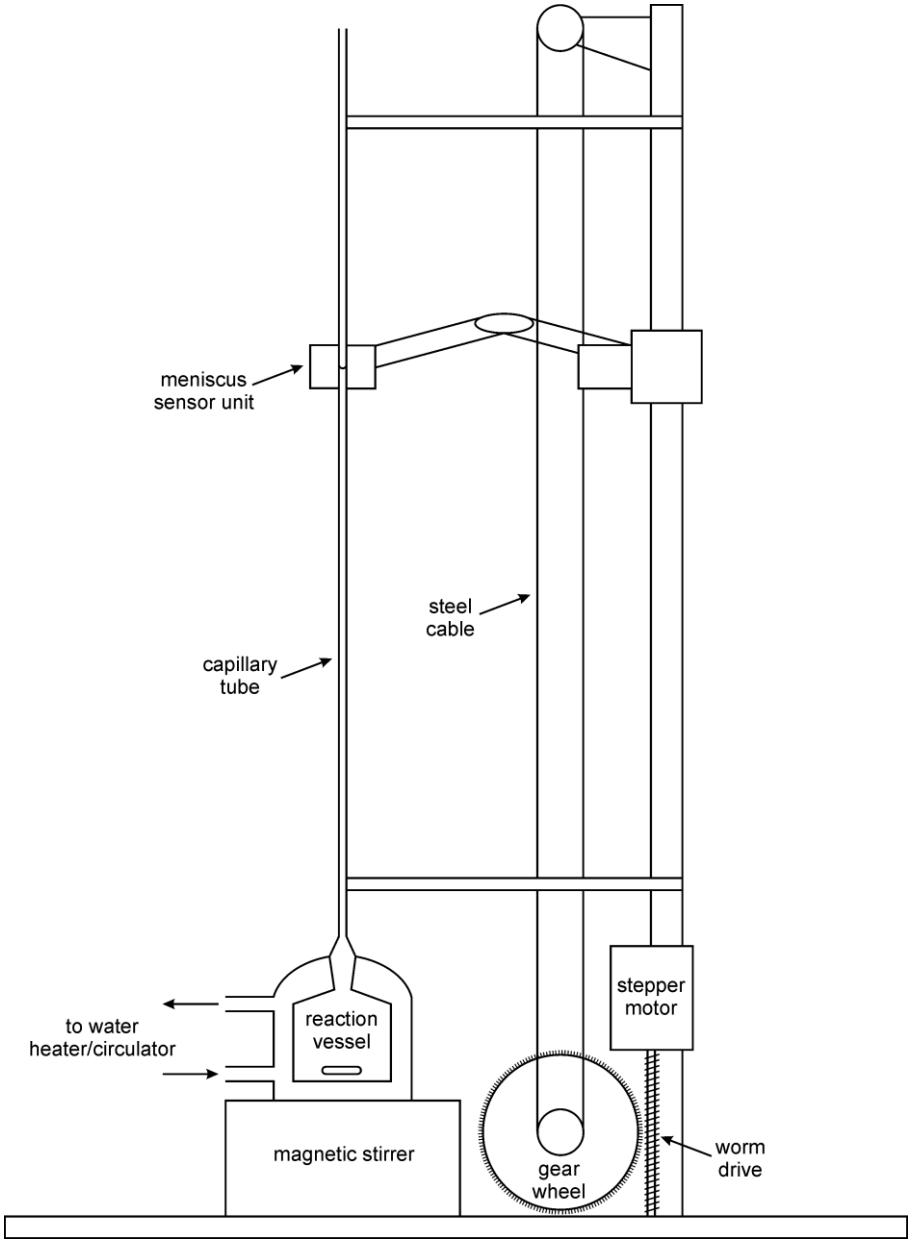

Figure 2.5. Schematic illustration for the dilatometer used at the University of Canterbury.

1) The internal part is a glass bulb, which is where the reaction occurs. The top of this bulb has a conical form, at which the bottom of the capillary can be placed after the preparation for the experiment. During the reaction, this bulb contains all the chemicals mentioned above, in addition to a magnetic flea.
2) The external part of the reaction vessel is a jacket with an inlet and outlet glass pipes connected to it. The inlet is connected to a water heater through a thermally isolated plastic pipe, and it keeps pumping water at 50^{o}C (or any other desired temperature) as long as the reaction is being run.

The dilatometer vessel is placed above a stirrer which is kept running at a constant speed for the whole experiment, to make sure the reaction vessel components are thoroughly mixed. Components are left stirring overnight, and the capillary top is closed with a glass stopper, to avoid any monomer loss due to evaporation.

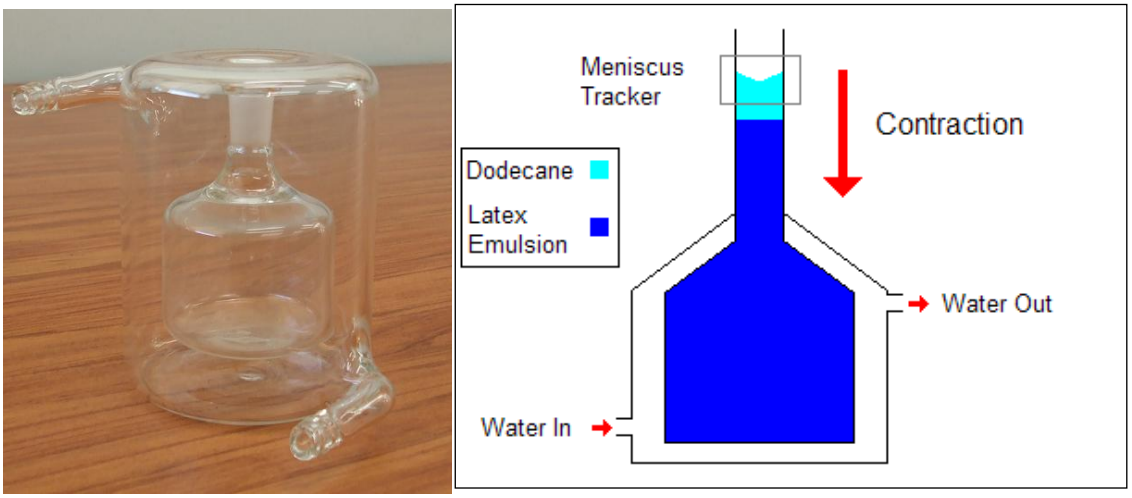

(a) (b)

Figure 2.6. (a) picture of the dilatometer vessel, and (b) schematic view of the dilatometer vessel during kinetic experiments.

In experiments involving use of CD, the monomer-CD complexation is done through stirring. The required amount of CD is added to the mixture, and the overnight stirring ensures that complexation takes place.

2.4.2 Dilatometry: kinetic experiments

Before the experiment starts, vessel components are to be degassed in order to avoid any retardation due to the presence of oxygen.[15] The degassing was done by heating the vessel to 60 ^{o}C. The glass stopper is removed and replaced by the degassing glass tube, which is mainly a vacuum tap connected to the vessel by a ground glass joint and having a rubber suva seal at the end. A needle is inserted through the suva seal and a 5mL glass syringe is used to suck the air to outside. Evacuation is repeated until the monomer starts to boil, which ensures that the mixture has been degassed.

After degassing the reaction mixture, the water which is to be added is also degassed.

This is done by placing this water into a round-bottom flask under vacuum, and while the vacuum pump is running, boiling water is passed around the round-bottom flask. The water boiling ensures it has been degassed, and then it is placed into a glass syringe.
When the experiment is ready to start, the vacuum tap is removed from the top of the dilatometer vessel, the initiator solution is injected, then the capillary tube is placed at the top of the vessel. Previously degassed water is then injected through a polyethylene hose (external diameter about 1 mm), filling any space within the vessel which is still void with air, then filling the glass capillary to a height of about 60 cm. A layer of dodecane with thickness of about 4 cm is injected into the capillary above the degassed water. The tracker, which will be described shortly, follows the dodecane meniscus down as it moves, because of the continuous contraction of the monomer as it converts to polymer. After this procedure is completed, the tracker is ordered to follow the meniscus, and stirring starts. Stirring is very important to avoid inhomogeneities, for example in initiator concentration, a problem which eventually happened during the course of the work as in one of the styrene experiments stirring was unintentionally not started at the beginning, and a nonlinear increase of conversion with time was obtained for that experiment, which could be because of the lack of stirring. Such experiment was not considered in the analysis of the experimental results.

2.4.3 Dilatometry: tracker

The main role of the tracker is to provide the exact details regarding the movement of the dodecane meniscus with time. The tracker has a solid metallic base, over which the tracker motor is fixed and the magnetic stirrer is placed during experiments. The tracker motor is connected to the meniscus sensor (Figure 2.7), which is attached to the base through a very smooth stainless steel rod.

Before the experiment is started, the tracker is calibrated using a glass capillary which includes a stainless steel bar whose length is exactly 10 cm. This calibration gives the "step length" the tracker takes in moving for that day; this is necessary because the current intensity from the power line changes from day to day, resulting in changes of step length in the range of $\pm$ 5%. The step length can be defined as the number of steps the tracker moves through the 10 cm length, the effect of changes of the ambient temperature on the length was neglected. In all the experiments done the tracker never

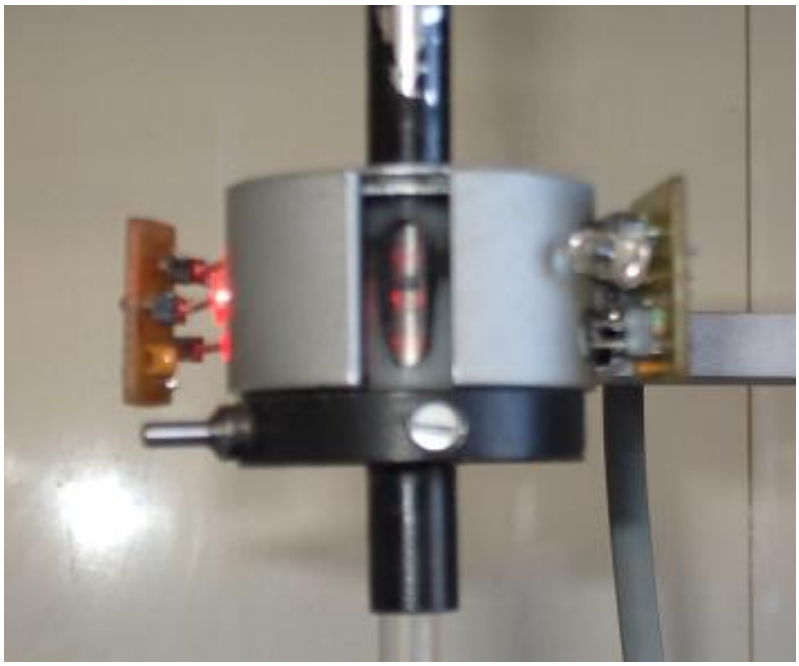

Figure 2.7. Picture showing the meniscus sensor used to track the height of the liquid column in the dilatometer, which can be seen in the centre of the photograph. Light enters from the left and is detected by the array on the right.

counted less than 190,000 steps over the 10 cm, which means that the maximum length of one step was 5.23 x 10^{-4} mm. With such very small steps, measurement of the meniscus movement was ensured to be very accurate. By far the larger source of error is due to meniscus position not being so precisely identifiable.

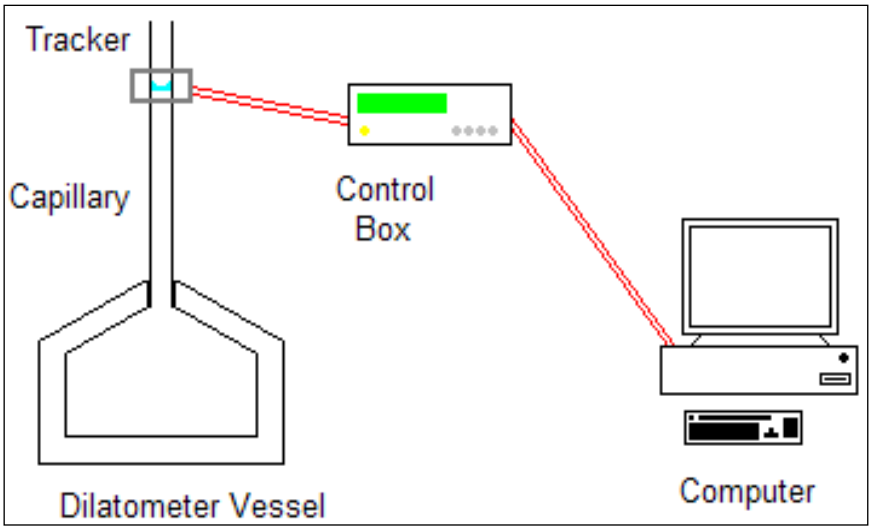

Figure 2.8. Schematic of the experimental set-up for automated dilatometry.

The meniscus sensor is controlled through a control unit connected to a computer (Figure 2.8). From the control unit the tracker was calibrated, then after setting up the experiment and injecting the dodecane into the glass capillary, commands were given through the computer for the meniscus sensor to follow the meniscus over specific periods of time, 20 seconds for initiator initiated and γ-radiolysis experiments, and 60 seconds for spontaneously initiated experiments. Tracker movement was recorded for every period, and by the end of the experiment the computer gives a table having two long columns, one for time and the other for number of steps the sensor moved. A more detailed description for the tracker has been previously written elsewhere.[16]

2.4.4 Equipment calibration

In addition to the calibration of the tracker before every experiment, specific characteristics of two types of equipment had to be calibrated; the volume of each dilatometer vessel and the radius of each capillary tube.

Calibration of the dilatometer vessel was a straight-forward process. The vessel was weighed on a scale, filled with milli-Q water then weighed again. Knowing the temperature at the time of measurement, the volume of water, which is equal to the volume of the vessel in this case, can be calculated:

$$V_{\text{vessel}} = \frac{m_{\text{wv}}}{d_{\text{water}}}$$

where m_{wv} is the mass of water within the dilatometer vessel, and d_{water} is the density of water at the ambient temperature.[17]

Calibration of the capillary tube was a more complicated process. The very small diameter of the capillary tube makes the use of water or any other material having a density similar to or lower than water, very hard to obtain highly accurate results. In addition, most liquids have low surface tension, which will result in having some liquid attached to the capillary wall when empty, not to mention possible bubbles when the capillary is full.

Mercury was found to solve these two problems, with its high density and high surface tension. Determining the diameters of capillaries having very small diameters (less than 2mm) was not a very hard problem to solve. The calibration was done through the tracker. First the tracker was calibrated as mentioned above, then the capillary is mounted on the tracker and a small vial containing about 80 grams of mercury, which was previously weighed, was placed at the bottom of the capillary. Then a syringe whose needle was replaced by a rubber hose was placed at the top of the capillary, so that the rubber hose surrounds the external side of the capillary for the length of about 1 cm. The syringe was used to suck the mercury within the capillary. After the mercury column is stable and not moving within the capillary, the mercury vial is removed from the bottom and weighed. The difference from the initial weight gives the weight of mercury column m_{Hg} The tracker was used to count how many steps the length of the mercury column represents. The length of the mercury column l_{Hg} present within the capillary is thus determined. Knowing the density of mercury d_{Hg},[17] the radius of the capillary can be calculated as:

$$r_{\mathrm{cap}} = \sqrt{\frac{m_{\mathrm{Hg}}}{\pi l_{\mathrm{Hg}} d_{\mathrm{Hg}}}}$$

2.4.5 Data Analysis

In the case of styrene, its solubility in water is 4.3 mM at 50 ^{o}C,[7] which can be considered negligible. Consequently, calculating conversion for styrene experiments was a straight forward process. From the data of time and steps obtained from the tracker, the conversion at any moment can be calculated as follows:

$$x = \frac{\pi {r_{\mathrm{cap}}}^2 \Delta h}{m_{\mathrm{M}}^0 \left(\frac{1}{d_{\mathrm{M}}} - \frac{1}{d_{\mathrm{P}}}\right)}$$

where Δh is the change in height as calculated from number of steps moved, according to the tracker calibration on the day of the experiment. In all calculations, Δh is always associated with the movement downward. In the calculations, monomer conversion to polymer was considered to be the only reason for volume contraction. This directly implies that all other reasons for volume change, like bubble formation and thermal

instability, have been certainly controlled through a very good control over temperature from the water bath, and the absence of any bubbles during the course of every experiment.

It is good to mention here that the decomposition of V-50 yields nitrogen gas, but during all interval II calculations the conversion increased linearly with time, highlighting the negligible amount of nitrogen gas formed, otherwise the formation of bubbles would have disrupted this linear relationship or even resulted in an expansion for the reaction medium volume. It can then be assumed that all formation of nitrogen bubbles took place during interval III, which was not considered in the calculations for this work.

But when calculating the conversion for MMA, calculations are much more complicated. This is because of the relatively high solubility of MMA in water, 0.15 M at 50 ^{o}C,[7] coupled with its non-ideal mixing in water. This means that there is volume change in the system as the total amount of MMA in the aqueous phase changes, it having different specific volumes in the water and latex-particle phases. This contribution must be accounted for in determining the conversion of monomer into polymer via dilatometry, which of course delivers only the total volume change for the system. The algorithm used for doing this was developed by Ballard et al.[11] Conversion was calculated by solving the following equations iteratively:

$$x = \frac{\pi {r_{\text{cap}}}^2 \Delta h + ({m_{\text{W}}}^0 - m_{\text{W}})\left(\frac{1}{d_{\text{M}}} - \frac{1}{d_{\text{M,aq}}}\right)}{m_{\text{M}}^0\left(\frac{1}{d_{\text{M}}} - \frac{1}{d_{\text{P}}}\right)} \tag{2.5}$$

$$C_{\text{P}} = \frac{x m_{\text{M}}^0 / M_0}{\frac{m_{\text{M}}^0(1-x) - m_{\text{W}}}{d_{\text{M}}} + \frac{m_{\text{particles}} + m_{\text{M}}^0 x}{d_{\text{P}}}} \tag{2.6}$$

$$\frac{C_{\text{W}}}{{C_{\text{W}}}^{\text{SAT}}} = \left(\frac{C_{\text{P}}}{{C_{\text{P}}}^{\text{SAT}}}\right)^{0.6} \tag{2.7}$$

where C_{W} is the monomer concentration in water, m_{W} is the mass of monomer in water, ${m_{\text{W}}}^0$ is the mass of monomer in water at the beginning of the experiment and $d_{\text{M,aq}}$ is the density of the monomer dissolved in the water, a quantity which was not used at all in the calculations done for the conversion of styrene. m_{W} can be calculated from:

$$m_{\mathrm{W}} = C_{\mathrm{W}} V_{\mathrm{W}} M_0$$

where V_{W} is the volume of the aqueous phase in water.

Solving equations (2.5), (2.6) and (2.7) iteratively yields the values of conversion for every period at which the dilatometer reading was recorded. From the data of conversion and time, other kinetic parameters can be calculated.

At the end of every experiment, the vessel components were inhibited with hydroquinone to prevent any more conversion taking place, and a sample of this product was analyzed through gravimetry to calculate its solids ratio. From calculated and original solids ratios the conversion can be calculated. This was used as crosscheck to ensure that conversion calculated from the dilatometry data is true, and that problems like monomer leakage have not been encountered during the course of the experiment.

2.5 γ-radiolysis kinetic experiments

Initiation with γ-radiolysis has a major advantage over chemical initiators. In cases where KPS or V-50 were used, once the initiator is added there is no way to stop its effect without affecting the experiment itself, which makes calculating exit and termination rates very hard from experiments in which chemical initiator is used.

This problem was solved by using the γ-radiolysis equipment at ANSTO, Figure 2.9, which is mainly a hollow cylinder of ^{60}Co continuously emitting γ rays with a dose rate of 1.18 Gy/min. The ^{60}Co cylinder was surrounded from all directions with lead to prevent any radiation leak.

The experiment starts by having the dilatometer vessel lowered with an electric motor, enabling it to be exposed to the γ rays, so initiation takes place, the vessel remains in the source for about 10 to 15 minutes as desired, then it is raised away from the radiation for a period of about 30-40 minutes as desired, enabling the reaction rate to relax. From the relaxation rate data, exit and termination rates can be calculated.

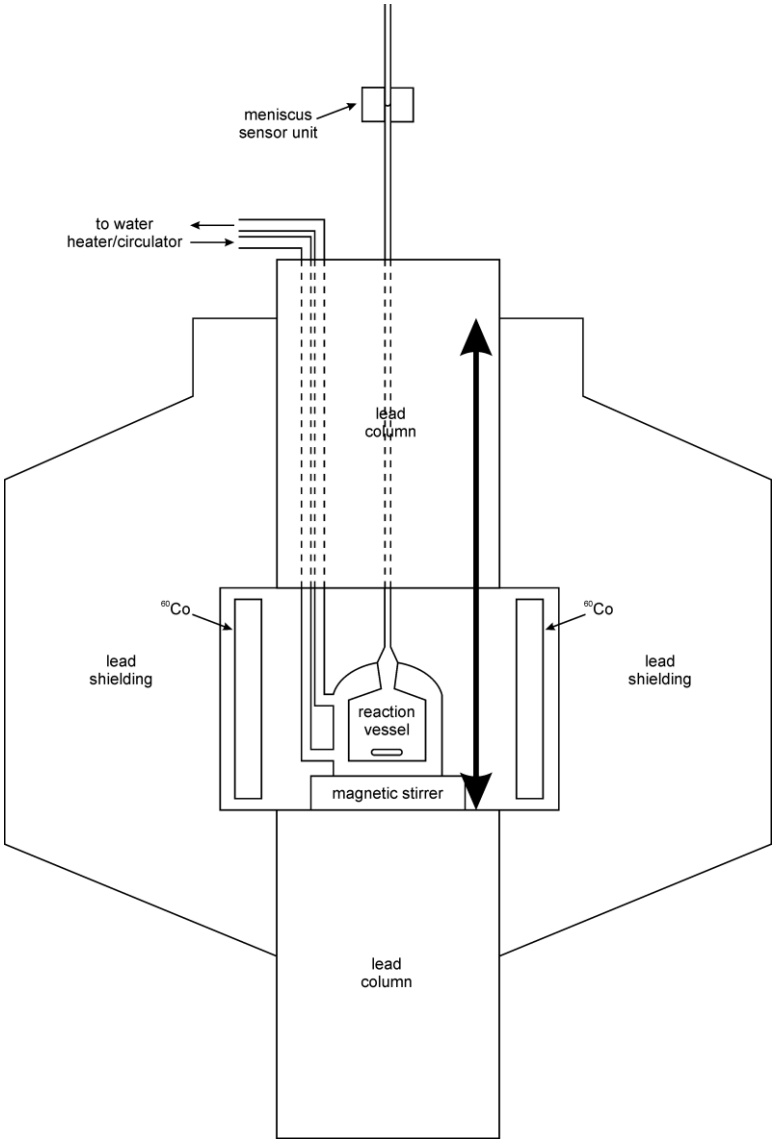

Figure 2.9 Schematic diagram for the γ-radiolysis equipment used in ANSTO.

2.6 Monomer solubility measurements

These experiments were not originally planned to be done as part of this project. They were first thought about to solve the question of why CD in some experiments and under some conditions does not speed up the reaction, to the contrary it was even found to slow down the reaction under specific conditions. The most logical explanation for this is that CD, under such conditions, did not act to increase the monomer solubility. To the contrary, CD in such situations reduces the monomer solubility.

This assumption has been already made in previous work,[18] that surfactant and monomer compete for CD cavities, but this is the first time such assumptions have been verified experimentally.

Solubility measurement experiments were all done using a Varian Cary 100 Bio UV-Vis spectrophotometer. UV is good at detecting multiple bonded and heteroaromatic compounds. [19] The spectrophotometer uses wavelength of 200-800 nm. Earlier experiments on styrene showed that it has a peak wavelength very close to 248 nm, and MMA has its peak wavelength at 203 nm. Both wavelengths are in range.

The solubility measurement itself was not direct. This is because the solubility of both monomers used during the course of this work was high compared to the maximum concentrations the spectrophotometer can detect. So the measurement of solubility was done on a few steps. First, a mixture similar to the seed latex kinetic experiments mixture was prepared within one of the dilatometer vessels. This includes stabilized monomer, water, and may include surfactant and/or CD, depending on the conditions required. Seed latices were not used in any of the solubility experiments. Although the lack of seed latices might have made the situation not exactly the same, but having any seed latices in the mixture with monomer (even if the monomer was stabilized with hydroquinone as in the case of this part of the work) would have resulted in particle swelling. Consequently, measuring the solubility in this case would have included both the monomer dissolved within the latex particles and that dissolved in the aqueous phase. For this reason, all solubility measurements experiments did not include the use of any latex particles prepared earlier; they were purely on aqueous phase.

Another variable to be decided here is the amount of surfactant. First, the amount of surfactant used in any kinetic experiment was not exactly known. This is because some of the surfactant remained with the latex even after the dialysis. Second, not all the surfactant remains in the aqueous phase in the form of micelles, as some of it gets adsorbed on the latex particles. And as long as the amount of surfactant adsorbed is unknown, the amount of surfactant in the aqueous phase is also unknown.

The amount of surfactant used, following the concept of imitating the kinetic experiments, was the same amount of surfactant which was added to the mixture used in preparing all kinetic experiments. This is based on the assumption that the surfactant adsorbed on the latex particles was not removed during the dialysis, and that dialysis removed only the aqueous phase surfactant. Consequently, all surfactant added to the kinetic experiments

remains dispersed in the aqueous phase, and this was the situation followed during solubility measurement experiments including surfactant.

After mixing all the components together for enough time at 50 ^{o}C, the mixing was stopped and the mixture stood still for about one hour, in order to make sure that all monomer which was not dissolved in the water went out of the aqueous phase. Then two ml of the aqueous phase were taken with a syringe and diluted to 200 mL in a volumetric flask in order to obtain reasonable absorbances. The absorbance of this solution was measured and recorded using the spectrophotometer.

Using a previously prepared calibration line of a monomer/water mixture, as shown in figure 2.10, the exact amount of styrene within the diluted solution can be calculated. From which the amount of monomer in the aqueous phase, which is C_W^{SAT} at those conditions, can be calculated with very low error.

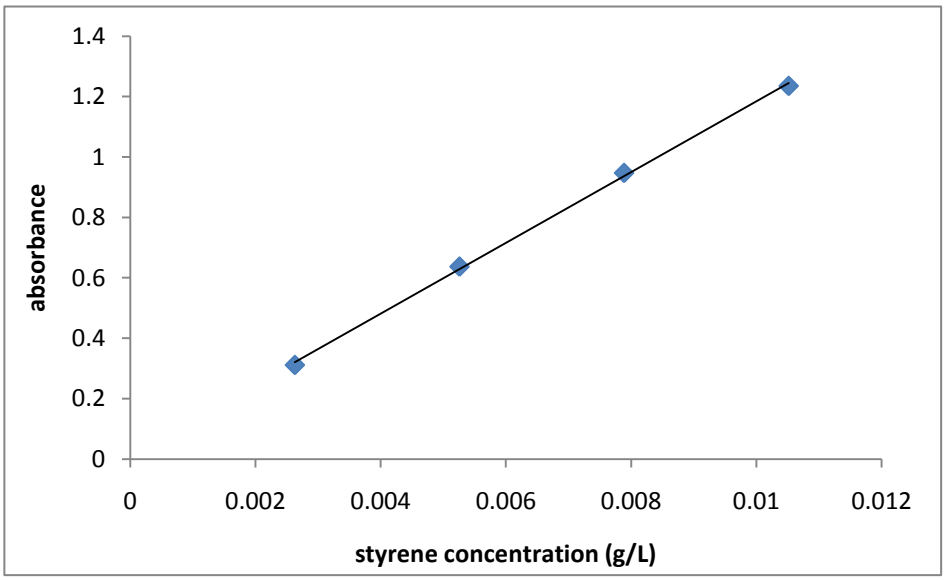

Figure 2.10. Calibration line for absorbance at 248 nm of solutions of styrene in water. Clearly there is a linear (Beer's law) relationship.

References

(1) Stickler, M. and Meyerhoff, G., *Makromol. Chem.*, **1978**, 179, 2729.

(2) Szejtli, J., *Chem. Rev.*, **1998**, 98, 1743

(3) Easton, C. and Lincoln, S., *Modified Cyclodextrins*, **1999**, Imperial College Press, London.

(4) Hu, J., Huang, R., Cao, S. and Hoa, Y., *e-polymers*, **2008**, 171

(5) Dahlstrom, D. *et al*., *Liquid Solid Operations and Equipment*, in Perry, R., Green, D. and Maloney, J., *Perry's Chemical Engineer's Handbook, Seventh Edition*, **1999**, McGraw-Hill, New York.

(6) Ferguson, C. J., *Core-Shell Polymers from Styrene and Vinyl Acetate for Use as Wood Adhesives*, PhD thesis, **2000**, University of Canterbury.

(7) Gilbert, Robert G., *Emulsion polymerisation, a mechanistic approach*, **1995**, Academic Press, London.

(8) Polymer Laboratories Ltd., now a part of Varian Inc., *PL-PSDA Operator's Manual*

(9) Small, H. and Langshort, M., *Anal. Chem.*, **1982**, 54, 892.

(10) Malvern Instruments, DLS Technical Notes.

(11) Ballard, M., Napper, D., and Gilbert, R., *J. Polym. Sci. Polym. Chem. Edn.*, **1984**, 22, 3225.

(12) Halnan, L., Napper, D. and Gilbert, R., *J. Chem. Soc. Faraday Trans.1*, **1984**, 80, 2851.

(13) Lovell P.A., and El-Aasser M.S. (editors), *Emulsion polymerization and emulsion polymers*, German L. Anton *et al*., *Latex Polymerization Characterization*, **1997**, John Wiley and sons, New York.

(14) Sudol, E., El-Asser, M., Micale, F. and Vanderhoff, J., Rev. Sci. Instrum., **1986**, 57, 2332.

(15) De Bruyn, H., Gilbert, R. and Hawkett, B., *polymer*, **2000**, 41, 8633.

(16) van Berkel, K., *Entry and the Kinetics of Emulsion polymerization*, a PhD thesis, University of Canterbury, 2004.

(17) Lide, D.(editor), *Handbook of Chemistry and Physics*, **2005**, Taylor and Francis, Florida

(18) Hu, J., Li, S. and Liu, B, *Journal of Polymer Material*, **2005**, 22, 213.

(19) Furniss, B., Hannaford, A., Smith, P. and Tatchell, A., *Vogel's Textbook of Practical Organic Chemistry*, 1989, Longman Scientific and Technical, Essex, England.

Chapter III

Effect of Cyclodextrin on the γ-Radiolysis Initiated Emulsion Polymerization of Styrene

3.1 Introduction

As one of the earliest monomers historically utilized in commercial emulsion polymerization, styrene is also one of the most widely studied monomers academically. Kinetic studies can be easily done for styrene because many of the rate parameters related to its emulsion polymerization have already been determined. However, establishing such parameters in the presence of small amounts of cycodextrins (CD) has never been published before. This chapter outlines the kinetic effect of the presence of CD, especially on the entry and exit rates of free radicals to and from latex particles, during Interval II of the emulsion polymerization of styrene.

It has been proven that the Maxwell-Morrison model for entry[1] has been validated through the work done by other researchers.[2,3] This work done by Maxwell and Morrison was validated only through the use of a latex stabilized anionically, and KPS was the only initiator used by them. More work was done later by van Berkel, which included the use of four polystyrene systems. Two were anionically stabilized and the other two were cationically stabilized.[2,3] In each case two initiators were used in the mentioned work, one being KPS, the initiator mostly used in emulsion polymerization experiments, and the other 2,2'azobis(2-methylpropionamidine)dichloride, known as V-50. The mentioned work also included the use of γ-rays as an initiation technique. This chapter concentrates on the γ-radiolysis experiments done with styrene. Details about chemically initiated experiments will be given in Chapter IV.

Cyclodextrins (CDs) can be briefly defined as cyclic oligosaccharides, formed of a number of glucopyranose units.[4] Because of their semi-natural and environmentally friendly characteristics, they are produced in huge amounts every year and sold for very cheap prices.[5] CDs have a truncated conical shape with a cavity in the middle, according to X-ray crystallography.[6] The internal side of the molecule is hydrophobic, while the

exterior is hydrophilic.[7] Consequently, a molecule with this form will increase the monomer solubility in water, which will increase the rate of the polymerization of styrene, as was found previously under specific conditions.[8]

CD has also been used in other research on emulsion polymerization, like the work done by Hu[9] and by Ritter *et al.*[10]. However no research has been done previously on the effect of CD on the kinetics of the emulsion polymerization of styrene using γ-radiolysis. As per the current available knowledge there is only one paper about the kinetics of the aqueous phase polymerization of styrene in presence of methyl-β-CD using 2,2'-azobis[N,N'-dimethyleneisobutyramidine] dihydro-chloride as initiator.[11] Moreover, there is no previous research done on the effect of the presence of CD on the entry and exit rates of free radicals to and from particles.

3.2 Theoretical Background

Before discussing the details of the γ-rays and their effect on the initiation reaction, it is useful to highlight the presence of another method of initiation, which takes place and eventually causes the polymerization reaction to start even without the use of initiator or γ-radiolysis.

3.2.1 Thermal initiation and entry

It was first found by Mayo[12] that styrene can polymerize either as bulk polymerization or in a solution of styrene in bromobenzene, in the lack of any initiating medium. A similar behavior was found in emulsion polymerization by Hawkett *et al*[13]. As seen in equations (1.42) – (1.46), thermal entry represents a non-negligible part of the entry rate in the emulsion polymerization process, as the thermal entry was found to correspond to the effect of the presence of 10^{-5} mol/L initiator concentration,[13] if the reaction is run at 50 ^{o}C and the average particle diameter is 50 nm (this was during a series of experiments when 10^{-3} mmol/L KPS was the concentration used for a typical run). Thermal entry was found to increase significantly with larger particles.[14]

The exact reason behind the thermal initiation for styrene is not certainly defined, but recent research[15] suggested that the Diels-Alder dimer of styrene is the most important

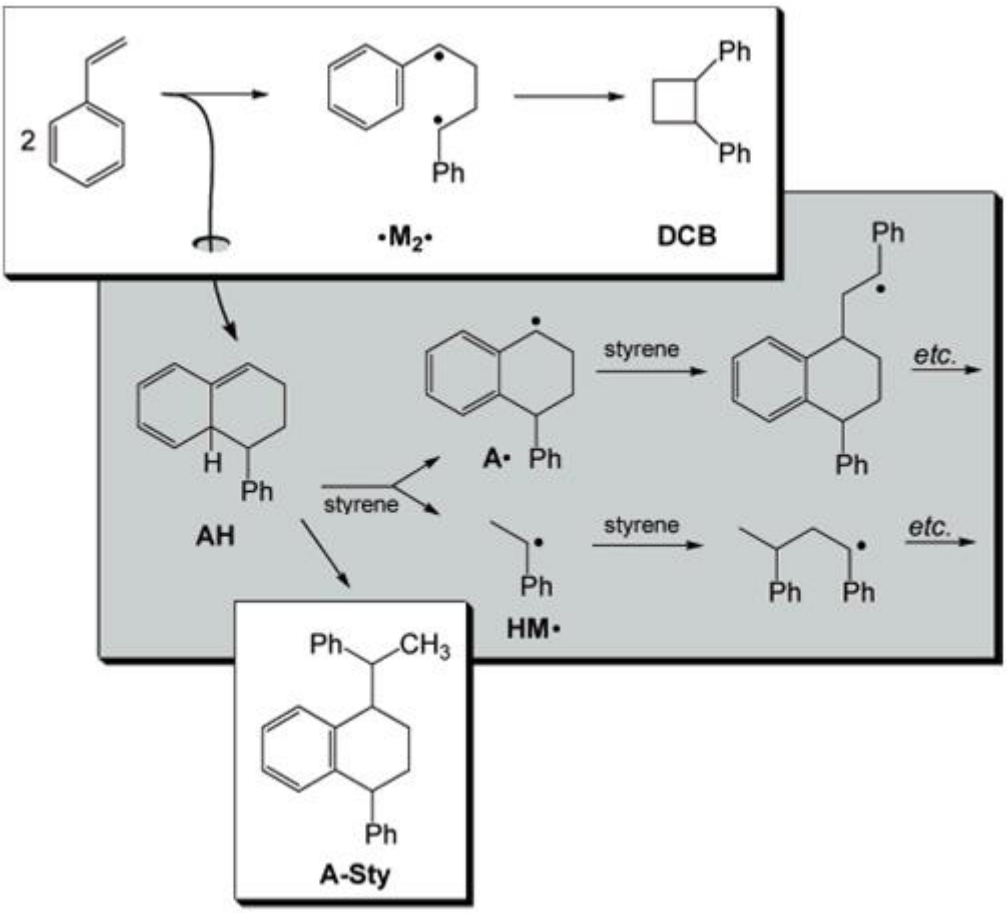

Scheme 3.1. Suggested mechanism for thermal polymerization.[15] AH denotes the Diels-Alder dimer of styrene.

intermediate. It reacts spontaneously to form a free radical, though the side reaction of the formation of diphenylcyclobutane (DCB) also takes place. Through the thermal dimerization reaction the dimer becomes the free radical (together with a monomeric free radical), which can start the initiation process. With the continuous presence of the free radical within styrene, or within the seeded emulsion polymerization mixture (which was described in more detail in chapter II), polymerization starts and continues at a very slow rate. Other reactions of the polymerization process are to be discussed shortly.

It is very important to obtain accurate data for the reaction rate in the lack of any initiating medium; this is because the (total) entry rate coefficient ρ is calculated from the equation:

$$\rho = \rho_{\text{thermal}} + \rho_{\text{initiator}} \tag{3.1}$$

The equation shows that the value of $\rho_{thermal}$, though usually low, still has an impact on ρ, and the effect of $\rho_{thermal}$ has to be deducted from the total value of ρ obtained experimentally, in case ρ is to be used in calculating the entry efficiency for chemically initiated experiments (as will be thoroughly discussed in chapter IV), or the entry and exit rate coefficients in case of γ-radiolysis experiments.

3.2.2 Initiation through γ-radiolysis

The source from which γ-rays are emitted is the nuclei of some metal isotopes, as these nuclei move down from an excited state to a lower energy state.[16] In some cases this happens through β-decay, which can be explained as the emission of a negatron or a positron from the nuclei.[17] This is the case of ^{60}Co, the source of γ-rays used during the course of this work.

A number of chemical reactions are considered to be "radiation-induced" reactions; two famous examples are the production of ozone from oxygen and the production of nitrogen dioxide from a mixture of oxygen and nitrogen.[5] Both are done through irradiation of the reacting gases. γ-radiolysis is also used to transfer monomers into free radicals, a technique through which the initiation process can take place.

A common factor between thermal initiation and γ-radiolysis is that in both cases a chemical initiator of known concentration is not present. Consequently, equations (1.11)-(1.32), and any other equation which deals with the chemical initiator cannot be used in this case. Otherwise, for both thermal initiation and γ-radiolysis cases the reaction sequence is as follows:[18]

Initiation: $M \longrightarrow M^{\bullet}$ (3.2)

Propagation: $M^{\bullet} + M \longrightarrow MM^{\bullet}$ (3.3)

$M_i^{\bullet} + M \longrightarrow M_{i+1}^{\bullet}$ (3.4)

Termination:

- Combination: $M_i^{\bullet} + M_j^{\bullet} \longrightarrow P_{i+j}$ (3.5)

- Disproportionation $M_i^{\bullet} + M_j^{\bullet} \longrightarrow P_i + P_j$ (3.6)

where M is a monomer molecule and P is a polymer molecule.

The γ-radiolysis experiments involve running the emulsion polymerization reaction in a dilatometer glass vessel surrounded by a ^{60}Co hollow cylinder. The flux of γ-rays enables the polymerization to run at a very high rate. After a few minutes of polymerization, the vessel is taken away from the γ-ray source, and the rate of polymerization starts declining slowly, until it reaches a constant and low rate. From all this data the exit rate constant *k* can be calculated.

3.2.3 Determination of entry and exit rate coefficients

Kinetic experiments do not directly provide any details about the entry and exit rates of free radicals to and from the particles. The only set of data which could be obtained from the dilatometer is a list of times and their corresponding heights of the dodecane layer within the capillary tube (for more details refer to section 2.4). Corresponding conversions can be calculated from heights, and from the data of time and conversion, the average number of free radicals per latex particle $\bar{n}$, can be calculated as follows:

$$\frac{\mathrm{d}x}{\mathrm{d}t} = \frac{k_\mathrm{p} C_\mathrm{P} N_\mathrm{c}}{{m_\mathrm{M}}^0 N_\mathrm{A}} \bar{n} \tag{3.7}$$

where x is the fractional conversion of monomer to polymer, t is the time, k_p is the propagation rate coefficient, C_P is the monomer concentration within the latex particles, N_c is the number of latex particles per unit volume of aqueous phase, ${m_\mathrm{M}}^0$ is the amount of monomer added to the latex at the beginning of the reaction and N_A is Avogadro number.

After calculating $\bar{n}$, the following step is to calculate the value of the exit rate constant *k*, which can be calculated from the equations governing the entry-exit relationship to $\bar{n}$. As explained in section 1.5, for zero-one systems there are the following possibilities:[19,20,21]

Limit 1a: $\frac{\mathrm{d}\bar{n}}{\mathrm{d}t} = \left(\rho_{\text{thermal}} + \rho_{\text{initiator}}\right)(1 - 2\bar{n}) - k_{\text{ct}}\bar{n}$ (3.8)

Limit 1b: $\frac{\mathrm{d}\bar{n}}{\mathrm{d}t} = \left(\rho_{\text{thermal}} + \rho_{\text{initiator}}\right)(1 - 2\bar{n}) - 2k_{\text{ct}}\bar{n} + 2k_{\text{ct}}\bar{n}^2$ (3.9)

Limit 2a: $\frac{\mathrm{d}\bar{n}}{\mathrm{d}t} = \left(\rho_{\text{thermal}} + \rho_{\text{initiator}}\right)(1 - 2\bar{n}) - 2k_{\text{cr}}\bar{n}^2, k_{\text{cr}} = \frac{k_{\text{tr}}\,k_{\text{dM}}}{k_{\text{p}}^1}$ (3.10)

Limit 2b: $\frac{\mathrm{d}\bar{n}}{\mathrm{d}t} = \left(\rho_{\text{thermal}} + \rho_{\text{initiator}}\right)(1 - 2\bar{n}) - 2k_{\text{cr}}C_{\text{p}}\bar{n}$ (3.11)

These equations are all cases of the following general equation:

$$\frac{\mathrm{d}\bar{n}}{\mathrm{d}t} = (\rho + \alpha k\bar{n})(1 - 2\bar{n}) - k\bar{n} \tag{3.12}$$

For α = +1, equation (3.12) becomes the equation for limit 2a; for α = 0 one obtains the equations for limits 1a and 2b (which, mathematically, are the same); and for α = -1 the limit 1b equation is recovered. It is convenient to rewrite equation (3.12) as a quadratic equation:

$$\frac{\mathrm{d}\bar{n}}{\mathrm{d}t} = \omega\bar{n}^2 + g\bar{n} + \rho \tag{3.13}$$

where ω = -2αk, and g= -2ρ - (1-α)k. The solution of this equation[1] is:[19]

$$\bar{n} = \frac{p - \lambda\delta\exp(-\theta t)}{1 - \delta\exp(-\theta t)} \tag{3.14}$$

[1] The solution can be written in its full form as

$$\bar{n} = \frac{\frac{-2\rho-(1-\alpha)k+\sqrt{[-2\rho-(1-\alpha)k]^2+8k\alpha\rho}}{-4\alpha k}}{1-\left\{\frac{-2\rho-(1-\alpha)k+\sqrt{[-2\rho-(1-\alpha)k]^2+8k\alpha\rho}-\bar{n}_0}{-2\rho-(1-\alpha)k-\sqrt{[-2\rho-(1-\alpha)k]^2+8k\alpha\rho}-\bar{n}_0}\right\}e^{-\left(\sqrt{[-2\rho-(1-\alpha)k]^2+8k\alpha\rho}\right)t}} - \frac{\left\{\frac{-2\rho-(1-\alpha)k-\sqrt{[-2\rho-(1-\alpha)k]^2+8k\alpha\rho}}{-4\alpha k}\cdot\frac{-2\rho-(1-\alpha)k+\sqrt{[-2\rho-(1-\alpha)k]^2+8k\alpha\rho}-\bar{n}_0}{-2\rho-(1-\alpha)k-\sqrt{[-2\rho-(1-\alpha)k]^2+8k\alpha\rho}-\bar{n}_0}\right\}e^{-\sqrt{[-2\rho-(1-\alpha)k]^2+8k\alpha\rho}}}{1-\left\{\frac{-2\rho-(1-\alpha)k+\sqrt{[-2\rho-(1-\alpha)k]^2+8k\alpha\rho}-\bar{n}_0}{-2\rho-(1-\alpha)k-\sqrt{[-2\rho-(1-\alpha)k]^2+8k\alpha\rho}-\bar{n}_0}\right\}e^{-\left(\sqrt{[-2\rho-(1-\alpha)k]^2+8k\alpha\rho}\right)t}} \tag{3.14a}$$

where

$$p = \frac{-g-\theta}{2\omega} \quad ; \quad \delta = \frac{p-\bar{n}_0}{\lambda-\bar{n}_0} \quad ;$$

$$\lambda = \frac{-g+\theta}{2\omega} \quad \text{and} \quad \theta^2 = g^2 - 4\omega\rho$$

A complete derivation of equation (3.14) from equation (3.13) is given in Appendix 3.1.

The version of equation (3.14) that will be used in the present work is that for α = +1, i.e., limit 2a. This is because small-particle styrene systems have been shown to follow this limit most closely.[21] Out of interest, some fitting of data was also carried out with α = 0, i.e., limit 1a. Not surprisingly, it was found that γ data (both relaxation and insertion) could be fitted equally well by this limit, but obviously quite different values of *k* and ρ were obtained. However it makes no sense to compare such values with ones obtained from previous work using limit 2a. For this reason the only values reported here are ones using limit 2a equations. It is stressed that current knowledge holds this limit to be most correct for the systems being studied.

Although the values of both ρ and *k* can be obtained by fitting equation (3.14) to the approach to steady state of a chemically initiated experiment,[13] a problem with this methodology is the uncertainty caused by the possible presence of oxygen.[22] If present this will cause retardation, and consequently the value of *k* will be too large, leading also to error in ρ. Therefore a better procedure is to use γ-relaxation data, because by this stage of a polymerization one can be confident that any oxygen has been consumed. By generating $\bar{n}$ values with equation (3.14), these may be compared with the experimental values. A MathCAD error-minimization program was developed and used to find the best fit of equation (3.14) to experimental values.

Having obtained *k* from fitting as described above, this value may then be used in the steady-state limit ($\frac{\mathrm{d}\bar{n}}{\mathrm{d}t}$ = 0) of equation (3.10), which is

$$\rho = 2k\frac{\bar{n}_{ss}{}^2}{1-2\bar{n}_{ss}} \qquad (3.15)$$

In this way the value of ρ may be obtained from a steady-state experiment. This

procedure will be used in this chapter to analyze thermally initiated experiments, and to compare the obtained value of ρ with that from analysis of γ-relaxation experiments, as described above.

3.3 Experimental details

3.3.1 Synthesis and purification of seed latex

Two latices have been used during the course of this work, AN05 and CA01, the surfactant in each of them has a different charge, and both have low particle-size polydispersity index (PDI), and both of them were used in all the thermally and γ-ray initiated experiments. The formulation for preparing the latices is in table 3.1, and some of their properties are in table 3.2.

Styrene was purchased stabilized with hydroquinone. Inhibitor was removed through a column of basic activated aluminium oxide, and then distilled under low pressure. When the purity reached 99.99%, the purified styrene was stored at low temperature (< 4^{o}C) and used only during the first two weeks after distillation. The initiator KPS was re-crystallized twice from water, and V-50 was re-crystallized from water/acetone (1:1 by weight) before use. Other chemicals including AMA-80, DTAB, and sodium bicarbonate were all used without further purification.

Ingredient	AN05	CA01
Milli-Q water	600	600
styrene	92	92
surfactant	12 (AMA-80)	4.57 (DTAB)
$NaHCO_3$	1.25	-
Polystyrene beads	0.96	0.93
Initiator	1.3 (KPS)	0.298 (V-50)
Temperature	92^{o}C	94^{o}C
Reaction Time	24 h	24 h

Table 3.1. Seed Latex Preparation, all amounts are in grams

Characteristics	AN05	CA01
Average Particle Diameter (nm)		
TEM	63.70	76.64
PSDA	65.43-69.70	-
HPPS	69.69	73.02
Value used for kinetic analysis	**63.70**	**76.64**
PDI*	1.031	1.045
% Solids	12.46	13.54
C_P^{SAT} (mol/L)	5.735	5.581

* PDI equals weight-average particle diameter / number-average particle diameter

Table 3.2. Seed latex properties

The seed latex synthesis consisted of mixing the water, surfactant and sodium bicarbonate together in the reactor, which consists mainly of a 1 L glass cylinder surrounded by a water jacket to control the temperature. In the mean time, styrene is mixed with a small amount (less than 1 g) of polystyrene beads, in order to improve radical capture efficiency especially at the beginning of the polymerization process, which increases the polymerization rate and number of polymer particles produced,[23,24,25] and gives a higher rate of radical capture which enables better control over polydispersity,[23] which results in a lower polydispersity latex. The styrene and the polystyrene beads are added to the reactor, and the mixture is heated together to the required temperature until thermal equilibrium is achieved. Initiator, previously dissolved in a small amount of water (about 10 mL), is then added to the reactor, and the polymerization continues for the specified time to make sure all styrene is converted to polystyrene. The whole polymerization process in the reactor is run under an inert atmosphere of nitrogen gas, in order to avoid any oxygen effect on the process.

After synthesis, the seed latex is dialyzed in Milli-Q water for around 5 weeks in a 5 L beaker. Water is changed twice a day in the first week, then daily in the remaining period. Dialysis ensures the latex is purified of any non-reacted water-soluble chemicals (like extra surfactant, buffer, and non-reacted initiator).

3.3.2 Determination of seed latex characteristics

Solids ratio was measured by simple gravimetry. Particle size distribution and average particle diameter were measured by TEM, Particle Size Distribution Analyzer (PSDA), and by High Performance Particle Sizer (HPPS). PSDA and HPPS results were used as an indication that TEM measurements were true. In all analysis of kinetic experiments only the average particle diameter determined by TEM was used.

PSDA was used twice to give the average particle diameter of the AN05 latex, although the first value (65.43 nm) is quite close to TEM value, the second (69.70 nm) is slightly larger. During the course of the analysis, using the TEM value was giving reasonable values for $\bar{n}_{ss}$, between 0 and 0.5, typical for zero-one system, while the second value obtained with the PSDA gave $\bar{n}_{ss} > 0.5$, which is unlikely for a zero-one system, as small-particle styrene is believed to be.

C_P^{SAT} measurement was slightly more complicated. To measure it a known mass of seed latex was diluted in water and a known amount of stabilized monomer was added (to avoid any polymerization occurrence during the experiment). The amount of monomer which did not dissolve in the water and the particles was separated and its volume measured. This technique is also known as "static swelling" and more details have already been given in section 2.3.3.

All the above mentioned experiments were run at least three times for each latex, as they were found to differ from one latex to another as previously shown in table 3.2.

3.3.3 Kinetic Experiments

To avoid any interval I nucleation interference (which can certainly affect the kinetics) in the work done, all experiments run were designed to start at interval II. This had an advantage over starting in interval I, which is that the characteristics of the latex (including the % solids, C_P^{SAT} and the average particle diameter) are known at the beginning of interval II, reducing the number of unknowns required to calculate $\bar{n}$ through equation (3.7).

The kinetic experiments were run as follows: known amounts of seed latex, monomer and CD were added to the dilatometer vessel, and then diluted with water until the vessel is nearly full. Adequate time was left for mixing, then hot water was run in the jacket surrounding the vessel, and air was taken out until the monomer starts to boil. When degassing was complete the vessel was thermally equilibrated through water running at 50 ^{o}C. A capillary of known diameter was placed at the top of the dilatometer vessel, degassed water was used to fill the capillary, and then dodecane was added at the top. An automated tracker was used to follow the movement of the dodecane, whose meniscus goes down because of the reduction of the volume of the monomer as it reacts to become a polymer. For experiments run to determine the value of ρ_{thermal} through equation (3.14), the experiment is kept running for more than 12 hours, to ensure that interval II has ended, while for γ-radiolysis experiments, the dilatometer vessel is moved down to the γ-rays source and kept there for a specific period of time, before it was taken up and left to relax for at least 30 minutes. A few γ-relaxation experiments included two relaxations, while the majority included three. For all experiments N_c = 5.1 x 10^{16} particles/L for AN05 and N_c = 3.2 x 10^{16} particles/L for CA01. The amounts of other chemicals added depended on the volume of the capillary used, and no initiator was used in any of the experiments discussed in this chapter. Experiments were run either with no CD added, or with 2% and 4% CD (relative to total monomer) for AN05 experiments, or only 4% CD in CA01 kinetic experiments. For example 4% CD means $\frac{\text{mass of CD}}{\text{mass of monomer}}$ = 0.04.

From the data of time and dodecane movement, the value of $\mathrm{d}x/\mathrm{d}t$ in equation (3.7) can be measured, from which $\bar{n}$ can be calculated. By having a set of data of time and the corresponding $\bar{n}$, both ρ_{thermal} and k can be calculated from equation (3.14).

3.4 Analysis of γ-relaxation data

One of the decisions which had to be made during the course of this work is to define the period of time during which the relaxation reaches a constant $\bar{n}_{ss}$ value. It has been observed that running the γ-relaxation experiment for short periods of time might result in inaccuracy problems when calculating ρ and k, which will inevitably affect the accuracy of the $\bar{n}_{ss}$ value. Having an inaccurate k will even cause a bigger problem, as all entry efficiency data, which will be discussed thoroughly in chapter IV, will have a high error.

Consequently, an error analysis had to be done, to give an indication of whether the k values obtained really reflect accurate values. For all experiments, γ-relaxation took 30 minutes. But the error analysis was done very simply by assuming the relaxation experiment was stopped after 10, 15, 20, 25 or 30 minutes. Results (table 3.3) show that the length of the time period certainly affects the accuracy.

time	$\bar{n}_{ss}$ x 10^2	k x 10^2 s	$\rho_{thermal}$ x 10^5 s
10 minutes	-2.81	1.07	-2.69
15 minutes	5.85	1.22	9.46
20 minutes	5.54	1.20	8.28
25 minutes	5.37	1.19	7.68
30 minutes	5.82	1.23	9.42

Table 3.3. Results calculated from experiment XSN508 R2, depending on the length of the relaxation period.

The results in table 3.3 show a number of facts. One is that the longer the γ-relaxation period was, the higher the values of $\bar{n}_{ss}$, k and $\rho_{thermal}$. In addition to this, it is clear from figure 3.1 that if relaxation was only done for ten minutes, steady state would not have been reached and so the values obtained for k and $\rho_{thermal}$ from this short period data would have had very high error in them, especially that, as shown in table 3.3, determined values for both $\bar{n}_{ss}$ and the entry rate coefficient ρ at 10 minutes is certainly wrong, as it is not possible to have a negative $\bar{n}$ or a negative rate coefficient. On the contrary, figure 3.1 shows that steady state for that relaxation experiment was reached at around 18 minutes. And this can be seen from the data in table 3.3, which show that the values of $\bar{n}_{ss}$, k and $\rho_{thermal}$ are quite close whether the relaxation was stopped after 20 or 30 minutes. The difference may be because of the effect of the short steady-state period taken in the case of relaxation for 20 minutes. At such conditions the values of $\bar{n}_{ss}$, k and $\rho_{thermal}$ might have been affected by the long approach to steady state period. As a result, all relaxation experiments took at least 30 minutes.

The above results are important in that they establish that γ-relaxations might look complete after 20 minutes, but in fact it is necessary to run them for longer – a minimum of 30 minutes is suggested – in order to obtain to higher accuracy in parameter values. In

particular, the fits in Figure 3.1 for 0-20 min and 0-30 min look identical, but Table 3.3 shows there are differences in the fitted parameter values.

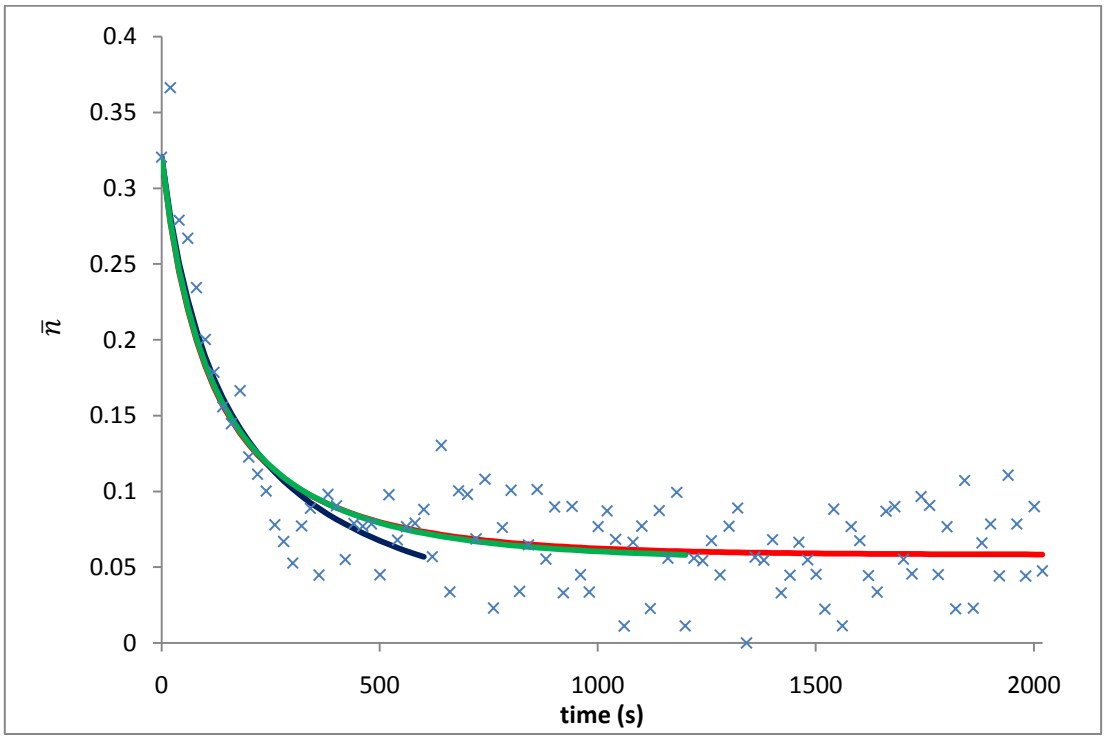

Figure 3.1. $\bar{n}$ as a function of time for a typical γ-relaxation experiment (XNS508 R2). Blue crosses: experimental values. Curves: equation (3.14) fitted over three different time periods: 0-10 min(blue line), 0-20 min (green line) and 0-30 min(red line).

3.5 Experiments without cyclodextrin

3.5.1 γ-relaxation experiments without CD

Experiments including γ-relaxation were carried out for both AN05 and CA01. Figure 3.2 shows typical results for two experiment, 3.2a shows typical results of an experiment done with latex AN05, and 3.2b shows typical results of an experiment done with CA01. All experiments were run at 50 ^{o}C. Figure 3.2 shows the difference for the rate while reaction vessel was in source, represented by sharp increases in the value of $\bar{n}$, and when the vessel is taken out of source. Data fitting of the relaxations provides the values of k and ρ_{thermal}. $\bar{n}$ values as a function of time (as calculated from equation (3.7) from experiment results), from this data and through an error minimizing function, k and ρ_{thermal} can be calculated, then all values are substituted in the model, equation (3.14). $\bar{n}$ is

calculated as a function of time from both model and experimental data, and the results are shown in figure 3.3, which represents $\bar{n}$ as a function of time for two of the relaxations presented in figure 3.2, one for each latex. Figure 3.3 shows how the calculated values of k and $\rho_{thermal}$ allow the model results to go smoothly between the experimental points to a good level of accuracy.

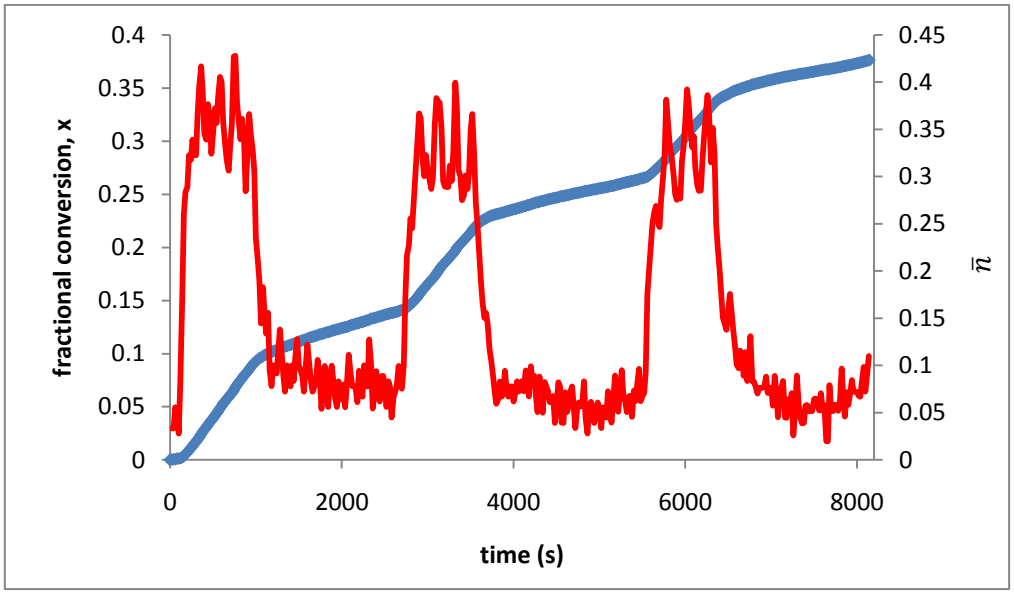

Figure 3.2a. Conversion (blue) and $\bar{n}$ (red) as functions of time for γ-relaxation experiment XSN508 (with anionic latex)

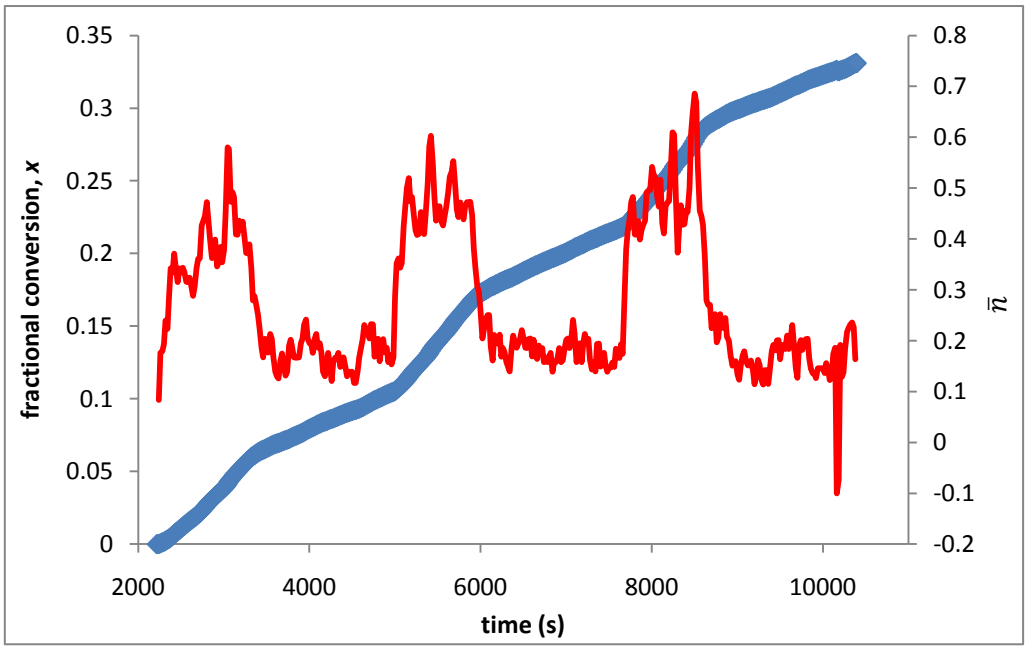

Figure 3.2b. Conversion (blue) and $\bar{n}$ (red) as functions of time for γ-relaxation experiment XSC104 (with cationic latex)

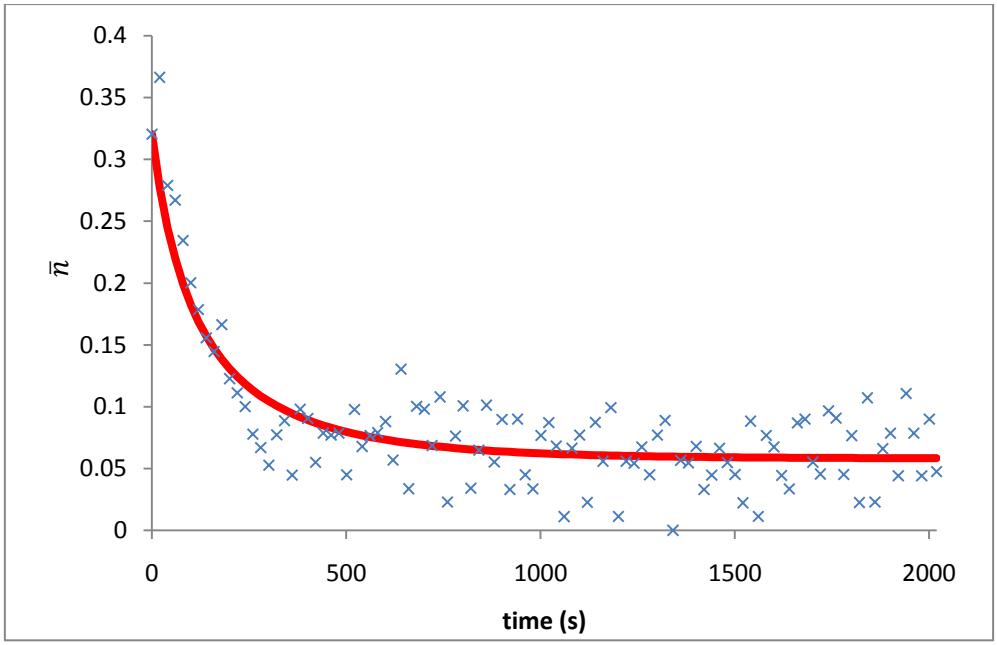

Figure 3.3a. $\bar{n}$ as a function of time for a typical γ-relaxation experiment (XSN508 R2, with anionic latex). Blue crosses: experimental values. Curve: equation (3.14) (best fit)

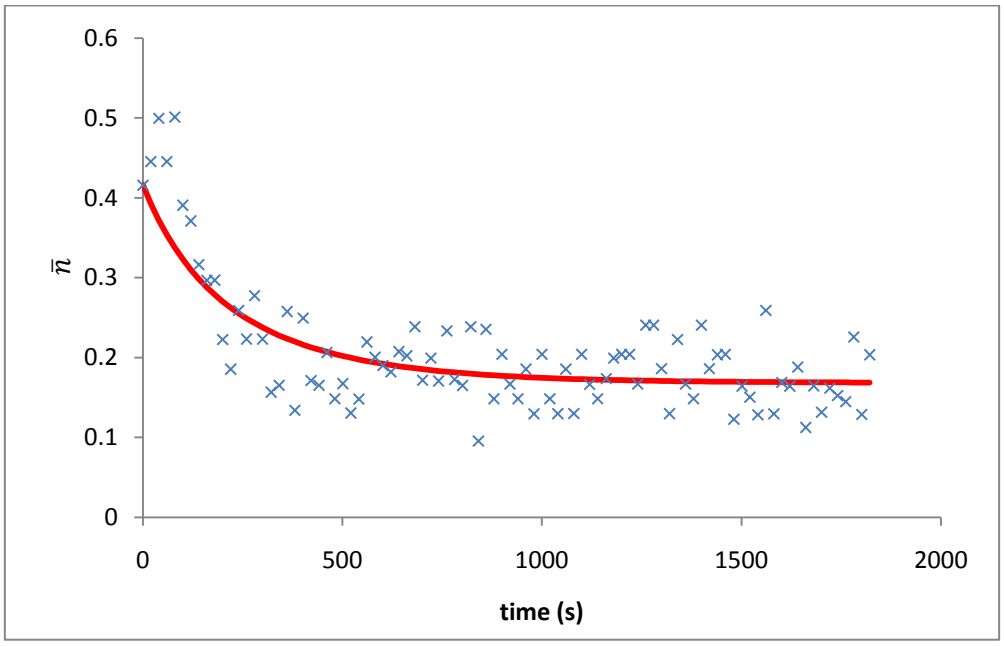

Figure 3.3b. . $\bar{n}$ as a function of time for a typical γ-relaxation experiment (XCS104 R2, with cationic latex). Blue crosses: experimental values. Curve: equation (3.14) (best fit)

As per the time difference between figure 3.2 and 3.3, substituting the actual value of the time in equation (3.14) does not really represent the time by which the relaxation started, which would give wrong results. Consequently, time was substituted with the value zero at the beginning of every relaxation, as seen in figure 3.3.

$\bar{n}$ oscillation, as shown in both figure 3.2 and 3.3, are mainly because the thread of the tracker used in γ-relaxation experiments is not uniform, but varies in a cyclic way. As the model used depended on the overall average, then this should not have an effect on the calculated values of ρ and k.

Results of all successful γ-relaxation experiments done are presented in table 3.4. The table includes values of $\rho_{thermal}$ and k as determined from equation 3.14. It should be noted that values for relaxations which started during interval III are not included in calculating the average values of $\bar{n}_{ss}$, k and $\rho_{thermal}$ for each latex used.

Seed Latex	Experiment	$\bar{n}_{ss}$ x 10^2	k x 10^2 s	$\rho_{thermal}$ x 10^4 s
AN05	XSN503 R1	5.62	1.13	0.78
	XSN503 R2	5.13	1.55	0.90
	XSN508 R1	7.89	1.25	1.85
	XSN508 R2	5.84	1.23	0.94
	XSN510 R1	7.78	1.19	1.71
	XSN513 R1	6.65	1.79	1.82
	XSN513 R2	3.95	1.38	0.46
	Average	**6.12**	**1.36**	**1.21**
CA01	XSC104 R1	17.08	0.57	5.06
	XSC104 R2	17.08	0.51	4.63
	XSC104 R3	15.31	1.02	6.86
	Average	**16.49**	**0.70**	**5.68**

Table 3.4. Results of γ-relaxation polymerization experiments.

3.5.2 Thermal polymerization experiments:

A set of experiments was run for both latices to calculate the value of $\rho_{thermal}$, knowing the value of $\bar{n}_{ss}$ from the conversion/time data, and k from the γ-radiolysis experiments. The results of these experiments are given in table 3.5. A typical result of a thermal initiation experiment is shown in figure 3.4. $\bar{n}_{ss}$ was calculated from the average slope of the conversion/time curve, which follows almost a straight line path, as styrene is known to

hold a straight line relationship between conversion and time in Interval II.[19] The induction time for these experiments was typically 15 min for the anionic latex (see figure3.5a) and 18 hours for the cationic latex (see figure 3.5b). The cause of this massive difference is unknown.

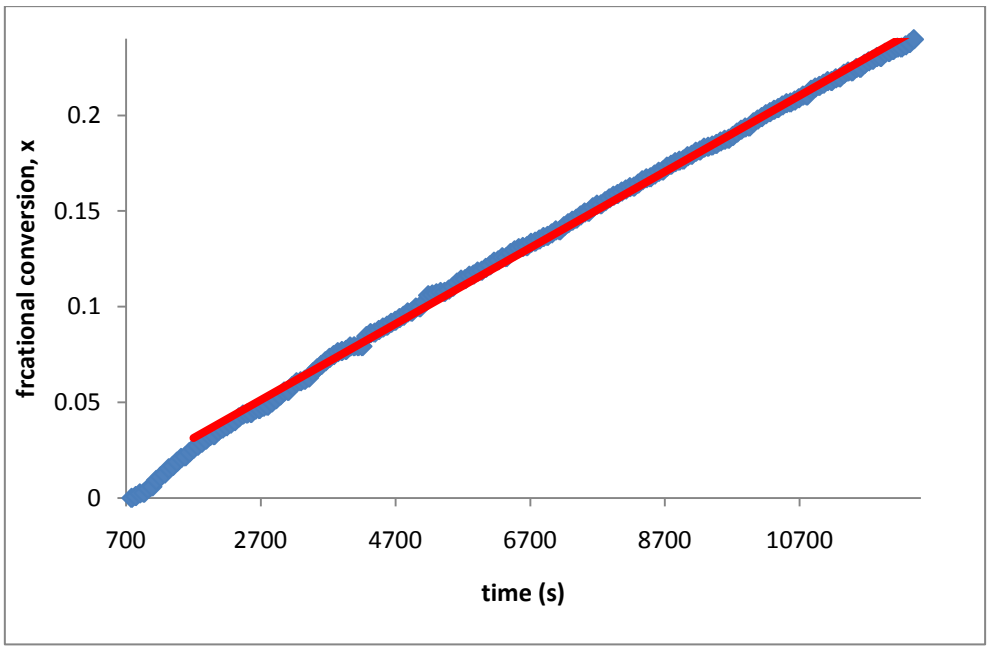

Figure 3.4a. Results for thermal polymerization experiment SN501 (with anionic latex). Blue: experimental data, red: straight-line fit to steady-state period.

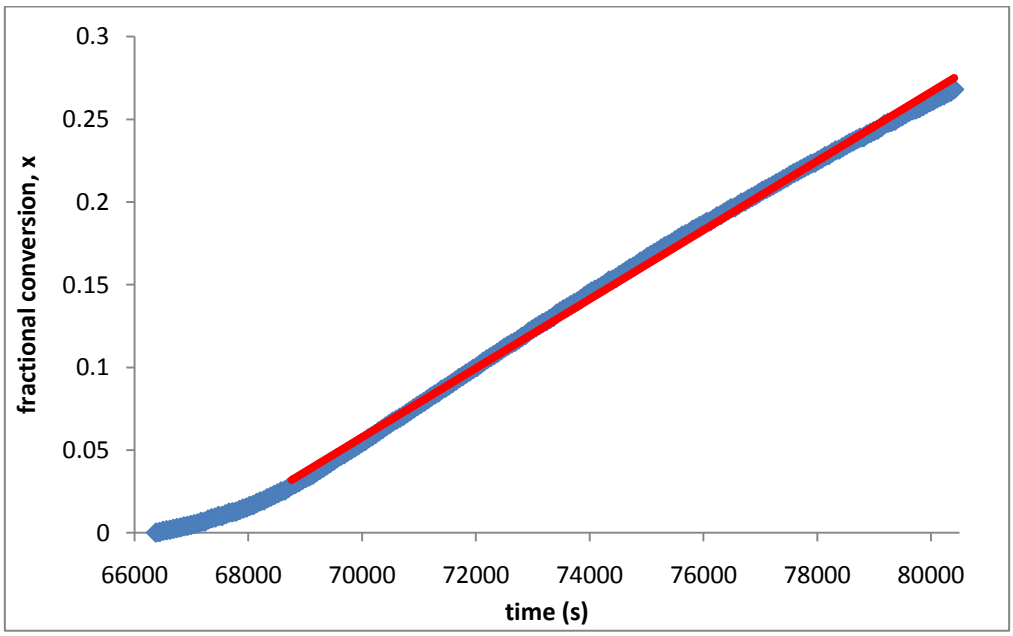

Figure 3.4b. Results for thermal polymerization experiment SCT151 (with cationic latex). Blue: experimental data, red: straight-line fit to steady-state period.

The aim of thermal polymerization experiments is to calculate $\rho_{thermal}$, which can be calculated through this technique and also through γ-radiolysis, as discussed in section 3.5.1. The advantage of this technique is that it totally excludes any initiation method, which makes its results considered the most accurate.

For all thermal initiation experiments for AN05, the value of $k = 1.36 \times 10^{-2}$ s^{-1} was used, and for experiments for CA01, the value of $k = 7.0 \times 10^{-3}$ s^{-1} was used. These values are the average values as calculated in table 3.4.

Seed Latex	Experiment	$\bar{n}_{ss}$ x 10^2	$\rho_{thermal}$ x 10^4 s
AN05	SN501	6.01	1.11
	SN502	8.39	2.29
	SN504	4.72	0.67
	SN505	6.84	1.47
	Average	**6.49**	**1.32**
CA01	SCT150	9.67	1.26
	SCT151	11.76	1.96
	Average	**10.71**	**2.04**

Table 3.5. $\rho_{thermal}$ as calculated from thermal initiation experiments data for both lattices. These experiments do not include experiments done to analyze the effect of surfactant and CD on $\rho_{thermal}$.

Data shown in table 3.5 highlight the reproducibility of results for thermally initiated experiments. The data also shows that $\bar{n}_{ss}$ and $\rho_{thermal}$ for these two latices are quite close to each other. The reproducible values confirm the accuracy of this method.

Comparing data in tables 3.4 and 3.5 shows the reproducibility of the average values of $\bar{n}_{ss}$ and $\rho_{thermal}$ for the anionic latex. This was not the case for the cationic latex where $\bar{n}_{ss}$ and $\rho_{thermal}$ values obtained through γ-relaxation were quite different from their values obtained through thermally initiated experiments. This can be explained by the presence of small amounts peroxides within the cationic latex which caused this effect. More details about peroxides, their formation and effect will be discussed in section 3.5.4.

3.5.3 γ-insertion experiments without CD

Another method for calculating k is from the γ-irradiation period, in the same way followed to calculate entry and exit parameters from equation (3.14). A typical example for this is given in figure 3.5.

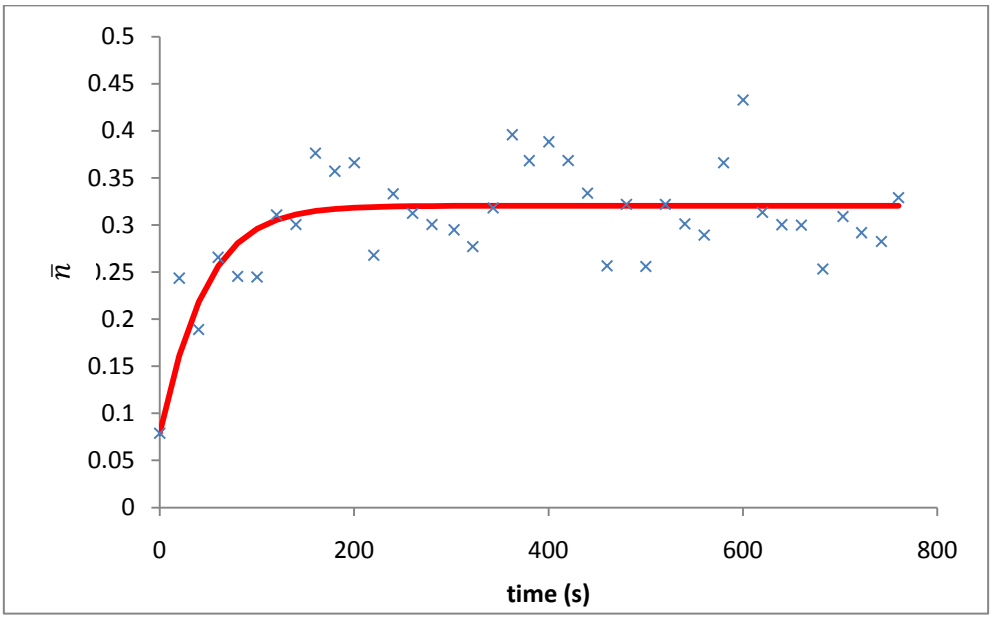

Figure 3.5a. $\bar{n}$ as a function of time for a typical γ-relaxation experiment (XSN508 I2, with anionic latex). Blue crosses: experimental values. Curve: equation (3.14) (best fit)

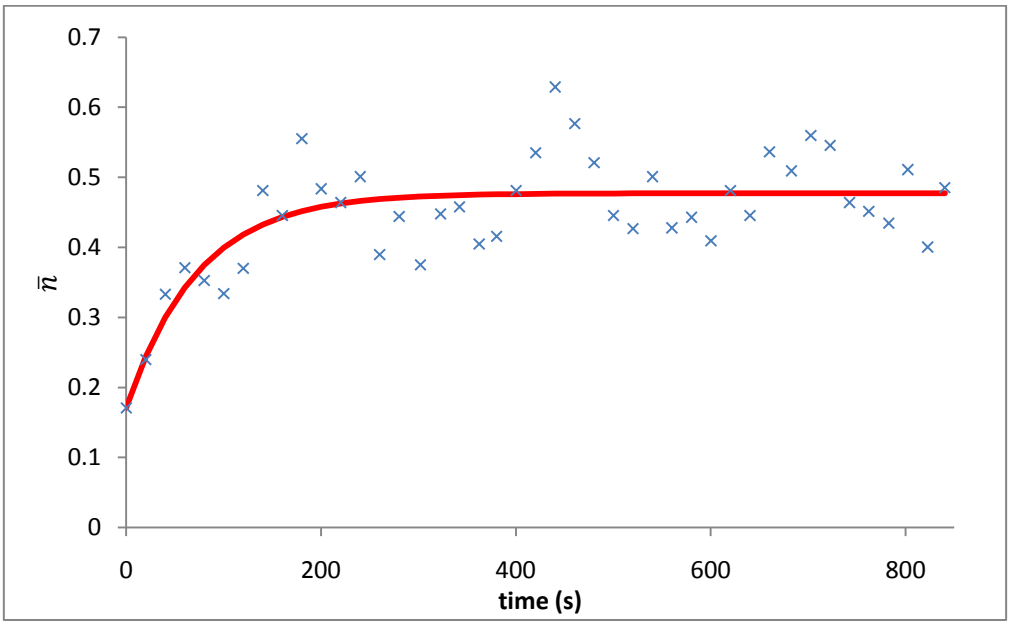

Figure 3.5b. $\bar{n}$ as a function of time for a typical γ-relaxation experiment (XSC104 I2, with cationic latex). Blue crosses: experimental values. Curve: equation (3.14) (best fit)

Figure 3.5 shows some of the drawbacks of this technique, one of them is the short period the monomer sample can remain within the source, which certainly impacts the accuracy of the results, as was discussed in section 3.4. Furthermore, the value of $\rho_{thermal}$ cannot be calculated from this graph because the actual ρ acting here is $\rho_{thermal} + \rho_{\gamma}$, and there are no available details on the value of ρ_{γ} or how to accurately calculate it. Finally, the presence of oxygen in the first γ-irradiation period of each experiment can affect the results.

		$k \times 10^2 \times s$		$(\rho_{\gamma} + \rho_{thermal}) \times s$	$\rho_{thermal} \times s$
Seed Latex	Experiment	γ-irradiation	γ-relaxation	γ-irradiation	γ-relaxation
AN05	XSN503 I&R 1	0.51	1.13	4.20×10^{-3}	7.83×10^{-5}
	XSN503 I&R 2	2.66	1.55	0.016	8.99×10^{-5}
	XSN508 I&R 1	0.18	1.25	1.92×10^{-3}	1.85×10^{-4}
	XSN508 I&R 2	1.02	1.22	5.86×10^{-3}	9.42×10^{-5}
	XSN508 I&R 3	0.65	1.48	2.71×10^{-3}	9.08×10^{-5}
	XSN510 I&R 1	0.81	1.19	4.21×10^{-3}	1.71×10^{-4}
	XSN510 I&R 2	0.44	1.36	2.43×10^{-3}	6.14×10^{-5}
	XSN513 I&R 1	0.50	1.79	3.26×10^{-3}	1.82×10^{-4}
	XSN513 I&R 2	1.77	1.38	7.05×10^{-3}	4.62×10^{-5}
	XSN513 I&R 3	0.96	1.32	2.78×10^{-3}	1.85×10^{-5}
CA01	XSC104 I&R 1	0.12	0.57	2.51×10^{-3}	5.06×10^{-4}
	XSC104 I&R 2	0.06	0.51	6.35×10^{-3}	4.63×10^{-4}
	XSC104 I&R 3	0.06	1.02	1.44×10^{-2}	6.86×10^{-4}

Table 3.6. *k* values from γ-irradiation and γ-relaxation. Results in red are totally (or partially) in interval III.

To calculate *k* using this technique, results of the first irradiation period for each experiment were neglected. This adds another issue as the maximum number of relaxations for every experiment is three, thus reducing the number of data points available before averaging, so increasing the error. But with all such drawbacks, table 3.6 gives a summary of the results of the values of *k* calculated from γ-irradiation. Table 3.6 includes results for I&R1 for many experiments, I&R1 means (1st insertion and 1st relaxation, i.e., I1 is the very beginning of the experiment). For the cationic latex, *k*

calculated for I1 experiment is larger than its value from other insertions, a clear sign of the presence of oxygen and its retardation effect. On the other hand, for the anionic latex, for all I1 results, *k* calculated is less than its value from I2 and I3. This can be interpreted that, under some conditions, dissolved oxygen can play an initiating role. In any case, results for all I1 experiments were excluded when calculating the averages. Averages for all γ-insertion experiments are shown in table 3.11.

It is clear that for the anionic latex the results are very similar, which gives some credibility to this technique. Cationic latex results here do not have a similar agreement. One of the reasons for this can be assumed to the increased effect of the amine/peroxide side reactions in presence of γ-rays, which certainly affect the reaction kinetics. With all previously mentioned drawbacks, *k* calculated from this method was not used in any calculations during the course of this work.

3.5.4 Interpretation of entry and exit rate coefficients

Knowing that styrene follows Limit 2a kinetics, with its assumption of complete re-entry and minimum re-escape, the exit rate can be defined as a function of free radical diffusivity in water. The fate of the free radical already present within the particle is either that the free radical will transfer to monomer and a monomeric free radical will exit, or that the free radical may propagate within the particle, and will not be able to exit. With these assumptions the exit rate coefficient can be calculated as follows:

$$k_{\text{theor}} = \frac{3D_{\text{w}}C_{\text{W}}}{{r_{\text{s}}}^2 C_{\text{p}}}\frac{k_{\text{tr}}}{k_{\text{p}}^1} \tag{3.16}$$

Where D_{W} is the diffusion coefficient of monomer in water, k_{tr} is the rate coefficient by transfer to monomer, k_{p}^1 is the rate coefficient of propagation for monomeric radicals and r_{s} is the average radius of a swollen latex particle. With the assumption that only monomeric free radicals desorb, the coefficient of desorption of this free radical is assumed to be equal to that of a monomer molecule, as has been previously derived.[26] As the aim of this work is only for interval II analysis, both C_{p} and C_{W} were substituted with their saturated values, so the following values were used to calculate k_{theor}: $D_{\text{W}} = 1.5 \times 10^{-9}$ m^2/s,[27] ${C_{\text{W}}}^{\text{sat}} = 4.4 \times 10^{-3}$ mol/L,[28] $k_{\text{tr}} = 9.3 \times 10^{-3}$ mol/L.s,[29] $k_{\text{p}}^1 = 4\ k_{\text{p}} = 1 \times 10^3$ mol/L.[19]

k_{theor} was found to be equal to 1.43 x 10^{-2} for AN05, and 1.06 x 10^{-2} for CA01, values which are close enough to the exit rate coefficients as shown in table 3.4. The difference between these values is primarily due to the cationic latex having a larger size (value of r_s for the anionic latex was 46.58 nm, and for the cationic latex was 55.01 nm at the beginning of interval II). Especially given the uncertainty in k_p[1,30] the agreement here between experiment and theory is good. Values of $\rho_{thermal}$ in table 3.4 were not calculated by substituting k (from γ-relaxation data) and using $\bar{n}_{ss}$ of thermal initiation experiments, but were taken directly from the analysis of γ-relaxation experiments. The results are close to those calculated from relaxation data, which is a good indication for the accuracy of the model used in this work.

Although tables 3.4 and 3.5 are similar for most values, the results shown for $\bar{n}_{ss}$ for the cationic latex, obtained throughout γ-relaxation experiments, are slightly higher than those of the thermal initiation experiments, resulting in a slightly higher value of $\rho_{thermal}$. Although the difference is not very high, a deeper discussion about this issue might help clarify this point.

During the preparation of the two latices used during this work, no degasification took place either for the water or the monomer. This is because of the big amounts of water and monomer used (as shown in table 3.1), which might have required a lengthy process for effective degasification. Consequently, oxygen presence in the reaction medium is inevitable and the following reactions take place:[31]

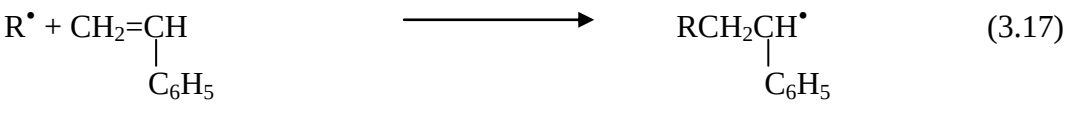

(3.17)

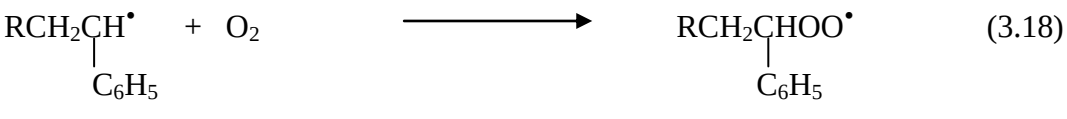

(3.18)

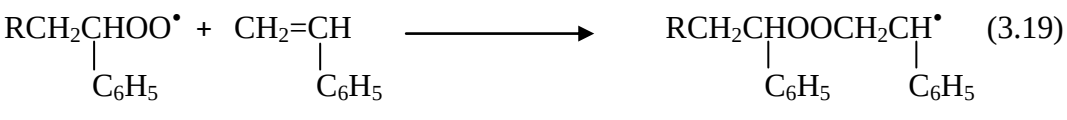

(3.19)

At atmospheric pressure, oxygen reactivity with styrene is approximately a million times higher than styrene polymerization on a molar basis.[32] The rate constant for the reaction of free radical with the monomer, equation (3.17) is considered to be equal to 10^9 or greater. Although the rate was not calculated for styrene, somewhat similar reactions, like reactions of hydroxyalkyl radicals with oxygen,[33] including some short chain alcohols and carbohydrate,[34]or reactions of some inorganic radicals with hypophosphite ions to form peroxides[35] , both cases gave values $\geq 10^9$ mol/L.s, so assuming a value in this range for styrene will not be a problem. The propagation reaction of the monomer with oxygen, equation (3.18) has a lower rate constant, for styrene at 25 ^{o}C its rate constant is 41mol/L.s[36]. Reaction kinetics of styrene with oxygen have been studied by Mayo,[32,37,38] who found that peroxide radicals reaction with styrene is much slower than termination with a styrene radical, such conclusions lead to the later findings by Gilbert[22] that oxygen is a main reason for retardation and/or radical losses during the initiation periods of seeded emulsion polymerization reactions. Another reason for the propagation of peroxide radicals is that oxygen-centered radicals are more reactive than carbon-centered radicals, so it can be assumed that the first peroxide radicals will form hydroperoxides and generate new radicals wherever hydrogen bonded within other molecules can be reacted with, example for this is the methine group within other styrene molecule or on the polymer chain. The product of this reaction will be polymer-bound peroxides which are not as easy to remove as postulated oligomers. [39] Styrene peroxide can still be produced under special conditions,[31,40] and is used as a polymeric fuel,[40] and as initiator for photopolymerization of methyl methacrylate even at low temperatures.[41,42]

As peroxides must be present in the latex already prepared, their effect on the reactions run during the course of this work has to be studied. Oxygen maximum concentration in water at 100 ^{o}C water is 1.10 mmol/L (as calculated from data in[43]), and in styrene is 1.5 mmol/L,[32] and from the amounts of water and styrene used to prepare each latex, and assuming all oxygen present in the medium reacted with styrene to form peroxides, the concentration of peroxides can be calculated as 1.2 mmol/L. Because of the higher rate of termination of peroxide polymerization reactions (compared to propagation), most of the peroxides are not supposed to form long chain polymers, but rather they form small oligomers which tend to remain within the latex. Because dialysis cannot remove all such oligomers from the latex, an assumption of the presence of some peroxide oligomers can be a sound assumption.

Can the thermal decomposition of peroxide oligomers be considered negligible? A previous study by van Berkel[2,3] has shown that of $\bar{n}_{ss}$ becomes slightly lower in case the latex was heat treated under argon gas for four days, which resulted in a de-oxygenation of the cationic latex prepared during his work, so decomposing any peroxide oligomers already present. The long period of heat treatment (compared for example to the heat treatment of anionic latex which lasted only for 24 hours) resulted in slightly lower $\bar{n}_{ss}$. Because the difference was not major, heat treatment for all latices synthesized during the course of this work lasted for only 24 hours under nitrogen. The success of this process can be seen from the low $\bar{n}_{ss}$ values as shown in table 3.5.

The last question can then be asked, why is there a difference for the cationic latex $\bar{n}_{ss}$ value between thermal polymerization results (table 3.4) and γ-relaxation results (table 3.5)? Why did the anionic latex not have a similar difference?

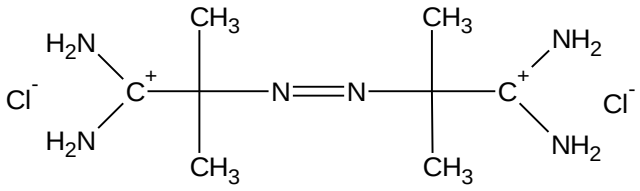

Scheme 3.2. Chemical structure of V-50

This is easily answered knowing that V-50 was the initiator used to prepare the cationic latex. Because of the way it decomposes, V-50 (scheme 3.2) releases nitrogen in the form of azo and amidine groups[44] resulting in the formation of some amine groups, especially in a medium already containing a variety of organic compounds, like styrene (with dimers and higher molecular weight polymers). These amine groups are likely to induce a redox reaction with the peroxide oligomers[39], as per the reaction in scheme 3.3

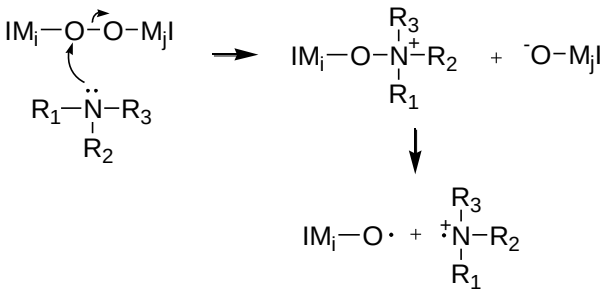

Scheme 3.3. Redox mechanism of amine induced decomposition of oligomer peroxide.[2]

It is clear from the above mentioned explanation that amine induced decomposition of peroxide oligomers had a minor impact on thermal polymerization experiments. Meanwhile, this impact was magnified under the effect of γ-rays. A possible explanation about that is the high initiation efficiency obtained during γ-initiated experiments. As will be seen in chapter IV, values of $\bar{n}_{ss}$ obtained from γ-rays are close enough to those obtained with 4 mmol/L V-50 concentration in the aqueous solution. This very high initiation efficiency can be assumed to have induced the redox mechanism, which was halted during the latex synthesis because of the heat treatment. This redox mechanism has obviously increased the entry rates, as seen with the increased value of $\bar{n}_{ss}$, even during γ-relaxation. In addition to this, γ-rays help generating hydroxy radicals in the aqueous phase.[18] With the role oxygen-centered radicals play in generating peroxides, this can give an possible factor causing the differences in $\rho_{thermal}$. Consequently, all values used for $\rho_{thermal}$ during the calculations done for chemically initiated experiments will depend only on the values obtained from thermal initiation.

3.6 Experiments with cyclodextrin

3.6.1 Effect of surfactant on thermal polymerization in the presence of CD

Thermal experiments have shown the effect of the surfactant and of CD, as shown in table 3.7 on thermal polymerization. Experiments were all run on latex CA01.

Figure 3.6 and the results in table 3.7 show clearly the impact of the presence/absence of surfactant. The exact amount of surfactant required was determined through a set of chemically initiated experiments, for which a deeper discussion will be presented in section 4.4.3. The results show that the presence of an exact amount of surfactant is required for the emulsion polymerization process to reach its highest rate. The exact amount of surfactant used in the experiment is very hard to identify, simply because the latex used already contains an unknown amount of surfactant which remained through dialysis.

Experiment	Reaction conditions	$\bar{n}_{ss}$ x 10^2	average
SC146	No surfactant, no CD	9.04	8.59
SC147		8.15	
SCT150	0.09g surfactant, no CD	9.67	10.71
SCT151		11.76	
SC173	0.09g surfactant, 4% CD	9.68	10.94
SC174		12.19	

Table 3.7. Results of thermal polymerization at different conditions.

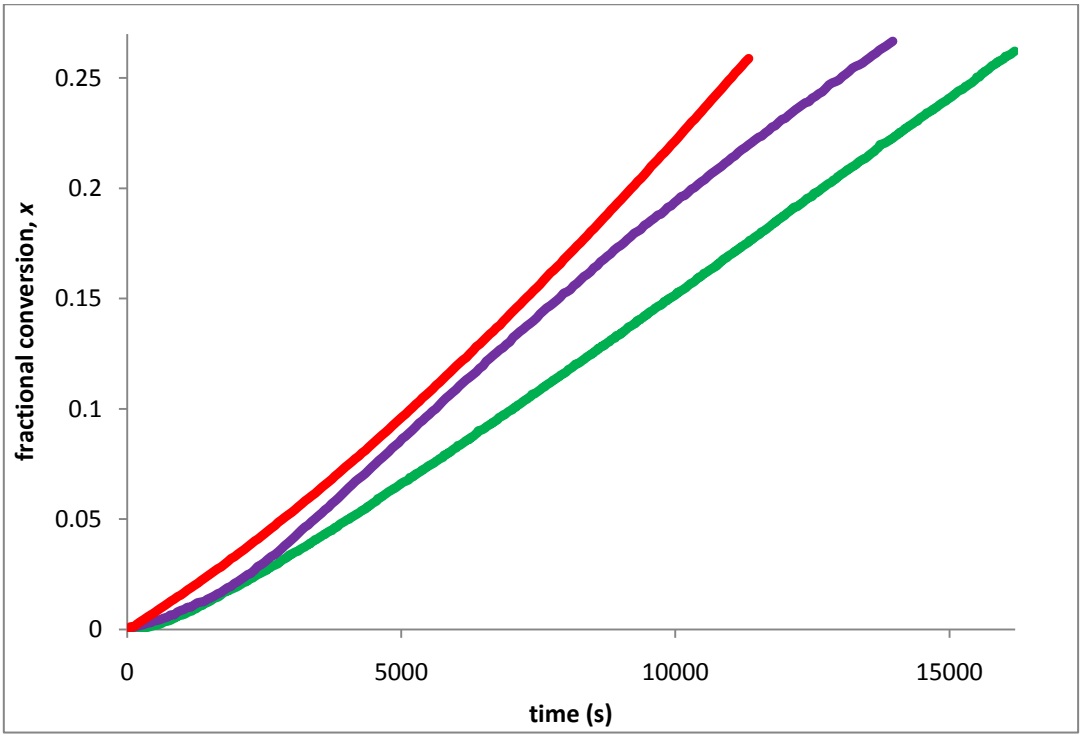

Figure 3.6. Effect of surfactant and CD on thermally initiated experiments (with cationic latex). Green line represents a "no surfactant no CD" experiment (SC146). The big gap between the green line and other lines shows the major impact of surfactant on thermal polymerization reaction rate. Violet line represents a "0.09g surfactant no CD" experiment (SCT151), and the red line represents a "0.09g surfactant 4% CD" experiment (SC174). The small gap between the violet and red lines shows the minor effect of CD on thermal polymerization reaction rate.

Although the amount of surfactant was found to affect the polymerization rate in interval

II, which was already expected knowing the basics of the emulsion polymerization process,[45,46] the effect of CD on thermal polymerization needs some explanation. Table 3.7 makes it clear that at the absence of an initiating medium, CD does not have any impact on the polymerization kinetics. To the contrary, the free radicals formed at the earliest moments of the reaction depend mainly on the presence of surfactant. Certainly, they can still form if no surfactant or CD is present, but the presence of surfactant is the main parameter affecting ρ_{thermal} .

Another important conclusion to be made here is that the spontaneous polymerization of styrene is not an aqueous phase reaction. This disagrees with the original assumptions of the Harkins theory.[47,48,49] Furthermore, it indicates that the mechanism of spontaneous polymerization with the lack of surfactant is different from its mechanism with surfactant present in the aqueous phase.

This brings about a question, if the exit has increased with the presence of CD, why does the presence of CD not change the value of $\bar{n}_{\text{ss}}$?

To answer this question, it is better to have a closer look at the actual role of CD in the mixture. The main role of CD is to increase the solubility of styrene C_{W}, and with the increased solubility the exit rate will increase, according to equation (1.36):

$$k_{\text{dM}} = \frac{3D_{\text{mon}}D_{\text{W}}}{\left(\frac{C_{\text{P}}}{C_{\text{W}}}D_{\text{mon}}+D_{\text{W}}\right)r_{\text{s}}{}^2} \approx \frac{3D_{\text{W}}C_{\text{W}}}{C_{\text{P}}r_{\text{s}}{}^2} \tag{3.20}$$

where k_{dM} is the first order rate coefficient for desorption of radical from particles, D_{mon} is the diffusion coefficient of the radical inside the particle, and D_{W} is the diffusion coefficient of a free-radical into the aqueous phase. Knowing that k is a function of k_{dM}, from equation (1.43) k can be calculated as:

$$k = \frac{k_{\text{tr}}k_{\text{dM}}}{k_{\text{p}}^1} \tag{3.21}$$

where k_{tr} is the rate coefficient for transfer, and k_{p}^1 is the propagation rate coefficient for the (monomeric) free radical formed by transfer. It has been experimentally proven that k

increases with increasing $C_{W,}$ using methanol to increase C_W of styrene in water.[50]

Equations (3.20) and (3.21) show that k increases with increasing C_W, which explains the increased value of k in gamma relaxation experiments. But does $\rho_{thermal}$ increase with increasing CD concentration? The answer must be yes, so that $\bar{n}_{ss}$ can remain constant. On the other hand, $\rho_{thermal}$ was found not to change with the presence of CD, as will be discussed shortly.

The only possible explanation for the lack of change in the value of $\rho_{thermal}$ is that CD can only play a role in the presence of an initiating medium, while its effect becomes negligible when no chemical initiator or γ-rays are used. This can be concluded from equation (3.1)

$$\rho = \rho_{thermal} + \rho_{initiator} \tag{3.1}$$

As $\rho_{thermal}$ is found not to change with CD, $\rho_{initiator}$ is known to be directly affected by the monomer solubility, as in equation (1.30)

$$\rho_{initiator} = \frac{2fk_d[I]N_A}{N_c}\left(\frac{2\sqrt{k_d[I]k_{t,aq}}}{k_{p,aq}C_W}+1\right)^{1-z} \tag{3.18}$$

where k_d is the initiator decomposition rate coefficient, $k_{t,aq}$ is the rate coefficient for termination in aqueous phase, and z is the critical degree of polymerization. With $z \geq 1$, $\rho_{initiator}$ will certainly increase with an increased $C_{W.}$

It is then clear from these results that as long as no initiation technique (other than thermal initiation) is used, CD effect on both entry and on exit will be negligible.

3.6.2 γ-relaxation experiments with CD

These experiments are similar to those previously discussed in section 3.5.2., except that experiments discussed here include the use of 2% and 4% CD (of the weight of monomer)

with anionic latex, and only 4% CD of the weight of monomer added with cationic latex.

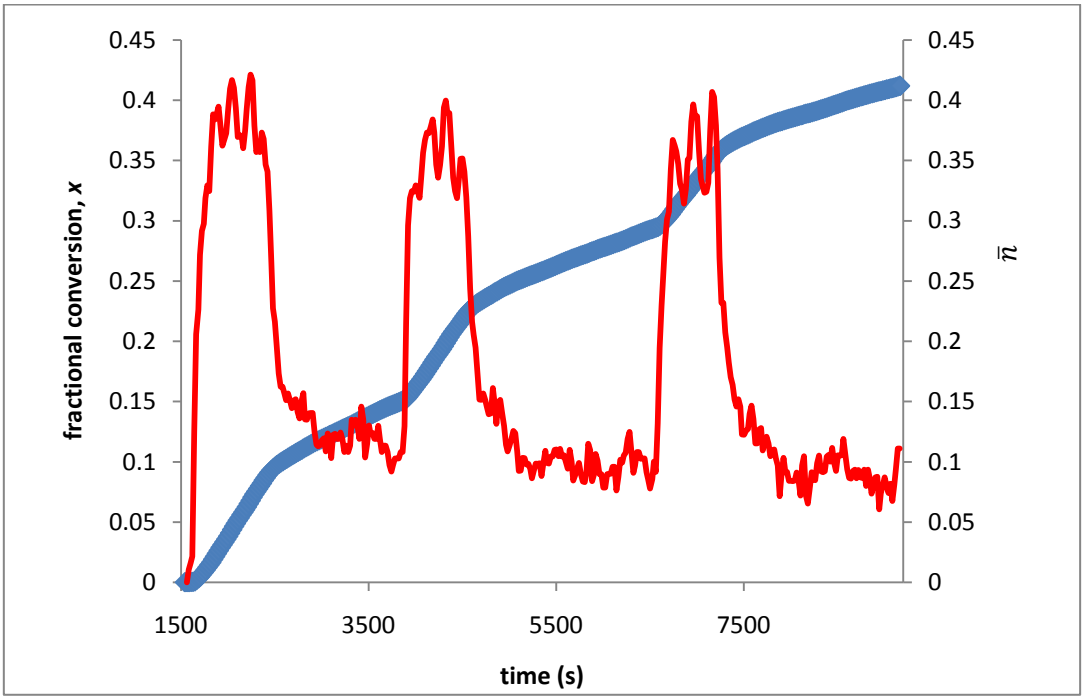

Figure 3.7a. Conversion (blue) and $\bar{n}$ (red) as functions of time for γ-relaxation experiment XSN507 (with anionic latex)

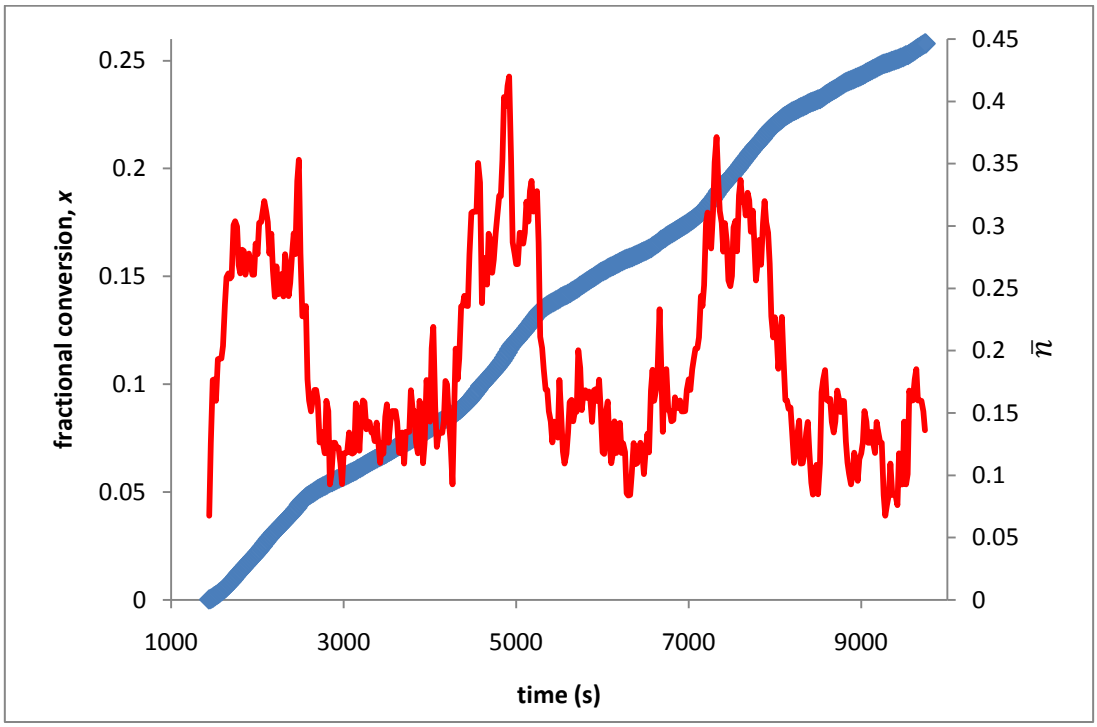

Figure 3.7b. Conversion (blue) and $\bar{n}$ (red) as functions of time for γ-relaxation experiment XSN105 (with cationic latex)

Figures 3.7 shows the typical results of two 4% CD experiments, one with AN05 and the

other with CA01. Figure 3.8 shows the analysis two relaxations for two 4% CD experiments.

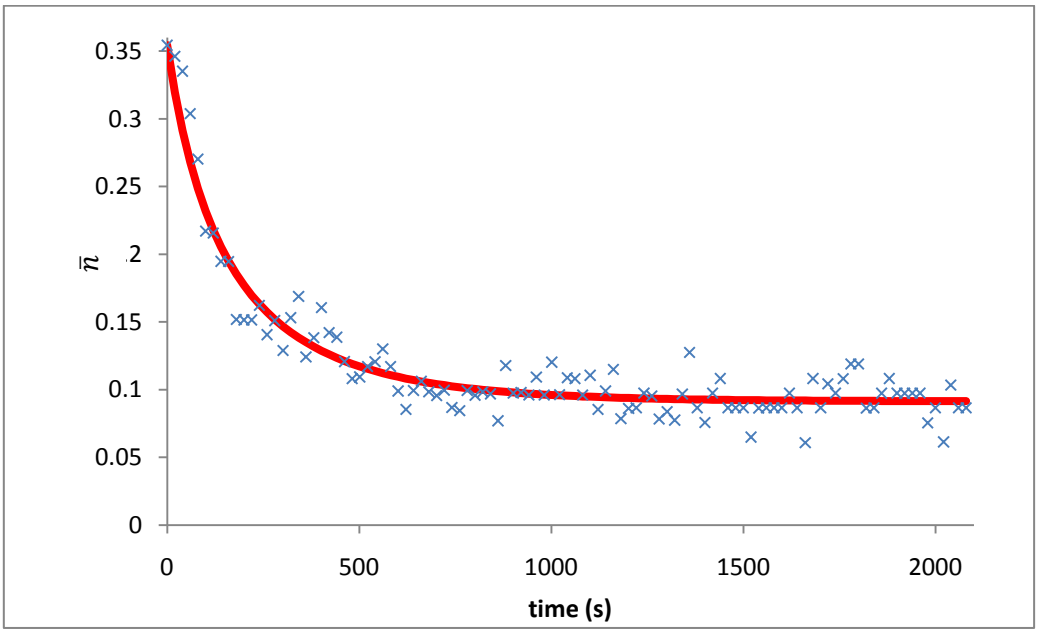

Figure 3.8a. $\bar{n}$ as a function of time for a typical γ-relaxation experiment (XSN507 R2, with anionic latex). Blue crosses: experimental values. Curve: equation (3.14) (best fit)

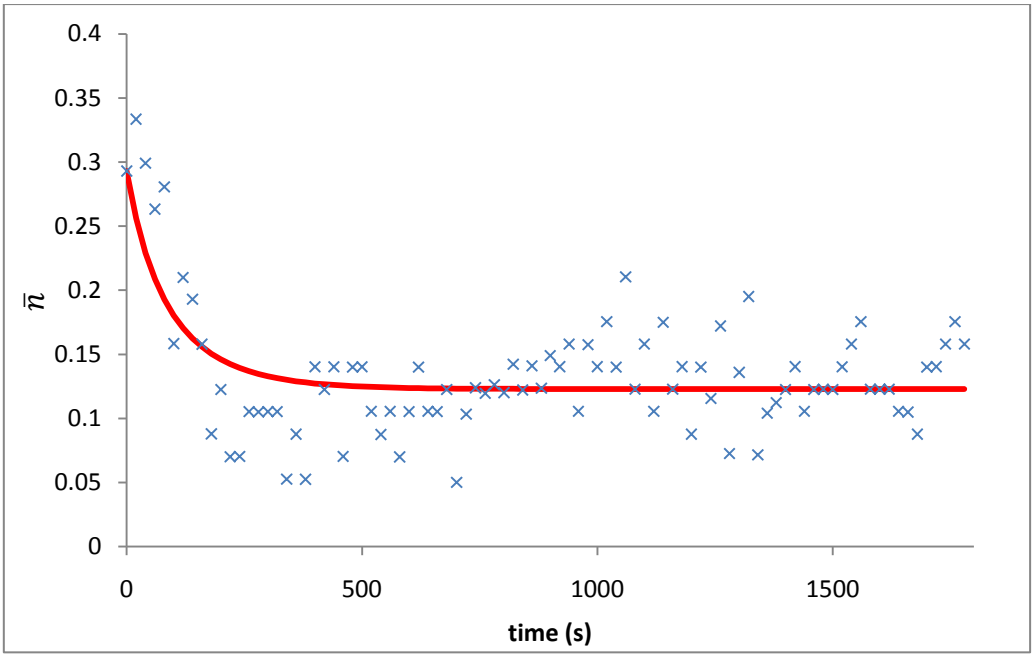

Figure 3.8b. $\bar{n}$ as a function of time for a typical γ-relaxation experiment (XSC103 R1, with cationic latex and 4% CD). Blue crosses: experimental values. Curve: equation (3.14) (best fit)

A comparison between figures 3.7 and 3.8 on one hand, and figures 3.2 and 3.3 on the

other, shows one of the advantages of using CD in emulsion polymerization experiments, which is that CD increases the latices stability.[51] This can be concluded from the lower level of scattering seen in case CD is used. The lower level of scattering means that $\bar{n}$ value does not change significantly from one moment to another, but rather it remains nearly constant once steady state has been reached.

Table 3.8 shows the effect of CD on $\bar{n}_{ss}$, entry and exit. During the experiments the 2% CD concentration was found to have negligible effect on $\bar{n}_{ss}$ for the anionic latex. So when the cationic latex was prepared and seeded emulsion polymerization experiments were run, only 4% CD concentration was used.

Seed Latex	CD concentration	Experiment	$\bar{n}_{ss}$ x 10^2	k x 10^2 s	$\rho_{thermal}$ x 10^4 s
AN05	2%	XSN511 R1	5.00	1.27	0.71
		XSN511 R2	3.55	1.14	0.29
		Average	**4.28**	**1.21**	**0.48**
AN05	4%	XSN507 R1	11.5	0.88	3.00
		XSN512 R1	7.02	0.82	0.90
		XSN512 R2	6.45	1.13	1.08
		XSN512 R3	6.39	1.02	0.95
		Average	**6.12**	**0.96**	**1.21**
CA01	4%	XSC103 R1	12.29	1.40	5.63
		XSC103 R2	9.59	1.69	3.85
		XSC105 R1	13.64	1.25	6.38
		XSC105 R2	14.11	0.85	4.74
		XSC105 R3	12.16	0.70	2.75
		Average	**12.36**	**1.18**	**4.67**

Table 3.8. Effect of the addition of CD on kinetic parameters of the latices during γ-relaxations.

Although the results have the same problem discussed above, of having a slightly higher value of $\bar{n}_{ss}$ than the values obtained from thermal experiments for the cationic latex, these values can still be used to give a comparative indication on the effect of CD, with

the assumption that the amine/peroxide reaction does not have a different path, kinetics or effect because of the presence of CD. Such an assumption needs to be validated later, but it will be followed just for this part of the analysis. With this assumption, the same discussion of section 3.5.4 can be used to analyze the results of experiments mentioned in table 3.8.

3.6.3 Discussion of γ-relaxation results

The first conclusion to be drawn from table 3.8 is that for the anionic latex, at 2% CD the $\bar{n}_{ss}$ value goes against the expected trend, which appears in the 4% CD. This agrees with earlier findings that the anionic surfactant used competes with styrene on CD cavities,[8,52] these findings go against the fact that k increases with C_W. But this conclusion is not to be taken to be completely accurate, because increasing the amount of CD can still speed up the emulsion polymerization process, to a small extent (as will be discussed in more details in chapter IV), which means that surfactant has been complexed within CD molecules to a level high enough that it no longer competes with styrene. On the other hand, a common factor in all the research previously done about CD effect on emulsion polymerization is that it was either surfactant free[8] or using sodium lauryl sulphate (or other anionic surfactants) as surfactant.[52] This should explain why the anionic latex had this problem while the cationic latex did not.

In all experiments run using anionic latex, AMA-80 surfactant was used. This surfactant has 80% of its amount (by mass) as sodium di(1,3-dimethylbutyl)sulfosuccinate. From its structure, sodium di(1,3-dimethylbutyl)sulfosuccinate has 16 carbon atoms, and knowing that sodium lauryl sulphate has 14 carbon atoms, the assumption that both of them have similar molecular sizes can be considered valid. Consequently, the results drawn before[52] that CD forms a complex with the surfactant can be also applied to the case of AMA-80, which clarifies why the rate of polymerization with the anionic latex did not change very much when anionic latex was used.

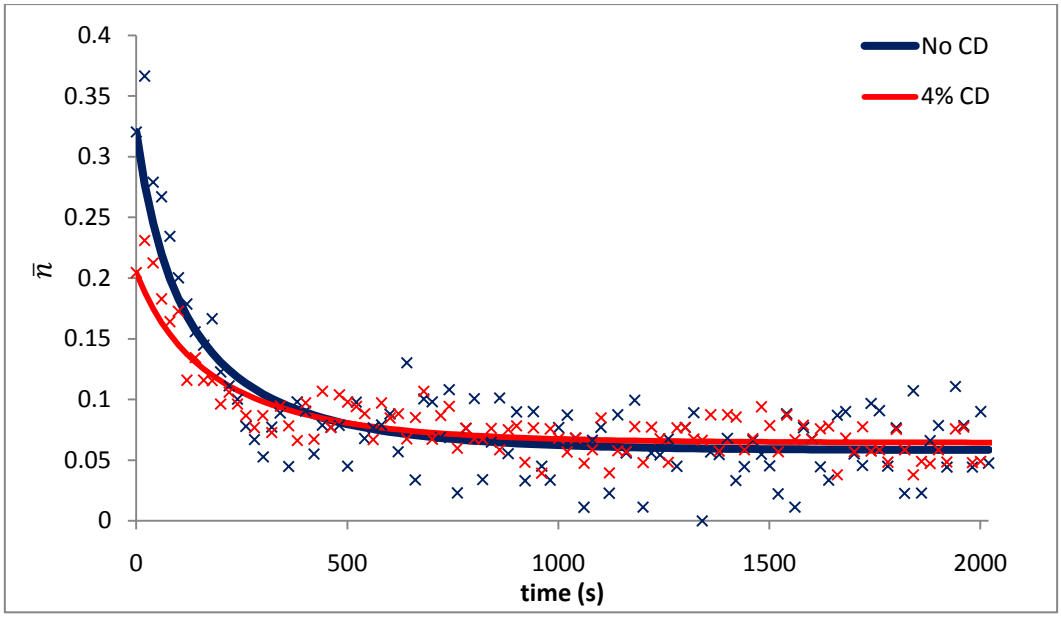

Figure 3.9a. $\bar{n}$ as a function of time for two γ-relaxation experiment with anionic latex (XSN508 R2, with no CD and XSN512 R2 with CD). Crosses: experimental values. Curves: equation (3.14) fitted. The curves show the effect of the addition of 4% CD to the reaction mixture. As CD has no major effect on the entry and exit rate coefficients, the steady-state part of the curves for both experiments are almost identical.

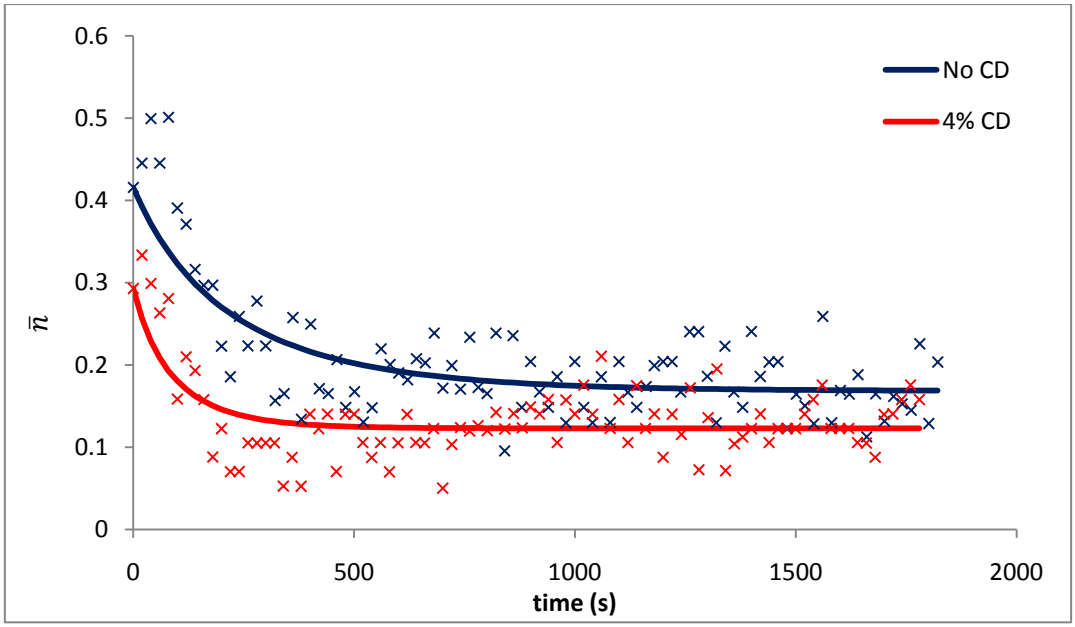

Figure 3.9b. $\bar{n}$ as a function of time for two γ-relaxation experiment with cationic latex (XCS104 R2, with no CD and XSC103 R1 with CD). Crosses: experimental values. Curves: equation (3.14) fitted. The curves show the effect of the addition of 4% CD to the reaction mixture. As the exit rate coefficients increases with constant thermal entry rate coefficient, $\bar{n}$ decreases with CD addition.

Although this conclusion seems true for the anionic surfactant, the cationic surfactant used DTAB (dodecyltrimethylammonium bromide) seems to act in a different way with CD. This surfactant has a smaller structure, the carbon chain has only 12 carbon atoms, so it can be considered to be more competitive with styrene for complexation with CD. But this was not found to be the case. The increase in the value of *k* with the use of CD makes it clear that the solubility of styrene has increased in water and so the free radical exit rate has increased.

But why would styrene complexation with CD go in two different paths with different surfactants? A simple way of answering would be the environment type. In the case of an anionic environment styrene complexation is not going to happen very easily, while in a cationic environment it is easier. But this assumption would not be valid because of the hydrophobic nature of the CD cavity, which should not be affected by the charges in the surrounding medium.

What can be the reason then? Sometimes basic chemistry can help answer some questions which may not find an answer with advanced chemistry. This is a good example for such a question. Looking at the structure of both compounds, it is easy to notice that the hydrophilic side of the anionic surfactant has an $-SO_3^-\ Na^+$ group, for which the electronegativity[53] of the bond between the oxygen and sodium is 2.4, which makes the bond highly polar. While the hydrophilic side of the cationic surfactant has an $-N(CH_3)^+\ Br^-$ group, for which the electronegativity of the nitrogen-bromide bond is 0.2, which makes the polarity of the bond very low. When the anionic surfactant is complexed within the CD, styrene can be easily expelled from the CD cavity because of the high polarity present at the cavity, a result of the high electronegativity. On the other hand, complexing the cationic surfactant within CD does not represent any problem for styrene to be complexed, both compounds have low polarity and can be easily exchanged between the CD cavities, allowing even the styrene and the surfactant to co-exist within the CD cavity, which gives the CD complexation an advantage which was not available in the anionic environment.

Although such an explanation appears to be true, as per the current knowledge available, further research should be done about this, using anionic surfactants whose hydrophilic groups have lower electronegativity.

For the anionic latex, the previous explanation makes it clear why *k* has decreased with increasing CD concentration, as shown in table 3.8. The continuous decrease of *k* with increasing CD concentration can be explained by the inability of the styrene monomers to fit into the CD cavity with the AMA-80 surfactant present. It was noted though that $\rho_{thermal}$ and $\bar{n}_{ss}$ increased slightly at 4% CD concentration, which can be explained by the fact that $\rho_{thermal}$ is independent of surfactant concentration, [54] so the only reason for this increase is the slight increase in styrene solubility in water at 4% CD concentration. The reason why this slight increase in C_W did not affect *k* remains obscure, but a possible explanation is that *k* decreases with a decrease in surfactant, a more focused study on surfactant effect on exit in the future may clarify this point.

The most important conclusion from these results is that the effect of the aqueous phase solubility of the monomer on the value of *k*. with no CD in the aqueous medium, the exit rate coefficient $k = 7 \times 10^{-3}$ s^{-1} as shown in table 3.4, and with 4% CD $k = 1.18 \times 10^{-2}$ s^{-1} as shown in table 3.8. In presence of DTAB surfactant without CD, styrene $C_W = 5.83 \times 10^{-3}$ mol/L, and with 4% CD, $C_W = 9.42 \times 10^{-3}$, as will be further discussed in chapter IV.

The ratio between the values of C_W with and without CD is equal to the ratio between the values of *k* with and without CD. This conclusion shows excellent agreement between equation (3.21) and the results of this work, confirming the accuracy of the model used to analyze the results of this work.

3.6.4 γ-insertion experiments with CD

Calculating the effect of CD on *k* using the γ-irradiation periods show an effect for CD for the cationic latex, results for all γ-irradiation experiments with CD are shown in table 3.9.

The change of values for the cationic latex is similar to what has been discussed in section 3.5.4., the amine/peroxide redox reaction has a similar effect with the presence of CD, and the increase in *k* with 4% CD because of this side reaction is similar to that without CD. The only difference is that the increase in the value of *k* with CD half the increase in the value of *k* without CD. This can be explained by the stabilizing effect of CD[51], which has diminished, though could not remove the amine/peroxide side reaction effect.

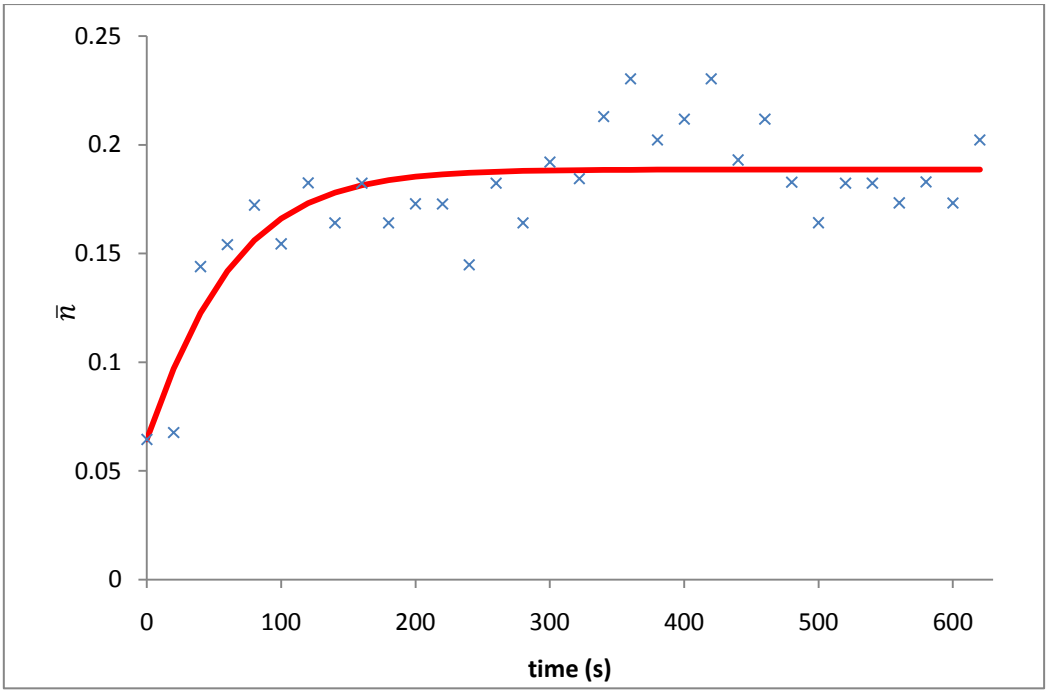

Figure 3.10a. $\bar{n}$ as a function of time for a typical γ-relaxation experiment with 4% CD (XSN512 I3, with anionic latex). Blue crosses: experimental values. Curve: equation (3.14) (best fit)

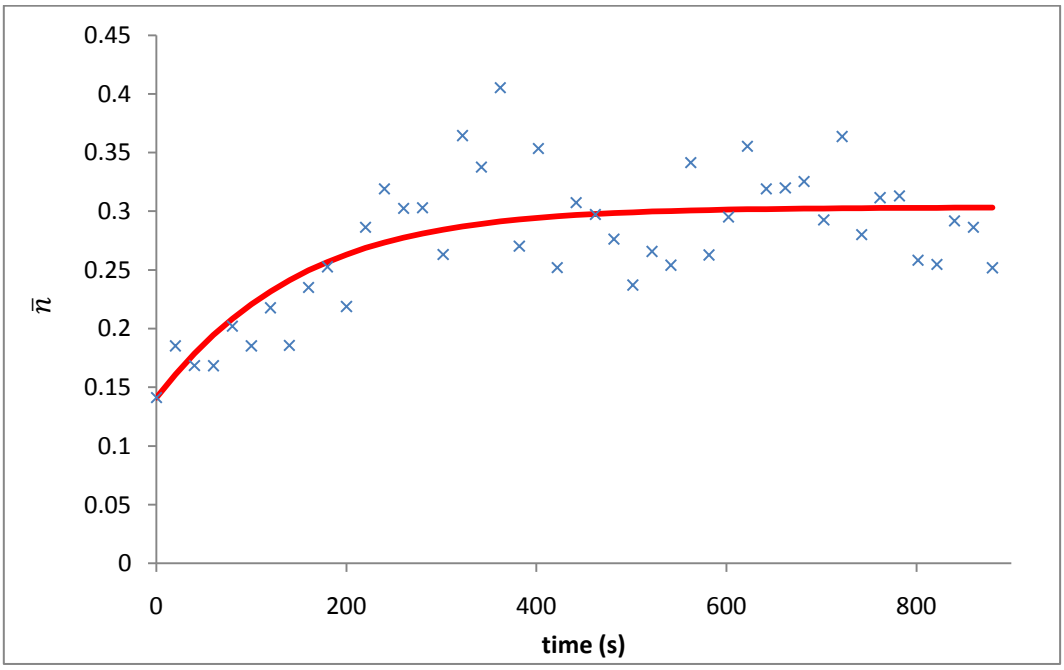

Figure 3.10b. $\bar{n}$ as a function of time for a typical γ-relaxation experiment with 4% CD (XSC105 I3, with cationic latex). Blue crosses: experimental values. Curve: equation (3.14) (best fit)

The last question to be answered is about the effect of CD on the anionic latex results for *k* obtained from γ-irradiation. The value of *k* obtained from γ-irradiation in case of 2% CD is smaller than that obtained from γ-relaxation. In the case of 4% CD, *k* from γ-irradiation is greater. This can be explained by the fact that a number of factors were not tightly controlled. Changing surfactant concentrations, and the effect of peroxide polymerization whose rate can increase with increasing CD, in addition to all other disadvantages of using γ-irradiation data to calculate *k*, already discussed in 3.5.3. All these factors together might shed some light on why the values of *k* obtained from γ-irradiation data might not be considered accurate.

Seed Latex and % CD		$k \times 10^2$ s		ρ_γ x s	$\rho_{thermal}$ x s
	Experiment	γ-irradiation	γ-relaxation	γ-irradiation	γ-relaxation
AN05 2% CD	XSN511 I&R 1	0.46	1.27	4.84×10^{-3}	7.07×10^{-5}
	XSN511 I&R 2	0.39	1.14	4.06×10^{-3}	2.86×10^{-5}
	XSN511 I&R 3	0.72	1.29	4.63×10^{-3}	1.70×10^{-5}
AN05 4% CD	XSN507 I&R 1	1.27	0.88	2.10×10^{-3}	3.00×10^{-4}
	XSN507 I&R 2	1.61	0.79	1.39×10^{-2}	1.62×10^{-4}
	XSN512 I&R 2	1.95	0.82	2.59×10^{-3}	9.01×10^{-5}
	XSN512 I&R 3	0.98	1.13	1.39×10^{-3}	1.08×10^{-4}
	XSN512 I&R 1	1.98	1.02	2.27×10^{-3}	9.53×10^{-5}
CA01	XSC103 I&R 1	0.42	1.40	1.76×10^{-3}	5.63×10^{-4}
	XSC103 I&R 2	0.54	1.69	2.75×10^{-3}	3.85×10^{-4}
	XSC105 I&R 1	0.67	1.25	2.29×10^{-3}	6.38×10^{-4}
	XSC105 I&R 2	0.35	0.85	1.90×10^{-3}	4.74×10^{-4}
	XSC105 I&R 3	0.35	0.70	1.65×10^{-2}	2.75×10^{-4}

Table 3.9. *k* values from γ-irradiation and γ-relaxation. Results in red are totally (or partially) in interval III.

Seed latex, CD	*k* from γ-irradiation x s	*k* from γ-relaxation x s
AN05, NO CD	1.37×10^{-2}	1.36×10^{-2}
AN05, 2% CD	4.22×10^{-3}	1.23×10^{-2}
AN05, 4% CD	1.65×10^{-2}	9.62×10^{-3}
CA01, NO CD	9.24×10^{-4}	5.42×10^{-3}
CA01, 4% CD	4.13×10^{-3}	1.18×10^{-2}

Table 3.10. *k* values as averaged from results in table 3.6 and 3.9. These averages do not include the first irradiation of every experiment and do not include interval III results.

3.7 Summary of results

Seed Latex	$\bar{n}_{ss}$ x 10^2	*k* x 10^2 s	$\rho_{thermal}$ x 10^4 s
AN05	6.49	1.36	1.32
CA01	10.82	0.70	2.09

Table 3.11. Results of thermal and γ-relaxation polymerization experiments

Table 3.11 gives a summary for the results of all experiments done to calculate $\rho_{thermal}$ and *k*, in case of complete CD absence. The value of $\rho_{thermal}$ was calculated from the thermal polymerization experiments, while *k* was calculated only from the γ-relaxation experiments which do not involve the use of CD. To the opposite of that, some thermal initiation experiments included the use of 4% CD (of the total weight of monomer), and $\bar{n}_{ss}$ for such experiments was found to have a negligible change from the values of $\bar{n}_{ss}$ in absence of CD. The values presented in table 3.11 are the values used throughout all calculations of this work, unless otherwise specified.

Another fact obtained from table 3.11, is that the value of $\rho_{thermal}$ is not very different between the anionic and cationic latices, contrary to a situation faced in an earlier research[2,3]. The problem was mainly because of the formation of some amine and peroxide products because of the thermal decomposition of the V-50 initiator. Such compounds interact with the reaction kinetics resulting in high value for $\bar{n}_{ss}$, and consequently a very high value for $\rho_{thermal}$.

During the course of this work, this problem was avoided through a very simple technique; the cationic latex was prepared at a high temperature (94^{o}C), and remained heated for 24 hours under nitrogen atmosphere. It is believed that under such conditions any peroxides or amines formed will easily decompose. The success of this technique is clear from the comparative results of $\rho_{thermal}$ for both anionic and cationic latices.

It is good to mention that the average values of $\bar{n}_{ss}$ and $\rho_{thermal}$ for the cationic latex include results of experiments done with CD. As will be discussed in section 3.6.1, CD was found not to affect thermal polymerization experiments.

3.8 Comparison with previous work[2,3]

	Anionic		Cationic	
	$\rho_{thermal}$ x s	k x s	$\rho_{thermal}$ x s	k x s
Current work	1.32 x 10^{-4}	1.36 x 10^{-2}	2.09 x 10^{-4}	7.00 x 10^{-3}
Van Berkel	1.1 x 10^{-4}	1.2 x 10^{-2}	2.5 x 10^{-5}	9.0 x 10^{-3}

Table 3.12. Comparison between results of entry and exit rate coefficients obtained through the current work and through the previous work of van Berkel. Results of the current work include only no CD experiments.

Table 3.12 shows that entry and exit rate coefficients for the anionic latex were similar. Cationic latex results are different, especially in the value of $\rho_{thermal}$. The main reason for this was the long period of heat treatment used by van Berkel to confirm the absence of styrene peroxides from the latex.

As a general conclusion, it is clear that because the physical properties of latices used in the current and previous work are similar (this includes average particle diameter and C_p^{sat}), obtaining similar kinetic parameters confirms the accuracy of the results of this current work.

3.9 Conclusions

The effect of CD on the kinetic parameters of emulsion polymerization has been studied

for two different polystyrene emulsion polymerization systems, one anionic and one cationic. Both systems have been studied thoroughly using thermal polymerization and γ-radiolysis to get the values of entry and exit rate coefficients, in absence of any chemical initiator.

Results for the cationic latex have shown an agreement with the fact that increasing the aqueous phase solubility of the monomer increases the values of its entry and exit rate coefficients, but overall the reaction rate increases with presence of CD in the aqueous phase. Moreover, the presence of a cationic surfactant within the mixture was found not to have any negative effect on the reaction rate. Furthermore, spontaneous polymerization is not an aqueous phase process.

The anionic latex results showed that CD does not have the expected effect of increasing the reaction rate because of increasing the solubility. This is mainly because of competitive effect that both styrene and surfactant on the CD present. But it was concluded that increasing the amount of CD will reduce this problem, and will speed up the reaction rate, but not to a high level.

As both thermal entry and exit rate coefficients have been calculated and their values have been confirmed through the work done in this chapter, both with and without CD, having a thorough analysis for the chemically initiated experiments and calculating their entry efficiency with and without CD can now be done, and this will be discussed in the next chapter.

Appendix 3.1. Derivation of equation (3.14)

$$\frac{\mathrm{d}\bar{n}}{\mathrm{d}t} = (\rho + \alpha k\bar{n})(1 - 2\bar{n}) - k\bar{n}$$

$$\frac{\mathrm{d}\bar{n}}{\mathrm{d}t} = \rho - 2\bar{n}\rho + \alpha k\bar{n} - 2\alpha k\bar{n}^2 - k\bar{n}$$

$$\frac{\mathrm{d}\bar{n}}{\mathrm{d}t} = -2\alpha k\bar{n}^2 + [-2\rho - (1 - \alpha)k]\bar{n} + \rho$$

$$\frac{\mathrm{d}\bar{n}}{\mathrm{d}t} = \omega\bar{n}^2 + g\bar{n} + \rho$$

where ω = -2αk, and g= -2ρ - (1-α)k. Integrating time (from 0 to t) and $\bar{n}_0$ from $\bar{n}$ to $\bar{n}$ yiels

$$t = \frac{1}{\omega}\int_{\bar{n}_0}^{\bar{n}} \frac{\mathrm{d}\bar{n}}{\left(\bar{n}+\frac{g}{2\omega}\right)-\left(\frac{g^2}{4\omega^2}-\frac{\rho}{\omega}\right)}$$

$$t = \frac{-1}{2\omega\sqrt{\frac{g^2}{4\omega^2}-\frac{\rho}{\omega}}}\left[\ln\left(\frac{\bar{n}+\frac{g}{2\omega}+\sqrt{\frac{g^2}{4\omega^2}-\frac{\rho}{\omega}}}{\bar{n}+\frac{g}{2\omega}-\sqrt{\frac{g^2}{4\omega^2}-\frac{\rho}{\omega}}}\right) - \ln\left(\frac{\bar{n}_0+\frac{g}{2\omega}+\sqrt{\frac{g^2}{4\omega^2}-\frac{\rho}{\omega}}}{\bar{n}_0+\frac{g}{2\omega}-\sqrt{\frac{g^2}{4\omega^2}-\frac{\rho}{\omega}}}\right)\right]$$

$$-2\omega t\sqrt{\frac{g^2}{4\omega^2}-\frac{\rho}{\omega}} = \ln\left[\frac{\left(\frac{\bar{n}+\frac{g}{2\omega}+\sqrt{\frac{g^2}{4\omega^2}-\frac{\rho}{\omega}}}{\bar{n}+\frac{g}{2\omega}-\sqrt{\frac{g^2}{4\omega^2}-\frac{\rho}{\omega}}}\right)}{\left(\frac{\bar{n}_0+\frac{g}{2\omega}+\sqrt{\frac{g^2}{4\omega^2}-\frac{\rho}{\omega}}}{\bar{n}_0+\frac{g}{2\omega}-\sqrt{\frac{g^2}{4\omega^2}-\frac{\rho}{\omega}}}\right)}\right]$$

$$\frac{\bar{n}+\frac{g}{2\omega}+\sqrt{\frac{g^2}{4\omega^2}-\frac{\rho}{\omega}}}{\bar{n}+\frac{g}{2\omega}-\sqrt{\frac{g^2}{4\omega^2}-\frac{\rho}{\omega}}} = \frac{\bar{n}_0+\frac{g}{2\omega}+\sqrt{\frac{g^2}{4\omega^2}-\frac{\rho}{\omega}}}{\bar{n}_0+\frac{g}{2\omega}-\sqrt{\frac{g^2}{4\omega^2}-\frac{\rho}{\omega}}}e^{-2\omega t\sqrt{\frac{g^2}{4\omega^2}-\frac{\rho}{\omega}}}$$

$$\frac{\bar{n}+\frac{g}{2\omega}+\frac{1}{2\omega}\sqrt{g^2-4\omega\rho}}{\bar{n}+\frac{g}{2\omega}-\frac{1}{2\omega}\sqrt{g^2-4\omega\rho}} = \frac{\bar{n}_0+\frac{g}{2\omega}+\frac{1}{2\omega}\sqrt{g^2-4\omega\rho}}{\bar{n}_0+\frac{g}{2\omega}-\frac{1}{2\omega}\sqrt{g^2-4\omega\rho}}e^{-t\sqrt{g^2-4\omega\rho}}$$

$$\bar{n}+\frac{g}{2\omega}+\frac{1}{2\omega}\sqrt{g^2-4\omega\rho} =$$

$$\left(\bar{n}+\frac{g}{2\omega}-\frac{1}{2\omega}\sqrt{g^2-4\omega\rho}\right)\left(\frac{\bar{n}_0+\frac{g}{2\omega}+\frac{1}{2\omega}\sqrt{g^2-4\omega\rho}}{\bar{n}_0+\frac{g}{2\omega}-\frac{1}{2\omega}\sqrt{g^2-4\omega\rho}}\right)e^{-t\sqrt{g^2-4\omega\rho}}$$

$$\bar{n}+\frac{g+\sqrt{g^2-4\omega\rho}}{2\omega} = \left(\frac{\bar{n}_0+\frac{g+\sqrt{g^2-4\omega\rho}}{2\omega}}{\bar{n}_0+\frac{g-\sqrt{g^2-4\omega\rho}}{2\omega}}\right)\left(\bar{n}+\frac{g-\sqrt{g^2-4\omega\rho}}{2\omega}\right)e^{-t\sqrt{g^2-4\omega\rho}}$$

$$\bar{n} + \frac{g+\sqrt{g^2-4\omega\rho}}{2\omega} =$$

$$\bar{n}\left(\frac{\bar{n}_0+\frac{g+\sqrt{g^2-4\omega\rho}}{2\omega}}{\bar{n}_0+\frac{g-\sqrt{g^2-4\omega\rho}}{2\omega}}\right)e^{-t\sqrt{g^2-4\omega\rho}} + \frac{g-\sqrt{g^2-4\omega\rho}}{2\omega}\left(\frac{\bar{n}_0+\frac{g+\sqrt{g^2-4\omega\rho}}{2\omega}}{\bar{n}_0+\frac{g-\sqrt{g^2-4\omega\rho}}{2\omega}}\right)e^{-t\sqrt{g^2-4\omega\rho}}$$

$$\bar{n}\left[1 - e^{-t\sqrt{g^2-4\omega\rho}}\left(\frac{\bar{n}_0+\frac{g+\sqrt{g^2-4\omega\rho}}{2\omega}}{\bar{n}_0+\frac{g-\sqrt{g^2-4\omega\rho}}{2\omega}}\right)\right] =$$

$$\frac{g-\sqrt{g^2-4\omega\rho}}{2\omega}e^{-t\sqrt{g^2-4\omega\rho}}\left(\frac{\bar{n}_0+\frac{g+\sqrt{g^2-4\omega\rho}}{2\omega}}{\bar{n}_0+\frac{g-\sqrt{g^2-4\omega\rho}}{2\omega}}\right) - \frac{g+\sqrt{g^2-4\omega\rho}}{2\omega}$$

$$\bar{n} = \frac{\frac{-g-\sqrt{g^2-4\omega\rho}}{2\omega} - \frac{-g+\sqrt{g^2-4\omega\rho}}{2\omega}e^{-t\sqrt{g^2-4\omega\rho}}\left(\frac{\bar{n}_0+\frac{g+\sqrt{g^2-4\omega\rho}}{2\omega}}{\bar{n}_0+\frac{g-\sqrt{g^2-4\omega\rho}}{2\omega}}\right)}{1-e^{-t\sqrt{g^2-4\omega\rho}}\left(\frac{\bar{n}_0+\frac{g+\sqrt{g^2-4\omega\rho}}{2\omega}}{\bar{n}_0+\frac{g-\sqrt{g^2-4\omega\rho}}{2\omega}}\right)} \qquad \text{(a)}$$

taking $\theta^2 = g^2 - 4\omega\rho$; $p = \frac{-g-\theta}{2\omega}$; $\delta = \frac{p-\bar{n}_0}{\lambda-\bar{n}_0}$ and $\lambda = \frac{-g+\theta}{2\omega}$, equation (a) can be written as

$$\bar{n} = \frac{p-\lambda\delta\exp(-\theta t)}{1-\delta\exp(-\theta t)}$$

which is equation (3.14)

Appendix 3.2 Formulations for all γ-relaxation and thermal initiation experiments for latices AN05 and CA01

Latex AN05 – γ-relaxation experiments

Experiment	Component mass				Vessel
	latex	monomer	AMA-80	CD	volume
XSN502	1.75	1.32	0.08	0	32.514
XSN503	1.84	1.27	0.086	0	36.160
XSN505	1.72	1.30	0.095	0.024	32.514
XSN506	1.77	1.25	0.091	0.050	32.514
XSN507	1.78	1.27	0.098	0.053	29.317
XSN508	1.73	1.28	0.097	0	36.160
XSN509	1.85	1.27	0.088	0	30.478
XSN510	1.87	1.22	0.090	0.0253	30.478
XSN511	1.77	1.37	0.117	0	29.317
XSN512	2.00	1.40	0.098	0.026	36.160
XSN513	1.84	1.35	0.099	0.051	30.478

All component masses are in grams, vessel volume is in cm^3.

Latex CA01 – γ-relaxation experiments

Experiment	Component mass				Vessel
	latex	monomer	DTAB	CD	volume
XSC102	1.61	1.32	0.07	0	29.317
XSC103	1.66	1.32	0.07	0.06	29.317
XSC104	1.57	1.43	0.07	0	29.317
XSC105	1.73	1.46	0.074	0.054	36.160

All component masses are in grams, vessel volume is in cm^3.

Latex AN05 – thermally initiated experiments

Experiment	Component mass				Vessel
	latex	monomer	AMA-80	CD	volume
SN501	3.01	2.03	0.07	0	57.14
SN502	3.04	2.00	0.08	0	57.04
SN503	3.04	2.10	0.08	0	57.14
SN504	3.12	2.35	0.07	0	57.04
SN505	3.04	2.08	0.07	0	57.14
SN506	3.04	2.13	0.08	0	57.14

All component masses are in grams, vessel volume is in cm^3.

Latex CA01 – thermally initiated experiments

Experiment	Component mass				Vessel
	latex	monomer	DTAB	CD	volume
SC146	3.24	2.32	0	0	57.81
SC147	3.23	2.31	0	0	57.81
SCT150	3.17	2.24	0.0980	0	57.14
SCT151	3.21	2.47	0.0967	0	57.14
SC172	3.22	2.30	0.0995	0.0935	57.04
SC173	3.18	2.24	0.0982	0.0925	57.14

All component masses are in grams, vessel volume is in cm^3.

References

(1) Maxwell, I., Morrison, B., Napper, D. and Gilbert, R., *Macromolecules*, **1991**, 24, 1629.

(2) van Berkel, K., Russell, G., Gilbert, R., *Macromolecules*, **2003**, 36, 3921.

(3) van Berkel, K., *Entry and the Kinetics of Emulsion polymerization*, a PhD thesis, University of Canterbury, 2004

(4) Easton, C. and Lincoln, S., *Modified Cyclodextrins*, **1999**, Imperial College Press, London

(5) Loftsson, T. and Duchêne, D., *International Journal of Pharmaceuticals*, **2007**, 329, 1

(6)Makoto M. and Monflier E., *Cyclodextin Catalysis* in Helena D. (editor), *Cyclodextrins and their complexes*, , **2006**, Wiley-VCH, Weinheim

(7) Szejtli, J., *Chem. Rev.*, **1998**, 98, 1743

(8) Hu, J., Li., Y., Ji, H. and Chen, Z., *Gaofenzi Xuebao*, **2007**, 3, 246

(9) Hu, J., Li, S., Wang, D. and Liu, B., *Polymer International*, **2004**, 53, 1003

(10) Ritter, H., Storsberg, J., van Aert, H. and Roost, C., *Macromolecules*, **2003**, 36, 50.

(11) Ritter, H., Steffens, C. and Storsberg, J., *e-polymers*, **2005**, 34, 1.

(12) Mayo, F. R., *Journal of the American Chemical Society* **1968**, 90 (5), 1289.

(13) Hawkett, B., Napper, D. and Gilbert, R., *Journal of the Chemical Society, Faraday Transactions 1*, **1980**, 76, 1323.

(14) Scheren, P., Russell, G., Sangster, F., Gilbert, G. and German, A., *Macromolecules*, **1995**, 28, 3637.

(15) Khuong, K., Jones, W., Pryor W. and Houk, K., *J. Am. Chem. Soc.*, **2005**, 127, 1265.

(16) Lieser, K., *Nuclear and Radiochemistry Fundamentals and Applications*, **1996**, VCH Verlagsgesellschaft, Germany

(17) McKay, H., *Principles of Radiochemistry*, **1971**, Butterworth & Co Ltd, London

(18) O'Donnell, J. and Sangster, D., *Principles of Radiation Chemistry*, **1970**, Edward Arnold Ltd, London

(19) Gilbert, Robert G., *Emulsion polymerisation, a mechanistic approach*, **1995**, Academic Press, London.

(20) Casey, B., Morrison, B., Maxwell, I., Gilbert, R. and Napper, D., *J. Polym. Sci. A: Polym. Chem.*, **1994**, 32, 605

(21) Morrison, B., Casey, B., Lacik, I., Leslie, G., Sangster, D., Gilbert, R. and Napper, D., *J. Polym. Sci. A: Polym. Chem.*, **1994**, 32, 631

(22) De Bruyn, H., Gilbert, R. and Hawkett, B., *polymer*, **2000**, 41, 8633.

(23) Miller, C., Sudol, E., Silebi, C. and El-Aasser, M., *Macromolecules*, **1995**, 28, 2754

(24) Miller, C., Sudol, E., Silebi, C. and El-Aasser, M., *Macromolecules*, **1995**, 28, 2765

(25) Miller, C., Sudol, E., Silebi, C. and El-Aasser, M., *Macromolecules*, **1995**, 28, 2772

(26) Ugelstad, J., Hansen, F., *Rubber Chem. Technol.*, **1976**, 49, 536

(27) Wilke, C. R., Chang, P., *A.I.Ch.E.J.*, **1955**, *1*, 264

(28) Lide, D.(editor), *Handbook of Chemistry and Physics*, **2005**, Taylor and Francis, Florida

(29) Tobolsky, A. and Offenbach, J., *J. Polym. Sci*., **1955**, 16, 311.

(30) Heuts, J. and Russell, R., *European Polymer Journal*, **2006**, 42, 3
(31) Hawkins, E., *Organic Peroxides*, **1961**, E. and F. F. SPON Ltd., London
(32) Mayo, F., A., *J. American Chemical Soc.*, **1958**, 80, 2465
(33) Maillard, B., Ingold, U., and Scaiano, J., *J. American Chemical Soc.*, **1983**, 105, 5095.
(34) Adams G. and Wilson, R., *Trans. Faraday. Soc.*, **1969**, 65, 2981
(35) Shastri., L., Huie, R. and Neta, P., *J. Phys. Chem.*, **1990**, 94, 1895
(36) Howard, J., *Free-Radical reaction mechanisms involving peroxides in solution*, Patai, S. (editor), *The chemistry of peroxides*, **1983**, John Wiley and Sons ltd.
(37) Mayo, F. and Miller, A., *J. American Chemical Soc.*, **1956**, 78, 1017
(38) Mayo, F. and Miller, A., *J. American Chemical Soc.*, **1956**, 78, 1023
(39) Moad, G. and Solomon, D., *The chemistry of radical polymerization 2nd fully revised edition*, **2006**, Elsevier.
(40) Singh, R., Desai, S., Sivaram, S. and Kishore, K., *Macromol. Chem. Phys*., **2002**, 203, 2163
(41) Mukundan, T., Bhanu, V. and Kishore, K., Journal of the Chemical Society, Chemical Communications, **1989**, 12, 780
(42) Subramanian, K., Murthy, K., and Kishore, K., *Polymer*, **1997**, 38, 527
(43) Weast, R.(editor), *Handbook of Chemistry and Physics*, **1984**, CRC press
(44) Dougherty, T., *J. Am. Chem. Soc.*, **1961**, 83, 4849
(45) W.D. Harkins, Journal of the American Chemical Society, **1947**, 69, 1428
(46) W.V. Smith and R.H. Ewart, *Journal of Chemical Physics*,**1948**, 16,592
(47) W.D. Harkins, *Journal of Chemical Physics*,**1945**, 13,381
(48) W.D. Harkins, *Journal of Chemical Physics*,**1946**, 14,47
(49) W.D. Harkins, *Journal of the American Chemical Society*, **1947**, 69, 1428
(50) Adams, M., Napper, D. and Gilbert, R., *J. Chem. Soc. Faraday Trans. 1*, **1986**, 82, 1979
(51) Ritter, H., Storsberg, J., van Aert, H. and Roost, C., *Macromolecules*, **2003**, 36, 50.
(52) Hu, J., Li, S. and Liu, B, *Journal of Polymer Material*, **2005**, 22, 213.
(53) Chang, R., *Chemistry*, 9th Edition, **2007**, McGraw Hill Higher Education, New York
(54) Adams, M., Trau, M., Gilbert, R., Napper, D., Sangster, D., *Aust. J. Chem.*, **1988**, 41, 1799

Chapter IV

Effect of Cyclodextrin on the Chemically Initiated Emulsion Polymerization of Styrene

4.1 Introduction

Emulsion polymerization of styrene was first developed in the 1930s,[1] and then was expanded for mass production during World War II. During that time, the main technique used to initiate the polymerization reaction was the use of a chemical initiator, which was called "catalyst" during that period.[2] Currently, the most commonly used initiation technique is the use of chemical initiators, for example the salts of persulphuric acid, like potassium persulphate (KPS).[1] This is mainly because of the cheap price of chemical initiators compared to other techniques, like γ-rays, whose cost is relatively high because of the high cost of the radioactive isotope.[3] Moreover, polymerization initiation is not considered as one of the most common uses of radioactive materials.[4]

The present work is inspired by the work done previously by Maxwell and Morrison and their model for entry.[5] The Maxwell-Morrison model was validated by the authors through the use of chemically initiated emulsion polymerization experiments. The latex used was stabilized using an anionic surfactant, and the initiator used was KPS (scheme 4.1).

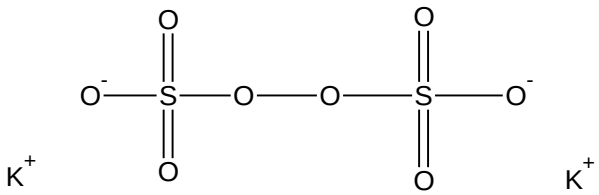

Scheme 4.1. Chemical structure of potassium persulphate (KPS)

The work of Maxwell and Morrison was further validated later on through the work of van Berkel, who worked with four latices, two were stabilized with anionic surfactants, and the other two were stabilized through the use of cationic surfactants.[6,7] Through the work of van Berkel the effect of 2,2'azobis(2-methylpropionamidine)dichloride (scheme

4.2), commercially known as (V-50), which is a cationically charged initiator, was tested. Similarly for KPS.

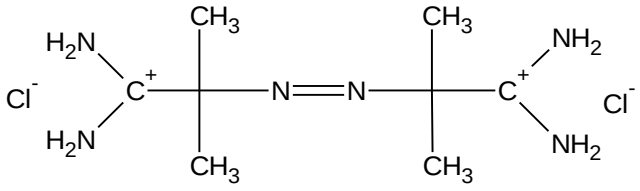

Scheme 4.2. Chemical structure of 2,2'-azobis(2-methylpropionamidine)dichloride (V-50)

This work uses the same technique as that followed by van Berkel in his work. The difference in this work is the use of cyclodextrin (CD) as a "phase transport catalyst".[8] CD has been used before in chemically initiated emulsion polymerization experiments, like in the work done by Storsberg and Ritter,[9] where KPS was used to initiate the polymerization of styrene. One of the results concluded during this work, because of the styrene/CD ratio (1:1 by mole), was that the kinetics of the polymerization did not follow the already established emulsion polymerization kinetics, obviously because of the major increase of styrene solubility in water, which changed the reaction kinetics to be even faster than the kinetics of polymerization in an organic solvent. In addition to this, Hu *et al*.[10] have also demonstrated the possibility of having higher reaction rates for polymerization when using CD (with KPS as initiator), in the absence of surfactant.

Because of the use of KPS in the majority of emulsion polymerization work previously done on styrene/CD complexes, and because of the high price of V-50, in addition to the fact that it releases nitrogen gas when it decomposes, not a lot of work has been done with it. From the current available literature, only Ritter *et al*. used 2,2'-azobis[N,N'-dimethyleneisobutyramidine] dihydro-chloride initiator for emulsion polymerization work with CD.[11] This was the only kinetic study done on the effect of CD on the rate of emulsion polymerization of styrene in aqueous phase polymerization, and it has shown for the first time that polymerization kinetics of styrene/CD 1:1 mixture follow solution polymerization kinetics.[11] However the present work will use a more controlled technique – specifically, that of seeded emulsion polymerization– in order to obtain a more definitive answers on the effect of CD on emulsion polymerization kinetics.

The work discussed in this chapter is based on the results obtained from chapter III. Here

the discussion will focus on the effect of CD on reaction rate for both anionic and cationic latices in the cases where a chemical initiator is used, and the reasons why CD can sometimes increase the reaction rate while in other situations it will be seen to have a negative or negligible effect.

4.2 Theoretical Background

4.2.1Maxwell-Morrison model for entry for chemically initiated experiments

Although thermal and γ-radiolysis initiation techniques are used in research, chemical initiation remains the most commonly used technique to initiate free radical polymerization, either in laboratory scale or industrially.[12] Chemical initiators have a cost advantage over γ-radiolysis, and a time advantage over thermal initiation. During the course of this work some thermal experiments took more than 18 hours to start; this time is also called "induction period". Having a chemical initiator, even at a very low concentration (0.03 mmol/L) reduced this time to a maximum of five hours, but typically it was much briefer than this.

Because of its wider use, chemically initiated emulsion polymerization has been thoroughly studied. The model which will be used during the analysis of all experimental results here is the Maxwell-Morrison model.[5] According to the model, the kinetics of the emulsion polymerization are totally dependent on the chemistry of the aqueous phase. Knowing that the initiator decomposes in the aqueous phase, and that the first steps of a propagating monomer molecule take place in the aqueous phase, the following procedure take place. The reaction starts by the decomposition of the initiator:

$$\mathrm{I{-}I} \xrightarrow{k_d} 2\mathrm{I}^{\bullet} \qquad (4.1)$$

where k_d is the first order rate coefficient for initiator decomposition (note that I denotes initiator, not its usual chemical meaning of iodine). The initiator free radical ($\mathrm{I}^{\bullet}$) starts to react with monomer molecules dissolved in the aqueous phase:

$$\mathrm{I}^{\bullet} + \mathrm{M} \xrightarrow{k_{pi}} \mathrm{IM}^{\bullet} \qquad (4.2)$$

where k_{pi} is the second order rate coefficient for aqueous phase propagation between initiator free radical and monomer. The free radical produced in equation (4.2) will then undergo subsequent propagation:

$$IM_i^{\bullet} + M \xrightarrow{k_{p,aq}^{i}} IM_{i+1}^{\bullet} \quad (4.3)$$

$k_{p,aq}^{i}$ is the rate coefficient for aqueous phase propagation of the free radical whose degree of polymerization is *i*. For entry to happen, the growing free radical degree of polymerization has to reach critical value, *z*, while still in the aqueous phase. This can be written as:

$$IM_z^{\bullet} + \text{latex particle} \xrightarrow{\rho_{initiator}} \text{entry} \quad (4.4)$$

Finally, if the free radical $IM_i^{\bullet}$ reacted with any other free radical present in the aqueous phase, $T^{\bullet}$, then

$$IM_i^{\bullet} + T^{\bullet} \xrightarrow{k_{t,aq}} \text{inert products} \quad (4.5)$$

where $i < z$ and $k_{t,aq}$ is the second order rate coefficient for termination between free radicals in the aqueous phase.

From equations (4.1) to (4.5) a set of rate equations can be derived, which has been discussed in more detail in chapter I. From these rate equations and with some approximation, Maxwell and Morrison arrived to the following equation to calculate the initiator component of the first order rate coefficient for entry:

$$\rho_{initiator} = \frac{2fk_d[I]N_A}{N_c}\left(\frac{2\sqrt{k_d[I]k_{t,aq}}}{k_{p,aq}C_W} + 1\right)^{1-z} \quad (4.6)$$

where *f* is the initiator decomposition efficiency (implicit in equation 4.1), and C_W is the monomer concentration in the aqueous phase. Entry efficiency can be calculated as:

$$F = \frac{\rho_{\text{initiator}}}{\rho_{\text{initiator100\%}}} = \left(\frac{2\sqrt{k_{\text{d}}[\text{I}]k_{\text{t,aq}}}}{k_{\text{p,aq}}C_{\text{W}}} + 1 \right)^{1-z} \tag{4.7}$$

The value of z was found to be 2 for styrene with KPS[12] and 1 for styrene with V-50.[6,3]

4.2.2 Comparison of kinetic parameters at different conditions

Equation (4.6) shows that $\rho_{\text{initiator}}$ should not be used as the defining factor for the rate of emulsion polymerization. This is because any change in N_{c}, the number of particles per unit volume in the aqueous phase, can heavily affect the initiator component $\rho_{\text{initiator}}$ of the entry rate coefficient ρ. It has been suggested earlier[2,3] that comparing the values of the entry efficiency F gives a more reliable mechanistic method for comparing the effect of changing the different emulsion polymerization variables (initiator concentration, particle number,…etc).

F is affected by any change in C_{W}, which should vary with CD level. Therefore F is the best index to use to study the effect of CD on entry. It will be shown later how this increase in solubility increases the values of both the entry efficiency and $\rho_{\text{initiator}}$.

4.2.3 Measurement of entry rate coefficients:

At the end of every kinetic experiment, the dilatometer gives two sets of data, one for the times at which the height of the dodecane layer (placed in the capillary above the reaction medium) is taken, and the other is the corresponding number of steps the tracker moved to record the dodecane position in the capillary. By calibrating the tracker before every experiment, the number of steps can be converted into the distance the dodecane layer moved. Knowing the capillary diameter, the volume contraction of the reaction medium can be calculated. As the densities of styrene and polystyrene have already been determined in the literature[13], calculating the conversion thus follows.

With data for conversion-time, $\bar{n}$ can be calculated from:

$$\frac{\mathrm{d}x}{\mathrm{d}t} = \frac{k_\mathrm{p} C_\mathrm{P} N_\mathrm{c}}{{m_\mathrm{M}}^0 N_\mathrm{A}} \bar{n} \tag{4.8}$$

where x is the fractional conversion of monomer to polymer, t is the time, k_p is the propagation rate coefficient, C_P is the monomer concentration within the latex particles, N_c is the number of latex particles per unit volume of aqueous phase, ${n_\mathrm{M}}^0$ is the amount of monomer added to the latex at the beginning of the reaction and N_A is Avogadro number. As k has already been known for the latices used in chemically initiated experiments, the entry rate coefficient, ρ, can be calculated from the following equation:

$$\rho = 2k \frac{{\bar{n}_\mathrm{ss}}^2}{1-2\bar{n}_\mathrm{ss}} \tag{4.9}$$

It is useful to mention here that the procedure used to calculate k from γ-radiolysis experiments (as previously discussed in chapter III) can still be used with the chemically initiated experiments, though the value of k obtained from such experiments may not be considered precise. This is because of the effect of oxygen present in the reaction medium, which retards the reaction.[14] Nevertheless, it has been noticed throughout this work, that the effect of oxygen decreases with increasing initiator concentration, which agrees with earlier findings[14]. This will be discussed in more detail in section 4.4.4. The other problem is that approach to steady-state is relatively rapid, meaning there is not a lot of data points to fit to obtain k.

The entry rate coefficient ρ has more than one component, one from the thermal entry and one from the initiator. ρ calculated from experiments can be expressed as:

$$\rho = \rho_\mathrm{thermal} + \rho_\mathrm{initiator} \tag{4.10}$$

and by knowing ρ_thermal , which has already been calculated (as discussed in chapter III), the effect of changing concentration on $\rho_\mathrm{initiator}$ can be studied thoroughly.

4.3 Experimental Part

4.3.1 Synthesis, purification and determination of characteristics of seed latices

In addition to the two latices mentioned earlier in chapter III (AN05 and CA01), a few more latices have been synthesized during the course of this work, but they were either not used in kinetic experiments or were used but gave low quality results. The problem of having unacceptable latices happened mainly because of the high particle size polydispersity (PDI) of the latices. Latices used in seeded emulsion polymerization experiments are highly recommended as they have low PDI.[12]

In addition to the two latices already mentioned in chapter III, five more anionic latices have been used through the course of this work. One latex remained from the work previously done van Berkel[3], Latices AN01 and AN03 had high PDI. AN01 had a PDI of 1.059, AN03 showed very high PDI only from a quick look at the TEM images.

The two other latices, AN02 and AN04 have lower PDI. Both of them have also had physical properties close enough to AN05. But no γ-radiolysis experiments were performed for any of these two latices. Because of the close properties for the two latices, entry efficiency calculations for both latices were done based on the *k* values obtained from γ-radiolysis experiments done with the AN05 latex. Even if these values are slightly

Characteristics	AN04K*	AN01	AN02	AN04	AN05	CA01
Average Particle Diameter (nm)						
TEM	64.00	56.13	64.51	61.44	63.70	76.64
PSDA	-	-	-	-	65.43	-
HPPS	-	-	-	-	69.69	73.02
Value used for kinetic analysis	**64.00**	**56.13**	**64.51**	**61.44**	**63.70**	**76.64**
PDI*	1.02	1.059	1.033	1.034	1.031	1.045
% Solids	10.49	10.07	6.67	10.59	12.46	13.54
C_P^{SAT} (mol/L)	5.32	5.58	5.56	5.596	5.735	5.581

* Latex AN04K was prepared and mainly used by van Berkel.

Table 4.1. Physical properties for seed latices used throughout the present work

incorrect for other latices, that will not undermine the trend obtained with these other latices. A typical TEM image for latex AN04 is shown in figure 4.1. Table 4.1 shows the physical properties of all latices synthesized and used during the course of this work.

For latices AN01, AN02 and AN04, TEM was the only technique used to determine the average particle diameter. As shown in figure 4.1, most particles for latex AN04 have similar size, which guarantees a low PDI.

Details about the synthesis and purification of the latices are provided in detail in 3.3.1, and details about determining the latices characteristics are in 3.3.2.

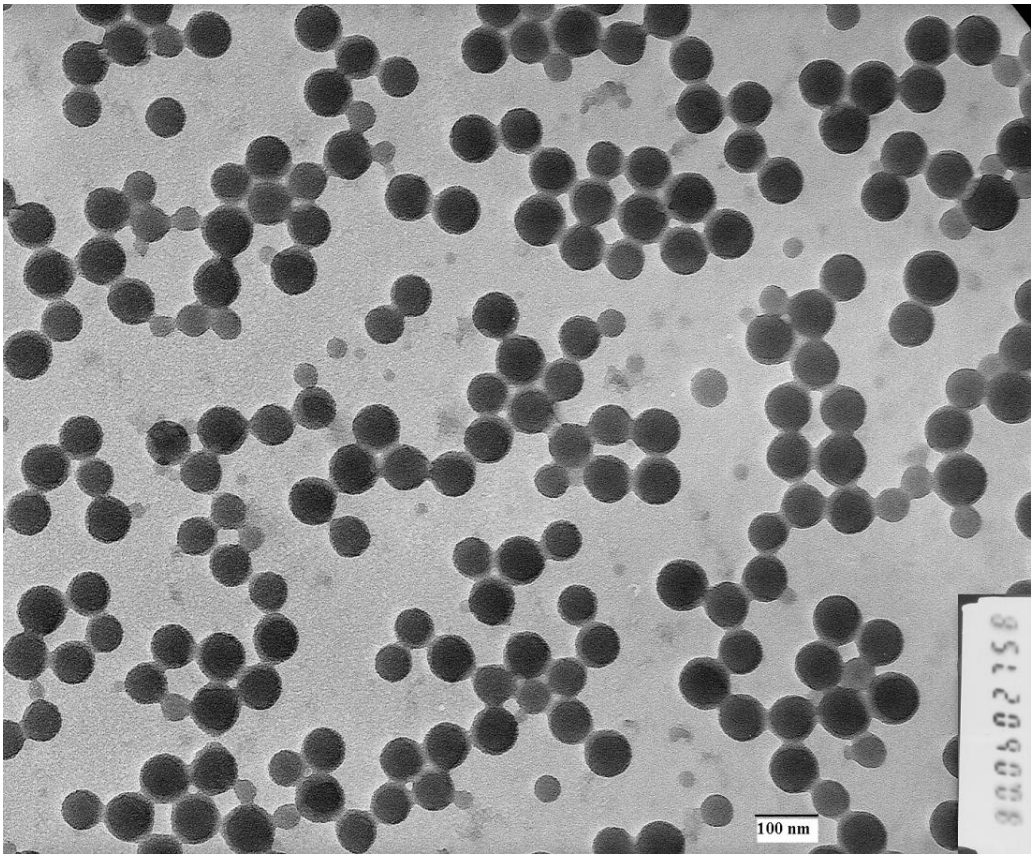

Figure 4.1. Typical TEM image for latex AN04

4.3.2 Kinetic experiments

All chemically initiated experiments run throughout this work were started at Interval II, to avoid introducing more unknown parameters to the calculations. Starting with seeded experiments gives a clear idea on the characteristics of the latex at the beginning of the

experiment, as these are the same latex characteristics already determined.

Chemically initiated kinetic experiments were run in a similar way to that described earlier in section 2.4. The main difference between these experiments and thermally initiated experiments is that an aqueous solution of the initiator is prepared before the experiment. After degassing the dilatometer vessel (where the reaction takes place), the initiator solution is injected to the reaction medium, then the capillary is placed at the top of the dilatometer vessel, filled with degassed water then with dodecane. Through this technique the reaction can start in Interval II with known initiator concentration.

In order to keep an electrostatically stable environment for all experiments, and to avoid acid-base side reactions between initiator and surfactant, all experiments were run with the same charge of surfactant and initiator. For example, the initiator KPS, as shown in scheme 4.1, and the surfactant sodium dihexyl sulphosuccinate, both have a negative charge. Having both negatively charged surfactant and initiator within the mixture reduces the possibility of having both of them reacting acid-base reactions with each other. Although it has been stated previously that charge-charge interactions for chemically initiated experiments have negligible effect[2,3], this was stated in a case in which CD was not present. CD presence in this case might have raised more questions which are beyond the topic of this research.

All chemically initiated experiments were run at 50 ^{o}C. One of the problems faced at this temperature with the CA01 latex was the decomposition of the added V-50 to nitrogen gas and other products.[15] However, this was found not to affect the reaction kinetics during interval II.

4.3.3 Solubility experiments

As it was noticed that styrene solubility is affected not only by the amount of CD present, but also by the presence of other components, especially the surfactant, styrene solubility in water was measured in the presence of 2% and 4% CD concentration, relative to the total mass of monomer used. The mixture was prepared by mixing styrene, and/or surfactant, and/or CD in water. The mixing took place in the dilatometer vessel. The amounts used were the exact amounts added to the latex used in kinetic experiments, to

imitate the situation present within the aqueous phase of the emulsion polymerization mixture, in order to obtain a value of styrene solubility which is close to its value in the aqueous phase of the polymerization mixture.

Samples were taken of the mixture, diluted to a known amount, and then the concentration of the diluted styrene samples was found using a Varian Cary 100 Bio UV-Vis spectrophotometer. Knowing the amounts used for dilution, C_W^{SAT} at different conditions was easily and accurately calculated. More information about solubility measurement can be found at section 2.6.

4.4 Results and discussion

4.4.1 Main role of CD in emulsion polymerization reactions

It has been previously found that the overall reaction rate of the emulsion polymerization process increases with increasing monomer solubility in water. This happens generally by adding chemicals like glucose which increase the monomer solubility in water[16]. This general rule applies also to CD, which was found to increase the overall reaction rate for the emulsion polymerization of styrene under different conditions[17,18,19,20]. As this research focuses on the mechanistic approach for this conclusion, the solubility of styrene was measured at the two CD concentrations used during the course of this work (2% and 4% of the monomer weight).

The calibration was done by dissolving 0.27 g of styrene in 1 L of water. 20 mL of this solution were taken and further diluted to 0.2 L. Three other portions (40, 60 and 80 mL) were all taken from the original styrene solution and diluted in the same ratio.

	Styrene solubility (x 10^3 L/mol)		
	No surfactant	AMA-80	DTAB
No CD	4.06	7.43	5.83
2% CD	4.26	7.14	6.50
4% CD	5.32	8.57	9.42

Table 4.2. Solubility of styrene in water at different conditions

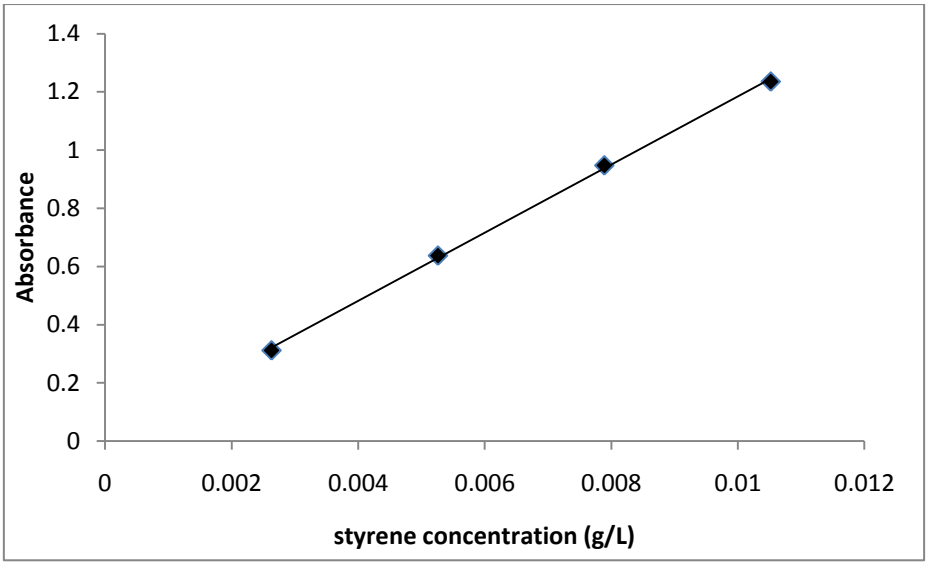

Figure 4.2. Calibration line used for styrene solubility measurement. This line shows that styrene absorbance follows Beer's law. All absorbance were taken at wavelength 248 nm.

Absorbances of all samples were obtained. By plotting the data, figure 4.2 was obtained.

When determining the solubility of styrene using this technique, it should be noted that it was assumed there is no contribution of CD and surfactant to absorbance. It was also assumed that CD and surfactant do not affect styrene absorbance. It was noted however that there was a minor change for the styrene spectrum when CD was used, but this change was neglected in all the calculations done.

To determine the solubility of styrene at different conditions, mixtures of styrene, CD and both surfactants were prepared in dilatometer volumetric flasks, in the same way of mixing and preparing the mixture before kinetic experiments, with the main difference is the absence of seed latex particles. From each mixture 2 mL were taken and diluted to 0.2 L volume. Samples from this diluted solution had their solubilities measured. Appendix 4.1 shows all the experiments done for measurement of styrene maximum concentrations at different conditions.

Table 4.2 shows the aqueous phase solubility of styrene at different conditions. The first column from the left shows that the more the CD, the more the styrene can be dissolved. A similar value of styrene solubility was found to be 4.4×10^{-3} mol/L[21], which is in close agreement to the value of 4.3×10^{-3} mol/L which was found earlier[22], both values are very

close to the value found during the course of this work. Furthermore, another β-CD derivative (hydroxypropyl-β-cyclodextrin) was also found to increase styrene oxide solubility in water[23]. From such previous work done, the increase of styrene solubility with increasing CD can be a logical conclusion, and can give a good indication that the results obtained here do not contradict work previously done on CD. Such results and conclusion are very logical regarding the structure of CD.

The reason CD increases the solubility of monomers, and organic compounds generally in water, is because of its structure. CD has a form of a truncated cone, with a hydrophobic cavity and a hydrophilic exterior[24]. With this structure, the cavity can contain the hydrophobic compound, which is styrene in this case, and the CD molecule will be dissolved into water, thanks to its hydrophilic exterior. Consequently, the solubility of styrene will increase because of its inclusion and complexation within CD molecules.

Moving along the first row of the column, where there is no CD used, it is clear that AMA-80 increases the styrene solubility in water. But it has to be noticed that this is not a real increase in solubility. What happens is that some of the surfactant, which is in the mixture at a concentration higher than its critical micelle concentration, remains in the mixture in micellar form. These micelles keep some of the monomer within them, and this is where the nuclei start forming at the earliest stage of the polymerization process. Because of the presence of some of the monomer within those micelles, the solubility of styrene in water appears to increase both in presence of anionic and cationic surfactants.

The second column shows a trend opposite to the trend shown in the first column. This trend is that there is a decrease in monomer solubility at 2% CD concentration, and then with more CD, the monomer solubility increases again. This reduced solubility of styrene at such conditions has been explained earlier as a result of the competition between styrene and surfactant for CD cavities[18]. Although this assumption has not been experimentally proven earlier, the effect of 2% CD with AMA-80 shows clearly that such competition takes place.

But why did the monomer solubility decrease at 2% CD then increase at 4%? The simplest explanation for this is that equilibrium has been reached between the styrene, the

CD and the surfactant used. In other words, at 2% CD concentration the equilibrium between the three components was in favour of complexing more surfactant within the CD cavities, so less styrene was complexed within CD, and as the amount of surfactant, and so the micelles decreased, the total amount of styrene soluble in water has also decreased. To the contrary, at 4% CD the equilibrium favoured complexing more monomer within the CD cavities, which is logical regarding doubling the mass of CD used. In short, with AMA-80, small amounts of CD will affect the solubility of styrene negatively, and so the reaction rates. While with more CD used, the solubility of styrene will increase, as do the reaction rates. Such results agree with what was discussed in chapter III, and, as will be discussed in 4.4.2, give a good background to explain the negative effect of small amounts of CD on the reaction rate.

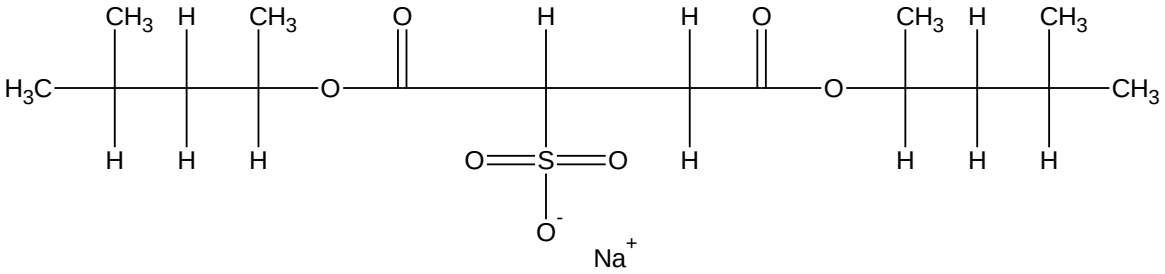

Scheme 4.3. Chemical structure of sodium dihexyl sulphosuccinate, main component of AMA-80.

From the structure of sodium dihexyl sulphosuccinate, scheme 4.3, it is clear that it has 16 carbon atoms, not all of them are on a straight chain. Consequently, the hydrophobic part can be assumed to take the form of a pyramid within the CD cavity, the top of the pyramid, which points outside the cavity will be the SO_3^- group. This structure will keep the hydrophobic side of the surfactant within the CD cavity, but with any other hydrophobic compound which can co-exist with the surfactant, the structure of the surfactant in this case will push it away. This assumption can be proven through X-ray crystallography, but this is out of the scope of this work.

In light of this explanation, it will be very hard to explain why DTAB, the cationic surfactant used, did not have the same effect on styrene solubility. The third column in table 4.2 shows that increasing the concentration of DTAB and/or CD, increases styrene solubility in water, which goes against earlier findings regarding the anionic surfactant.

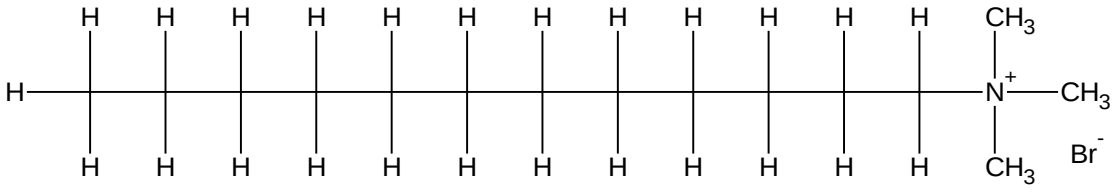

Scheme 4.4. Chemical structure of dodecyltrimethyl ammonium bromide (DTAB).

Scheme 4.4 highlights two reasons why the competition for CD cavities does not change the CD effect negatively as happens in case anionic surfactants were used. A main difference between DTAB and sodium dihexyl sulphosuccinate is the structure. DTAB has a straight chain structure, with a shorter chain length than sodium dihexyl sulphosuccinate, which makes its binding to the CD cavity weaker.[25] Furthermore, the electronegativity difference[26] for the nitrogen and bromide, the atoms forming the bonds of the $—NCH_3^+\ Br^-$ group in the DTAB, is only 0.2, much less than the difference between oxygen and sodium, as in the $—SO_3^-\ Na^+$, where the difference in electronegativity is 2.4. Such a high polarity in the surfactant hydrophilic side makes it very unlikely for sodium dihexyl sulphosuccinate to co-exist in the CD cavities with styrene. For these two reasons, it can be assumed that both CD and DTAB work together to increase styrene solubility. With such reasoning the solubilities shown in table 4.2 are very logical and acceptable.

4.4.2 Effect of CD on reaction rate for the anionic latices/KPS system

For this part of the work, only 3 initiator concentrations were used at three different CD concentrations. Experiments were run with 0.15, 0.5 and 1.5 mmol/L KPS. These are the concentrations of KPS in the aqueous phase within the system. All different initiator concentrations were used in experiments with no CD, and in experiments using 2% and 4% CD concentration. The percentages show the relative mass of CD to the total mass of the monomer used. Because of the small number of initiator concentrations used for the anionic latices/KPS system, the comparison will focus mainly on the effect of CD on conversion rate, as will be shown in the figures. Results for all systems were very similar, except for the highest initiator concentration case which will be discussed shortly. Tables 4.3 – 4.7 present values of F and $\rho_{\text{initiator}}$, for all experiments done throughout the course of this work.[3] %CD means (mass of CD / mass of monomer at the beginning of the reaction) x 100.

Table 4.3 presents the results of experiments done with latex AN04K, previously prepared by van Berkel during the course of his work. For this latex, ρ_{thermal} = 1.5 x 10^{-4} s^{-1}, and k = 7.5 x 10^{-3} s^{-1}. Both values have already been calculated[6,3].

Entry efficiency F for all experiments was calculated from the equation:

$$F = \frac{\rho_{initiator} \ N_c}{2 f k_d [I] N_A} \tag{4.11}$$

Equation (4.11) is a result of substituting $\rho_{\text{initiator } 100\%}$ from equation (1.31), into the equation defining entry efficiency (4.7).

Experiment	N_c x 10^{-17}	[KPS] x L/mmol	$\bar{n}_{ss}$	$\rho_{\text{initiator}}$ x 10^4 s	F	%CD
SNT4K09	1.015	0.000	0.054	-	-	-
SNT4K10	1.072	0.000	0.095	-	-	-
SNT4K18	1.349	0.546	0.188	7.021	0.131	-
SNT4K17	1.407	0.546	0.188	6.948	0.135	-
SNT4K15	1.032	0.559	0.254	18.081	0.252	-
SNT4K07	1.011	0.560	0.316	39.272	0.535	-
	1.200	**0.553**	**0.237**	**17.831**	**0.263**	
SNT4K14	0.779	0.522	0.294	29.787	0.336	2%
SNT4K12	0.778	0.575	0.230	13.242	0.135	2%
	0.779	**0.549**	**0.262**	**21.515**	**0.236**	**2%**
SNT4K11	0.780	0.520	0.372	79.666	0.902	4%
SNT4K04	1.012	1.090	0.164	4.466	0.031	-
SNT4K01	1.084	1.631	0.268	21.729	0.109	-
SNT4K02	1.014	1.631	0.460	396.568	1.860	-
SNT4K03	1.072	1.644	0.374	82.287	0.405	-
SNT4K08	1.075	5.426	0.440	241.703	0.361	-
	1.051	**2.284**	**0.341**	**149.351**	**0.553**	**-**

Table 4.3. Summary of results for all chemically initiated experiments done using latex AN04K. Averages for every initiator/CD concentration are presented in bold font.

Results shown in table 4.3 show that, at [KPS] = 0.5 mmol/L, the highest entry efficiency was at 4% CD, while at 2% CD the entry efficiency was around the same range of no CD.

The first latex prepared during the course of this work is AN01. No thermally initiated or γ-relaxation experiments were done for AN01. It will be assumed to have ρ_{thermal} = 1.32 x 10^{-4} s^{-1}, equal to that of latex AN05. As for *k*, it will be calculated from equation (3.16)

$$k_{\text{theor}} = \frac{3D_{\text{w}}C_{\text{W}}}{r_{\text{s}}{}^2 C_{\text{p}}}\frac{k_{\text{tr}}}{k_{\text{p}}^1} \tag{4.12}$$

For latex AN05, *k* was found to change in presence of CD. Consequently, for every CD concentration there will be a specific value for *k*. Experiments done with AN01 did not involve the use of any CD. Consequently, the value of *k* for no CD will be used for them. This value will be scaled down according to equation (4.12). *k* will be calculated from

$$\frac{k_{\text{AN 01}}}{k_{\text{AN 05}}} = \frac{r_{\text{AN 05}}{}^2}{r_{\text{AN 01}}{}^2} \tag{4.13}$$

From this, *k* for latex AN01 = 1.75 x 10^{-2} s^{-1}. Results of all AN01 experiments are presented in table 4.4.

Experiment	N_c x 10^{-17}	[KPS] x L/mmol	$\bar{n}_{ss}$	$\rho_{\text{initiator}}$ x 10^4 s	*F*	%CD
SNT122	2.013	0.532	0.107	3.830	0.112	-
SNT119	1.970	0.536	0.116	4.874	0.139	-
SNT125	2.027	0.536	0.139	7.985	0.234	-
SNT123	1.950	0.542	0.187	18.231	0.514	-
SNT121	1.839	0.556	0.363	167.425	4.454	-
SNT124	1.729	0.598	0.480	2037.019	50.943	-
SNT120	1.732	0.624	0.298	75.671	1.896	-
	1.99	**0.537**	**0.137**	**8.730**	**0.250**	

Table 4.4. Summary of results for all chemically initiated experiments done using latex AN01. Experiments written in red faced technical problems, usually leaks. Averages are presented in bold, values in red are not included in calculation of averages.

Experiments done using latex AN02 included the use of CD, with 2% and 4% CD concentration. There were no γ-relaxation experiments done for latex AN02. Consequently, *k* for no CD, 2% and 4% CD was calculated from *k* values for latex AN05, using equation (4.13). For no CD, $k = 1.32 \times 10^{-2}$ s^{-1}, for 2% CD, $k = 1.20 \times 10^{-2}$ s^{-1}, and for 4% CD $k = 0.94 \times 10^{-2}$ s^{-1}. $\rho_{thermal} = 1.39 \times 10^{-4}$ s^{-1}, as was calculated from the results of experiments SNT233 and SNT234. Table 4.5 shows results of all AN02 experiments.

Experiment	N_c x 10^{-17}	[KPS] x L/mmol	$\bar{n}_{ss}$	$\rho_{initiator}$ x 10^4 s	F	%CD
SNT233	1.194	0.000	0.115	-	-	-
SNT234	1.146	0.000	0.106	-	-	-
SNT230	1.120	0.168	0.122	3.305	0.166	-
SNT231	1.106	0.174	0.144	6.402	0.307	-
SNT238	1.142	0.183	0.163	3.267	0.154	-
SNT235	1.140	0.184	0.181	2.503	0.117	-
	1.127	**0.177**	**0.153**	**3.869**	**0.186**	
SN203	1.157	0.158	0.212	3.273	0.181	2%
SN201	1.151	0.172	0.205	3.519	0.178	2%
SN202	1.128	0.179	0.193	4.339	0.206	2%
	1.145	**0.170**	**0.203**	**3.710**	**0.188**	**2%**
SN216	1.082	0.187	0.239	8.314	0.364	4%
SNT226	1.142	0.530	0.066	4.270	0.069	-
SNT228	1.171	0.551	0.120	14.907	0.239	-
SNT227	1.141	0.555	0.063	17.958	0.278	-
SNT232	1.143	0.575	0.131	9.410	0.141	-
	1.149	**0.553**	**0.095**	**11.636**	**0.182**	**-**
SN207	1.360	0.491	0.236	2.540	0.053	2%
SN206	1.144	0.537	0.164	8.180	0.132	2%
SN205	1.172	0.538	0.141	45.263	0.745	2%
SN204	1.084	0.558	0.206	5.378	0.079	2%
	1.190	**0.531**	**0.187**	**15.340**	**0.252**	**2%**

Table 4.5. Summary of results for all chemically initiated experiments done using latex AN02. Averages are presented in bold.

Experiment	N_c x 10^{-17}	[KPS] x L/mmol	$\bar{n}_{ss}$	$\rho_{initiator}$ x 10^4 s	F	%CD
SN209	1.130	0.544	0.218	12.091	0.189	4%
SN208	1.127	0.552	0.243	13.459	0.207	4%
	1.129	**0.548**	**0.231**	**12.775**	**0.198**	**4%**
SNT236	1.202	1.603	0.111	28.004	0.158	-
SNT229	1.163	1.617	0.115	21.610	0.117	-
SNT239	1.153	3.257	0.287	27.666	0.074	-
	1.173	**2.159**	**0.171**	**25.760**	**0.116**	**-**
SN212	1.107	1.585	0.220	19.010	0.100	2%
SN210	1.124	1.611	0.240	13.001	0.069	2%
SN211	1.124	1.647	0.191	16.190	0.083	2%
	1.118	**1.614**	**0.217**	**16.067**	**0.084**	**2%**
SN213	1.143	1.574	0.226	20.220	0.111	4%
SN214	1.097	1.636	0.206	16.245	0.082	4%
SN215	1.146	1.546	0.633	18.521	0.104	4%
	1.129	**1.585**	**0.355**	**18.329**	**0.099**	**4%**

Table 4.5 (cont'd). Summary of results for all chemically initiated experiments done using latex AN02. Averages are presented in bold.

It is noticed again, with latex AN02, that the trend is that entry efficiency F increases noticeably with 4% CD concentration. With 2% CD concentration there was a general slight increase in F, but not as noticeable as with 4%.

Another latex used was latex AN04. No thermally initiated experiments were done for AN04, so it was assumed that its $\rho_{thermal} = 1.32 \times 10^{-2}$ s^{-1}, equal to that of latex AN05. As for k, it was calculated in the same way done for latex AN02. For no CD, $k = 1.46 \times 10^{-2}$ s^{-1}, for 2% CD, $k = 1.33 \times 10^{-2}$ s^{-1}, and for 4% CD $k = 1.03 \times 10^{-2}$ s^{-1}. Results for all experiments done with latex AN04 are presented in table 4.6.

It is noticed in table 4.6 that for latex AN04, CD had almost no effect at 4% CD concentration, while at 2% CD it mostly had a negative effect on the reaction rate. There is no clear reason behind this behaviour for CD with latex AN04. A possible explanation

might be that the amount of surfactant which remained after dialysis was above the amount which remained from other latices, and this increased amount of surfactant, in presence of CD, worked as a retarder. Discussion about the surfactant negative effect on the role of CD was in section 4.4.1.

Experiment	N_c x 10^{-17}	[KPS] x L/mmol	$\bar{n}_{ss}$	$\rho_{initiator}$ x 10^4 s	F	%CD
SN423	1.183	0.160	0.083	1.112	0.062	-
SN425	1.121	0.174	0.130	4.795	0.233	2%
SN424	1.112	0.174	0.075	0.455	0.022	2%
	1.117	**0.174**	**0.103**	**2.625**	**0.128**	**2%**
SN426	1.163	0.171	0.155	5.940	0.304	4%
SN427	1.108	0.545	0.128	5.125	0.079	-
SN428	1.143	0.551	0.140	5.885	0.092	2%
SN429	1.103	0.553	0.107	2.556	0.038	2%
	1.123	**0.552**	**0.124**	**4.221**	**0.065**	**2%**
SN430	1.182	0.549	0.182	9.483	0.154	4%
SN433	0.544	1.562	0.181	13.750	0.036	-
SN431	0.537	1.569	0.244	32.467	0.084	-
SN434	0.516	1.578	0.211	21.265	0.052	-
SN435	0.526	1.610	0.230	27.207	0.067	-
SN418	1.140	1.682	0.208	20.308	0.104	-
SN417	1.506	1.715	0.179	13.256	0.088	-
SN421	1.153	1.746	0.197	17.507	0.087	-
	0.846	**1.637**	**0.207**	**20.823**	**0.074**	**-**
SN432	0.522	1.551	0.217	20.622	0.052	2%
SN420	1.105	1.559	0.180	12.074	0.065	2%
SN436	0.519	1.584	0.199	16.238	0.040	2%
SN419	1.096	1.633	0.166	9.683	0.049	2%
	0.811	**1.582**	**0.191**	**14.654**	**0.052**	**2%**

Table 4.6. Summary of results for all chemically initiated experiments done using latex AN04. Averages are presented in bold.

Experiment	N_c x 10^{-17}	[KPS] x L/mmol	$\bar{n}_{ss}$	$\rho_{initiator}$ x 10^4 s	F	%CD
SN437	0.503	1.580	0.302	46.253	0.111	4%
SN422	1.153	1.662	0.216	15.624	0.082	4%
	0.828	**1.621**	**0.259**	**30.939**	**0.097**	**4%**

Table 4.6 (cont'd). Summary of results for all chemically initiated experiments done using latex AN04. Averages are presented in bold.

Results of experiments done with latex AN05 are shown in table 4.7. Three experiments were done without using additional surfactant. Results of these experiments were not included, as the three experiments faced the problem of forming coagulum, although these experiments gave values for $\bar{n}_{ss}$ which are similar to those obtained from experiments without latex. For AN05, $\rho_{thermal}$ = 1.32 x 10^{-4} s^{-1}, and k = 1.36 x 10^{-2} s^{-1} for no CD, 1.23 x 10^{-2} s^{-1} for 2% CD and 0.96 x 10^{-2} s^{-1} for 4% CD.

Experiment	N_c x 10^{-16}	[KPS] x L/mmol	$\bar{n}_{ss}$	$\rho_{initiator}$ x 10^4 s	F
SN513	4.972	0.160	0.117	3.515	0.082
SN512	4.929	0.534	0.172	10.949	0.076
SN519	4.969	1.527	0.189	14.275	0.035

Table 4.7a. Summary of results for chemically initiated experiments done using latex AN05 in absence of CD.

Experiment	N_c x 10^{-16}	[KPS] x L/mmol	$\bar{n}_{ss}$	$\rho_{initiator}$ x 10^4 s	F
SN513	4.982	0.160	0.119	3.254	0.077
SN512	4.930	0.534	0.160	7.997	0.056
SN519	4.977	1.527	0.200	1.522	0.037

Table 4.7b. Summary of results for chemically initiated experiments done using latex AN05 with 2% CD concentration.

Experiment	N_c x 10^{-16}	[KPS] x L/mmol	$\bar{n}_{ss}$	$\rho_{initiator}$ x 10^4 s	F
SN513	4.907	0.160	0.152	5.069	0.118
SN512	4.946	0.534	0.226	1.654	0.116
SN519	5.036	1.527	0.249	2.231	0.056

Table 4.7c. Summary of results for chemically initiated experiments done using latex AN05 with 4% CD concentration.

Results confirm results reached earlier with latex AN02, that CD has almost no effect (or a minor negative effect) with 2% concentration, while at 4% concentration it has a more noticeable positive effect.

Focusing on the effect of CD on reaction rate, and neglecting its effecting on other parameters like $\rho_{initiator}$ and F, figure 4.3 shows that CD acts as a "phase transfer catalyst"[8]. CD has an obvious catalytic effect on the emulsion polymerization rate. Furthermore, using initiator concentration of 0.15 mmol/L, the reaction rate increased at both 2% and 4% CD concentration (compared to the rate when CD was not used) and this

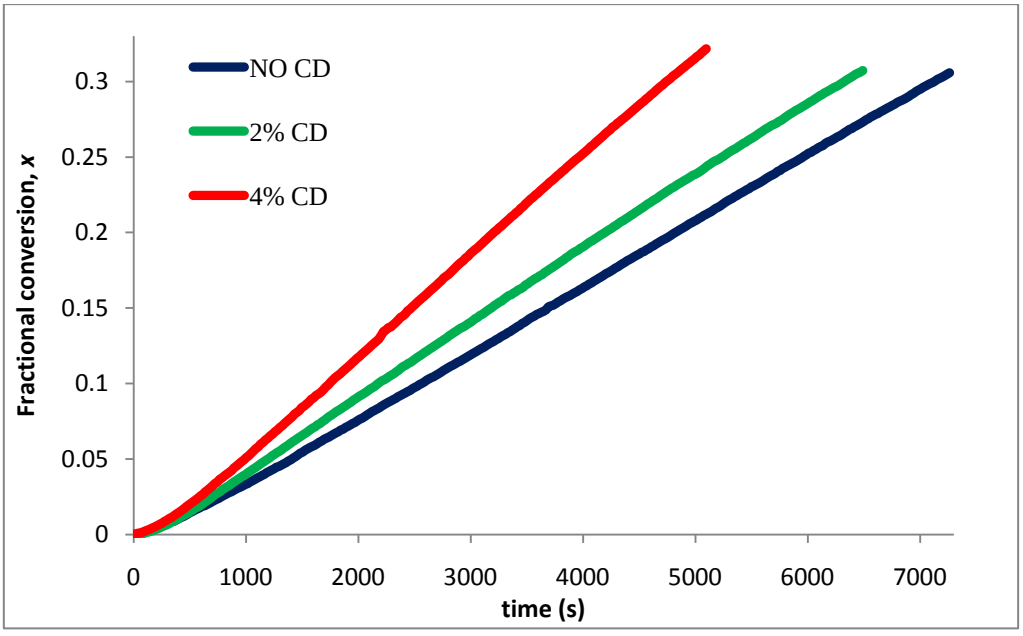

Figure 4.3. Effect of CD on reaction rate at KPS concentration of 0.15mmol/L for latex AN02. Conversion time curves are for experiments SNT235 (no CD), SN201 (2% CD) and SN216 (4%CD). Increasing CD concentration has an increasingly positive effect on the reaction rate.

can lead to the conclusion that increasing the amount of CD speeds up the reaction. Similar results were obtained with latices AN04 and AN05.

But such conclusions cannot be taken as a general rule, as figure 4.4 shows that, although increasing the amount of CD can increase the reaction rate, this does not happen under all conditions.

Figure 4.4 shows that at 2% CD concentration, and with 0.5 mmol/L initiator concentration, there is a minor increase in reaction rate between the reaction at which no CD was used and the reaction at which 2% CD was used. Compared to that, when CD concentration used is 4% of the monomer concentration, the reaction rate had a major increase. Similar curves have been obtained for latices AN04 and AN05.

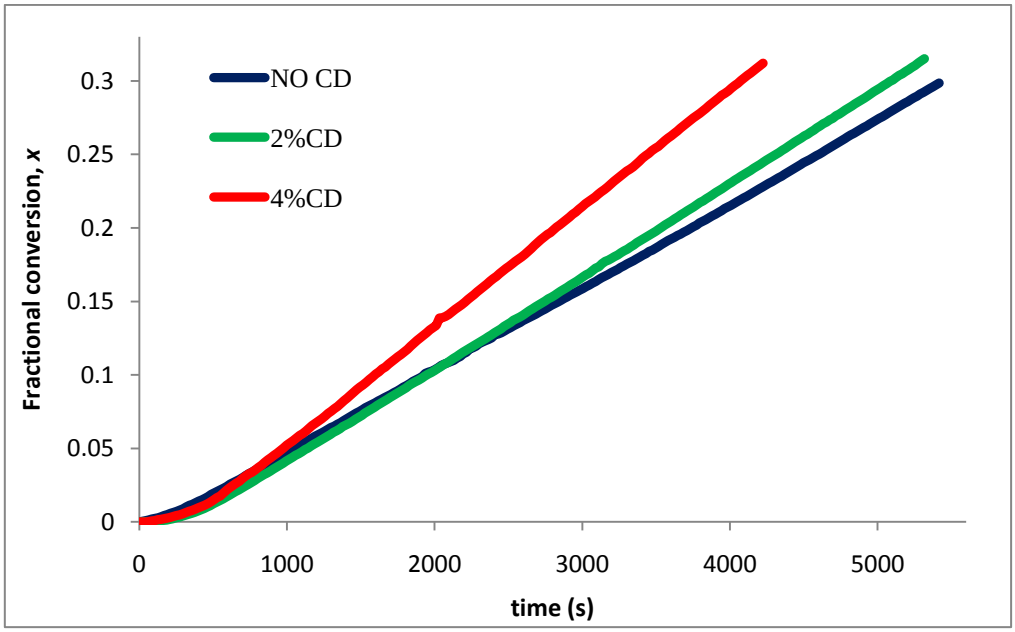

Figure 4.4. Effect of CD on reaction rate at KPS concentration of 0.5 mmol/L for latex AN02. Conversion time curves are for experiments SNT226 (no CD), SN206 (2% CD) and SN209 (4%CD). Highest CD concentration has the most positive effect on the reaction rate, while lower CD concentration does not have the same effect.

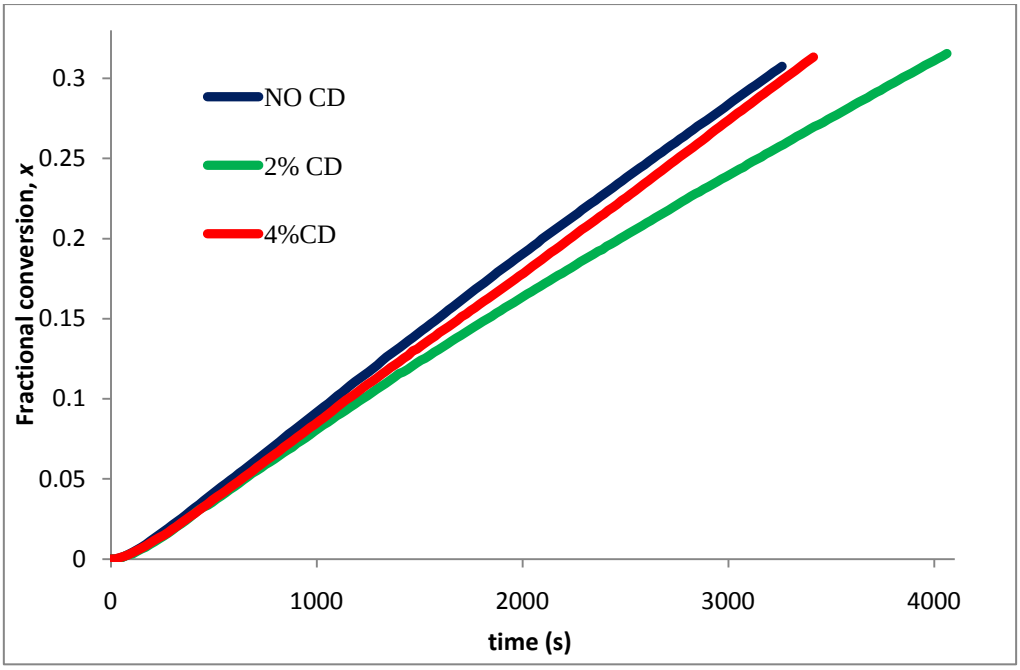

Figure 4.5. Effect of CD on reaction rate at KPS concentration of 1.5 mmol/L, for latex AN02. Conversion time curves are for experiments SNT236 (no CD), SN211 (2% CD) and SN213 (4%CD). 2% CD concentration has a negative effect on reaction rate, while 4% CD concentration has a negligible effect.

But what if the initiator concentration was further increased? In this situation, as shown in figures 4.5 and 4.6, the CD at 2% concentration has an overall negative effect, which is not even noticed through the initial slope of the curve shown in figure 4.6. To the opposite of that, at 4% CD concentration the reaction rate was found to remain at a value close to its original value without CD, as shown in figure 4.5, or to have a slight increase as shown in figure 4.6, a result quite similar to the results obtained for γ-initiated emulsion polymerization experiments run with 4% CD concentration.

A possible explanation for this is, what has been previously proposed, that both monomer and surfactant compete on CD cavities[10,18]. Such competition reduces the effect of surfactant and CD.

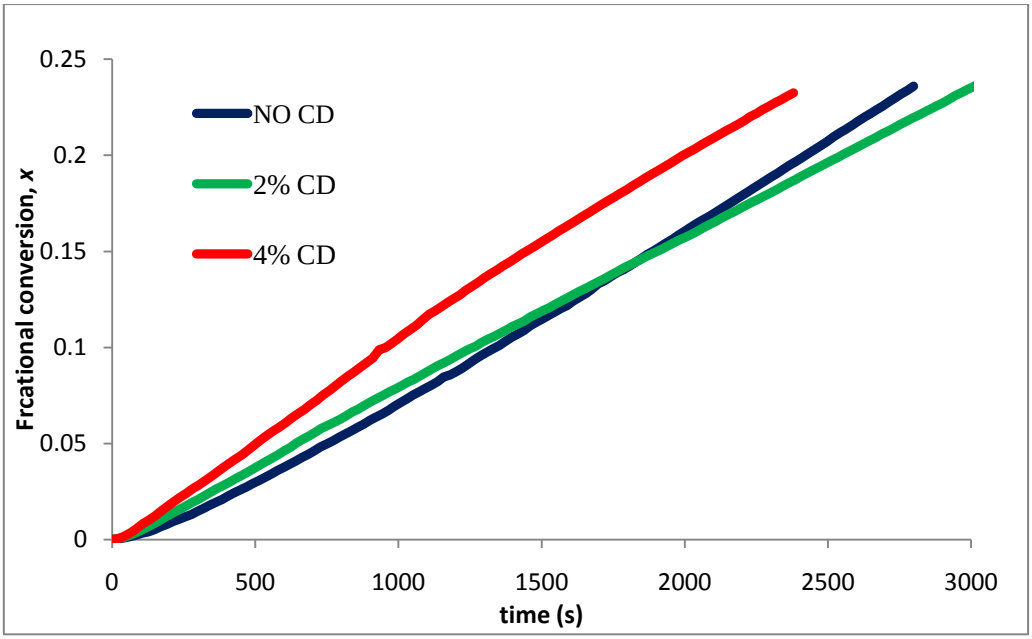

Figure 4.6. Effect of CD on reaction rate at KPS concentration of 1.5 mmol/L, for latex AN04. Conversion time curves are for experiments SN421 (no CD), SN420 (2% CD) and SN422 (4%CD). 2% CD concentration has a negligible effect on reaction rate, while 4% CD concentration has a noticeable positive effect.

It should be noted that experiments for both AN02 and AN04 with 1.5mmol/L KPS and 4% CD which gave different results were both run at very similar conditions, including similar monomer mass used and similar N_c. Results for both latices were reproducible. The higher the initiator concentration is, the less likely the rate will be affected by increased CD concentration is a possible hypothesis.

The effect of CD on entry efficiency is similar to its effect on reaction rate. It is noted in figure 4.7 that with 4% CD there is always an increase in entry efficiency. However, this was not the case with 2% CD concentration. The exact reason behind that is not known, though the assumption of competition between monomer and surfactant molecules for CD cavities can be a reasonable assumption.

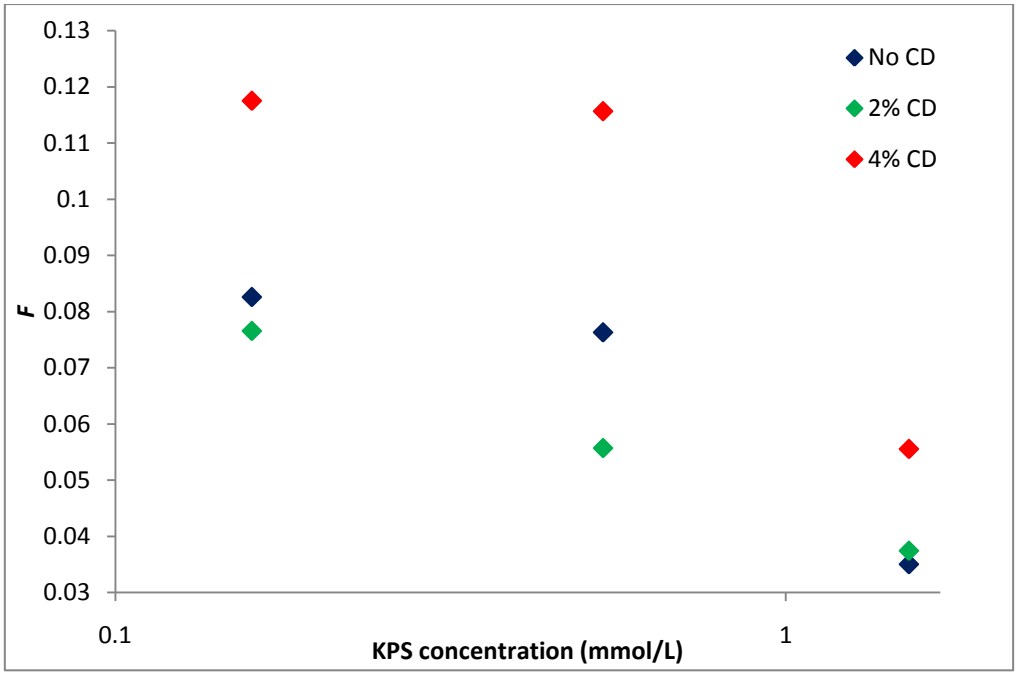

Figure 4.7. Effect of CD on entry efficiency for AN05 latex. Results show an increase in *F* with highest amount of CD.

Results above show that the conclusion drawn before, that there is competition between monomer and surfactant for CD cavities, is not true under all conditions. It has been shown that at a low initiator concentration (0.15 mmol/L KPS), CD has an effect which is more significant than its effect of higher initiator concentration (1.5 mmol/L KPS). So, would the initiator concentration play a role in the effect of CD on reaction rate?

4.4.3 Effect of CD on reaction rate and entry efficiency for the CA01/V-50 system

It was clear from the results of the AN05/KPS system that the 2% CD concentration has minor effect on the reaction rate, especially when high initiator concentration was used. So, experiments done for the CA01/V-50 system were either done with no CD or with 4% CD.

Another factor which was also found to affect the reaction rate was the surfactant. The added amount of surfactant was found to have a direct impact on the reaction rate as shown in figure 4.8.

Figure 4.8 shows that $\bar{n}_{ss}$ (the parameter representing and expressing reaction rate) has a linear increase with increasing surfactant concentration. This conclusion contradicts

earlier findings about surfactant effect on reaction rate[27], but it should be noted that such findings were done on a sodium dodecyl sulphate stabilized latex, and experiments were initiated using γ-rays. Because of the effect changing surfactant concentration might have on ρ and k, which might results in further uncertainty with their values, entry efficiency was not used for the calculations done for such experiments.

The experiments for the effect of surfactant concentration on $\bar{n}_{ss}$ were performed because the first experiments done for CA01 were without added surfactant, which means the seeds added only included the surfactant which remained after the dialysis process. The experiments failed because of the significant amount of coagulum formed during interval II. Coagulation has to be avoided during kinetic experiments, because of the effect of the formation of coagulum on different kinetic parameters. Adjusting the ionic strength of the

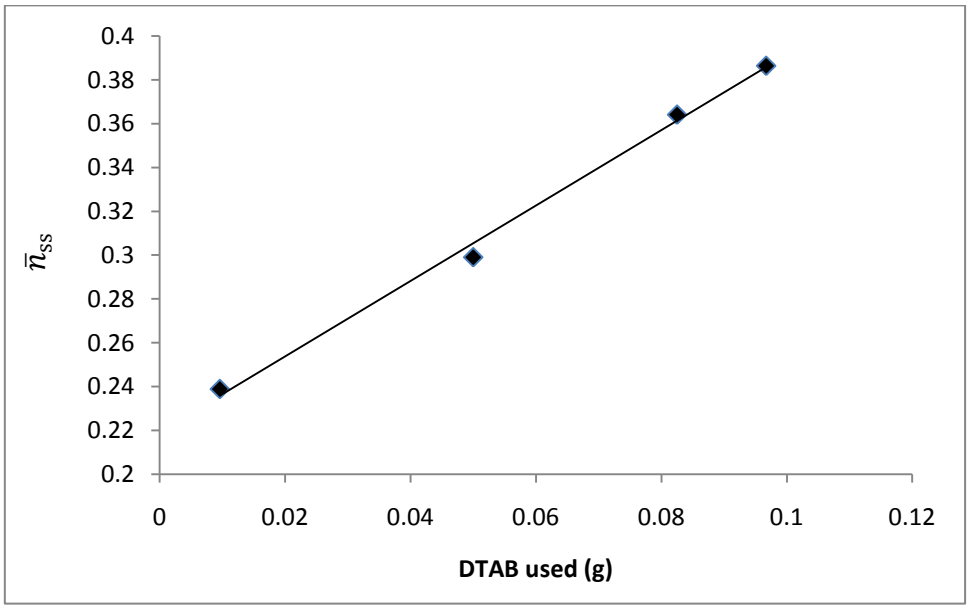

Figure 4.8. Effect of the amount of surfactant on reaction rate. Results are for experiment SCT145 (0.0994 g DTAB), SCT147 (0.05 g DTAB), SCT149 (0.0825 g DTAB) and SCT146 (0.0967 g DTAB). Experiments were done with V-50 concentration of 1 mmol/L. solution is a known method to avoid coagulum formation[12,27].

One method to get the correct ionic strength for the experiment is to keep adjusting the amount of surfactant used in the kinetic experiment, until no coagulum is formed. By keeping all other parameters constant, including V-50 concentration and N_c, the effect of changing the amount of DTAB used was very clear. For all other CA01/V-50 experiments,

no coagulum was found to form during interval II, and very small amounts were formed during interval III.

For the anionic latex, coagulum formation also occurred, through lesser amounts of coagulum formed, compared to the amounts formed with the cationic latex. Furthermore, the right amount of surfactant was just found after one trial. The effect of another anionic surfactant (sodium lauryl sulphate) has already been studied, so results for the current work are not expected to be different[12,28].

Before finding the amount of additional surfactant required, some experiments have been done using no additional surfactant, or using the wrong amount of surfactant, as discussed earlier. Results of these experiments are in table 4.8, it should be noted that results of five experiments done with V-50 concentration around 1 mmol/L were not included in table 4.8, as these experiments were the earliest to have the problem of coagulum formation. Coagulum formation in these experiments was the main motive for trying to identify the amount of surfactant by which no coagulum forms. Table 4.8 does not include results of thermally initiated experiments with no surfactant, as their results were discussed in section 3.6.1.

After finding the right amount of surfactant, experiments were undertaken to find the effect of CD, 4% concentration (relative to the total mass of monomer used), on the overall emulsion polymerization rate at different initiator concentrations. Results are shown in table 4.9.

For all entry efficiencies shown in table 4.8, $\rho_{thermal} = 2.09 \times 10^{-4}\ s^{-1}$, $k = 0.70 \times 10^{-2}\ s^{-1}$ for no CD and 2% CD experiments. $k = 1.18 \times 10^{-2}\ s^{-1}$ only for experiment SC156 as the only experiment in table 4.8 done with 4% CD.

Experiment	N_c x 10^{-17}	[V-50] x L/mmol	$\bar{n}_{ss}$	$\rho_{initiator}$ x 10^4 s	F	%CD
SC145	0.186	0.028796	3.916	5.620	0.929	-
SC154	0.223	0.032783	3.184	10.501	0.919	2%
SC155	0.254	0.033594	3.423	16.202	0.918	2%
SC153	0.185	0.033999	3.332	5.530	0.917	-
SC156	0.242	0.034045	3.459	24.696	0.917	4%
SC138	0.180	0.361371	12.279	4.998	0.509	-
SC144	0.210	0.038282	3.284	8.573	0.907	-
SC152	0.193	0.039369	3.156	6.421	0.905	-
SC142	0.172	0.096044	3.092	4.247	0.796	-
SC143	0.242	0.10555	3.140	13.730	0.780	-
SC151	0.214	0.109127	3.373	9.080	0.774	-
SC150	0.213	0.111369	3.083	8.936	0.771	-
SCT142	0.279	0.314002	3.412	22.595	0.544	-
SC141	0.238	0.322879	2.901	13.042	0.537	-
SC148	0.246	0.327768	3.016	14.584	0.533	-
SC139	0.105	0.33512	11.816	-0.138	0.527	-
SC149	0.234	0.340191	3.222	12.268	0.524	-
SCT140	0.282	0.34045	3.366	23.421	0.523	-
SCT141	0.320	0.34045	3.332	37.820	0.523	-
SC140	0.242	0.354121	12.819	13.771	0.514	-

Table 4.8. **.** Summary of results for chemically initiated experiments done using latex CA01. All experiments in the table were run with no additional surfactant.

Results of experiments done with the optimum amount of surfactant are given in table 4.9. For all these experiments $\rho_{thermal}$ = 2.09 x 10^{-4} s^{-1}, k = 0.70 x 10^{-2} s^{-1} for no CD experiments. For 4% CD experiments k = 1.18 x 10^{-2} s^{-1}. Results of experiments done with no CD are in table 4.9a, while those done with CD are in table 4.9b. It is clear from table 4.9 that entry efficiency for 4% CD experiments was much higher than for experiments at which no CD was used, especially at low initiator concentrations

Experiment	N_c x 10^{-17}	[KPS] x L/mmol	$\bar{n}_{ss}$	$\rho_{initiator}$ x 10^4 s	F
SC171	3.243	0.001	0.117	0.431	0.219
SC169	3.167	0.011	0.215	9.272	0.461
SC168	3.353	0.035	0.279	22.428	0.368
SC164	3.243	0.105	0.373	74.150	0.396
SC165	3.400	0.105	0.325	40.089	0.224
SC163	5.571	0.332	0.292	26.701	0.078
SC170	3.247	0.335	0.355	58.901	0.099
SC157	3.282	1.122	0.372	74.022	0.037
SC158	3.343	2.135	0.384	86.870	0.024
SC162	3.214	4.249	0.430	181.703	0.024
SC159	3.313	4.279	0.323	39.370	0.005
SC160	3.209	4.518	0.395	102.303	0.013

Table 4.9a. Summary of results for chemically initiated experiments done using latex CA01. All experiments in the table were run with 0.09 g surfactant and no CD.

Experiment	N_c x 10^{-17}	[KPS] x L/mmol	$\bar{n}_{ss}$	$\rho_{initiator}$ x 10^4 s	F
SC174	3.349	0.001	0.124	2.767	1.458
SC175	3.232	0.011	0.202	14.036	0.726
SC176	3.202	0.108	0.323	67.225	0.345
SC177	3.227	0.323	0.390	161.258	0.279
SC178	3.256	1.072	0.357	103.537	0.054
SC179	3.268	2.131	0.380	139.445	0.037
SC180	3.172	4.257	0.349	92.928	0.012
SC181	3.249	3.261	0.278	39.044	0.007

Table 4.9b. Summary of results for chemically initiated experiments done using latex CA01. All experiments in the table were run with 0.09 g surfactant and 4% CD.

Further confirmation to the effect of CD on reaction rate for the cationic latex, figure 4.9 shows how the presence of CD increased the reaction rate for the lowest initiator concentration used. Increasing the initiator concentration does not nullify the positive

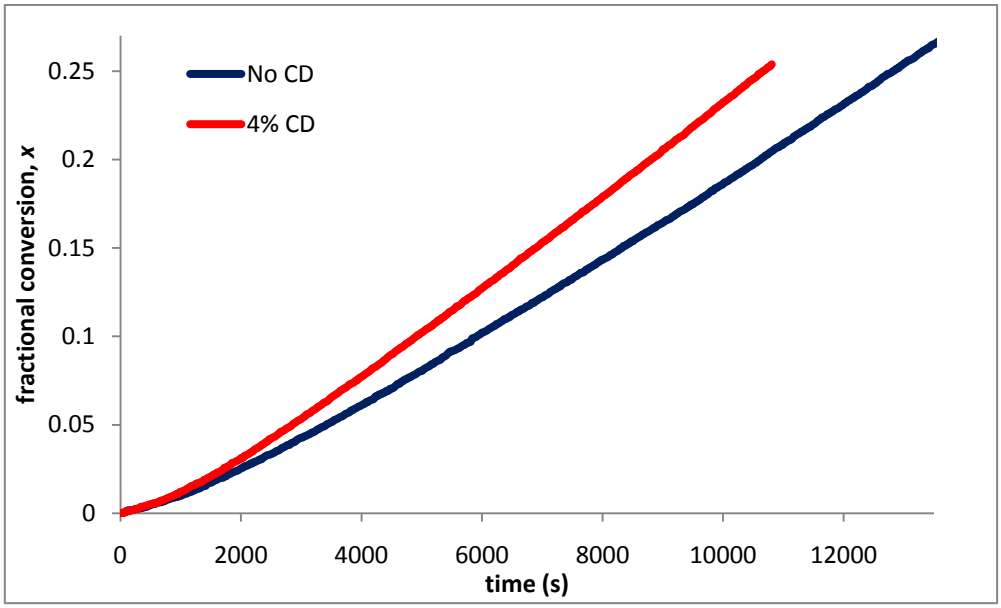

Figure 4.9. Effect of CD on reaction rate at V-50 concentration of 0.001 mmol/L, for latex CA01. Conversion time curves are for experiments SC171 (no CD) and SC174 (4%CD). 4% CD concentration has a noticeable positive effect on the reaction rate.

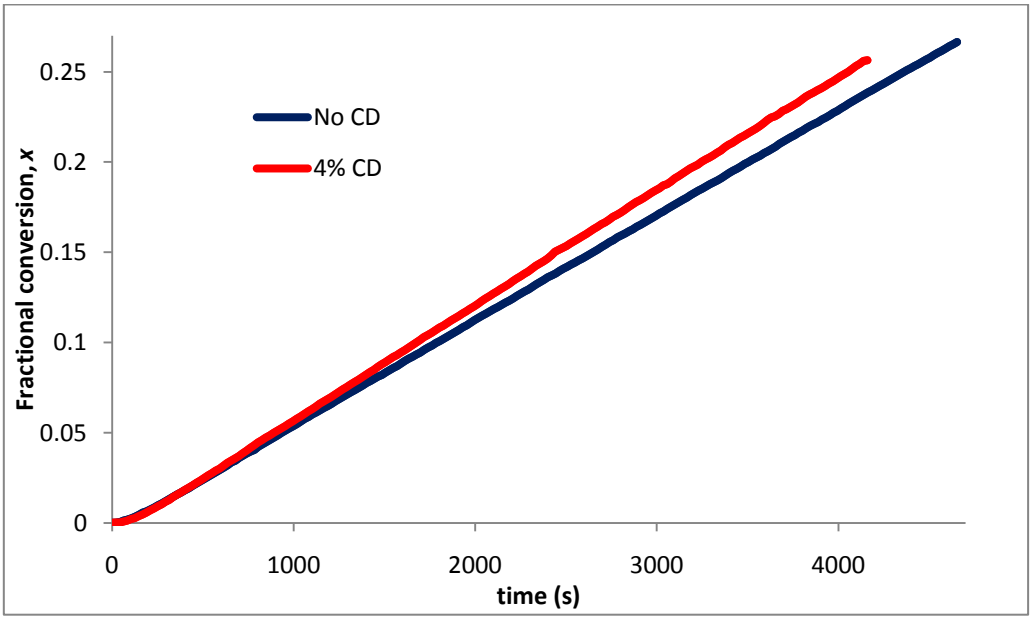

Figure 4.10. Effect of CD on reaction rate at V-50 concentration of 0.1 mmol/L, for latex CA01. Conversion time curves are for experiments SC165 (no CD) and SC176 (4%CD). 4% CD concentration has a noticeable positive effect on the reaction rate.

effect of CD, as shown in figure 4.10. The positive effect of CD on the reaction rate remains positive at medium V-50 concentrations (0.3 mmol/L) as shown in figure 4.11, and even at the highest concentration (4 mmol/L), as shown in figure 4.12.

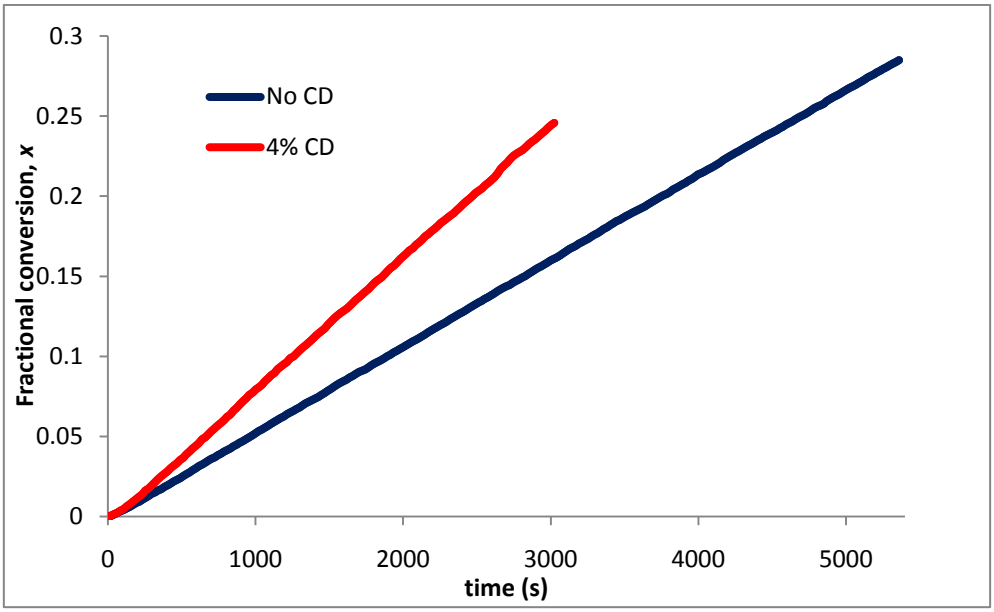

Figure 4.11. Effect of CD on reaction rate at V-50 concentration of 0.3 mmol/L, for latex CA01. Conversion time curves are for experiments SC170 (no CD) and SC177 (4%CD). 4% CD concentration has a noticeable positive effect on the reaction rate.

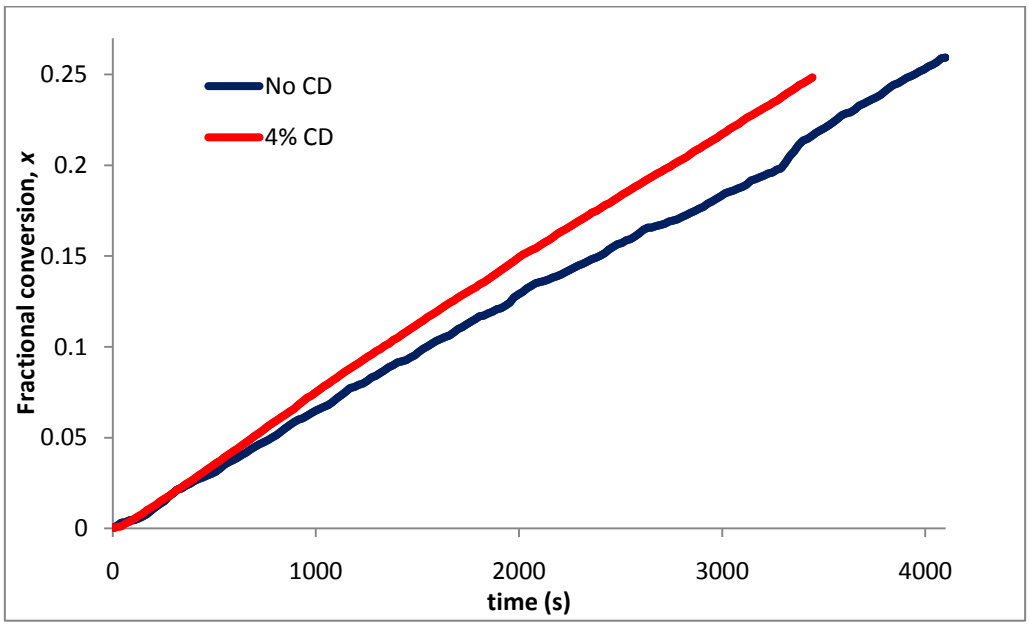

Figure 4.12. Effect of CD on reaction rate at V-50 concentration of 4 mmol/L, for latex CA01. Conversion time curves are for experiments SC159 (no CD) and SC180 (4%CD). 4% CD concentration has a noticeable positive effect on the reaction rate.

Figure 4.13 shows that *F* for all cases on which 4% CD concentration was used (as presented by red circles) is higher than the case at which no CD was used. Furthermore, the red and blue curves show two assumed exponential functions representing *F* as a function of initiator concentration, for 4% CD and no CD, respectively.

Figure 4.13 highlights another conclusion regarding the cationic latex/V-50 system, which is that *F* decreases with increasing initiator concentration, giving results similar to those obtained with the anionic latex, but opposite to those obtained earlier for seeded emulsion polymerization experiments run with anionically stabilized latices.[5,2] Interestingly, if *F* at the point of lowest initiator concentration with no CD was neglected, the curve representing *F* as a function of V-50 concentration (the blue dashed curve) will be starting with a value of *F* which is close to 100%., meaning that at very low initiator concentrations *F* is very close to 100%, which is similar to results found earlier for anionic latex/KPS system.[5,2] Assuming that *F* for the lowest concentration used was wrong, this assumption leads to the conclusion that initiator effect on entry efficiency does not show any major differences between KPS and V-50. With this assumption it can be concluded that *F* follows the generally known trend of limit 2a, of decreased entry efficiency with increased initiator concentration. CD results give further confirmation to this conclusion.

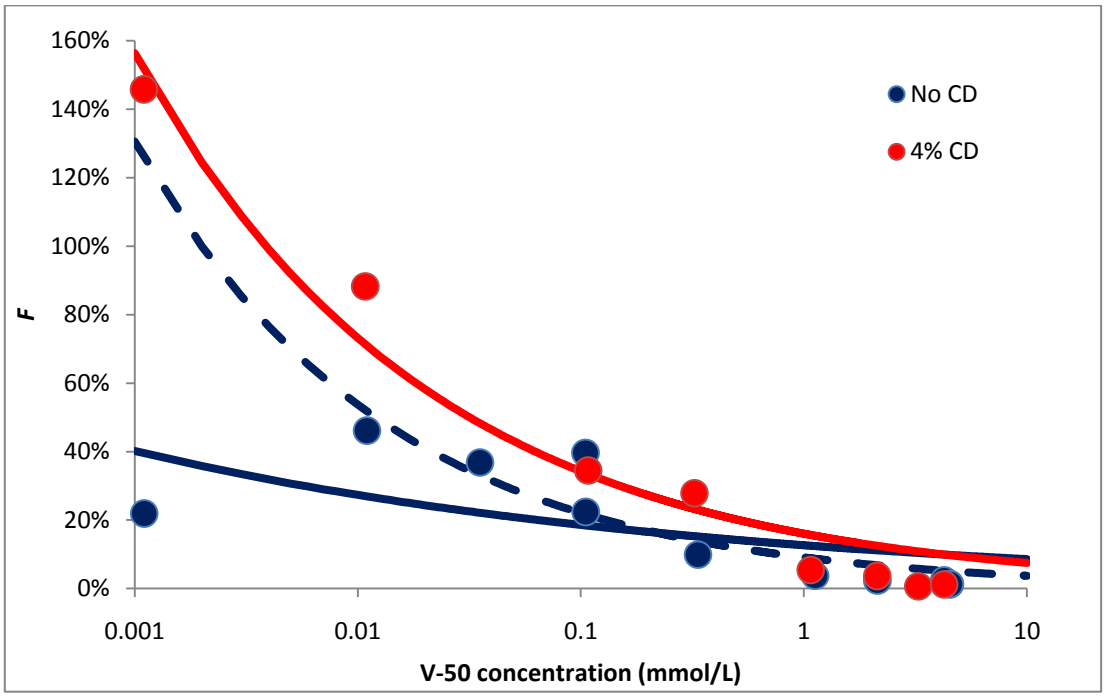

Figure 4.13a. Effect of CD on entry efficiency *F* at different initiator concentrations.

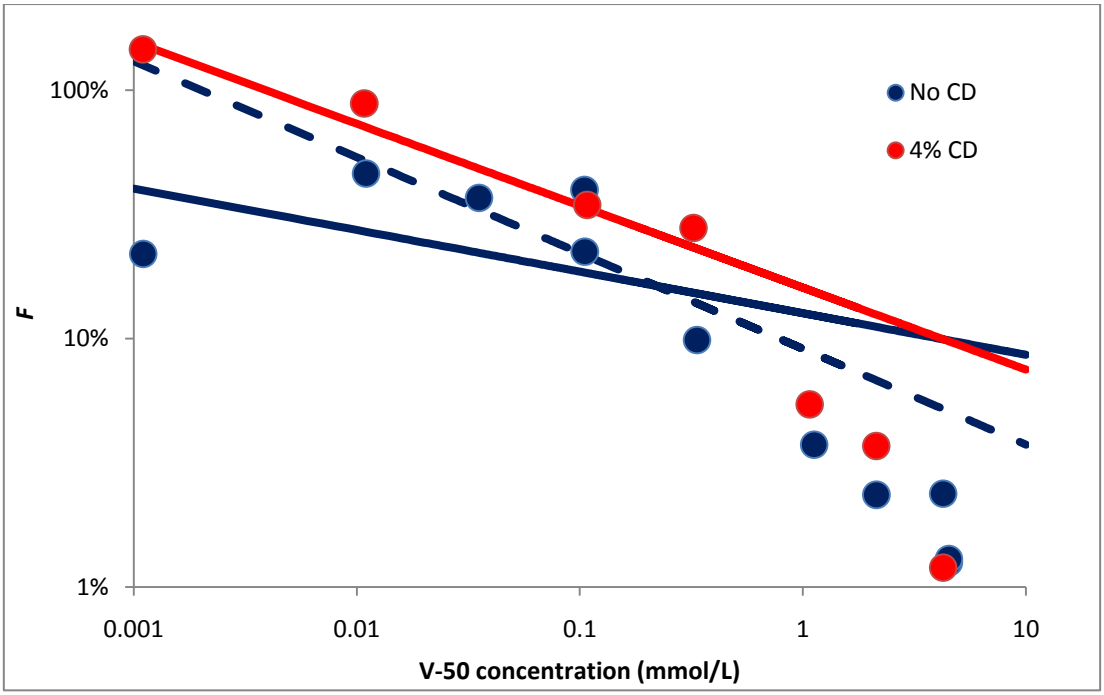

Figure 4.13b. Effect of CD on entry efficiency *F* at different initiator concentrations, axes in logarithmic scale.

Figure 4.13 also shows that, opposite to the conclusions drawn from the results of the anionic latex/KPS system, CD has a major effect on the overall reaction rate, and consequently on the entry efficiency. This effect is very clear at the very low initiator concentrations (0.001 mmol/L), and weakens gradually until it is nearly negligible. Interestingly, even at the highest initiator concentrations used for these experiments, *F* with 4% CD almost always remained higher than when CD was not used, though the difference between both values is very small to be easily noticed at concentrations higher than 2 mmol/L.

It can also be concluded that CD can push the reaction rate to its maximum limits. These limits are generally 2 for limit 2.a. First, $\bar{n}_{ss}$ can not exceed 0.5, because of the physical nature of systems following limit 2.a, which was further discussed in chapter I. Second, *F* should not be very high. Theoretically *F* should not exceed 100%, but this happened with the use of CD, which might suggest the need to amend the current entry efficiency calculating techniques. This is beyond the scope of this work.

A more significant conclusion can be drawn from comparing the effect of CD on both anionic and cationic latices. To answer the question by which section 4.4.2 was concluded,

the simple answer is that the initiator concentration plays an important role in determining the effect of CD on the reaction rate.

4.4.4 Comparing the efftect of CD on entry rate coefficient for both anionic and cationic latices

$\rho_{\text{initiator}}$, the entry rate coefficient, can be expected to increase with CD, thanks to the CD effect of increasing monomer solubility. Substituting $z = 2$ for styrene in equation (1.30), the equation takes the form:

$$\rho_{\text{initiator}} = \frac{2 f k_{\text{d}} [\text{I}] N_{\text{A}}}{N_{\text{c}} \left(\frac{2\sqrt{k_{\text{d}} [\text{I}] k_{\text{t,aq}}}}{k_{\text{p,aq}} C_{\text{W}}} + 1 \right)} \tag{4.12}$$

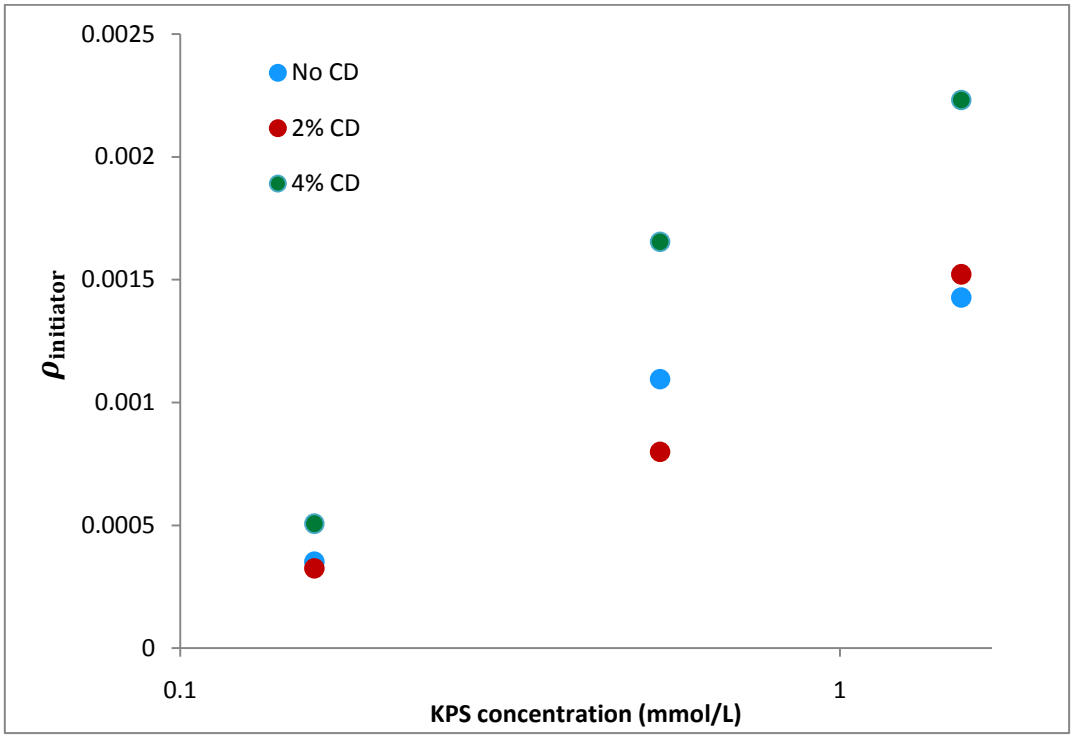

Figure 4.14. Effect of initiator and CD concentrations on the initiator component of the entry rate coefficient. $\rho_{\text{initiator}}$ increases with higher initiator concentration, and with the highest CD concentration used.

It is clear from equation 4.12 that $\rho_{\text{initiator}}$ is proportional to C_{W}. Consequently, an increase in $\rho_{\text{initiator}}$ and F is expected to be found with increasing either the initiator

concentration or the monomer solubility.

For the anionic latex, and as can be expected from the figures 4.3-4.6, both $\rho_{\text{initiator}}$ and F have been affected by increasing the initiator and increasing CD concentrations. Figures 4.7 and 4.14 show this effect.

When no CD is used, entry efficiency is at its lowest, and $\rho_{\text{initiator}}$ is also very low. This situation changes clearly at 4% CD, when F and $\rho_{\text{initiator}}$ values show substantial increase.

The effect of 2% CD is shown again to be compatible with what was shown earlier in figures 4.3-4.6. With both 0.15 and 0.5 mmol/L KPS, 2% CD has the lowest entry efficiency, and its slight increase at 4% CD is just a result for the decrease of the exit rate coefficient k.

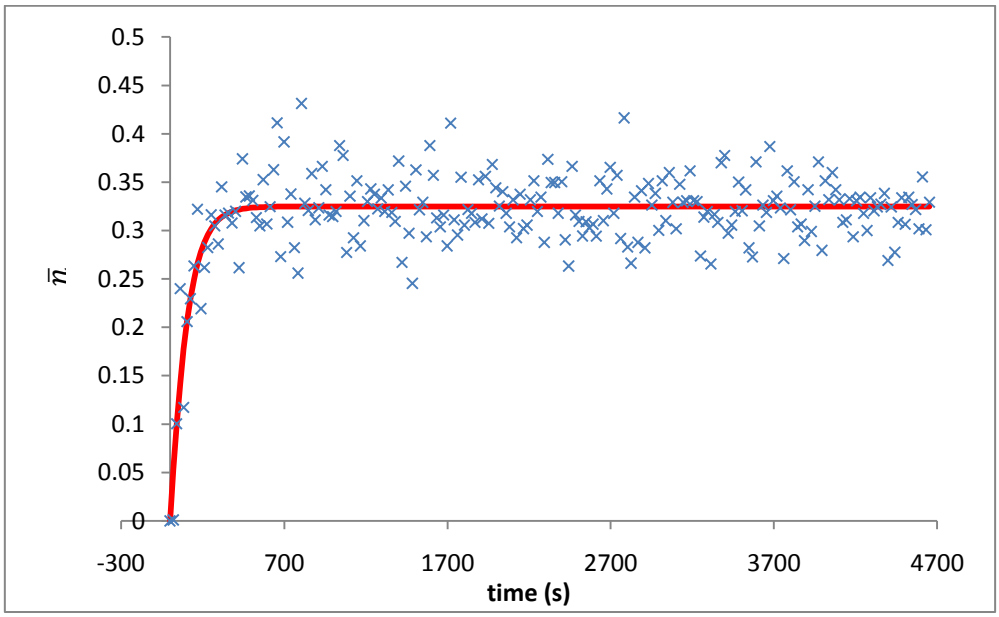

Figure 4.15. $\bar{n}$ as a function of time for a typical chemically initiated experiment (experiment SC165, 0.1 mmol/L V-50, no CD). Blue crosses: experimental values. Curve: equation (3.14) fitted. Lower stability can be seen from the relatively increased scattering around the fitted curve.

It is worth noting here that, similar to what was mentioned in chapter III, the stabilizing

effect of CD on the reaction progress was very clear. Figure 4.15 shows the relatively lower latex stability, as clear from the amount of scattering for the values of $\bar{n}$ values around the curve. Similar results of increased scattering were shown before during γ-relaxation experiments.

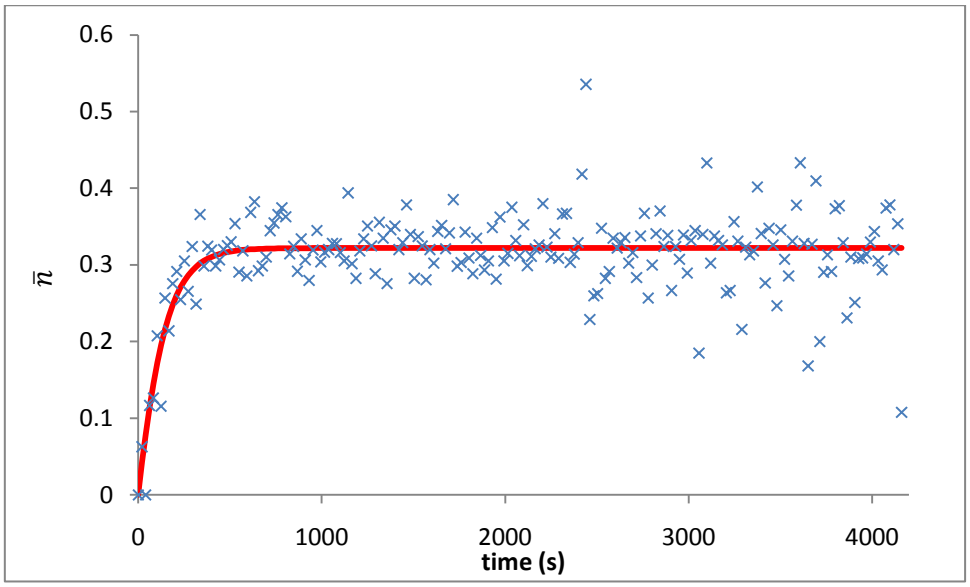

Figure 4.16. $\bar{n}$ as a function of time for a typical chemically initiated experiment (experiment SC176, 0.1 mmol/L V-50, 4% CD). Blue crosses: experimental values. Curve: equation (3.14) fitted. Higher stability can be seen from the relatively less scattering around the fitted curve.

Figure 4.12 shows the stabilizing effect of CD. The similarity of the stabilizing effect of CD confirms conclusions drawn earlier,[29] and adds another advantage to the use of CD in emulsion polymerization.

For the cationic latex, results are different when looking at the effect of CD on $\rho_{\text{initiator}}$. As shown in figure 4.17, $\rho_{\text{initiator}}$ increases with increasing initiator concentration and amount of CD.

The bigger increase at $\rho_{\text{initiator}}$ at 1.5 mmol/L V-50 is because the reaction at this point is away from the two limits. $\bar{n}$ is not very close to 0.5, and F is not very high. This could guarantee a high entry efficiency at special conditions. Otherwise, the general conclusion drawn from the graph can be, opposite to the anionic latex results, the presence of CD and

DTAB is always advantageous for the reaction rate of emulsion polymerization in cationic stabilized latices.

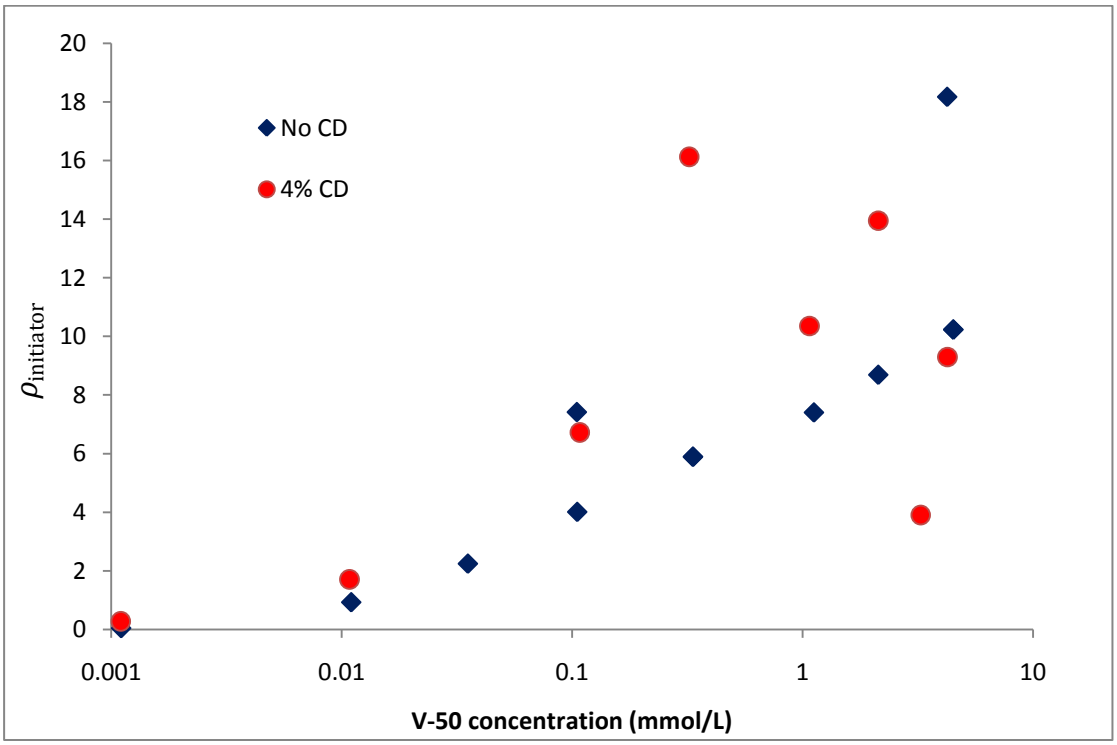

Figure 4.17. Effect of initiator concentration on $\rho_{initiator}$ at different CD concentrations for CA01 experiments. Experiment results show an increase in $\rho_{initiator}$, to a higher level that its increase with the anionic latices.

As has been mentioned earlier, all values of exit rate coefficient used in the calculations are the ones obtained from γ-relaxation calculations. But what will be the effect of initiator concentration on k if $\bar{n}$ data was analyzed only based on the chemically initiated experiments?

Best fit results obtained from figures similar to 4.15 and 4.16 were used to calculate ρ and k for chemically initiated experiments in the same way discussed and used throughout chapter III.

Values of k determined through this method at different initiator concentrations are shown in figure 4.18. Although such results can be considered close enough to the assumed true value of k (which was determined through γ-relaxation), these results are still affected by the oxygen present in the medium. Oxygen has been known earlier to have a retarding

effect on the reaction rate, and this effect diminishes with increasing initiator concentration.[14]

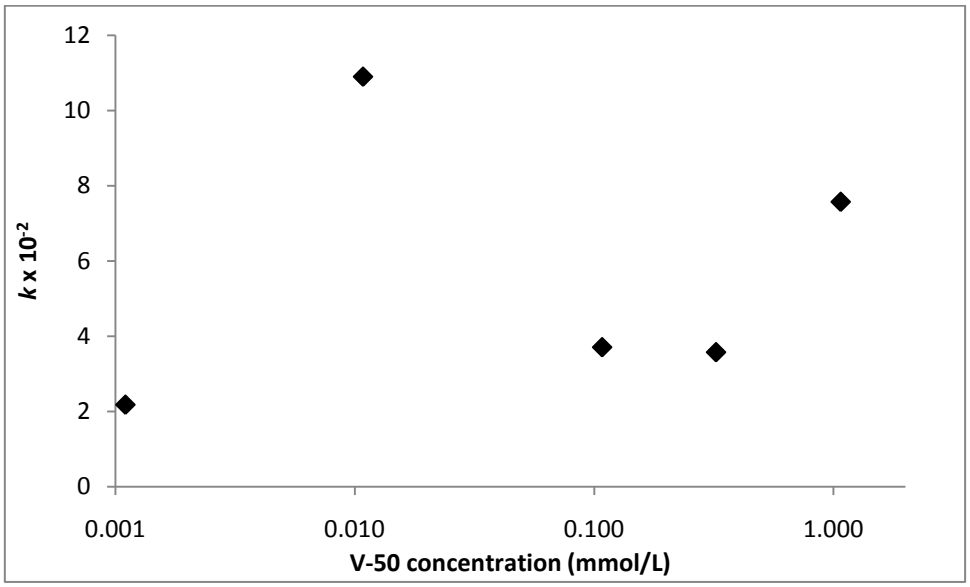

Figure 4.18. Effect of initiator concentration on exit rate coefficient, as *k* values were determined from best fit curves using equation 3.14.

k values were calculated using only equation (3.13) on chemically initiated experiments. It is clear that the calculated values get closer to the true value of *k*, which is 1.18 x 10^{-2}, as calculated from γ- relaxation experiments.

4.4.5 A mechanistic approach to the role of CD in emulsion polymerization systems

To have a deeper understanding on the actual effect of CD on the emulsion polymerization process, Harkins theory can be the starting point[30,31,32,33]. The theory states that the surfactant micelles are the main location at which the original nuclei form, this assumption will be shown shortly to fit directly with the CD experiments results.

Styrene has been found to penetrate deeply within the CD cavity,[34] a result which was found through ^{1}H NMR titration and quantum calculation. Both styrene and CD formed 1:1 inclusion complexes. With such a structure, the need for other chemicals which facilitate the solubility, especially surfactants and other organic solvents, can be completely replaced by CD.[35] This offers an environmentally friendly alternative to

surfactants and organic solvents. Another advantage here is the low price of CD,[36] which makes it a good catalyst not only in research but even industrially.

Following the assumption of Harkins, and knowing that CD increases the aqueous phase solubility of the monomer, there are two situations in which the role of CD can be discussed.

1. First is surfactant free aqueous phase polymerization, which is the case for a number of publications written about emulsion polymerization using CD.[11,16,20] CD was considered to be a complete replacement of surfactant,[37] it was even considered a surfactant itself.[38] If a chemical initiator is used, then the aqueous phase free radicals which resulted from the initiator decomposition will directly seek the styrene dissolved in water, including the molecules complexed within the CD molecules. In this case, for 1:1 CD : monomer mixture, the rate will be proportional to the square root of initiator concentration (typical emulsion polymerization kinetics).[11] Otherwise, the styrene dissolved in water, excluding any molecules complexed within CD cavities, will undergo spontaneous polymerization. The presence of CD here will not affect the reaction rate if no chemical initiator has been used, as was the case shown in table 3.7.

2. Second is the surfactant and CD emulsion polymerization, which is the case for the current research. In this case, when there is no chemical initiator, the presence of surfactant did increase the reaction rate, as appears in table 3.7. Explaining this in light of the Harkins theory can be simple. The most logical explanation will be that nuclei form both in surfactant micelles and in CD cavities. This is what speeds up the reaction when surfactant is used. In chemically initiated experiments, the free radicals produced from the initiator decomposition will seek the complexed styrene. In that case, and because the amount of styrene soluble in water increased due to the presence of CD, more styrene molecules can be attacked by free radical initiator molecules. Consequently, more styrene can be polymerized at the same period of time, speeding up the reaction.

Although this approach sounds logical, it still has not answered the question of why the

2% CD concentration had a noticeable effect on the reaction kinetics for the anionic latex/KPS experiments at the lowest initiator concentration used, and the reason of why CD loses its effect on entry efficiency at high initiator concentrations.

Using the same concepts from Harkins theory, and following the terminology of considering CD to be a surfactant,[38] what happens in the emulsion mixture when CD is present, in case of using an anionic surfactant, is not only a competition between the surfactant and the monomer. Actually, there is a thermodynamic equilibrium, which is never reached between three components, the initiated styrene molecules taking the form of free radicals, styrene molecules and surfactant.

Referring to the basic equations of emulsion polymerization, it is known that reactions start as:

$$\text{I—I} \xrightarrow{k_{\text{d}}} 2\text{I}^{\bullet} \qquad (4.13)$$

$$\text{I}^{\bullet} + \text{M} \xrightarrow{k_{\text{pi}}} \text{IM}^{\bullet} \qquad (4.14)$$

Equations (4.13) and (4.14) show that the two components, M and $\text{IM}^{\bullet}$ exist together in the aqueous phase of the medium. Knowing that these components are similar, but not the same, assuming an equilibrium between them in presence of the decomposed initiator is a logical assumption.

The decomposed initiator might not get complexed within the CD, because it is water soluble. But as the CD increases the styrene solubility in water, and knowing that the first free radicals formed are water insoluble (based on the conclusion drawn in chapter III that thermal polymerization is not an aqueous phase process, but rather depends mainly on surfactant), the reaction will proceed mainly with the small amount of styrene free radicals, $\text{IM}^{\bullet}$, which can exist in the aqueous phase.

The aqueous phase has three components competing for CD cavities, the monomer M, the initiated monomer free radicals $\text{IM}^{\bullet}$ and the surfactant. With a low initiator concentration (0.15 mmol/L), the concentration of the monomer free radicals is small. Le Chatelier's principle can be easily applied here. The component present at the lowest concentration

($IM^{\bullet}$) gets continuously consumed, so the equilibrium of equation (4.14) shifts towards producing more $IM^{\bullet}$, and even with small amounts of CD, the increased solubility of styrene at this case helps increasing the $IM^{\bullet}$ in the aqueous phase to maintain the equilibrium. Consequently, the surfactant-monomer competition for styrene cavities has a minor effect. This explanation is also valid for the case of the cationic latex, on which both the surfactant and the CD continuously speed up reaction (4.14). This explanation might go against current knowledge that reaction (4.14) is a very rapid reaction,[12] it should be noted that such knowledge is based on cases where CD was not present. Presence of CD has introduced some changes to the kinetics as previously shown, so this conclusion might still represent a valid explanation.

At higher KPS concentrations (0.5 and 1.5 mmol/L), more $IM^{\bullet}$ is present in the reaction medium, so it does not get consumed in a rate faster than its rate of formation. Consequently, the increased amount of $IM^{\bullet}$ and M, in addition to the surfactant, which is always present in the medium, keep competing for the CD cavities and so less $IM^{\bullet}$ can exist in the aqueous medium (in case of 2% CD concentration). Consequently, the reaction rate is slowed down.

4.5 Conclusions

The effect of CD on entry rate coefficients at different initiator concentrations was analyzed for four different latices. Experiments included the use of CD with different initiators, and this was done for latices stabilized with both anionic and cationic surfactants.

Using CD with chemical initiators was found to have an accelerating effect on the reaction rate of the emulsion polymerization of styrene. Entry efficiency and the initiator component of the entry rate coefficients were both found to increase with increasing the amount of CD used, unless increasing the CD decreases the solubility of styrene. This only happens when the surfactant used competes with styrene for CD cavities, and this was never the case with latices stabilized with a cationic surfactant.

For latices stabilized with anionic surfactant, CD did not have a similar effect to its effect on latices stabilized with cationic surfactants. As a general conclusion, CD should only be

used if it increases the solubility of styrene by increasing its concentration and the surfactant concentration. Otherwise, CD can have a negligible or sometimes even a negative effect on the reaction rate.

With this, the effect of CD on the emulsion polymerization of monomers having a very low solubility in water has been thoroughly studied. What about monomers having a higher solubility in water? This is the topic of discussion for the next chapter.

Appendix 4.1. Formulations for all styrene solubility measurement experiments with UV-Vis spectroscopy.

Component				Absorbance
Styrene	CD	AMA-80	DTAB	
1.64	-	-	-	0.507
2.08	-	0.077	-	0.876
2.07	-	0.079	-	0.962
2.04	0.0409	-	-	0.533
1.99	0.0405	0.077	-	0.885
2.05	0.0855	-	-	0.662
2.06	0.0832	0.080	-	1.058
2.07	-	-	0.0959	0.724
2.03	0.0430	-	0.0944	0.805
2.06	0.0819	-	0.0919	1.163

All amounts are in gram.

Appendix 4.2. Formulations for all styrene chemically initiated experiments

Latex AN04K experiments

Experiment	Component				Vessel
	latex	monomer	AMA-80	CD	volume
SNT4K01	10.11	3.41	0.07	-	57.12
SNT4K02	10.02	3.41	0.07	-	60.25
SNT4K03	10	3.42	-	-	57.12
SNT4K04	10.01	3.39	-	-	60.25
SNT4K05	10.01	3.39	-	-	60.25
SNT4K06	10	3.42	-	-	57.12
SNT4K07	9.99	3.42	-	-	60.25
SNT4K08	10.03	3.39	-	-	57.12
SNT4K09	10.04	3.4	-	-	60.25
SNT4K10	10	3.4	-	-	57.12
SNT4K11	7.45	2.56	-	0.1034	57.12
SNT4K12	7.43	2.55	-	0.052	57.12
SNT4K13	7.45	2.57	-	0.0515	59.18
SNT4K14	7.45	2.47	-	0.0503	57.12
SNT4K15	10.01	3.41	-	-	59.18
SNT4K16	9.97	3.41	-	-	57.12
SNT4K17	10.04	3.41	-	-	57.12
SNT4K18	10.01	3.4	-	-	59.18
SNT4K19	9.98	2.96	-	-	57.12

All component masses are in grams, vessel volume is in cm^3.

Latex AN01 experiments

Experiment	Component				Vessel
	latex	monomer	AMA-80	CD	volume
SNT120	10.02	3.39	-	-	57.12
SNT121	10.17	5.7	-	-	60.25
SNT122	10.1	3.4	-	-	57.12
SNT123	10.16	3.44	-	-	60.25

SNT124	10.01	3.33	-	-	60.25
SNT125	10.17	3.39	-	-	57.12

All component masses are in grams, vessel volume is in cm^3.

Latex AN02 experiments

Experiment	Component				Vessel
	latex	monomer	AMA-80	CD	volume
SNT226	13.69	3.37	-	-	59.18
SNT227	13.05	3.76	-	-	57.12
SNT228	13.32	4.02	-	-	57.12
SNT229	13.87	3.61	-	-	59.18
SNT230	12.91	3.44	-	-	57.12
SNT231	12.72	3.56	-	-	57.12
SNT232	13.13	3.56	-	-	57.12
SNT233	13.77	3.36	-	-	57.12
SNT234	13.22	3.38	-	-	57.12
SNT235	13.67	3.33	-	-	59.18
SNT236	13.84	3.43	-	-	57.12
SNT237	13.2	3.43	-	-	59.18
SNT238	13.16	3.42	-	-	57.12
SNT239	13.25	3.53	-	-	57.12
SN201	13.79	3.39	-	0.0698	59.18
SN202	12.99	3.46	-	0.0698	57.12
SN203	13.28	3.62	-	0.0673	57.12
SN204	12.99	3.4	-	0.0684	59.18
SN205	13.52	3.37	-	0.0667	57.12
SN206	13.18	3.42	-	0.069	57.12
SN207	16.24	3.38	-	0.0678	59.18
SN208	13.03	3.27	-	0.1374	57.12
SN209	13.05	3.33	-	0.1359	57.12
SN210	13.47	3.4	-	0.069	59.18
SN211	12.96	3.4	-	0.0691	57.12
SN212	13.27	3.38	-	0.0681	59.18

SN213	13.18	3.41	-	0.1346	57.12
SN214	13.14	3.41	-	0.1355	59.18
SN215	13.21	3.41	-	0.1353	57.12
SN216	12.94	3.53	-	0.1321	59.18

All component masses are in grams, vessel volume is in cm^3.

Latex AN04 Experiments

Experiment	Component				Vessel
	latex	monomer	AMA-80	CD	volume
SN417	9.8	3.36	-	-	59.18
SN418	7.45	3.36	-	-	59.18
SN419	7.31	2.4	-	0.4940	59.18
SN420	7.23	3.34	-	0.0706	59.18
SN421	7.26	3.34	-	-	57.12
SN422	7.53	3.38	-	0.1345	59.18
SN423	7.44	3.36	-	-	57.12
SN424	7.29	3.22	-	0.0631	59.18
SN425	7.31	3.46	-	0.0706	59.18
SN426	7.32	3.32	-	0.1293	57.12
SN427	7.26	3.27	-	-	59.18
SN428	7.21	3.24	-	0.0640	57.12
SN429	7.23	3.25	-	0.0639	59.18
SN430	7.47	3.15	-	0.1243	57.12
SN431	3.5	2.01	-	-	57.12
SN432	3.53	2.01	-	0.0407	59.18
SN433	3.55	2.01	-	-	57.12
SN434	3.49	2.02	-	0.0403	59.18
SN435	3.56	1.99	-	-	59.18
SN436	3.51	2.01	-	0.0415	59.18
SN437	3.42	2.09	-	0.0805	59.18

All component masses are in grams, vessel volume is in cm^3.

Latex AN05 Experiments

Experiment	Component				Vessel
	latex	monomer	AMA-80	CD	volume
SN507	3.06	2.14	-	-	57.14
SN508	3.01	2.24	-	0.0447	57.14
SN509	3.02	2.19	-	0.088	57.14
SN510	2.99	2.25	-	0.0885	57.13
SN511	3.05	2.23	0.0823	-	57.04
SN512	3.03	2.26	0.0786	-	57.13
SN513	3.06	2.2	0.0846	-	57.04
SN514	3.05	2.16	0.0770	0.0877	57.13
SN515	3.07	2.14	0.0831	0.0426	57.04
SN516	3.02	2.21	0.0786	0.0882	57.13
SN517	3.03	2.19	0.0808	0.0452	57.04
SN518	3.05	2.11	0.0801	0.0868	57.13
SN519	3.05	2.25	0.0801	-	57.04
SN520	3.06	2.25	0.0816	0.0461	57.13
SN521	3.1	2.19	0.0808	0.0867	57.04

All component masses are in grams, vessel volume is in cm^3.

Latex CA01 Experiments

Experiment	Component				Vessel
	latex	monomer	DTAB	CD	volume
SC138	11.6	3.19	-	-	57.12
SC139	11.61	3.17	-	-	59.18
SC140	11.42	3.93	-	-	57.12
SC141	2.96	2.33	-	-	59.18
SC142	3.03	2.46	-	-	57.12
SC143	3.08	2.41	-	-	57.12
SC144	3.23	2.27	-	-	57.12
SC145	3.84	2.34	-	-	57.12
SC148	3.08	2.28	-	-	59.18
SC149	3.17	2.28	-	-	57.14

SC150	3.15	2.24	-	-	59.18
SC151	3.31	2.38	-	-	57.14
SC152	3.22	2.31	-	-	59.18
SC153	3.28	2.24	-	-	57.14
SC154	3.25	2.27	-	0.0489	59.18
SC155	3.41	2.24	-	0.0453	57.81
SC156	3.4	2.29	-	0.0896	57.14
SCT140	3.35	2.3	-	-	57.81
SCT141	3.32	2.24	-	-	57.81
SCT142	3.35	2.36	-	-	57.14
SCT143	3.17	2.29	0.0096	-	57.81
SCT144	3.23	2.23	0.0095	-	57.14
SCT145	3.25	2.23	0.0094	-	57.81
SCT146	3.23	2.31	0.0967	-	57.81
SCT147	3.46	2.22	0.05	-	57.14
SCT148	3.55	2.25	0.071	-	57.81
SCT149	3.3	2.17	0.0825	-	57.14
SC157	3.21	2.47	0.0975	-	57.04
SC158	3.28	2.39	0.0966	-	57.14
SC159	3.25	2.32	0.0962	-	57.04
SC160	3.16	2.24	0.0943	-	57.14
SC161	3.3	2.24	0.0966	-	57.04
SC162	3.17	2.16	0.0939	-	57.14
SC163	5.41	2.55	0.096	-	57.04
SC164	3.19	2.28	0.0941	-	57.14
SC165	3.32	2.53	0.0963	-	57.04
SC166	3.14	2.25	0.0959	-	57.14
SC167	3.15	2.24	0.094	-	57.04
SC168	3.29	2.3	0.0964	-	57.04
SC169	3.11	2.28	0.0916	-	57.04
SC170	3.15	2.86	0.0964	-	57.04
SC171	3.18	2.44	0.0988	-	57.14
SC174	3.29	2.24	0.1005	0.0882	57.04

SC175	3.18	2.27	0.1019	0.091	57.14
SC176	3.15	2.19	0.0957	0.087	57.04
SC177	3.19	2.05	0.0979	0.0809	57.14
SC178	3.19	2.38	0.0992	0.0845	57.04
SC179	3.22	2.2	0.0974	0.0908	57.14
SC180	3.13	2.06	0.0968	0.082	57.04
SC181	3.24	2.21	0.0915	0.0926	57.04

All component masses are in grams, vessel volume is in cm^3.

References

(1) El-Aasser, M. and Sudol, E., *Features of Emulsion Polymerization*, El-Aasser, M. and Lovell, P., *Emulsion Polymerization and Emulsion Polymers*, **1997**, John Wiley and sons, New York.

(2) W.D. Harkins, *Journal of the American Chemical Society*, **1947**, 69, 1428

(3) Morrison , R., *An Economic Analysis of Electron Accelerators and Cobalt-60 for Irradiating food*, **1989**, U.S. Department of Agriculture.

(4) Lieser, K., *Nuclear and Radiochemistry Fundamentals and Applications*, **1996**, VCH Verlagsgesellschaft, Germany

(5) Maxwell, I., Morrison, B., Napper, D. and Gilbert, R., *Macromolecules*, **1991**, 24, 1629.

(6) van Berkel, K., Russell, G., Gilbert, R., *Macromolecules*, **2003**, 36, 3921.

(7) van Berkel, K., *Entry and the Kinetics of Emulsion polymerization*, a PhD thesis, University of Canterbury, **2004**.

(8) Lau, W., *Macromol. Symp.*, **2002**, 182, 283.

(9) Ritter, R. and Storsberg, J., *Macromol. Rapid Commun.*, **2000**, 21, 236.

(10) Hu, J., Li., Y., Ji, H. and Chen, Z., *Gaofenzi Xuebao 高分子学报*, **2007**, 3, 246

(11) Ritter, H., Steffens, C. and Storsberg, J., *e-polymers*, **2005**, 34, 1.

(12) Gilbert, Robert G., *Emulsion polymerisation, a mechanistic approach*, **1995**, Academic Press, London.

(13) Hawkett, B., Napper, D. and Gilbert, R., *Journal of the Chemical Society, Faraday Transactions 1*, **1980**, 76, 1323.

(14) De Bruyn, H., Gilbert, R. and Hawkett, B., *polymer*, **2000**, 41, 8633.

(15) Dougherty, T., *J. Am. Chem. Soc.*, **1961**, 83, 4849

(16) Hu, J., Li, S., Wang, D. and Liu, B., *Polymer International*, **2004**, 53, 1003

(17) Hu, J., Li, S. and Liu, B, *Journal of Polymer Material*, **2005**, 22, 213.

(18) Ritter, R. and Storsberg, J., *Macromol. Rapid Commun.*, **2000**, 21, 236.

(19) Ritter, H., Steffens, C. and Storsberg, J., *e-polymers*, **2005**, 34, 1.

(20) Ritter, H., Storsberg, J., van Aert, H. and Roost, C., *Macromolecules*, **2003**, 36, 50.

(21) Lide, D.(editor), *Handbook of Chemistry and Physics*, **2005**, Taylor and Francis, Florida

(22) Lane, W. H., *Ind. Eng. Chem.*, **1946**, 18, 295.

(23) Yeats, C., Krieg, H. and Breytenbach, J., *Enzyme and Microbial Technology*, **2007**, 40, 228.

(24) Lehn, J. *at al.* (Editor), *Comprehensive Supramolecular Chemistry*, Szejtli, J. and Osa, T., *Volume 3: Cyclodextrins*, **1996**, Pergamon, UK

(25) Wilson, L., *Binding Studies of Cyclodextrin-Surfactant Complexes*, a PhD thesis, University of Saskatchewan, **1998**.

(26) Chang, R., Chemistry, 9th Edition, **2007**, McGraw Hill Higher Education, New York

(27) Adams, M., Trau, M., Gilbert, R., Napper, D. and Sangster, D., *Aust. J. Chem.*, **1988**, 41, 1799.

(28) Thicket, S. and Gilbert, R., *Polymer*, **2007**, 48, 6965

(29) Ritter, H., Storsberg, J., van Aert, H. and Roost, C., *Macromolecules*, **2003**, 36, 50.

(30) Blackley D.C., *Emulsion polymerization theory and practice*, **1975**, Applied science publishers ltd, London

(31) W.D. Harkins, *Journal of Chemical Physics*,**1945**, 13,381

(32) W.D. Harkins, *Journal of Chemical Physics*,**1946**, 14,47

(33) W.D. Harkins, *Journal of the American Chemical Society*, **1947**, 69, 1428

(34) Cao, Y., Xiao, X., Lua, R. and Guo, Q., *J. Mol. Struct.*, **2003**, 660, 73.

(35) Hu, J., Huang, R., Cao, S. and Hoa, Y., *e-polymers*, **2008**, 171

(36) Loftsson, T. and Duchêne, D., *International Journal of Pharmaceuticals*, **2007**, 329, 1

(37) Rimmer, S. and Tattersall, P., *Polymer*, **1999**, 40, 6673

(38) Madison, P., and Long, T., *Biomacromolecules*, **2000**, 1, 615

Chapter V

Effect of Cyclodextrin on the γ-Radiolysis Initiated Emulsion Polymerization of Methyl Methacrylate

5.1 Introduction

After establishing a well based idea on the effect of CD on the rate of the emulsion polymerization of a monomer having low water solubility like styrene, the CD effect on a monomer with higher water solubility was studied next. What is required is a monomer which is widely used in research for emulsion polymerization, and that has been well studied previously, and most importantly, has higher water solubility than styrene. Methyl methacrylate (MMA) fulfils all these requirements.

Water solubility of MMA is much higher than that of styrene, as it was found to be 0.15 mol/L,[1] compared to 4.1×10^{-3} mol/L for styrene (the value found during the course of this work as mentioned in chapter IV).

Because of this higher solubility which makes the reaction procedure different than that of monomers with lower solubility, models have been derived for MMA since 1946,[2,3,4] around the same time Harkins derived his model. More advanced studies for the polymerization of MMA were done later, like the research on MMA water soluble oligomers,[5] and similar work on styrene-MMA copolymerization.[6]

MMA catalyzed emulsion polymerization kinetics have been thoroughly studied, an example is the use of Co^{2+} catalyst and its effect with V-50 and sodium dodecyl sulphate.[7] Another study was done using microwave irradiation with one anionic and one non-ionic emulsifier and KPS as initiator, and running the reactions in a commercial microwave reactor.[8] Both the catalyst and the microwaves had a positive catalytic effect on the reaction kinetics.

Using γ-radiolysis as an initiating technique with MMA, this work was done previously by only a small number of researchers.[1,9,10,11] It is appropriate to mention that from this

work, only two researchers worked for the sole purpose of the emulsion polymerization kinetics of MMA.[9,10]

There was one other investigation of the effect of CD on MMA in presence of a RAFT reagent, and it has shown that CD facilitates the transportation of the RAFT reagent across the aqueous phase.[12]

This current research is the first research done on the kinetics of MMA emulsion polymerization with cyclodextrin (CD). For the first time it uses the γ-radiolysis technique to show the effect of CD on the termination rate of MMA.

5.2 Theoretical background

5.2.1 Thermal initiation of MMA

In contrast to styrene, very little is known about the mechanisms of thermal polymerization of MMA. Examples of suggested mechanisms include the formation of "cyclic dimers and linear trimers", both of them having unsaturated bonds.[13] The rate of thermal polymerization of MMA was found to change under specific conditions, for example, chlorine-containing acrylates polymerize at much higher rates than MMA.[14] Another example was that transfer agents also speed up the thermal polymerization reaction of MMA.[15]

This mechanism suggests that the dimers formed have two unpaired electrons, which can form a bi-radical. Following this suggestion is not very easy, as it means that all chemical reactions used in deriving the current kinetic models will have to be readjusted to allow the presence of the bi-radical on the reactants side of the equations.

Regardless of the actual mechanism which really takes place during the thermal polymerization (and also the γ-initiated polymerization of MMA), the same approach for studying thermal polymerization is followed as in chapter III.

The importance of thermally initiated experiments is that such experiments give the most accurate method to calculate ρ_{thermal} , the thermal component of the free radical entry rate

coefficient to the particle ρ. As in the case of styrene, ρ_{thermal} represents one component of ρ which cannot be neglected, as shown equation (5.1):

$$\rho = \rho_{\text{thermal}} + \rho_{\text{init iator}} \tag{5.1}$$

If ρ_{thermal} is not known, then the value of $\rho_{\text{initiator}}$, the initiator component of the entry rate coefficient, cannot be accurately calculated. Consequently, any calculations for the entry efficiency will have wrong results. All chemically initiated experiments and their entry efficiency results will be discussed in chapter VI.

5.2.2 Initiation through γ-radiolysis

γ-rays are emitted from the nuclei of some metal isotopes as these nuclei move down from an excited state to a lower energy state.[16] In some cases this happens through β-decay, which is the emission of a negatron or a positron from the nuclei.[17] ^{60}Co, which is the only source of γ-rays used during the course of this work, releases γ-rays as a result of β-decay.

Neither thermal nor γ-radiolysis initiation experiments involve the use of a chemical initiator whose concentration is known. For both cases the reaction can be assumed to follow the following reaction sequence:[18]

Initiation: $M \longrightarrow M^{\bullet}$ (5.2)

Propagation: $M^{\bullet} + M \longrightarrow MM^{\bullet}$ (5.3)

$M_i^{\bullet} + M \longrightarrow M_{i+1}^{\bullet}$ (5.4)

Termination:

- Combination: $M_i^{\bullet} + M_j^{\bullet} \longrightarrow P_{i+j}$ (5.5)
- Disproportionation $M_i^{\bullet} + M_j^{\bullet} \longrightarrow P_i + P_j$ (5.6)

where M is a monomer molecule and P is a polymer molecule.

The γ-radiolysis experiments involve running the emulsion polymerization reaction in a dilatometer glass vessel surrounded by a ^{60}Co hollow cylinder. The flux of γ-rays enables the polymerization to run at a very high rate. After a few minutes of polymerization, the vessel is taken away from the γ-ray source, and the rate of polymerization starts declining slowly, until it reaches a constant very low rate. From this process the termination rate constant *c* can be calculated.

5.2.3 Measurements of entry and termination rate coefficients

As already mentioned in chapter III, the only parameter which can be directly calculated from the tracker data is the change in volume versus time. In the case of styrene, fractional conversion, *x*, can be calculated in a straight forward manner from this data. For the case of MMA, the increased solubility of the monomer in the aqueous phase, in addition to the non-ideal mixing between MMA and water makes it very hard to directly calculate the fractional conversion from the volumetric change. To overcome this problem, the following procedure[1,19] was followed.

$$m_x = \frac{\Delta V}{V_{sM} - V_{sp}} \tag{5.7}$$

where m_x is the mass of monomer converted into polymer. V_{sM} and V_{sp} are the partial specific volumes of the monomer and polymer, respectively. $V_{sM} = 1/d_M$ and $V_{sp} = 1/d_P$. d_M and d_P are the densities of the monomer and the polymer, respectively. For MMA at 50^{o}C, d_M = 0.909 g/cm^3, and d_P = 1.226 *g*/cm^3, as have been previously measured.[19]

Following this definition, from a general mass balance for the system, the mass of polymer within the system, m_p, and the mass of monomer within the particles, m_P, can be defined as follows:

$$m_p = m_p{}^{seed} + m_x \tag{5.8}$$

$$m_P = m_M{}^0 - m_w - m_x \tag{5.9}$$

where m_p^{seed} is the mass of monomer originally present within the system. $m_p^{seed} \neq 0$ for all seeded emulsion polymerization kinetic experiments done throughout the course of this work. m_M^0 is the mass of monomer present in the system at the beginning of the experiment, and m_w is the mass of monomer dissolved in the aqueous phase.

Knowing the amount of monomer present within the particles m_P, the concentration of the monomer within the particles can be calculated from

$$C_P = \frac{m_P/M_0}{m_M V_{sM} + m_p V_{sp}} \tag{5.10}$$

where M_0 is the molecular weight of the monomer. During interval II, $C_P = C_P^{sat}$, but the number calculated from equation (5.10) may exceed the value of C_P^{sat} because of the presence of monomer droplets in the reaction medium. Knowing C_P, m_x can be easily calculated from equation (5.7).

During interval III, the volume contraction is the result of the conversion of monomer into polymer and the movement of monomer from the aqueous phase to the particles. In this case, volumetric change can be considered to be

$$\Delta V = m_x\left(V_{sM} - V_{sp}\right) + \left(m_W{}^0 - m_W\right)\left(V_{sM,aq} - V_{sM}\right) \tag{5.11}$$

m_w^0 is the mass of the monomer in the aqueous phase at the beginning of the experiment, m_w is the mass of the monomer in the aqueous phase at any time. $V_{sM,aq}$ is the partial specific volume of the monomer in the aqueous phase, this parameter must be included in the calculations to oversee the problem caused bythe non-ideal mixing. For MMA $V_{sM,aq}$ = 1.022cm^3/g. m_w^0 is equal to $C_W V_W M_0$, where V_W is the volume of the aqueous phase. Equation (5.11) can be considered to be a more general form for equation (5.7)

Finally, the monomer concentrations in the aqueous phase and the particles can be calculated from

$$\frac{C_W}{C_W{}^{sat}} = \left(\frac{C_P}{C_P{}^{sat}}\right)^{0.6} \tag{5.12}$$

Solving equations (5.10), (5.11) and (5.12) iteratively, the three unknowns (C_P^{sat}, m_x and m_W) can be calculated. Knowing that m_x is actually equal to xm_M^0, the fractional conversion x can be obtained.

This procedure was followed mainly because of the non-ideal mixing of the monomer with water.

After calculating the fractional conversion x, average number of radicals per particle $\bar{n}$ can be calculated, from which other entry and termination parameters can also be calculated. $\bar{n}$ for MMA is expected to higher values than zero-one system as MMA is a "pseudo-bulk" system.

As this research focuses on the effect of CD on ρ, k and c, a similar procedure to the one for styrene is followed with MMA. Again, γ-relaxation experiments were used to determine the value of c. The technique was to start the reaction by exposing the reaction medium to a flux of γ-rays. As the reaction is initiated, the medium is removed from the γ-rays source, γ-relaxation takes place. The slowing down of the rate is mainly because of radical loss kinetics. Consequently, c can be calculated from the γ-relaxation data.

As with styrene, the "in-source" entry rate coefficient is supposed to be equal to $\rho_{thermal} + \rho_\gamma$, and this makes it hard to calculate the thermal entry rate coefficient from "in-source" data alone. In addition to the presence of oxygen gas within the system, "in-source" data were not used to calculate any kinetic parameters for this work.

5.2.4 Pseudo-bulk kinetics in the emulsion polymerization of MMA

This analysis is mainly based upon the work done earlier by two researchers.[1,10] Going back to the Smith-Ewart theory[20], the main theory currently used in the analysis of emulsion polymerization results, entry, exit and termination parameters can all be calculated from the general form of the Smith-Ewart equation, equation (1.4), which can be re-written for the pseudo-bulk systems in the form

$$\frac{d\bar{n}}{dt} = \rho - (1-\alpha)k\bar{n} - 2c\bar{n}^2 \qquad (5.13)$$

Equation (5.13) can be solved in a manner which is not very complicated, that is if the values of $\bar{n}$ are known, and they can be easily found if the conversions are known at different times. This can be done using the equation

$$\frac{\mathrm{d}x}{\mathrm{d}t} = \frac{k_\mathrm{p} C_\mathrm{P} N_\mathrm{c}}{{m_\mathrm{M}}^0 N_\mathrm{A}} \bar{n} \tag{5.14}$$

Using the actual values of $\bar{n}$ as calculated from the conversion data, and the values obtained from the model, equation (5.13), both sets of values of $\bar{n}$ can be compared to each other. Through this comparison, assumed values of ρ, k and c can be checked whether they are accurate enough or need to be adjusted. Through a series of trial and error with an error minimizing function, the values of these parameters can be calculated.

Another characteristic of equation (5.13) is that, as an approximation of the original Smith-Ewart model, equation (5.13) can be taken as an accurate approximation under the conditions that $k > c$ or $\rho > c$,[21] which helps ensure the accuracy of the results obtained through using this approximation.

In cases of low radical concentration, which is the case during the γ-relaxation periods, the concentration of free radicals within the aqueous phase decreases, which will reduce the possibility of exited radicals' termination. This reduces the value of the exit rate parameters in the process, resulting in $\alpha = 1$ and equation (5.13) takes the form

$$\frac{\mathrm{d}\bar{n}}{\mathrm{d}t} = \rho - 2c\bar{n}^2 \tag{5.15}$$

Equation (5.15) is same as equation (1.50), limit 3 equation. If c is known then the steady state value of $\bar{n}$ can be easily obtained from

$$\bar{n} = \sqrt{\frac{\rho}{2c}} \tag{5.16}$$

Alternatively, termination cab be expressed by k_t, the second order rate coefficient of bimolecular termination, which can be calculated knowing V_s, the swollen volume of the

latex particle as

$$k_t = cN_A V_s \tag{5.17}$$

5.2.5 The Trommsdorff-Norrish effect

One of the major differences between styrene and MMA is that the rate of polymerization depends on the chain length of the growing radicals. This effect of the chain length on the reaction rate is known as the "Trommsdorff-Norrish" effect, sometimes called also "gel effect". The effect was noticed for the first time in1942[22] when it was noticed that the rate of the reaction increased markedly after about 10-20% of conversion. At that early stage the assumption was that the increase is because of the increased temperature of the reaction medium,[22] resulting from the exothermic nature of the polymerization reaction.

More recent research[23,24,25,26] has shown that the reason for the reaction rate increase is not the temperature increase. It is actually because of the entanglement of short chains within the polymerization medium, which is the swollen particles in the case of emulsion polymerization. With an increase in weight fraction of polymer within the medium, w_p, it is easier to have entanglement between shorter and shorter chains. In this case, k_t is affected by the termination between a short chain which is propagating, so becoming less mobile, and a long chain which has very limited mobility. In a situation like this, the more conversion takes place the less the value of k_t will be. Consequently, the rate (expressed by $\bar{n}$) increases with increased conversion.

Figure 5.1 gives a simplified form of the entanglement which takes place within the swollen MMA particles with increased chain lengths of the forming polymer chains.

It has been found through the course of this work, and even in previous work done on emulsion polymerization of MMA,[1,10] that this increase in reaction rate starts at a very early stage of the reaction. But it is to be expected that during interval II, the effect of chain length on reaction kinetics is negligible, as the main reason for reaction rate increase during interval II is the increase in reaction medium volume because of the continuous increase in $V_{s,}$[1] as will be discussed in more details in chapter VI.

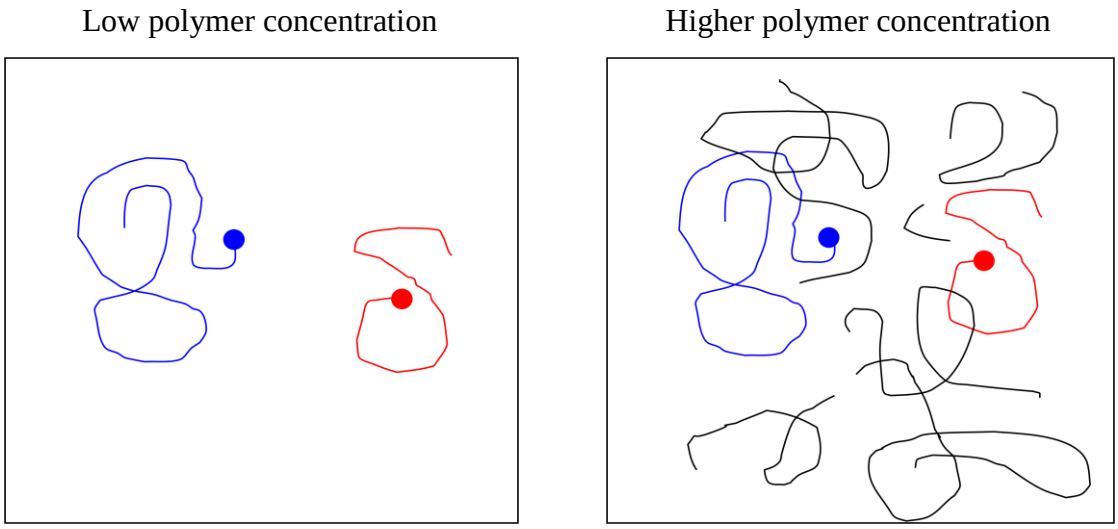

Figure 5.1. Simplified representation of chain length entanglement and its effect on viscosity.

5.3 Experimental Part

5.3.1 Synthesis and purification of seed latex

MMA was purchased stabilized with hydroquinone. Inhibitor removal was done by passing the MMA through a column of basic activated aluminium oxide. It was found earlier that the purity of the MMA monomer is a major factor which can affect the results of kinetic experiments.[27] GC tests done for purified MMA have shown that it is 100% pure, confirming that the basic aluminium hydroxide removed all the hydroquinone present. Consequently, no further distillation was applied for MMA. After removal of inhibitor, MMA was kept at 0 ^{o}C to avoid any spontaneous polymerization. Table 5.1 shows the formulations used for the latex synthesis.

As a main aim to this work is to study the effect of CD on experiments similar to what was previously done, MMA seed latex similar to the latices prepared during earlier research work was prepared.[1,10] As previous research was done only on anionically stabilized latices, similar work was done in this current project, and no cationically stabilized latex was prepared.

Latex was synthesized by mixing water, surfactant and sodium bicarbonate together in the reactor, which consists mainly of a 1 L glass cylinder surrounded with a water jacket to control the temperature. Mixing took place while the reactor wass being heated until it reached 90 ^{o}C, then MMA was added. Finally, a solution of 3.1 g KPS dissolved in about 55 g water is added to the reactor, and polymerization continues for the specified time, confirming that all monomer has been converted to polymer.

Ingredient	Amount (g)
Milli-Q water	765
MMA	195
Surfactant (AMA-80)	20
$NaHCO_3$	1
Initiator (KPS)	3.1
Temperature	92^{o}C
Reaction Time	24 h

Table 5.1. Seed Latex Preparation, all amounts are in gram.

The polymerization process within the reactor is run under an oxygen free environment (except for the oxygen which might be present within the water and monomer). This is guaranteed by continuously running nitrogen gas at the early stages (first 45 minutes) of the reaction, then closing the top of the reactor. Nitrogen gas introduced at the start is expected to have expelled most of the oxygen present within the system at the beginning of the reaction.

After synthesis, the seed latex is dialyzed in Milli-Q water for around 5 weeks in a 5 L beaker, water is changed twice a day in the first week, then daily in the remaining period. Dialysis ensures the latex is purified of any non-reacted water-soluble chemicals (like extra surfactant, buffer, and non-reacted initiator), and any minor amounts of monomer which might not have reacted.

5.3.2 Determination of seed latex characteristics

The % solid is determined through gravimetry. Both particle size distribution and average

particle diameter were determined through TEM, Particle Size Distribution Analyzer (PSDA), and by High Performance Particle Sizer (HPPS).

Characteristics	
Average Particle Diameter (nm)	
TEM	79.18
PSDA	103.91
HPPS	100.69
Value used for kinetic analysis	**103.91**
PDI*	1.011
% Solids	17.76
C_P^{SAT} (mol/L)	6.828

* PDI equals weight-average particle diameter / number-average particle diameter

Table 5.2. Seed latex properties

Contrary to the determination of PDI and average particle diameter in styrene, using TEM to determine such values for MMA is a very problematic process. This is because poly(MMA) particles deform under the electron beam, as was found earlier,[10] so it was very difficult to obtain accurate measurement for the sizes of the particles using TEM.

To avoid the particle deformation problem, carbon coating was used to protect the particles from the strong electron beam. Theoretically this can solve the problem, but practically this created another problem. The standard particles used for calibration of TEM measurements, whose average particle diameter is 234 nm, differ significantly in size from the poly MMA particles produced, which means that standard and MMA particles will both have carbon coatings of different thickness.

The approach followed was not to coat the standard particles and measure them independently, then measure the coated MMA particles. When measuring the MMA particles, the thick coating layer surrounding the particle was not included in the diameter, the diameter length measured was only for the clear centre of the particle, excluding the dark-coloured surrounding. This method, although theoretically solving the problem, was very inaccurate because it is very hard to define the border of the poly MMA particle when coated, which means that part of the actual particle diameter was not included in the

measurement. This explains why the average particle diameter determined through TEM is much less than its value determined through other techniques.

When doing kinetic calculations, average particle diameter as measured with PSDA was used, as it can be considered the most accurate method used to measure the particle sizes.

5.3.3 Determination of monomer solubility

During the course of the emulsion polymerization process, both the particles and the aqueous phase contain an amount of monomer. Equations (5.10) to (5.12) have to be solved to obtain the time conversion data, from which other parameters can be calculated. Equation (5.10) requires knowing the value of C_P, and equation (5.12) requires both C_P and C_W. Consequently, any trial to calculate the conversion without having accurate values of these two variables, especially in interval III, where $C_P < C_P^{sat}$, will certainly provide wrong results for conversion.

Knowing that the main effect of CD should be to increase the monomer solubility in the aqueous phase, C_W^{sat} was measured at 2% and 4% CD concentration, relative to the total mass of monomer used, in addition to measuring it with no CD.

C_P^{sat} was measured using static swelling method. A known amount of the latex was diluted with water in a dilatometer vessel, and a known amount of MMA was added to the mixture. Mixing was done overnight, then the vessel was heated to 50 ^oC (the temperature at which all kinetic experiments were run) with the stirrer still running. After about an hour stirring is stopped, and the vessel is left for another hour to make sure all dispersed MMA is separated from the aqueous phase. Finally, a capillary tube with known internal diameter is inserted at the top of the vessel and water is injected to the mixture. The MMA layer is pushed within the capillary tube where its height can be measured using a Vernier caliper. By knowing the amount of MMA which was not separated from the mixture, the amount of MMA dissolved in water (as calculated using literature values[1] of C_W^{sat}) , and the original amount of MMA used, then the amount of MMA dissolved within the particles can be calculated, from this calculating C_P^{sat} is a straight forward step. For more information about static swelling check chapter I.

C_W^{sat} was calculated in a different method. Similar to the procedure followed with C_P^{sat}, a mixture of known amounts of monomer and water is prepared (no seed latex is used in this case). CD and surfactant are added in some experiments, as will be discussed later. The mixture is heated to 50 ^oC for a few hours then stirring is stopped for one hour. Samples were taken of the mixture, diluted to a known amount, and then the concentration of the diluted MMA samples was found using a Varian Cary 100 Bio UV-Vis spectrophotometer. Knowing the amounts used for dilution, C_W^{SAT} at different conditions was calculated. More information about solubility measurement can be found at section 2.6. Results of solubility measurements for MMA are presented in section 6.3.3.

5.3.4 Kinetic experiments

To avoid any interference with interval I kinetics, all experiments were started at interval II. This was done by using the seed latex previously prepared, as mentioned in section 5.3.2. Starting the kinetic experiment at interval II gives the advantage of knowing the latex characteristics, like % solids, C_P^{SAT} and the average particle diameter. Knowing the values of such parameters makes it easier to calculate $\bar{n}$ through equation (5.14)

$$\frac{dx}{dt} = \frac{k_p C_P N_c}{{m_M}^0 N_A} \bar{n} \tag{5.14}$$

where x is the fractional conversion of monomer to polymer, t is the time, k_p is the propagation rate coefficient, C_P is the monomer concentration within the latex particles, N_c is the number of latex particles per unit volume of aqueous phase, ${n_M}^0$ is the amount of monomer added to the latex at the beginning of the reaction and N_A is Avogadro number.

Kinetic experiments were run as per the following procedure, known amounts of latex, monomer, surfactant and CD are mixed together in a dilatometer vessel of known volume. The whole mixture is diluted with water until vessel components can almost fill it. Components were mixed for suitable time, and then hot water was passed through the jacket, and air was taken out through a small syringe until the monomer starts to boil. Water at 50 ^oC was passed through the vessel until thermal equilibrium is reached. A capillary tube with known diameter was placed at the top of the dilatometer vessel, and then water, previously degassed, was injected into the dilatometer vessel and the capillary

tube. A small amount of dodecane was added at the top of the water. As the reaction proceeds, the volume of the reaction medium will decrease because of the conversion of MMA monomer to the denser poly(MMA). Consequently, the dodecane layer goes down, and an automated tracker follows the movement of the meniscus of the dodecane layer.

For thermally initiated experiments, the experiment is left running for more than 48 hours, to ensure that interval II was over. On the other hand, for γ-radiolysis experiments, the dilatometer vessel was placed in the γ-rays source, until the reaction starts, then it was taken off the source for at least 30 minutes, then placed back in the source for a short period of time, then taken off again for at least 30 minutes. Most γ-relaxation experiments done included three relaxations, but results included only the first two relaxations, as the third relaxation usually started after the reaction has been running in interval III for too long, making the use of these results of the third relaxation completely unsuitable to analyze interval II data.

Experiments were run either with no CD, 2% or 4% CD, relative to the total weight of the monomer used at the beginning of the reaction. For all experiments, N_c = 1.7 x 10^{17} particles/L, and surfactant was used in all thermally and γ-initiated experiments.

From the dodecane movement with time, a series of volume/time data points can be obtained. Solving equations (5.10) to (5.12) simultaneously at each data point gives the conversion at that point, from which the value of $\mathrm{d}x/\mathrm{d}t$ at every point can be calculated. Knowing the rate of conversion, $\bar{n}$ can be directly calculated at each point from the steady-state solution of equation (5.15), which will be shown shortly.

5.4 Fitting of γ-relaxation results

In this section the analysis of Section 3.4 will be repeated, i.e., a typical γ-relaxation will be fitted over varying time intervals in order to establish the minimum length of time that is needed to fit data. The reason for needing to repeat this exercise is that now the nature of the kinetics is different: whereas in Chapter III the kinetics were zero-one, here they are pseudo-bulk, and thus a different kinetic equation must be used to fit data.

Specifically, one uses

$$\bar{n} = \sqrt{\frac{\rho}{2c}} \frac{\left[\left(\sqrt{\frac{\rho}{2c}} + \bar{n}_0\right) e^{t\sqrt{2\rho c}}\right] - 1}{\left[\left(\sqrt{\frac{\rho}{2c}} - \bar{n}_0\right) e^{t\sqrt{2\rho c}}\right] + 1} \tag{5.18}$$

This is the solution of equation (5.15).[1] Results of fitting this equation to a data set are given in Table 5.3 and presented in Figure 5.2.

time	$\bar{n}_{ss}$ x 10^2	c x 10^2 s	$\rho_{thermal}$ x 10^5 s
10 minutes	12.67	2.69	8.66
15 minutes	12.70	2.69	8.62
20 minutes	12.33	2.65	8.06
25 minutes	12.06	2.62	7.62
30 minutes	11.76	2.58	7.13
35 minutes	11.68	2.57	6.99
40 minutes	11.53	2.54	6.77
45 minutes	11.37	2.53	6.53

Table 5.3. Results calculated from experiment TM105 R1, depending on the length of the relaxation period.

Results shown in table 5.3 and figure 5.2 indicate that, although γ-relaxation might look complete after 15 minutes, the relaxation still needs to be run for longer, at least 30 minutes. The longer period confirms higher accuracy in parameter values. The fits for 15, 30 and 45 minutes of relaxation, as shown in figure 5.2, appear identical, but the data in table 5.3 shows the parameter values are different.

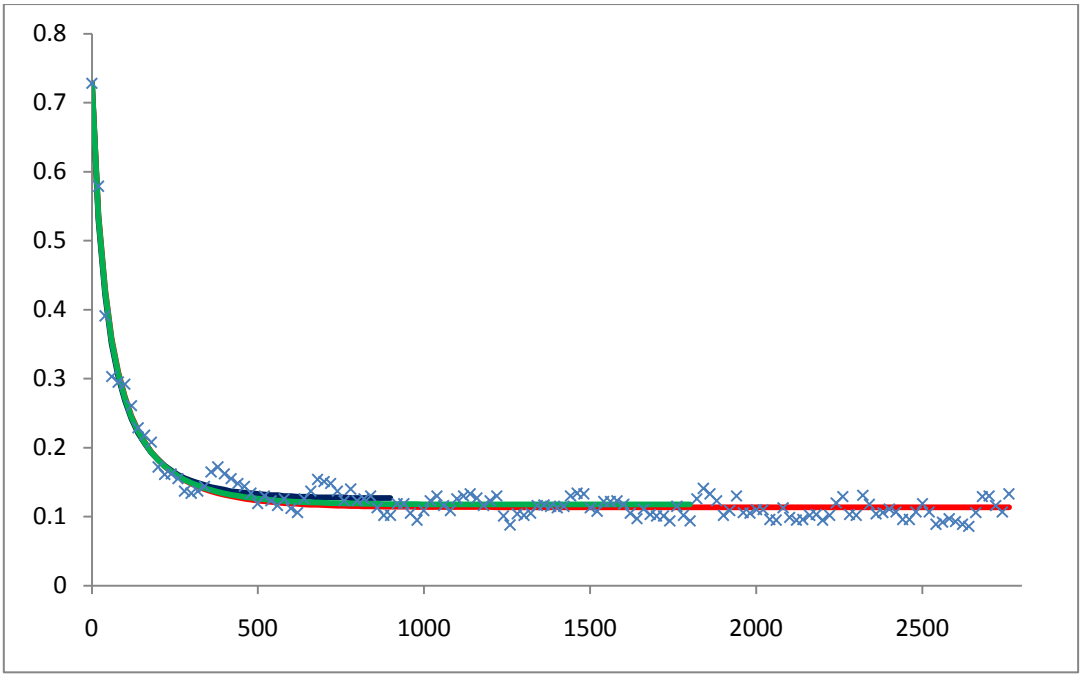

Figure 5.2. $\bar{n}$ as a function of time for a typical γ-relaxation experiment (TM105 R1). Blue crosses: experimental values. Curves: equation (5.18) fitted over three different time periods (0-15 min(blue curve), 0-30 min (green curve) and 0-45 min(red curve), as indicated). It is clear that the 0-30 min curve is almost ientical to the 0-45 min curve, strengthening the conclusion of running the relaxation for a minimum of 30 min.

5.5 Results and discussion

5.5.1 γ-relaxation experiments without CD

The main aim of γ-relaxation experiments is to calculate the termination rate parameter *c*. This was done using a γ-ray initiating unit, composed of a hollow cylinder of ^{60}Co, which initiates the reaction as long as the dilatometer vessel is placed within the cylinder. All experiments were run at 50 ^{o}C. A typical representation for one of the experiments (experiment TM108) is shown in figure 5.2.

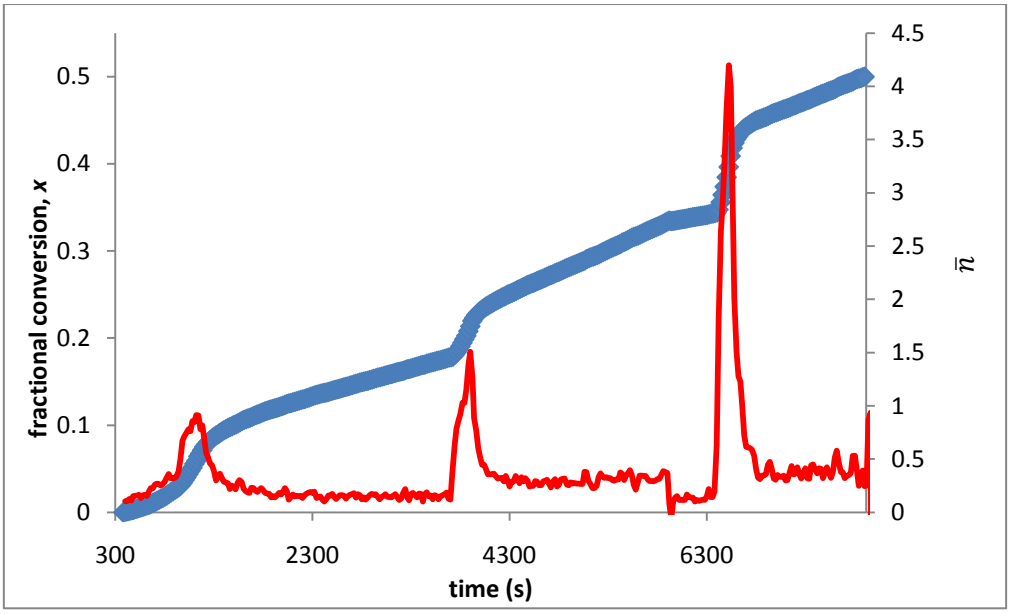

Figure 5.3. Conversion (blue) and $\bar{n}$ (red) as functions of time for γ-relaxation experiment TM108 for latex MMA01.

Figure 5.3 shows that the rate increases significantly when the reaction vessel is exposed to γ-rays, as shown by the sharp increases in the value of $\bar{n}$. Data fitting of the relaxation provides the values of c and ρ_{thermal} , this is done by using equation (5.15) for each relaxation. The increase in the value of $\bar{n}$ from one insertion to another presents enough evidence for the occurrence of gel effect.

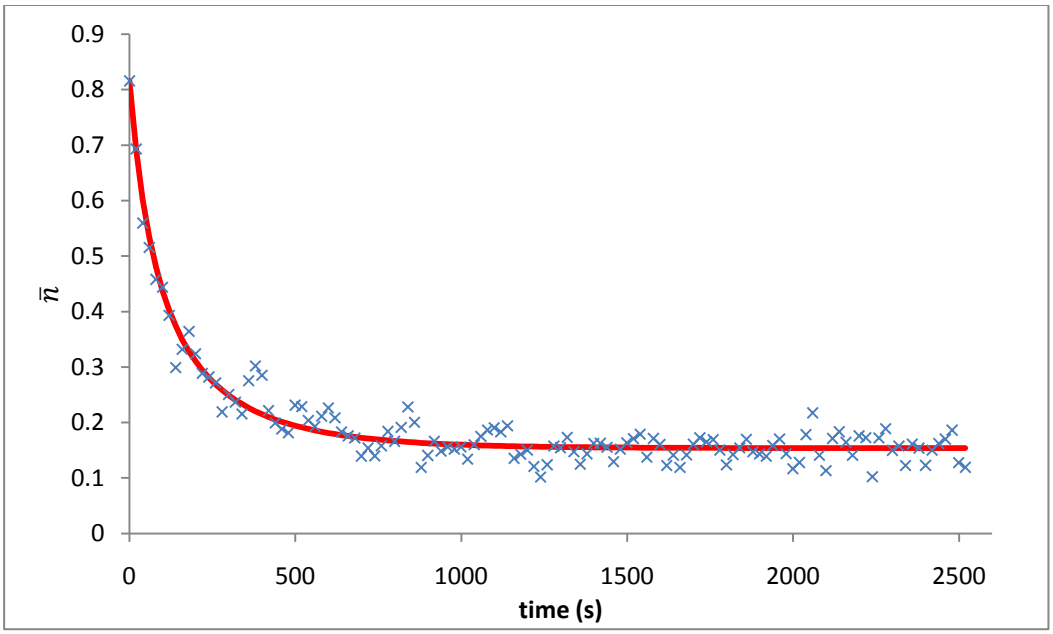

Figure 5.4. $\bar{n}$ as a function of time for a typical γ-relaxation experiment (TM108 R1). Blue crosses: experimental values. Curve: equation (5.18) (best fit).

Figure 5.3 shows clearly the Trommsdorff-Norrish effect, presented by sharp increases in the value of $\bar{n}$ as reaction progresses in-source and the reaction vessel is exposed to the γ-rays source.

For all γ-relaxation calculations, conversion was calculated from the tracker data, giving the change of volume versus time. This data was used in equations (5.10), (5.11) and (5.12) to simultaneously solve these equations, which yields a conversion as a function of time.

Experiment	w_p range	$\bar{n}_{ss}$ x 10^2	$\rho_{thermal}$ x 10^4 s	c x 10^2 s	k_t x 10^{-4} L.s.mol^{-1}
TM101 R1	0.41 – 0.53	20.48	15.22	1.82	2.99
TM101 R2	0.55 – 0.74	1.20	4.32	1.21	2.03
TM105 R1	0.31 – 0.48	11.37	6.53	2.53	4.05
TM105 R2	0.55 – 0.68	14.65	6.98	1.63	2.63
TM105 R3	0.72 – 0.76	26.44	17.71	1.27	2.07
TM108 R1	0.31 – 0.41	15.39	5.46	1.15	0.82
TM108 R2	0.45 – 0.57	26.12	21.00	1.54	8.55
TM108 R3	0.62 – 0.70	30.83	13.83	0.73	4.32
Average		**15.47**	**8.55**	**1.78**	**2.62**

Table 5.4. Results of γ-relaxation polymerization experiments with no CD. Because of the small number of data points available from γ-relaxation from interval II only, experiments include data up to the value of w_p = 0.68. Results highlighted in red are for experiments where w_p > 0.65, and they were not included in calculating averages.

To calculate c and $\rho_{thermal}$, $\bar{n}$ is calculated at each point from equation (5.14), using the data for conversion at different points of time. $\bar{n}$ is also calculated by substituting assumed values of c and $\rho_{thermal}$ in equation (5.16). Data fitting for both sets of values of $\bar{n}$ are shown in figure 5.4, which represents $\bar{n}$ as a function of time for one of the γ-relaxation experiments (experiment TM108 R1). From the curves in figure 5.4, using trial and error and minimizing the error, the exact values of c and $\rho_{thermal}$ can be calculated with the model, equation (5.18)

Results of rate constants as calculated from γ-relaxation experiments only are shown in table 5.4. Usually these experiments are carried out so that there is a significant portion of polymerization during interval II, enabling measurement of rate parameters strictly during interval II. Unfortunately this was not the case in these experiments, one reason for this is that not enough MMA was included in experimental recipes. Another is that the ^{60}Co source had very recently been replenished, resulting in very fast in-source polymerization rates, as is evident in figure 5.3.

5.5.2 Thermal polymerization experiments

A number of thermal polymerization experiments were run to calculate the value of ρ_{thermal} , which can be calculated if the value of $\bar{n}_{ss}$ is known. This set of experiments, as the title suggests, did not include any use of any initiating technique other than thermal initiation. Results of a typical experiment are shown below.

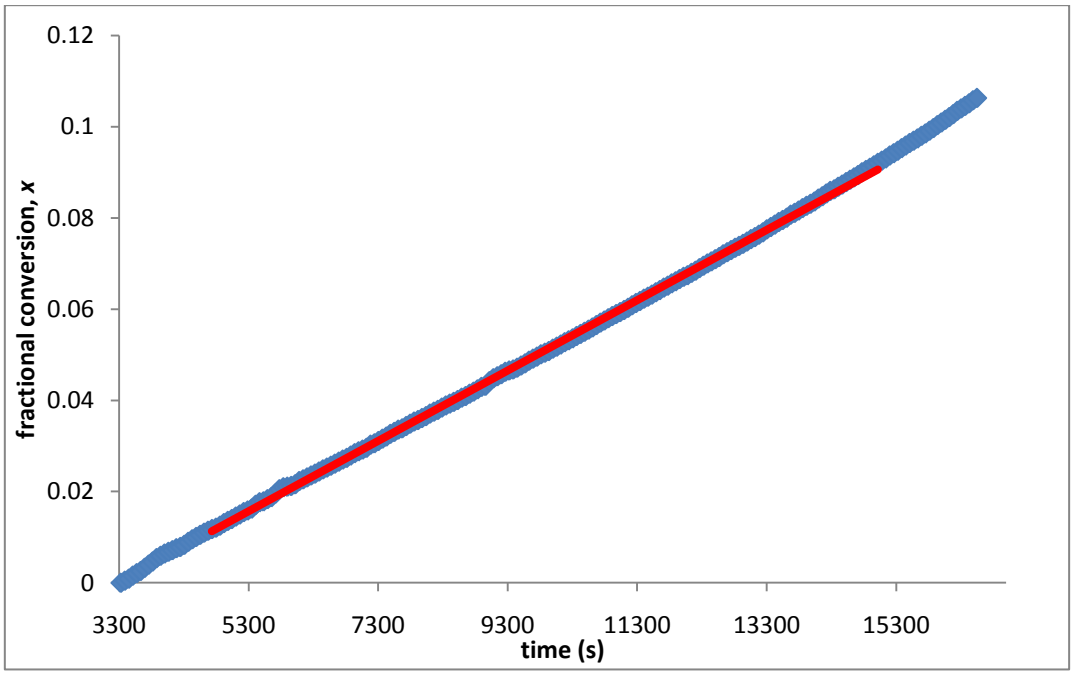

Figure 5.5. A typical result for an MMA01 thermal polymerization experiment (experiment M102)

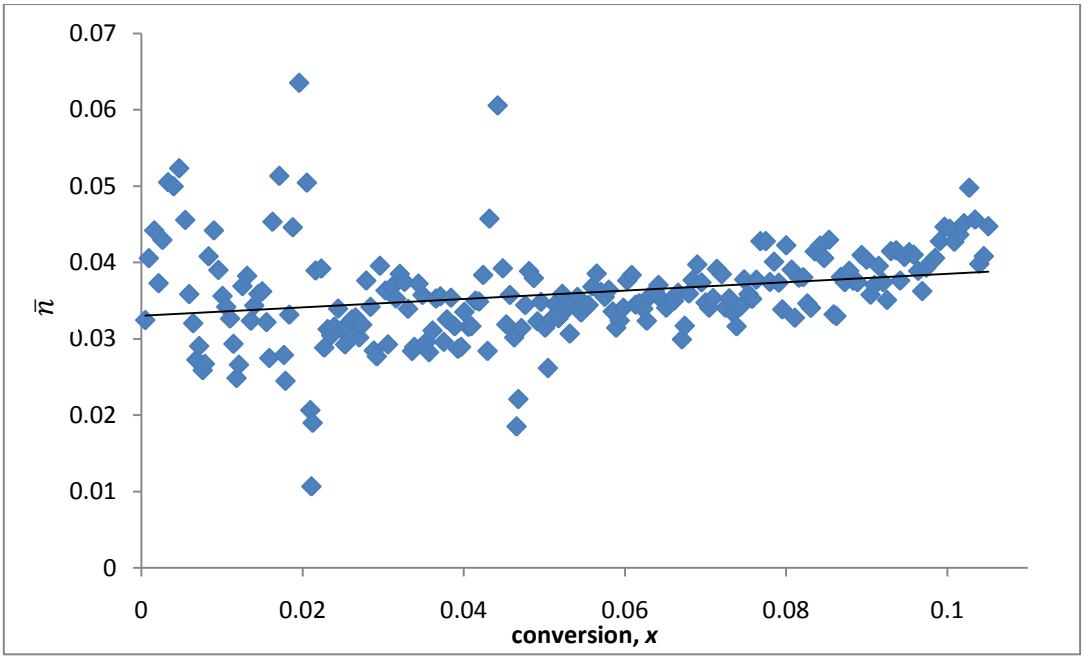

Figure 5.6. Increase of $\bar{n}$ as a function of conversion for experiment M102.

It is evident that there is a slight increase of $\bar{n}$ with time. This is expected with MMA polymerization and will be explained chapter VI. For these particular experiments this so-called acceleration is weak, meaning that there are two possible ways to analyze data:

(1) Ordinarily the acceleration is sufficiently pronounced that one must use $\bar{n}$ extrapolated back to zero conversion, as shown in Figure 5.6.

(2) In view of the weak acceleration, the average slope over the entire Interval II can be taken, as shown in Figure 5.4, and used to calculate the average $\bar{n}_{ss}$. Analysis of results obtained from both methods are shown in table 5.5.

For thermal polymerization experiments, $\bar{n}_{ss}$ was calculated using equation (5.14), and the value of dx/dt used in the equation was calculated from the average slope of the time/conversion curve, which almost follows a linear path. Although it has been established that the time/conversion relationship is not straight in interval II for MMA emulsion polymerization, thermal experiments results show only a minor deviation from linear relationship, this deviation was considered negligible in calculations done to calculate $\rho_{thermal}$, as this is shown from the graph in figure 5.5.

Figure 5.5 shows an almost linear relationship between time and conversion, as presented by the red straight line. This relationship deviates slightly from linearity at the beginning, because of the approach to steady state, and at the end, which can be explained by an

early impact for the Trommsdorff-Norrish effect, starting just at the end of interval II.

In order to find the exact values of thermal entry rate coefficients, a few experiments were run to test the impact of surfactant on the polymerization rate, and to find the right amount of surfactant which gives the lowest coagulum formation during interval III.

Before discussing the effect of surfactant concentration, it is good to refer to one of the parameters expressing the gel effect. Figure 5.5 shows the increase in $\bar{n}$ with increasing monomer conversion. The slope of the conversion/$\bar{n}$ straight line will be labeled $\mathrm{d}\bar{n}/\mathrm{d}x$.

More details about the increase of $\bar{n}$ with conversion will be discussed in chapter VI.

In the current work, results have shown a tendency of a positive value for $\mathrm{d}\bar{n}/\mathrm{d}x$ with a specific amount of surfactant. Decreasing or increasing this amount resulted in conversion/$\bar{n}$ curves giving a negative value for $\mathrm{d}\bar{n}/\mathrm{d}x$. Table 5.4 shows a summary of these results.

Experiment	AMA-80 (g)	$\mathrm{d}\bar{n}/\mathrm{d}x$	$\bar{n}_0$ x 10^2	$\bar{n}_{ss}$ x 10^2	$\rho_{thermal}$ x 10^5 s *
M101	0.092	-0.153	4.13	3.13	6.08
M102	0.147	0.055	3.30	3.45	3.88
M103	0.195	-0.015	3.19	3.09	3.62
M104	0.248	-0.074	2.07	1.57	1.53
M105	0.078	-0.10	5.25	2.79	9.82
M107	0.143	0.085	2.28	2.47	1.85
Averages			**2.92**	**3.02**	**3.04**

***** Calculated using $\bar{n}_0$ and c = 1.78 x 10^{-2} s^{-1}.

Table 5.5. Effect of amount of surfactant used on $\bar{n}$ and $\rho_{thermal}$. Rows written in red represent failed experiments, which were not included within the averages. Amounts of AMA-80 are all in grams. $\bar{n}_0$ is the value of $\bar{n}$ at the beginning of steady state period of interval II, which can be obtained from figure 5.6, while $\bar{n}_{ss}$ is calculated from $\mathrm{d}x/\mathrm{d}t$, the slope of the straight line portion of the time conversion graph, as in figure 5.5.

To calculate ρ_{thermal} , equation (5.16) was used in the form

$$\rho_{\text{thermal}} = 2c\bar{n}_0^{\,2} \tag{5.18}$$

c was substituted in the equation with its average value, 1.78 x 10^{-2} s^{-1}. This is the average value of *c* as calculated from all γ-relaxation experiments, including experiments in which CD was used.

As shown in table 5.5, increasing or decreasing the amount of surfactant outside a specific range (0.145-0.195 g) is likely to result in experimental failure. Experiment failure was very clear from the amount of coagulum formed. Furthermore, for the three successful experiments the value of $\bar{n}_{ss}$ and $\bar{n}_0$ are very close to each other. This is based on the weak acceleration for thermal polymerization of MMA, in case the true amount of surfactant is used.

Such results clearly show the sensitivity of MMA emulsion polymerization to the amount of surfactant used. Furthermore, as long as the right amount of surfactant is used, the expected result of having a positive value for $\mathrm{d}\bar{n}/\mathrm{d}x$ is achieved as seen in the three successful experiments, the only negative value obtained is almost zero. Obviously this was not the case for failed experiments where $\mathrm{d}\bar{n}/\mathrm{d}x$ had higher negative values.

Comparing these results to previously reported data[1,28] shows the importance of working accurately with surfactant. Results for both research projects done earlier did show negative values for $\mathrm{d}x/\mathrm{d}t$. Although in both cases deviation from zero was minor, there was no explanation for such results, which do not agree with the common knowledge of increasing $\bar{n}$ with increased conversion.

The increase in particle volume during the course of polymerization was assumed to be the reason for the increased rate of polymerization[1]. This theory does not explain at all why there is a decrease in polymerization rate in case different amounts of surfactant are used.

In emulsion polymerization, the main locus of particle formation is the surfactant

micelles[29,30,31], which simply leads to the fact that increasing the surfactant beyond a set limit causes secondary nucleation[19]. The surfactant plays other roles in emulsion polymerization. One of them is that, under specific conditions, the surfactant can act as a retarder or even as a chain transfer agent[32].

Although the surfactant is identified here as the reason behind such results, the simple explanation for the surfactant as a retarder cannot be taken as it is. The reason is the surfactant here acts in a way which is different from the way retarders usually act. Retarders are known to deactivate the propagating radicals[33], and they yield species which slowly re-initiate polymerization[34]. It is clear that the effect of the surfactants in both cases does not fulfill the mentioned characteristics for retarder. Nevertheless, it is clear that the surfactant reduces the reaction rate as the reaction progresses.

A possible explanation is that the surfactant facilitates the exit step within the reaction. The mechanism can thus be explained as follows: free radicals are initiated in the aqueous phase, and then they move to propagate within the particles. With high (or low) surfactant concentrations, the free radicals escape from the particles. As the reaction progresses, small free radicals are expelled from the particles to the more suitable aqueous phase. This explanation can be supported by the fact that in both chemically and γ-initiated experiments, the increasing number of free radicals increases the reaction rate to a level which makes the exit process negligible.

5.5.3 Comparison with previous work[10,28]

	$\rho_{thermal}$ x 10^4 s		c x 10^2 s	k_t x 10^{-4} L.s.mol^{-1}
	Thermal expts.	γ-relaxation		
Current work	0.3	8.5	1.8	2.6
Van Berkel	3.6	1.5	2.4	1.9

Table 5.6. Comparison between results of entry and termination rate coefficients obtained through the current work and through the previous work of van Berkel.

The comparison, as shown in table 5.6, highlights a few facts. First is that the termination rate coefficients are quite similar to each other. Such reproducibility of results between

two different latices confirms the accuracy for both previous and current work.

Interestingly, results of $\rho_{thermal}$ are very different for thermally initiated experiments. This was also the case as found from the determination of thermal entry rate coefficient $\rho_{thermal}$ from γ-relaxation experiments. This can be attributed to the fact that the γ-relaxations done during this part of the work were partially done during interval III. One of the results of running the experiments at interval III is that Trommsdorff-Norrish effect will take place, increasing the values of $\bar{n}_{ss}$, which will be mathematically interpreted as an increase in entry rate coefficient and a decrease in termination rate coefficient. Figures 5.9, 5.10 and the discussions in the next section will provide better details about that.

5.5.4 γ-relaxation experiments with CD

Having obtained an idea on the kinetics of emulsion polymerization without CD, and obtaining results which are comparable to results obtained in similar work done earlier[28], the next step was to use CD in the kinetic experiments with MMA. Figures 5.6 shows the results of experiment TM104 and TM106, and figure 5.7 shows the results of γ-relaxation for relaxation TM109 R1.

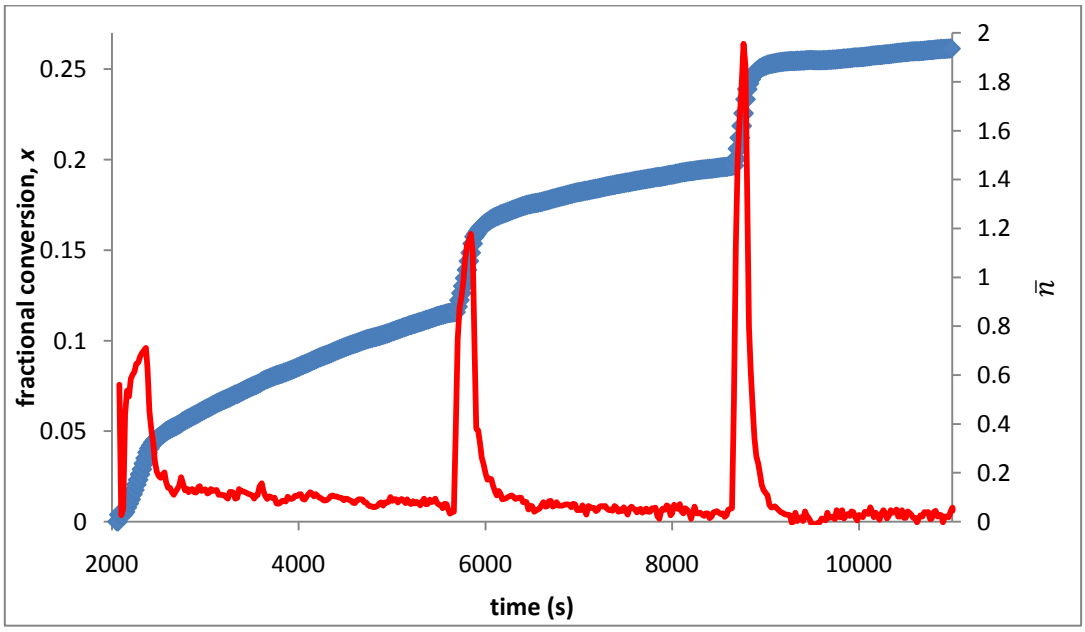

Figure 5.6a. Conversion (blue) and $\bar{n}$ (red) as functions of time for γ-relaxation experiment TM104 for latex MMA01. This experiment had reduced rate due to lead shielding.

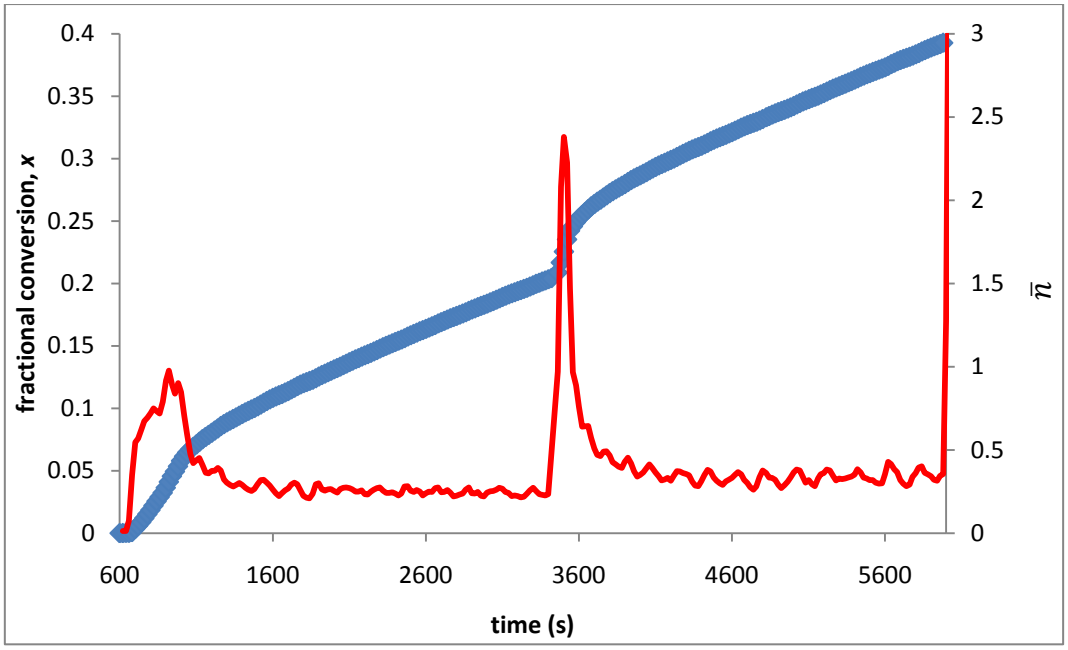

Figure 5.6b. **Figure 5.6a**. Conversion (blue) and $\bar{n}$ (red) as functions of time for γ-relaxation experiment TM106 for latex MMA01. No lead shielding

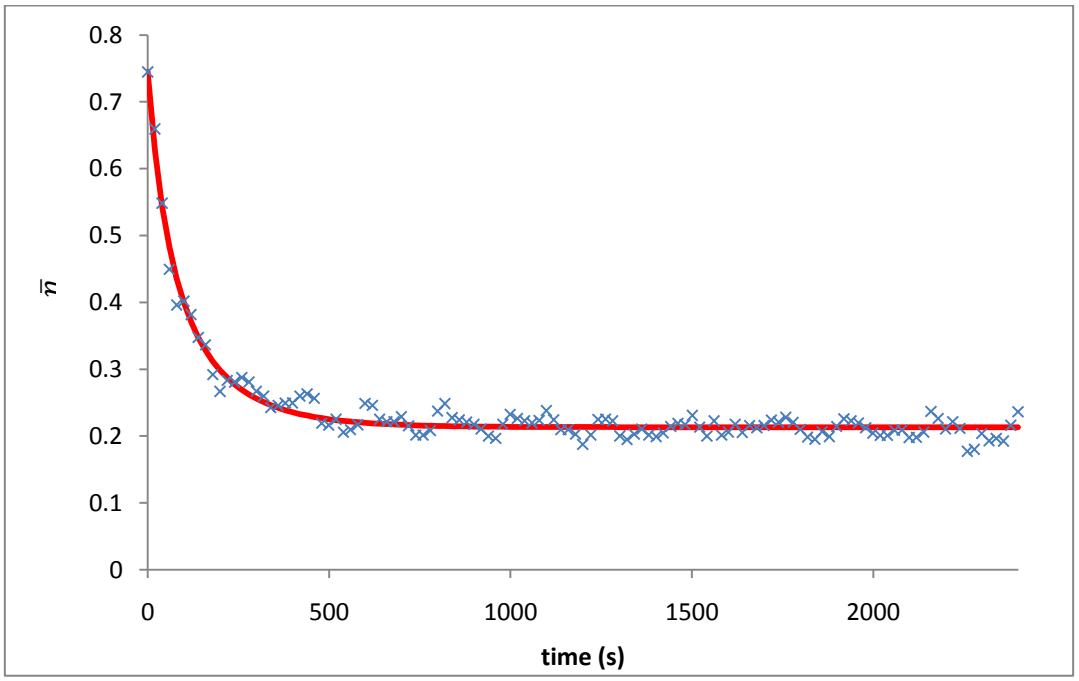

Figure 5.7. $\bar{n}$ as a function of time for a typical γ-relaxation experiment (TM109 R1). Blue crosses: experimental values. Curves: equation (5.18) fitted

Figure 5.8a shows the effect of CD on the values of $\bar{n}$. Figure 5.8b shows the $\bar{n}$-time curve of experiment TM102 R1 (the same curve shown in figure 5.8a) with an extra simulation. For this extra simulation, the value of $\rho_{thermal}$ (= 6.53 x 10^{-4} s^{-1}) from the

experiment in Figure 5.8a without CD (TM105 R1) was used. The value of c was adjusted so as to give the same value of $\bar{n}_{\text{thermal}}$ as in the experimental data with CD. It was obtained that c = 0.441 x 10^{-2} s^{-1}. What the simulation shows is that with this lower value of c, the relaxation portion of the kinetics is not at all reproduced: the relaxation is far too slow compared to the experiment. This illustrates that the data with CD can only be fitted with a higher ρ_{thermal} and the same c as for experiments without CD. This confirms the results shown in table 5.7, which show no change in the value of the termination rate coefficients with increasing CD, and confirms the change in $\bar{n}$ is mainly because of higher entry rate.

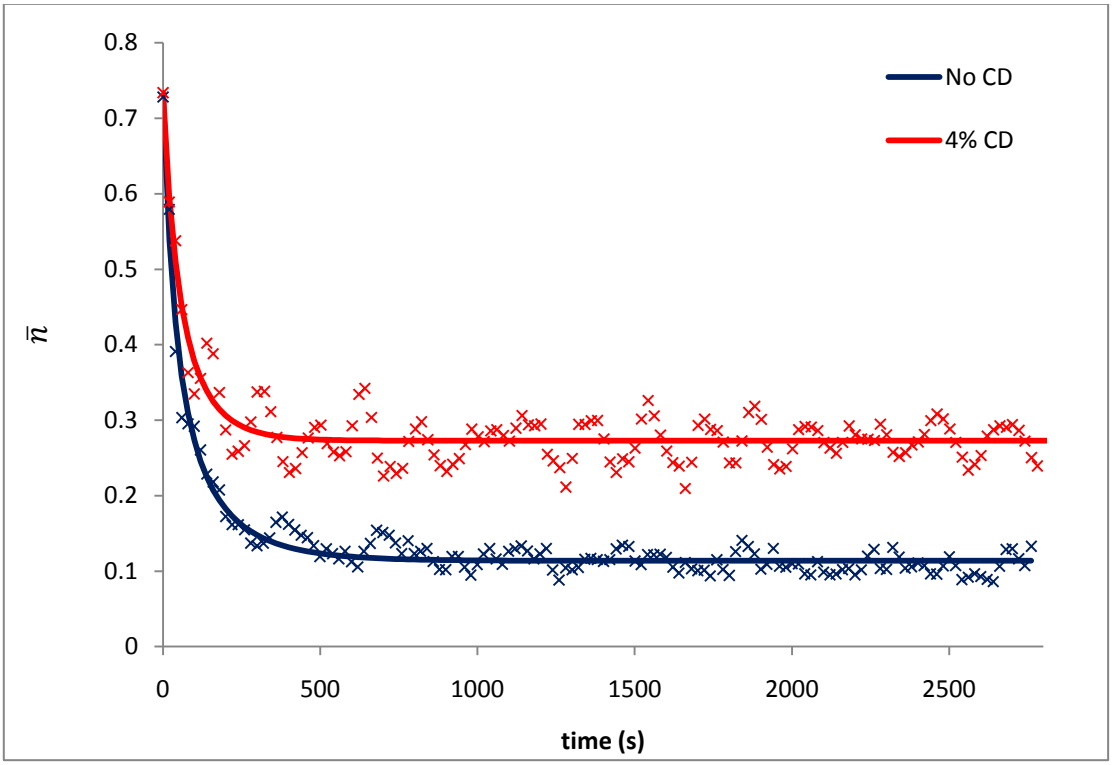

Figure 5.8a. $\bar{n}$ as a function of time for two γ-relaxation experiment with MMA01 (TM105 R1, with no CD and TM102 R1 with CD). Crosses: experimental values. Curves: equation (5.18) (best fit). The curves show the effect of the addition of 4% CD to the reaction mixture. As the termination rate coefficients remains constant with increasing thermal entry rate coefficient, $\bar{n}$ increases with CD addition.

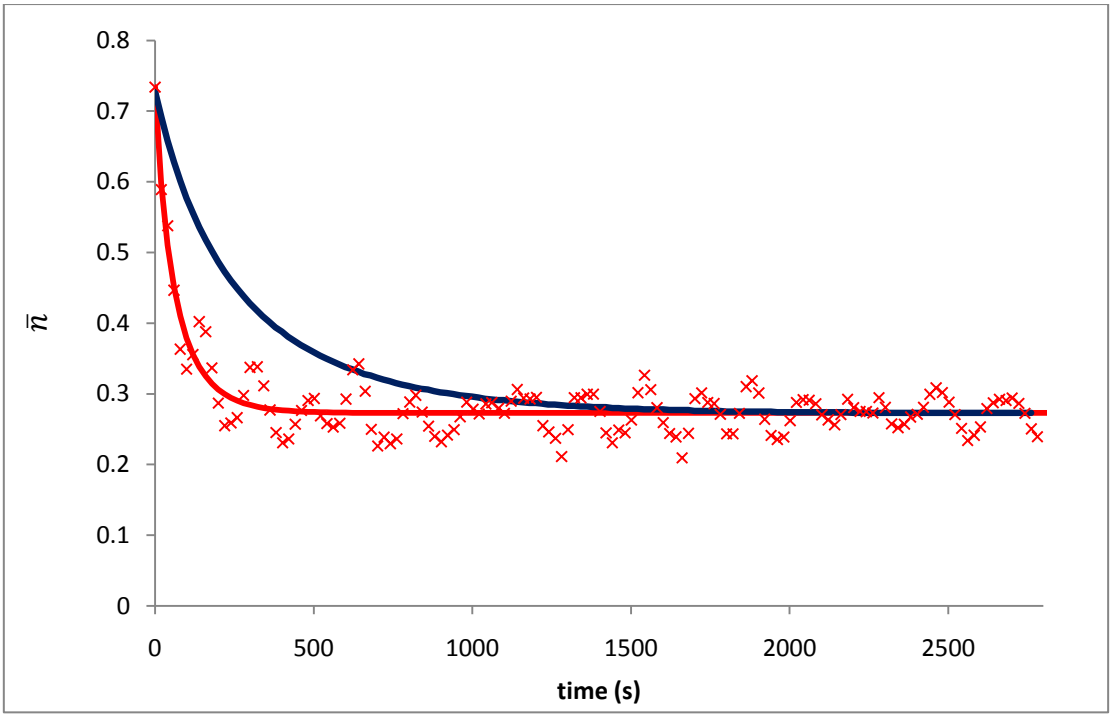

Figure 5.8b. $\bar{n}$ as a function of time for 4% CD data of Figure 5.8a. Crosses: experimental values (TM102 R1); red curve: best fit of Figure 5.8a (ρ = 28.4 x 10^{-4} s^{-1}, c = 1.91 x 10^{-2} s^{-1}). blue curve: equation (5.18) with ρ = 6.53 x 10^{-4} s^{-1}, c = 0.441 x 10^{-2} s^{-1}.

% CD	Experiment	w_p range	$\bar{n}_{ss}$ x 10^2	$\rho_{thermal}$ x 10^4 s	c x 10^2 s	k_t x 10^4 L.s.mol^{-1}
2%	TM103 R1	0.31 – 0.40	20.64	12.72	1.49	2.57
	TM103 R2	0.46 – 0.57	26.79	22.54	1.57	2.67
	TM106 R1	0.31 – 0.44	25.22	15.81	1.24	1.89
	TM106 R2	0.47 – 0.61	34.09	27.78	1.20	1.81
	TM106 R3	0.65 – 0.74	16.70	2.72	0.50	0.77
	TM107 R1	0.42 – 0.54	23.90	7.49	0.66	1.04
	TM107 R2	0.62 – 0.69	7.70	0.21	0.40	0.64
	TM107 R3	0.72 – 0.83	34.96	4.70	0.20	0.33
	Average		**26.69**	**19.71**	**1.38**	**2.23**
4% CD	TM102 R1	0.31 – 0.48	27.29	28.44	1.91	2.99
	TM102 R2	0.55 – 0.68	52.63	42.26	0.76	1.19
	TM102 R3	0.72 – 0.76	18.25	49.42	7.42	11.76
	TM104 R1	0.31 – 0.32	9.65	5.22	2.80	4.95
	TM104 R2	0.36 – 0.40	5.32	1.77	3.13	5.48

Table 5.7. Effect of the addition of CD on entry and termination rate.

% CD	Experiment	w_p range	$\bar{n}_{ss}$ x 10^2	$\rho_{thermal}$ x 10^4 s	c x 10^2 s	k_t x 10^4 L.s.mol^{-1}
	TM104 R3	0.44 – 0.46	1.84	0.18	3.69	6.41
	TM109 R1	0.31 – 0.39	21.33	12.87	1.42	2.36
	TM109 R2	0.42 – 0.52	22.38	14.59	1.40	2.31
	TM109 R3	0.58 – 0.66	16.78	3.47	0.63	1.05
	Average		**30.91**	**24.54**	**1.37**	**2.21**

Table 5.7 (cont'd). Effect of the addition of CD on entry and termination rate. Experiment TM104 is not included because during the experiment part of the reaction vessel was covered by a lead shield. Results in red are not to be included because of technical problems which happened during the experiment, or because of having working at very high w_p.

CD concentration	$\bar{n}_{ss}$ x 10	$\rho_{thermal}$ x 10^4 s^{-1}	c x 10^2 s^{-1}	k_t x 10^{-4} mol/L.s
No CD	1.55	8.55	1.78	2.62
2% CD	2.67	19.71	1.37	2.23
4% CD	3.09	24.54	1.38	2.21
Average of all γ-relaxation values			1.51	2.36

Table 5.8. Effect of addition of CD on kinetic parameters as obtained from γ-relaxation of latex MMA01. This table uses the averages from tables 5.4 and 5.6.

Comparison between kinetic parameters obtained from no CD experiments and from experiments using CD is shown in table 5.8. The main parameters aimed to be calculated from γ-relaxation experiments are the termination rate parameters, which are c and k_t. % CD shown in the table means the mass of CD used relative to the total mass of monomer added to the reaction medium at the beginning of the reaction.

Figure 5.8 and table 5.8a show a comparison between the reaction rates with and without CD. It is clear that thermal entry is the parameter mostly affected by the addition of CD, as it significantly increases with CD addition. This can also be easily noticed from the increase of the value of $\bar{n}_{ss}$, which almost doubles with the addition of 4% CD.

As γ-relaxation experiments were a simulation to experiments done with chemical initiators, the amount of monomer used was not enough to keep the system in interval II if it remained in the source for a long time. It can also be seen from figures 5.3 and 5.7 that

a short period of time in the source increases the conversion at a very high rate. As the reaction vessel remained in the source for very short periods of time, it was not possible to analyze the γ-irradiation data.

Figure 5.9 shows that k_t decreases with increased conversion, expressed by w_p, the weight fraction of polymer within the particles. Note that this increase is not very high, which suggests that using k_t as calculated in the earliest part of interval III will not be much different to that obtained using only interval II results. Furthermore, the decrease in the value of k_t with increased conversion gives additional evidence to the gel effect[22], and to subsequent work which obtained similar behavior.[1,36]

It is also noted from figure 5.9 that increased amounts of CD has only a minor effect on k_t. This is because k_t is the rate of an intra-particle process, where CD is not expected to have an effect, as its presence in mainly in the aqueous phase. It should be noted here that, although R3 for some experiments are shown in the figure, k_t values calculated from these relaxations are not included in calculating the averages, because of these values were taken at high values of w_p where conversion is very high and so the Trommsdorff-Norrish effect is high enough to a level where it cannot be neglected.

As per thermal entry, the trend obtained from previous work[1,36] is also followed here. $\rho_{thermal}$ was found to increase with conversion. The Trommsdorff-Norrish effect is not expected to play a role here, and actually there is no known reason why this is happening. It can be seen from figure 5.9 that $\rho_{thermal}$ increases between subsequent relaxations in the same experiment. An unknown parameter with the γ-irradiation which has this effect, but until this reason is know, exact details about the causes of increase of $\rho_{thermal}$ remain obscure. The increase in the value of $\rho_{thermal}$ can be explained by the formation of MMA peroxides in the aqueous phase. More details about peroxide formation are available in section 5.5.6.

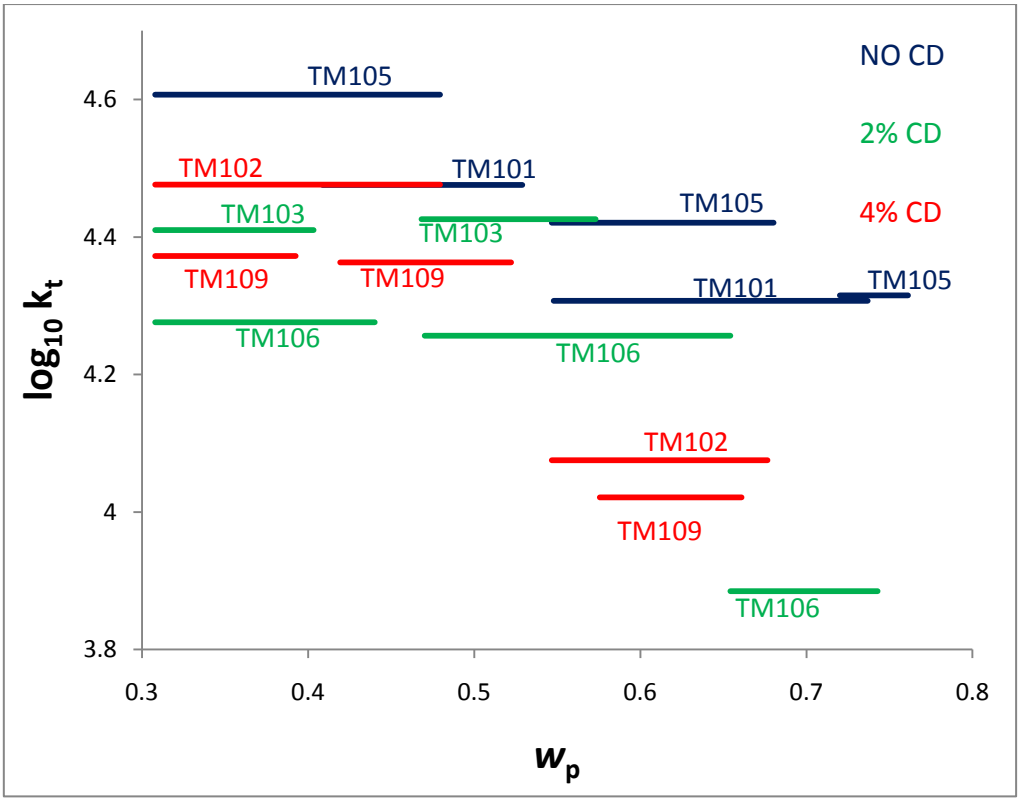

Figure 5.9. Change in k_t for experiments depending on w_p.

It is evident that the γ-relaxation experiments have found that $\rho_{thermal}$ seems to increase rather remarkably with the presence of CD, as seen in table 5.8. Consideration must be given to whether this effect also occurs in standard thermal experiments, as carried out in section 5.4.3. Unfortunately it was not possible to carry out such experiments, as the tracker at the University of Canterbury broke down soon after the MMA γ-relaxation experiments were carried out, and the tracker could not be fixed before the completion of this work.

This raises obvious issues for the analysis of chemically initiated experiments with CD: is $\rho_{thermal}$ the same as in section 5.4.3 (i.e., without CD) in the presence of CD, or is it increased, as in the γ-relaxations? There are arguments both ways. It is evident that products of γ-irradiation seem to be increasing the value of $\rho_{thermal}$. The question is whether these products act with CD to increase the value of $\rho_{thermal}$ still further, or

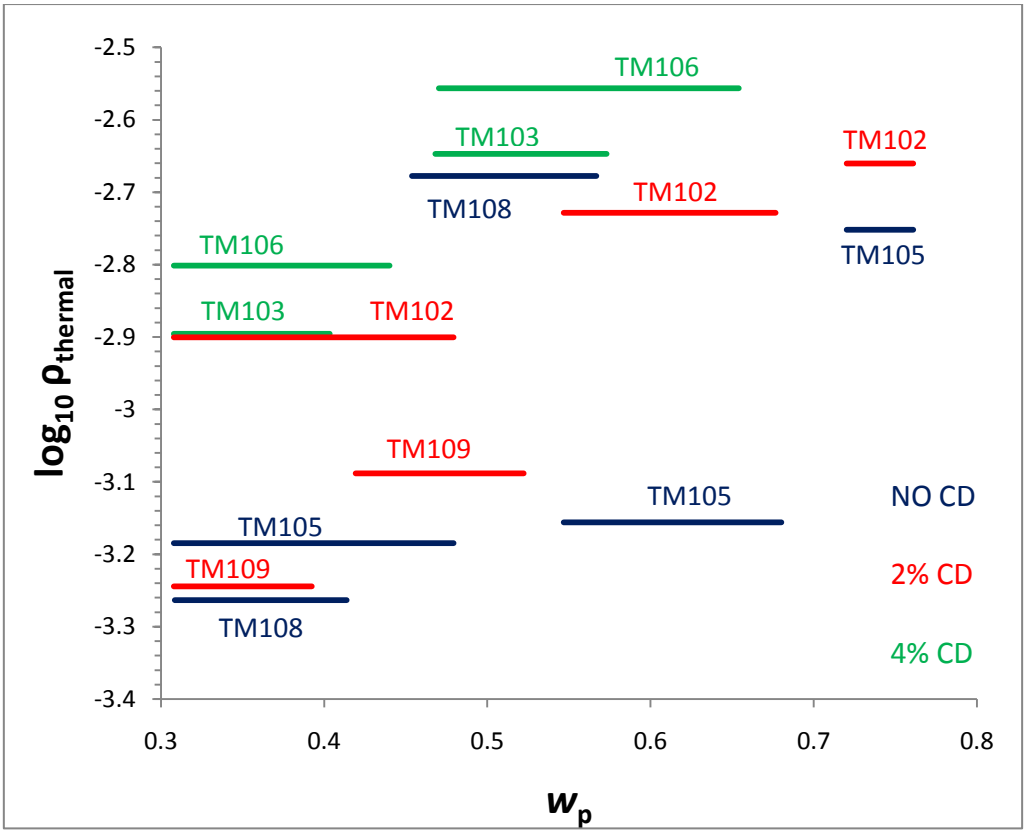

Figure 5.10. Change in $\rho_{thermal}$ for experiments depending on w_p.

whether CD acts alone, i.e., there are two separate effects. It is not possible to answer this question without doing the actual experiments.

5.5.5 Discussion of termination results

As has been highlighted earlier, the main aim of the γ-relaxation experiments is to determine c and k_t for experiments not including CD, then compare their values with those values from experiments containing CD, thereby obtaining an exact determination of the effect of CD on k_t.

The first conclusion to be made from these results is that they confirm conclusions already reached about emulsion polymerization of MMA. As MMA is polymerized in a pseudo-bulk system, termination takes place only within the latex particles.

Table 5.8 shows clearly that the effect of CD on termination rate coefficients is almost negligible. This goes along the original assumption that, for MMA, as a pseudo-bulk

system, termination is the rate determining step for ending the polymerization process. As termination is an intra-particle process, changes in the aqueous phase, or hypothetically any changes outside the particle, are not expected to have any impact on termination, as shown from the negligible effect of CD on termination rate coefficients. Adding CD, or changing its amount has no effect on k_t, as expected. CD can only influence emulsion polymerization rate via ρ and k. This is a very important result from this thesis.

5.5.6 Discussion of thermal entry results

As some unexpected results for thermal entry were obtained, as shown in table 5.8, a comparison between emulsion polymerization of styrene and MMA can be a good starting point. As already shown in table 3.7 and 3.9, $\rho_{thermal}$ for styrene had a negligible change with 4% CD concentration, which lead to the conclusion that thermal initiation for styrene is not an aqueous phase process. Results shown in table 5.8 show that thermal entry for the emulsion polymerization of MMA is clearly affected by the aqueous phase solubility.

One assumption which can be followed here is that CD has made a change to the aqueous phase presence of the monomer. This change can be assumed to be an increase in solubility, although solubility measurements (discussed in further details in 6.4.1) were not affected by the presence of CD. As CD molecules cannot penetrate within the poly(MMA) particles, their effect is only in the aqueous phase where they exist. They can be assumed to catalyze the formation of MMA free radicals, as will be discussed shortly.

Previous work done to find the exact location of thermal entry either concluded that it is an aqueous phase process[35], other work concluded that it is an inter-particle phase process[26,36]. All this work was done on styrene; no similar work was done for MMA.

A general conclusion to be drawn from the current work is that the main factor affecting thermal entry is the aqueous phase solubility of the monomer. Whether the monomer has low water solubility, like the case of styrene, thermal entry will not take place in the aqueous phase, although a minor amount of thermal entry might take place in the aqueous phase. The main loci in this case will be the surfactant micelles, as clear from table 3.7,

and the polymer particles themselves, as can be concluded from table 3.9, because of the negligible effect of CD on thermal entry. This theory can be further supported by the fact that at 2% CD concentration the value of ρ_{thermal} for styrene has decreased, because some of the surfactant was within the CD cavities and less micelles were formed, as shown from styrene solubilities in table 4.2, and the styrene/surfactant competition for CD cavities, as discussed in section 4.4.1. Negligible effect on increased styrene solubility (due to increased CD concentration) in the aqueous phase strongly strengthens the idea that thermal entry, in case of styrene, is not an aqueous phase process.

Thermal entry for MMA follows a totally different pattern, as it is clear from the increased value of ρ_{thermal} with increasing the concentration of CD. As the only known effect of CD on MMA is that it increases its solubility in water[37], the increased solubility can only be explained if the thermal entry is an aqueous phase process. Although CD might affect other monomer properties in the aqueous phase, like surface tension for example, which can have an impact on the kinetics of the reaction, the only data available for the effect of CD on surface tension is for some surfactants,[38] and this does not include sodium sulphosuccinate, which is the main component of AMA-80. Furthermore, no similar work was done to any of the monomers used in emulsion polymerization.

The theory of the dependence of thermal polymerization loci on monomer concentration can be further supported by the solubilities of the monomers used in this work. At 50 ^{o}C, MMA solubility in water (in mol/L) is more than 36 times styrene solubility. Referring back to the Harkins theory[29,30,13], polymerization starts in surfactant micelles, increasing the number of micelles will then increase the rate of formation of free radicals, while increasing the monomer concentration in the aqueous phase will have no impact at all on this rate, which is exactly what was found with styrene. On the other hand, when surfactant is not present, free radicals will start to form in the aqueous phase. What is concluded here is similar to that, when considering MMA solubility. With such a relatively high solubility in water, the number of free radicals formed (which move to enter into the particles) in the aqueous phase can be concluded to be big enough to consider the rate of formation of other radicals in the aqueous phase negligible.

Having established an understanding of the thermal entry, termination rate can then be discussed. Results shown in table 5.8 highlight the effect of CD on termination. For

MMA, intra-particle termination is the rate-determining step for emulsion polymerization. MMA then follows limit 3 kinetics, where polymerization happens in the particles and it is similar to bulk polymerization. From this description it is understood that reaction conditions in the aqueous phase have little or no impact on the reaction progress within the particles.

The main effect of CD is to increase the aqueous phase solubility of the monomer. Consequently, this effect should have no impact on the kinetics of the reactions taking place within the particles, including the termination reaction. This conclusion completely agrees to the results shown in table 5.8. It is clear from the table that CD presence did not have any effect on the kinetics of termination, as change in both c and k_t can be considered negligible between cases of no CD and when CD is present.

This result agrees to the earlier knowledge,[19] confirming the fact that MMA follows limit 3 and that intra-particle termination is the rate determining step for MMA. It is interesting to note that, although there might be some doubts about the explanation made regarding thermal entry, having a nearly constant value for c at different CD concentrations confirms the high level of accuracy follows throughout this work.

Comparison of the values of $\bar{n}_{ss}$ from table 5.5, and between reactions involving no CD, 2% CD and 4% CD cases as in table 5.8 shows a major difference in the value of $\bar{n}_{ss}$, which certainly affects all other calculated kinetic coefficients. The main reason for this difference of value is that, especially between thermally and γ-relaxation experiments, the value of $\bar{n}_{ss}$ with thermally initiated experiments was lower, as all these experiments were done only during interval II, which was not the case for the γ-relaxation experiments. Including experiments involving CD in the comparison adds another reason for this increase, which can be assumed to be the formation of peroxides during the preparation of the latex. As has been shown for styrene (section 3.5.2), peroxide formation is expected to happen, especially when the V-50 initiator was used.

In the presence of monomer and oxygen, peroxides form according to the following series of reactions[39]

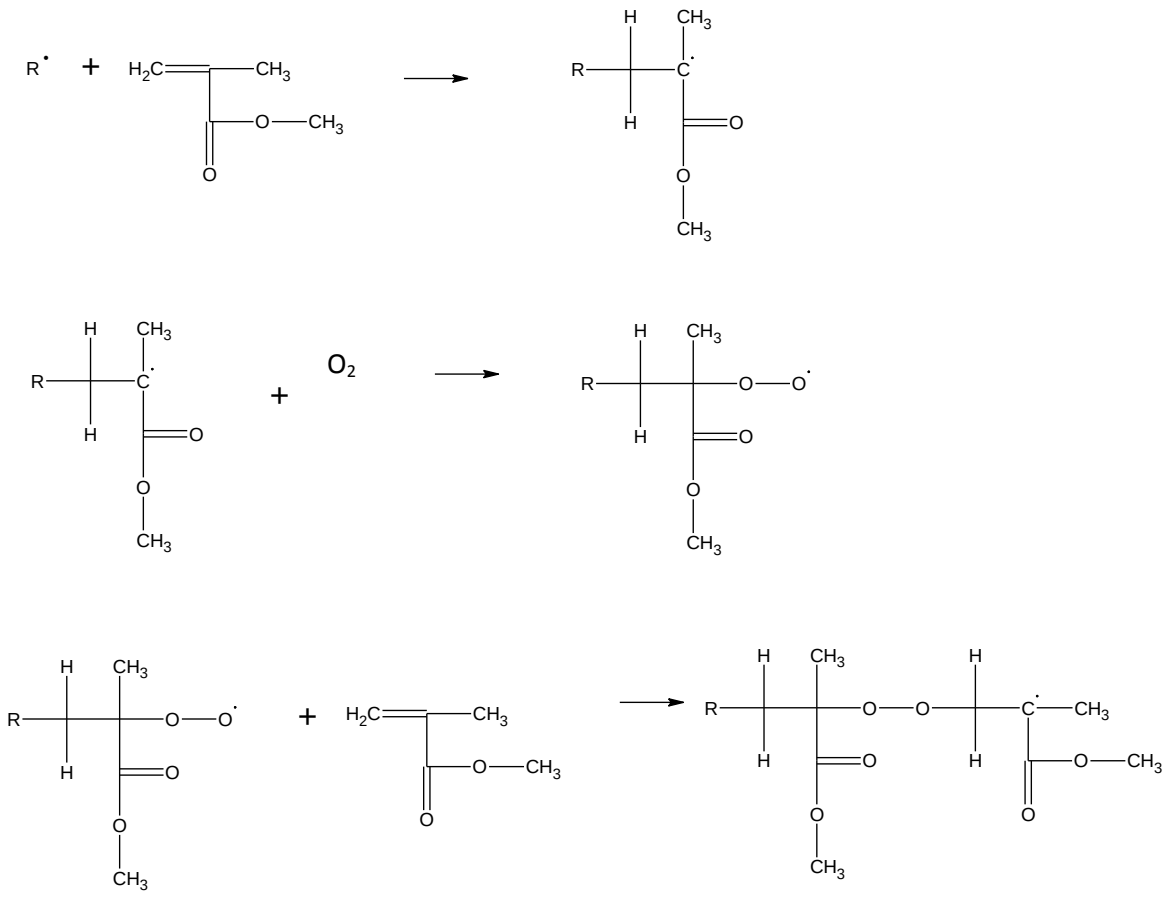

Scheme 5.1 reaction of MMA with oxygen gas yielding peroxide polymers.

The reactions in scheme 5.1 are based on earlier work done on peroxide formation for MMA.[40,41]

Table 5.9 shows the effect of the suggested formation of peroxides for three lattices used during the course of the current project. Because of the minor formation of peroxides in the AN05 latex, the peroxide effect was not present. For the cationic latex, the peroxide effect is clearer. For the MMA latex, the peroxide effect is bigger than both polystyrene lattices, in addition to all changes included because of interval II and interval III differences.

Seed Latex	AN05	CA01	MMA01
$\bar{n}_{ss}$ x 10^2 from thermal initiation	6.49	10.82	3.02
$\bar{n}_{ss}$ x 10^2 from γ-radiation	6.12	16.49	12.4

Table 5.9. Comparison for $\bar{n}_{ss}$ values for thermal relaxation periods during thermal initiation and γ-relaxation experiments

The question becomes why there is such effect for peroxide formation with MMA latex, although it is also formed with KPS initiator, an initiator that is not expected to cause peroxide formation as suggested from the AN05 latex experiments? This question can be answered by the fact that, because of the very high rate of formation of the $RCH_2C(COOCH3)OO^{\bullet}$ CH_3 radical, compared to the lower rate of propagation of the polymerization of MMA, polymerization of MMA can be considered to be inhibited until all the oxygen which is present in the reaction medium at the beginning if the reaction is used to form $RCH_2C(COOCH3)OO^{\bullet}$ CH_3.[31,42]

Another reason for the increased peroxide formation is the increased solubility of oxygen in MMA. Knowing the solubility of oxygen in styrene at 25 ^{o}C to be 7.1 mmol/L, and that of MMA is 10.6 mmol/L at the same temperature,[43] and knowing that the amount of MMA used in preparing the latex is more than double the amount of styrene used, this leads to the estimation that formation of MMA peroxides happened during the latex formation in bigger amounts than what happened with styrene.

But what about the nature of the formed MMA peroxides? Generally they have the empirical form $(C_5H_8O_4)_{n,}$[40] similar to the product of the reaction above. Furthermore, when isolated they have the physical form of a gummy substance,[40] this suggests that MMA peroxide have a high capacity to polymerize once polymerization is initiated. Bearing in mind that such substances remained inert in the latex, a strong initiating medium like γ-rays will initiate these peroxides in the form of free radicals again, and with such a high polymerizing rates, the effect of the presence of such potential chemical initiators in the reaction medium cannot be neglected.

This leads to the conclusion that ρ_{thermal} for the MMA latex can be calculated only from the thermal polymerization experiments, and that calculating this parameter using γ-radiolysis results can lead to a value of ρ_{thermal} much higher than the actual value.

Another conclusion to be drawn here is about the peroxide radicals (previously discussed in section 5.4.1), although peroxide compounds are still in the seed latex, their effect is negligible in thermal polymerization experiments, because they remain in a solid form

and they are not initiated, because of the lack of any strong initiating technique.

5.6 Summary of results

Seed Latex	$\bar{n}_{ss}$ x 10^2	$\rho_{thermal}$ x 10^5 s^{-1} •	c x 10^2 s^{-1} ■	k_t x 10^{-4} mol/L.s ■
MMA01	2.92	2.58	1.51	2.36

• Average from all thermal experiments, with table 5.5 values recalculated using average c here.

■ Average from all γ-relaxation experiments, with and without CD

Table 5.10. Results of thermal and γ-relaxation polymerization experiments

Table 5.10 summarizes all the results of experiments done to experiments done to calculate $\rho_{thermal}$ and c, in case CD was not present. Knowing c, k_t can be calculated from equation (5.17). Both entry and termination rate coefficients were calculated through different sets of calculations. $\rho_{thermal}$ was calculated from the thermal polymerization experiments, carried out with no use of any initiating techniques, except for the monomer's ability to polymerize spontaneously. Based on conclusions reached earlier on the effect of CD on $\rho_{thermal}$ CD was not used in thermal polymerization experiments for MMA, for more information refer to section 3.5.3. Values presented in table 5.3 are used throughout the calculations of this work, unless otherwise specified.

For all mathematical analysis done for γ-relaxation experiments, α is substituted in equation (5.13) to be equal to one, that is, intra-particle termination is considered the only mechanism to end the polymerization reaction, and the exit rate coefficient k was not included in any of the calculations done throughout this part of the research.

5.7 Conclusions

The effect of CD presence at two different concentrations on the emulsion polymerization of MMA in the absence of any chemical initiator has been studied using γ-radiolysis and thermal initiation. The aim of the experiments was to obtain the values of thermal entry and termination rate coefficients, and how CD presence can affect such parameters.

CD was found to increase the rate coefficient of thermal entry; this was the opposite of

what was found with styrene. This was explained to be due to the high solubility of MMA, which facilitates having thermal entry in the aqueous phase. Consequently, using CD will increase thermal entry rates, as was found through γ-relaxation experiments.

On the other hand, MMA termination was found to be completely unaffected by any changes in MMA aqueous phase properties. For the values of termination rate coefficients, negligible difference was found between running experiments with and without CD. Such conclusions confirm already established knowledge that the rate determining step for emulsion polymerization of MMA is intra-particle termination, with complete lack of any changes in the aqueous phase concentrations of chemicals on the termination rate.

Having calculated the values of thermal entry and exit rate coefficients both with and without CD, values of these coefficients are required to have a thorough analysis for the chemically initiated emulsion polymerization experiments of MMA, which will be discussed in the next chapter.

Appendix 5.1 Recipes for all γ-relaxation and thermal initiation experiments for latex MMA01

γ-relaxation experiments

Experiment	Component mass				Vessel
	latex	monomer	AMA-80	CD	volume
TM101	2.00	1.74	0.10	0	30.478
TM102	2.09	1.78	0.105	0.072	36.160
TM103	2.00	1.78	0.109	0.040	29.317
TM104	2.01	1.83	0.103	0.069	30.478
TM105	2.00	1.77	0.102	0	29.317
TM106	2.13	1.75	0.110	0.035	36.160
TM107	2.05	1.75	0.112	0.036	30.478
TM108	2.12	1.76	0.102	0	36.160
TM109	2.03	1.74	0.104	0.073	29.317
TM110	2.14	1.78	0.101	0	36.160

All component masses are in grams, vessel volume is in cm^3.

thermally initiated experiments

Experiment	Component mass (g)			Vessel volume
	latex	monomer	AMA-80	
M101	3.47	3.4	0.092	57.13
M102	3.86	3.56	0.147	57.04
M103	3.67	3.57	0.195	57.13
M104	3.78	3.5	0.248	57.13
M105	2.26	4.05	0.078	57.13
M106	2.26	3.52	0.109	57.04
M107	3.84	3.42	0.143	57.13

All component masses are in grams, vessel volume is in cm^3.

References

(1) Ballard, M., Napper, D., and Gilbert R., *J. Polym. Sci., Polym. Chem. Ed.*, **1984**, 22, 3225.

(2) Baxendale, J., Evans, M. and Park, G., *Trans. Faraday Soc.*, **1946**, 42, 155.

(3) Baxendale, J., Evans, M. and Kilham, J., *Trans. Faraday Soc.*, **1946**, 42, 668.

(4) Baxendale, J., Bywater, S. and Evans, M., *Trans. Faraday Soc.*, **1946**, 42, 675.

(5) Thomson, B., Wang, Z., Paine, A., Lajoie, G. and Rudin, A., *J. Polym. Sci. Part A – Polymer Chem.*, **1995**, 33, 2297.

(6) Wang, S. and Poehlein, G., *J. Appl. Polym. Sci.*, **1994**, 51, 593.

(7) Smeets, N., Heuts, J., Meuldjik, J., Cunningham, M. and van Herk, A., *J. Polym. Sci. Part A – Polymer Chem.*, **2009**, 47, 5078.

(8) Costa, C., Santos, A., Fortuny, M., Araújo, P. and Sayer, C., *Materials Science and Engineering C.*, **2009**, 29, 415

(9) Ballard, M., Napper, D., Gilbert, R. and Sangster, D., *Polym. Chem.*, **1986**, 24, 1027.

(10) van Berkel, K., Russell, G. and Gilbert, R., *Macromolecules*, **2005**, 38, 3214.

(11) Zhang, G. and Zhang, Z., *Radiation Physics and Chemistry*, **2004**, 71, 273

(12) Apostolovic, B., Quattrini, F., Butte, A., Storti, G. and Morbidelli, M., *8th International Workshop on Polymer Reaction Engineering, 2004*, 2004, 115.

(13) Lingnau, J., Stickler M. and Meyerhoff, G., *Eur. Polym. J.*, **1980**, 16, 785

(14) Lingnau, J. and Meyerhoff, G., *Macromolecules*, **1984**, 17, 941.

(15) Lingnau, J. and Meyerhoff, *Polymer*, **1983**, 24, 1437.

(16) Lieser, K., *Nuclear and Radiochemistry Fundamentals and Applications*, **1996**, VCH Verlagsgesellschaft, Germany

(17) McKay, H., *Principles of Radiochemistry*, **1971**, Butterworth & Co Ltd, London

(18) O'Donnell, J. and Sangster, D., *Principles of Radiation Chemistry*, **1970**, Edward Arnold Ltd, London

(19) Gilbert, Robert G., *Emulsion polymerisation, a mechanistic approach*, **1995**, Academic Press, London.

(20) W.V. Smith and R.H. Ewart, *J. Chem. Phys.*,**1948**, 16,592

(21) Ballard, M., Gilbert R. and Napper, D., *J.Polym. Sci., Polym. Letters Ed.*, **1981**, 19, 533.

(22) Norrish R.G.W., Smith R.R., *Nature*, **1942**, 150, 336

(23) Russell, G., Gilbert, R. and Napper, D., *Macromolecules*, **1992**, 25, 2459

(24) Russell, G., Gilbert, R. and Napper, D., *Macromolecules*, **1993**, 26, 3538

(25) O'Shaughnessy, B. and Yu, J., *Macromolecules*, **1994**, 27, 5067

(26) Scheren, P., Russell, G., Sangster, D., Gilbert, R. and German, A., *Macromolecules*, **1995**, 28, 3637

(27) Stickler, M. and Meyerhoff, G., *Makromol. Chem.*, **1978**, 179, 2729.

(28) van Berkel, K., *Entry and the Kinetics of Emulsion polymerization*, a PhD thesis, University of Canterbury, 2004

(29) W.D. Harkins, *J. Chem. Phys.*, **1945**, 13,381

(30) W.D. Harkins, *J. Chem. Phys.*, **1946**, 14,47

(31) W.D. Harkins, *J. Chem. Phys.*, **1947**, 69, 1428

(32) Dunn, A., *Effects of the Choice of Emulsifier in Emulsion Polymerization*, in Piirma, I.(Editor), *Emulsion Polymerization*, **1982**, Academic Press, New York.

(33) Moad, G. and Solomon, D., *The chemistry of radical polymerization 2nd fully revised edition,* **2006**, Elsevier.

(34) Lovell P.A., *Free-Radical Polymerization*, in Lovell P.A., and El-Aasser M.S. (editors), *Emulsion polymerization and emulsion polymers*, **1997**, John Wiley and sons, New York.

(35) Lacík, I., Casey, B., Sangster, F., Gilbert, G., and Napper, D., *Macromolecules*, **1992**, 25, 4065

(36) Adams, M., Russell, G., Casey, B., Gilbert, R. and Napper, D., *Macromolecules*, **1990**, 23, 4624

(37) Hu, J., Li, S., Wang, D., Li, H., Liu, B. and Liao, X., *Polymer*, **2004**, 45, 1511.

(38) Dharmawardana, U., Christian, S., Tucker, E., Taylor, R. and Scamehorn, J., *Langmuir*, **1993**, 9, 2258.

(39) Hawkins, E., *Organic Peroxides*, **1961**, E. and F. F. SPON Ltd., London

(40) Barnes, C. and Elofson, R., *J. Amer. Chem. Soc.*, **1947**, 72, 210.

(41) Mayo, F., A., *J. American Chemical Soc.*, **1958**, 80, 2493

(42) Schulz, G. and Henrici, G., *Makromol. Chem.*, **1956**, 18, 437

(43) Mayo, F. and Miller, A., *J. Amer. Chem. Soc.*, **1958**, 80, 2480

Chapter VI

Effect of Cyclodextrin on the Chemically Initiated Emulsion Polymerization of Methyl Methacrylate

6.1. Introduction

Poly(methyl methacrylate) was first developed in 1928, and was first available commercially in 1933. Currently it is commonly known as acrylic, and sold under the trade names Optix and Lucite, amongst others. Commercially, it is used in some cases as an alternative to glass. Currently, the use of water soluble chemical initiators is the most commonly used polymerization initiation technique for emulsion polymerization, including the emulsion polymerization of methyl methacrylate (MMA, scheme 6.1), for example the salts of persulphuric acid, like potassium persulphate (KPS),[1] which is the most commonly studied aqueous phase initiator for emulsion polymerization.[2] This is mainly because of the cheap price of chemical initiators compared to other techniques, like γ-rays, whose cost is relatively high because of the high cost of the radioactive isotope.[3] Because of the very high price of isotopes emitting γ-rays, polymerization initiation is not considered as one of the most common uses of radioactive materials.[4]

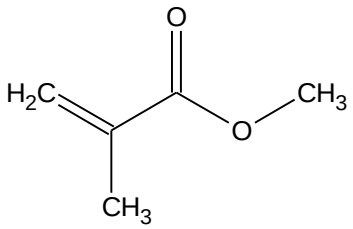

Scheme 6.1. Methyl methacrylate.

The following research is inspired by the Maxwell-Morrison model for entry.[5] This model was based on the experimental results of previous experiments. As the experimental work done for the Maxwell-Morrison model was on styrene emulsion polymerization, results of the work of Ballard *et al.*[6] were used to do the calculations required for MMA.

Work done in this project has some similarity to that done by Ballard,[6] and also to the

similar work done later by van Berkel *et al.*[7,8] Experiments done for MMA emulsion polymerization for both sets of work included the use of a latex which is stabilized by the AMA-80 anionic surfactant. Furthermore, both sets of work used KPS as the chemical initiator. The addition presented through this work is the use of cyclodextrin (CD) as a "phase transport catalyst"[9] to improve the reaction rate kinetics.

The inclusion of CD in research done on aqueous phase polymerization (including emulsion polymerization) started recently, as a result of the current cheap prices of CD. Such research was not done earlier because in 1970 the price of 1 kg of CD was US$ 2000, currently it is about $5 for the same amount.[10] Most of the research done was on monomers which are usually polymerized through emulsion polymerization, the use of equimolar amounts of monomer to CD led the polymerization to take a solution polymerization path, and this was the case with the work done by Ritter for aqueous phase polymerization of MMA.[11] A later research done by the same author[12] on styrene confirmed the fact that what was found earlier was solution polymerization, as it was found to follow solution polymerization kinetics.

Focusing on all this research about emulsion polymerization of MMA with CD, the kinetics of the reaction has not been studied to the same level of studying the emulsion polymerization of MMA without CD. A kinetic study of the emulsion polymerization of MMA with CD led to the conclusion that the increase of the amount of CD used leads to an increase in the polymerization rate and the monomer conversion, and a decrease in the particle size.[13] This research was done using benzoyl peroxide (BPO) initiator, and the emulsion particles were suspended in a water/methanol mixture.

The main objective of this research is to run MMA emulsion polymerization experiments similar to experiments previously done,[6,7] with the only difference to be the use of a small amount of CD (2% and 4% relative to the initial mass of monomer used), and monitoring the effect of the addition of CD on the reaction kinetics of the emulsion polymerization.

6.2 Theoretical Background

6.2.1 Maxwell-Morrison model for entry for chemically initiated experiments

Chemical initiators are the most common technique for emulsion polymerization, and the most widely studied through the study of chemistry of aqueous phase initiators. This is true for both laboratory scale and commercial scale emulsion polymerization. Chemical initiators are cheaper than γ-radiolysis isotopes, and they let the reaction run at a high rate compared to thermal initiation. Another advantage for chemical initiators is the reduction of the induction period. For all these reasons, early research done on emulsion polymerization considered the initiator to be a "catalyst".[14]

Analysing the effect of CD on reaction rate will follow the Maxwell-Morrison model.[15] This model has been used in the analysis for kinetic data for similar work done previously.[7] The model focuses on the free radical chemistry within the aqueous phase, as it controls the kinetics of the whole emulsion polymerization process. In the aqueous phase, the polymerization process starts by the initiator decomposition

$$\mathrm{I{-}I} \xrightarrow{k_\mathrm{d}} 2\mathrm{I}^{\bullet} \qquad (6.1)$$

where k_d is the first order rate coefficient for initiator decomposition. The initiator free radical ($\mathrm{I}^{\bullet}$) starts to react with monomer molecules suspended in the aqueous phase:

$$\mathrm{I}^{\bullet} + \mathrm{M} \xrightarrow{k_\mathrm{pi}} \mathrm{IM}^{\bullet} \qquad (6.2)$$

where k_pi is the second order rate coefficient for aqueous phase propagation between initiator free radical and monomer. The free radical produced in equation (6.2) will then go for subsequent propagation:

$$\mathrm{IM}_i^{\bullet} + \mathrm{M} \xrightarrow{k^i_\mathrm{p,aq}} \mathrm{IM}_{i+1}^{\bullet} \qquad (6.3)$$

$k^i_\mathrm{p,aq}$ is the rate coefficient for aqueous phase propagation of the free radical whose

degree of polymerization is *i*. According to the Maxwell-Morrison model, for entry to take place the radical chain length must reach a critical value *z*, at which the radical is no longer water soluble and entry to a particle must happen. This can be expressed by the following equation

$$IM_z^{\bullet} + \text{latex particle} \xrightarrow{\rho_{\text{initiator}}} \text{entry} \qquad (6.4)$$

For the free radical which react with other aqueous phase free radicals and terminate within the aqueous phase, the reaction is

$$IM_i^{\bullet} + T^{\bullet} \xrightarrow{\substack{i<z \\ k_{t,aq}}} \text{inert products} \qquad (6.5)$$

where $k_{t,aq}$ is the second order rate coefficient for termination between free radicals in the aqueous phase.

Rate equations can be derived based on equations (6.1) to (6.5), and this was discussed in details in chapter I. From these rate equations, and following some approximations, Maxwell-Morrison model uses the following equation to calculate initiator component of the first order rate coefficient for entry,

$$\rho_{\text{initiator}} = \frac{2fk_d[I]N_A}{N_c}\left(\frac{2\sqrt{k_d[I]k_{t,aq}}}{k_{p,aq}C_W}+1\right)^{1-z} \qquad (6.6)$$

where *f* is the initiator decomposition efficiency, the factor 2 is used as the two molecules produced from the initiator decomposition are capable of initiating polymerization, C_W is the monomer concentration in the aqueous phase. Entry efficiency can be calculated as:

$$F = \frac{\rho_{\text{initiator}}}{\rho_{\text{initiator100\%}}} = \left(\frac{2\sqrt{k_d[I]k_{t,aq}}}{k_{p,aq}C_W}+1\right)^{1-z} \qquad (6.7)$$

The Maxwell-Morrison original publication highlighted a value of *z* between 4 and 5[15].

This uncertainty in the value of *z* does not represent a problem in the calculation, as *F* is calculated through a different equation, equation (4.11)

$$F = \frac{\rho_{initiator} \quad N_c}{2 f k_d [I] N_A} \tag{6.8}$$

6.2.2 Comparison of kinetic parameters at different conditions

The entry efficiency rate coefficient ρ cannot be used as the defining parameter for the success of the entry process. ρ is divided into two components, thermal entry and initiator entry rate coefficient. The overall rate coefficient is calculated as

$$\rho = \rho_{\text{thermal}} + \rho_{\text{initiator}} \tag{6.9}$$

It was found earlier that $\rho_{\text{initiator}}$ for MMA can be affected by the aqueous phase solubility of the monomer. Furthermore, equations (6.6) shows clearly that $\rho_{\text{initiator}}$ can be affected by N_c, the number of particles per unit volume in the aqueous phase. For this $\rho_{\text{initiator}}$ can not be used by itself to define the efficiency of the entry process.

As this is the first research to study the entry efficiency in presence of CD, *F* was not calculated before under conditions at which C_W changes. As *F* is affected by any change in C_W, using *F* with its current definition has some inaccuracy in it. It will be shown later how this increase in solubility increases the values of both the entry efficiency and $\rho_{\text{initiator}}$.

6.2.3 Measurement of entry rate coefficients:

The only data obtained from the dilatometer tracker is the change in volume of the reaction mixtures at different times. To calculate the conversion from the change in volume, it should be noted that the mixing between MMA and water is not ideal. Consequently, it is wrong to consider the volume change as the between the monomer and polymer densities and base the calculations on that. It is then more accurate to follow the following procedure[6,16]

$$m_x = \frac{\Delta V}{V_{sM} - V_{sp}} \tag{6.10}$$

where m_x is the mass of monomer converted into polymer. V_{sM} and V_{sp} are the partial specific volumes of the monomer and polymer, respectively. $V_{sM} = 1/d_M$ and $V_{sp} = 1/d_P$. d_M and d_P are the densities of the monomer and the polymer, respectively. For MMA at 50^{o}C, d_M = 0.909 g/cm^3, and d_P = 1.226 g/cm^3, as have been previously measured[16].

Knowing m_p^{seed}, the mass of seed polymer originally present within the system, m_M^0, the mass of monomer present in the system at the beginning of the experiment, and m_w, the mass of monomer dissolved in the aqueous phase, a general mass balance to calculate the mass of polymer within the system, m_p, and the mass of monomer within the particles, m_P, leads to the following equations:

$$m_p = m_p^{seed} + m_x \tag{6.11}$$

$$m_P = m_M^0 - m_w - m_x \tag{6.12}$$

As all experiments done were seeded emulsion polymerization experiments, $m_p^{seed} \neq 0$ for all experiments.

The amount of monomer present within the polymer particles, C_P can be calculated from

$$C_P = \frac{m_P/M_0}{m_M V_{sM} + m_p V_{sp}} \tag{6.13}$$

where M_0 is the molecular weight of the monomer. Equation (6.13) implicitly assumes that the monomer and polymer mix ideally. As all experiments done were only interval II experiments, then $C_P = C_P^{sat}$ and conversion, x, can be calculated from equation (6.10).

As the focus is only on interval II calculations, there is no need to discuss interval III calculations here; as their only use is to identify the point of time at which interval III starts. Those equations have already been mentioned in section (5.2.3).

As conversion, *x*, has been calculated at different points of time throughout the experiment, then the corresponding $\bar{n}$, the average number of free radicals per particle, at each point of time can be calculated from

$$\frac{\mathrm{d}x}{\mathrm{d}t} = \frac{k_\mathrm{p} C_\mathrm{P} N_\mathrm{c}}{{m_\mathrm{M}}^0 N_\mathrm{A}} \bar{n} \tag{6.14}$$

Knowing $\bar{n}$, then the entry rate coefficient ρ can be calculated. As the value of ρ_{thermal} has already been calculated, then $\rho_{\mathrm{initiator}}$ can be easily calculated from equation (6.9), *F* can be calculated for every experiment accordingly.

6.2.4 Pseudo-bulk kinetics in the emulsion polymerization of MMA

This analysis follows the Smith-Ewart theory,[17] which is the main theory currently used for analysing emulsion polymerization results. From equation (6.14), a simplified form of the general form of Smith-Ewart equation (equation 1.4), entry, exit and termination parameters can be calculated.

$$\frac{\mathrm{d}\bar{n}}{\mathrm{d}t} = \rho - (1-\alpha)k\bar{n} - 2c\bar{n}^2 \tag{6.15}$$

As has been previously discussed, $\mathrm{d}\bar{n}/\mathrm{d}t$ can be calculated from conversion data, using equation (6.14). As equation (6.15) is the simplified form of the theory, it is considered an accurate approximation under the conditions that that $k > c$ or $\rho > c$.[18]

MMA emulsion polymerization system is known to be pseudo-bulk.[16] In γ-relaxation experiments, the system has a low concentration of free radicals, so it is a good approximation to assume $\alpha = 1$ in equation (6.15). But as has been previously found,[7,8] even during chemically initiated experiments, α was found to have values which are very close to 1 at low initiator concentration. For example at 0.03 mmol/L KPS, α was found to be equal to 0.97. At higher initiator concentrations $\alpha = 1$. For simplicity, throughout the calculations of this work, the assumption $\alpha = 1$ will be followed, and equation (6.15) takes the form

$$\frac{\mathrm{d}\bar{n}}{\mathrm{d}t} = \rho - 2c\bar{n}^2 \tag{6.16}$$

Equation (6.16) is the so called limit 3 equation. Knowing c (from γ-relaxation) and the steady state value for $\bar{n}$, then ρ can be calculated from

$$\rho = 2c\bar{n}^2 \tag{6.17}$$

Finally, another way to define c is through the second order rate coefficient of bimolecular termination k_t and the volume of the swollen latex particle V_s, as

$$c = \frac{k_t}{N_A V_s} \tag{6.18}$$

k_t used in the calculations of this chapter is the one calculated from γ-relaxation in chapter V, using equation (6.18). Using this constant value for k_t, $\bar{n}$ can be calculated at different times during any experiment from

$$\bar{n} = \sqrt{\frac{\rho N_A V_s}{2k_t}} \tag{6.19}$$

6.2.5 Acceleration during interval II[8]

One of the problems faced with the MMA system is that $\bar{n}$ is not constant even during interval II. In interval II this is because of the increase in particle volume during the course of polymerization. As the reaction is "pseudo-bulk", this increase in the volume of the reaction medium (particles) will increase the reaction rate[6]. For most calculations done, like calculations for $\rho_{\text{initiator}}$ and F, the value of $\bar{n}$ near the beginning of the reaction was calculated from the intercept of the conversion/$\bar{n}$ straight line relationship, as shown in figure 6.1.

The figure shows the linear increase in reaction rate, which can be expressed by the acceleration, $\bar{a}$, which quantifies the increase in the value of $\bar{n}$.

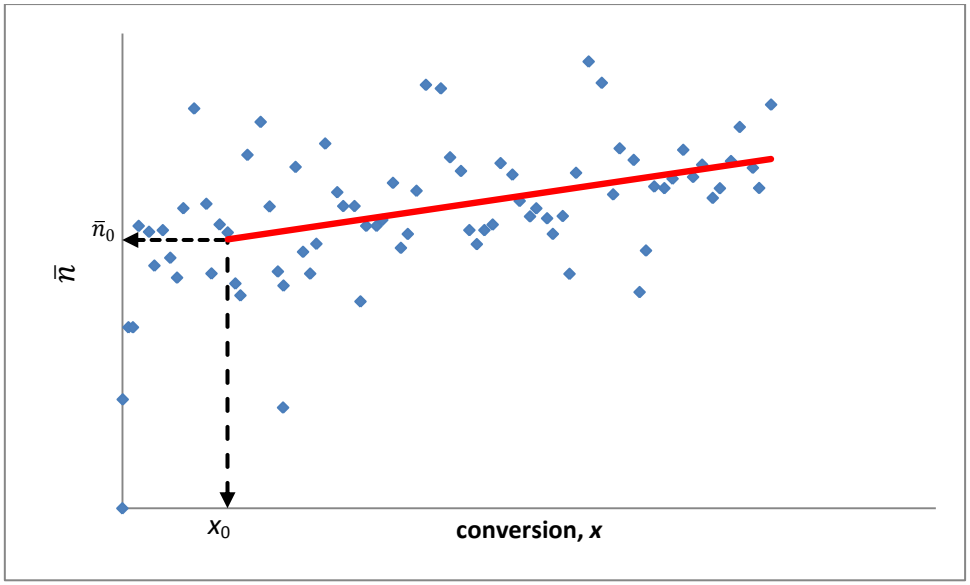

Figure 6.1. typical conversion/$\bar{n}$ curve resulting from one of the MMA experiments (M115).

As for the value of $\bar{n}$ which will be used in other calculations, like $\rho_{\text{initiator}}$ and F, the value used will be that of $\bar{n}$ at the beginning of the steady-state region, shown in figure 6.1 by the red straight line. This value is expressed as $\bar{n}_0$, and conversion at this point is x_0.

During the course of polymerization the particle volume keeps increasing, which results in an increase in the reaction rate, shown as a gradual linear increase in $\bar{n}$ with conversion, as shown in figure 6.1.

In work previously done[6], the following equation was derived and used to calculate the acceleration parameter $\bar{a}$, which is the quantitative representation for the increased value of $\bar{n}$.

$$\bar{a} = \frac{\frac{\mathrm{d}\bar{n}}{\mathrm{d}x}\frac{m_{\mathrm{P}}^{0}}{m_{\mathrm{M}}^{0}}}{\bar{n}_0} \tag{6.20}$$

$\mathrm{d}\bar{n}/\mathrm{d}x$ is the average change of $\bar{n}$ with conversion over the entire range of pseudo-steady state interval II, which can be calculated from the slope of the red line in figure 6.1. x_0 and $\bar{n}_0$ represent the starting point of the steady state period. $m_{\mathrm{M}}{}^{0}$ is the total mass of

monomer at the beginning of the reaction, and m_p^0 is the total mass of polymer at the start of interval II steady state period (these values are negligibly different to those at the beginning of the pseudo-steady state). m_p^0 can be calculated as

$$m_P^0 = m_p^{\text{seed}} + x_0 m_M^0 \tag{6.21}$$

To obtain a theoretical value of $\bar{a}$, the following equation was previously derived to calculate $\bar{n}$.

$$\bar{n} = \bar{n}_0 \sqrt{\left(1 + \frac{(x - x_0) m_M^0}{m_p^0}\right)} \tag{6.22}$$

The amount $(x - x_0)$ represents only the conversion which happened during the steady state period of interval II. Applying Taylor-series expansion to $(x - x_0)$ in equation (6.22), and taking only the first order of the expansion $\bar{n}$ can be expressed as

$$\bar{n} = \bar{n}_0 + \frac{\bar{n}_0}{2m_p^0}(x - x_0) m_M^0 \tag{6.23}$$

Substituting the value of $\bar{n}$ from equation (6.23) into equation (6.20) yields

$$\bar{a} = \frac{\frac{d\bar{n}}{dx}\frac{m_p^0}{m_M^0}}{\bar{n}_0} = \frac{\frac{\bar{n}_0}{2m_p^0} m_M^0 \frac{m_p^0}{m_M^0}}{\bar{n}_0} = 0.5 \tag{6.24}$$

This leads to the general conclusion that the value of $\bar{a}$ is constant at 0.5 for the steady state period of interval II. This means that changing reaction conditions (like initiator concentration, N_c, or temperature) should not affect this value. It should be noted, however, that this is an approximated value, as it has been noted that under different conditions $\bar{a}$ has different values. The lower the initiator concentration used in the experiment the lower the value of $\bar{a}$ was found to be.[8]

6.3 Experimental

As the experimental part for most work done on the MMA01 latex has already been mentioned in chapter V, here there is a summary for it, except in parts where the experiments were done differently.

6.3.1 Synthesis and purification of the seed latex

MMA, purchased stabilized with hydroquinone, was passed through a column of basic aluminium oxide . Extra care was taken to have MMA at the highest possible purity, as results of kinetic experiments are known to be very sensitive for MMA purity. The basic aluminium oxide removed all the hydroquinone present, as was seen by the 100% purity of the MMA used in this work. With this purity no further distillation was required. The purified monomer was kept at 0^{o}C, to avoid any spontaneous polymerization.

The reactor where the latex was synthesized is a jacketed glass cylinder, having an approximate size of 1 L. Before the reaction starts, oxygen is removed from the reaction medium, this is done by passing nitrogen gas over the reactants while they are being heated. Hot water is passed through the jacket to ensure temperature control, as the reactor has two thermometers, one in the reaction medium and the other in the jacket, to ensure precise temperature control. Miili-Q water (710 g) is heated within the reactor until its temperature approaches 92^{o}C, and then MMA (195 g) is added. 20 g of surfactant (Aerosol MA-80) and 1 g of sodium bicarbonate are added to the heated medium. Simultaneously, 3.1 g KPS was dissolved in 55 g water. When the mixture within the reactor reaches thermal stability, the initiator solution is added. The deoxygenation process ensures aerial oxygen does not interfere within the reaction, except for any amounts of oxygen which are dissolved in the monomer and water. The reaction is left to run for 24 hours.

As the latex has been synthesized it should then be purified. This is done by placing the latex in dialysis tubes and placing these tubes in milli-Q water for 5 weeks. Dialysis tubes separate water soluble components from the latex medium, this includes surfactant, any non-reacted initiator, buffer, and any extra monomer which might not have polymerized. Water is changed twice a day in the first week, then daily after that. The conductivity of

the milli-Q water is tested and is found to continuously decrease with time, until it reaches a nearly constant value after 4 weeks of dialysis.

6.3.2 Determination of seed latex characteristics

The amount of poly(MMA) within the latex was determined through gravimetry. Average particle diameter was determined through PSDA, as TEM images had the problem of unclear borders for the TEM particles. Figure 6.2 shows a TEM image for the poly MMA latex used during the course of the work. Although the particles should be spherical, figure 6.2 shows some of the problems of carbon coating (previously discussed in chapter V), which is that the coating hides the borders of the particles, and the "voids" in the centre of every particle makes it hard to distinguish the exact particle borders.

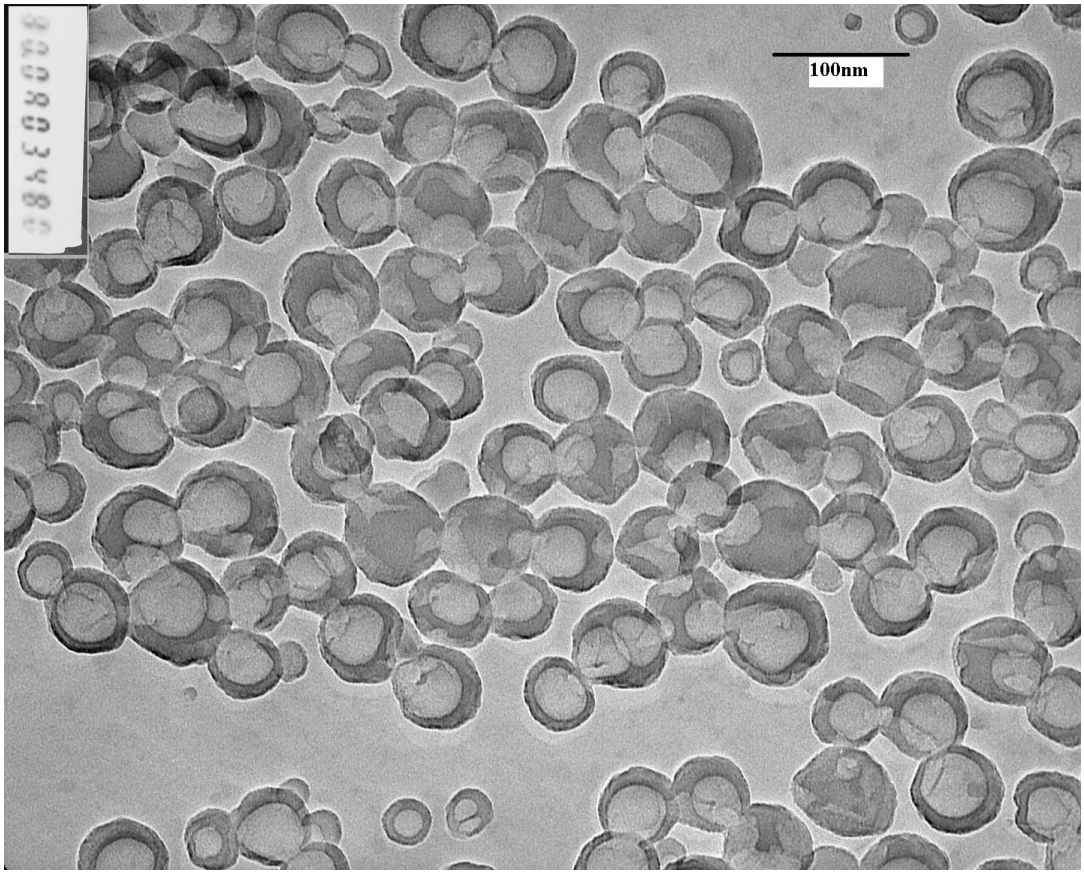

Figure 6.2. Typical TEM image for latex MMA01, image obtained through the Hitachi H600 TEM.

Because it was very hard to get an accurate average particle diameter through the use of such images, other images were obtained using a different TEM. Although figure 6.3

shows the particles to be more spherical, the borders of the particles are still unclear. Furthermore, the unclear borders may lead to a conclusion that even with carbon coating the particles might have been exposed to some deformation, resulting in such a “cloudy” image.

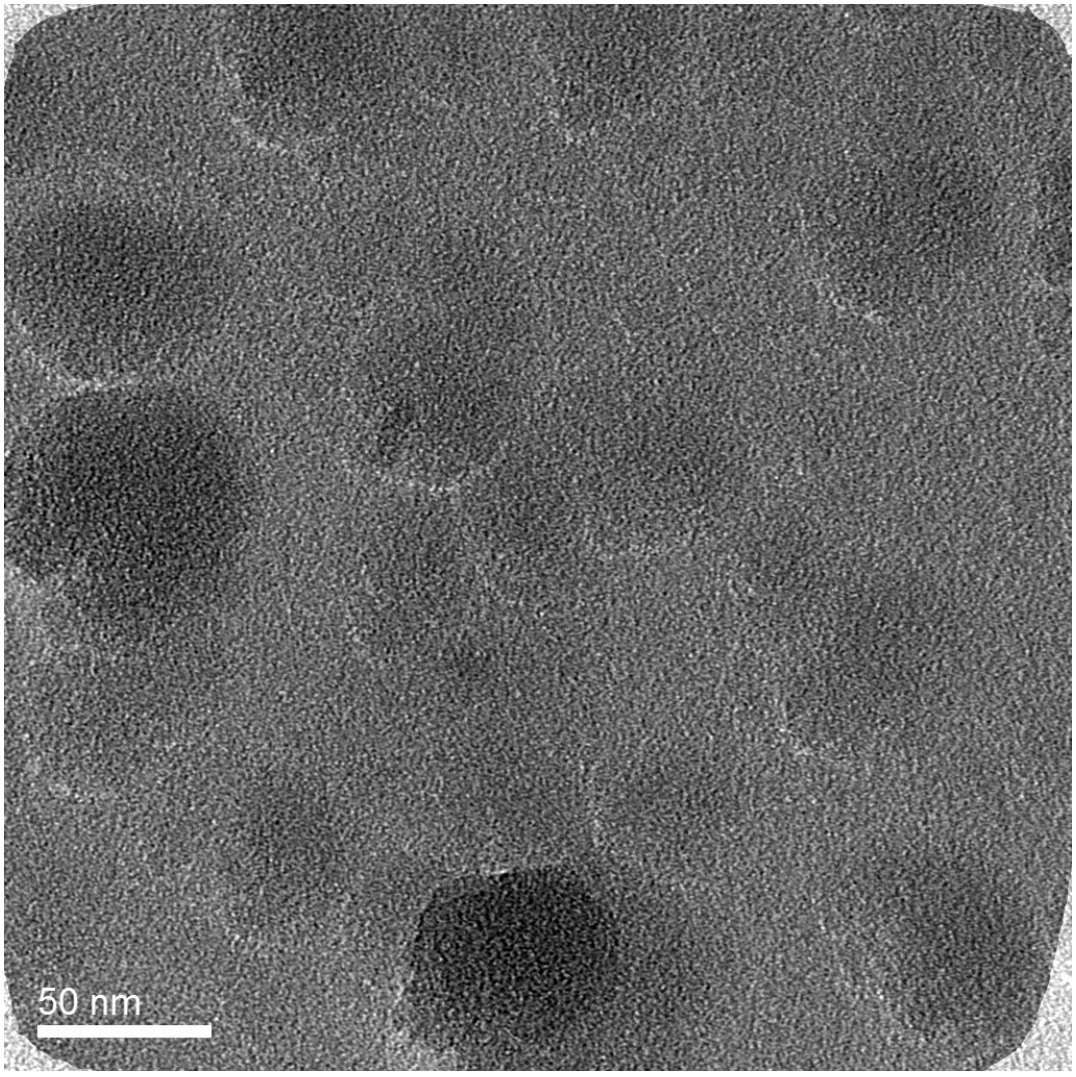

Figure 6.3. Typical TEM image for latex MMA01, image obtained through the Phillips CM200 TEM.

To avoid such problems, both PSDA and HPPS were used, and although the average particle diameter obtained through both techniques was similar, the PSDA value was the one used in all calculations, because it has higher accuracy than HPPS.

The average particle diameter for the MMA01 latex was determined to be 103.91 nm by PSDA.

6.3.3 Determination of monomer solubility

The solubility of the monomer in the latex, C_P^{sat}, was determined through the static swelling method. The monomer was mixed with the latex in a dilatometer capillary tube, heated to 50 ^oC then stirring was stopped. A capillary was inserted at the top of the dilatometer vessel, water was injected into the mixture and the amount of MMA which did not dissolve in the latex and water was pushed up through the capillary. For more details check 2.3.3 and 4.3.3.

The solubility of the monomer in water, C_W^{sat} was determined using UV-Vis spectroscopy. It should be noted, however, that the values of the solubility of MMA in water in presence of CD and surfactant did not explain the increased rate of polymerization in presence of MMA. An additional experiment was done, using NMR, and it gave some values for solubility which will be discussed in 6.4.1.

6.3.4 Kinetic Experiments

Kinetic experiments were run in a very similar way to chemically initiated styrene polymerization experiments, discussed more thoroughly in sections 2.4 and 4.3.2. The reactants are the seed latex particles and the monomer; they are both diluted in water to fill the dilatometer reaction vessel. CD was added in small amounts (2% and 4% of the weight of the monomer at the beginning of the reaction). Stirring was done overnight, then the reactants are heated to be degassed, and then cooled down to 50 ^oC. The initiator is prepared in an aqueous solution, and then it is added to the reaction mixture. A capillary is added at the top of the reaction vessel, and degassed water is used to fill the vessel and partially fill the capillary. A dodecane layer is added at the top of the water within the capillary, and the reaction is run. As the reactants volume decreases because of the polymerization of the monomer, the dodecane layer moves down, and the tracker follows it, providing a set of data of time versus height change.

Solving equations (6.10) - (6.12) iteratively provides the value of conversion at every point of time at which a reading of height has been taken.

Other than changing the initiator and CD concentrations, all other reaction conditions

remained the same, this includes the amount of surfactant (0.15 g AMA-80), the amounts of monomer and polymer used, and a constant N_c of 1.7 x 10^{16} particles/L.

6.4 Results and discussion

6.4.1 Effect of CD on monomer solubility in water

The rate of emulsion polymerization of MMA was found to increase with the addition of CD. This was the case with the work previously done, for example research done by Ritter *et al.*[19,20], and Hu *et al.*[13]. In all research previously done on effect of CD on MMA, the common understanding for the effect of CD and the reason that it increases the reaction rate was that it increases the aqueous phase solubility of the monomer because CD has hydrophobic cavity[21,22], enabling it to act as a "phase transfer catalyst".[8,23] This assumption has been followed for all previous work done on the effect of CD on aqueous phase polymerization, but no test on MMA solubility in water in presence of CD has previously been done.

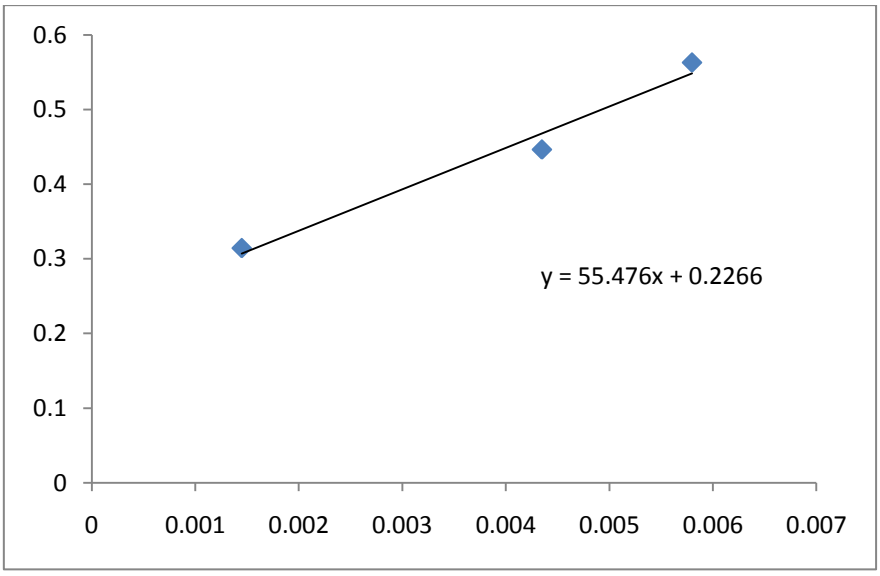

Figure 6.4. Calibration line used for MMA solubility measurement. This line shows that MMA absorbance follows Beer's law. All absorbance were taken at wavelength 203 nm.

all taken from the original styrene solution and diluted in the same ratio. By plotting the absorbances of these solutions, figure 6.4 was obtained.

The calibration was done by dissolving 0.29 g of MMA in 1 L of water. 10 ml of this solution were taken and further diluted to 0.2 L. Three other portions (30 and 40 ml) were

	MMA solubility (x 10^2 mol/L)	
	No surfactant	AMA-80
No CD	15.4	14.9
2% CD	10.9	9.0
4% CD	11.0	9.9

Table 6.1. Solubility of MMA in water at different conditions

A few assumptions were followed when this method was used to measure MMA solubility in water. First, CD and surfactant were assumed not to have any combinations with MMA which can affect the absorbance, and they were assumed not to affect MMA absorbance.

To determine the solubility of MMA at different conditions, mixtures of styrene, CD and surfactant were prepared in dilatometer volumetric flasks, in the same way of mixing and preparing the mixture before kinetic experiments, with the main difference is the absence of seed latex particles. From each mixture 1 ml was taken and diluted to 0.2 L volume, then 10 ml of this diluted solution were further diluted to 0.2 L. Samples from this most diluted solution had their solubilities measured. Appendix 6.1 shows all the experiments done for measurement of styrene maximum concentrations at different conditions.

Table 6.1 shows the aqueous phase solubility, as calculated through UV-Vis spectroscopy absorbance results. The numbers shown in the table highlights one of two possibilities, either these numbers are true, and that CD does not increase the solubility but it increases the rate through another mechanism, which is still unknown. Or that CD actually increases the MMA solubility, but UV is not the most suitable technique to measure this solubility.

It can be generally concluded that UV can be considered an accurate technique for measurement of MMA solubility, as the value of MMA solubility (with no CD or surfactant) is the same value obtained earlier,[6] This fact puts a heavier emphasis on the

assumption that UV is not the most suitable technique to detect MMA solubility in presence of CD. This can explained through a number of facts, one of them is that CD changes the UV-Vis spectra of its complexed guests,[24] although the change in spectrum can be small in most cases,[25] it is obviously not the case in the current work. Another alternative to UV-Vis spectroscopy can be gas chromatography, it can be used either as a confirmation for UV-Vis results, or as an independent concentration measurement technique.

Another reason for complexity is that having a double bond in the compound leads to changes in the whole absorption band.[25] MMA has two double bonds, one of them is a C=O bond. Although having a calibration curve of absorbance for different concentrations of MMA neutralizes such effects resulting from the double bond, it is very hard to detect the effect of these double bonds while MMA is complexed within CD cavities.

Similarity between the spectra of individual components increases the chance on inaccuracy of the analysis.[26] This was the case with this part of the work, as the available UV-Vis spectrophotometer works only in wavelengths of 200 to 800 nm. Both MMA and CD did not show a maximum for their spectra in this range, and both of them were showing an increase in the absorbance near the 200nm range. Such spectra similarity must have increased the inaccuracy of the analysis.

To avoid these problems a different technique was used. This was NMR, but results from NMR were even far from the values which have been found earlier. with no CD MMA concentration was found to be 0.0679 mol/L, with 2% CD it was 0.0747 mol/L, and with 4% CD it was 0.0684 mol/L. Such values are quite different from what was found with UV-Vis, but they can be taken from one prespective, which is that CD has a negligible effect on MMA solubility in water

For all the above mentioned reasons, the saturation values obtained through these measurements cannot be taken to be exact. Nevertheless, they highlight the fact that CD does not have a major effect on MMA solubility. This can be mainly because MMA has a relatively high water solubility compared to other monomers (styrene for example). As will be seen later, the increase of polymerization rates because of the presence of CD can

be considered minimal, compared to its effect for emulsion polymerization of styrene in the case of the cationic latex.

6.4.2 Chemically initiated MMA polymerization

Seeded emulsion polymerization experiments were all run at constant temperature of 50 ^{o}C, both initiator (KPS) and CD were used in experiments to quantitatively measure the effect of CD on the reaction rate. As has already been mentioned, there is a continuous increase in the reaction rate all along interval II. Figure 6.5 shows this increase.

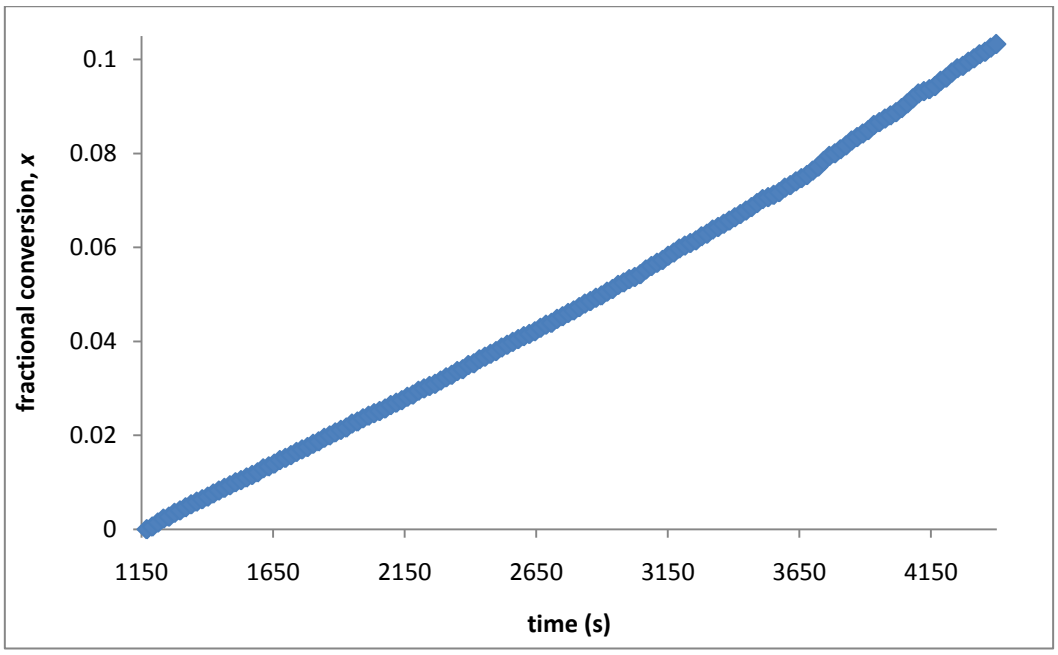

Figure 6.5. Typical conversion/time graph for a seeded emulsion polymerization experiment (experiment M122) during interval II.

The curve in figure 6.5 shows a continuous increase in conversion with time. The rate of this increase is almost constant; this is why the curvature of the curve is constant all over the range. Analysing the change in $\bar{n}$ over the range of conversion shows a linear increase in the rate of the reaction (expressed with $\bar{n}$) with conversion, as shown in figure 6.6. Because of the lack of the Trommsdorff-Norrish[27] effect over interval II, the rate of increase of $\bar{n}$ is slow. And the theory explaining this slow increase in reaction rate considers the reason of this increase to be due to the increase in the particle volume.[6] Results of the current work confirm such previously reached conclusions.

Emulsion polymerization of MMA in interval III follows a totally different path. After the end of interval II, there is a gradual increase in reaction rate until it reaches a maximum, followed by a decline in this increase.

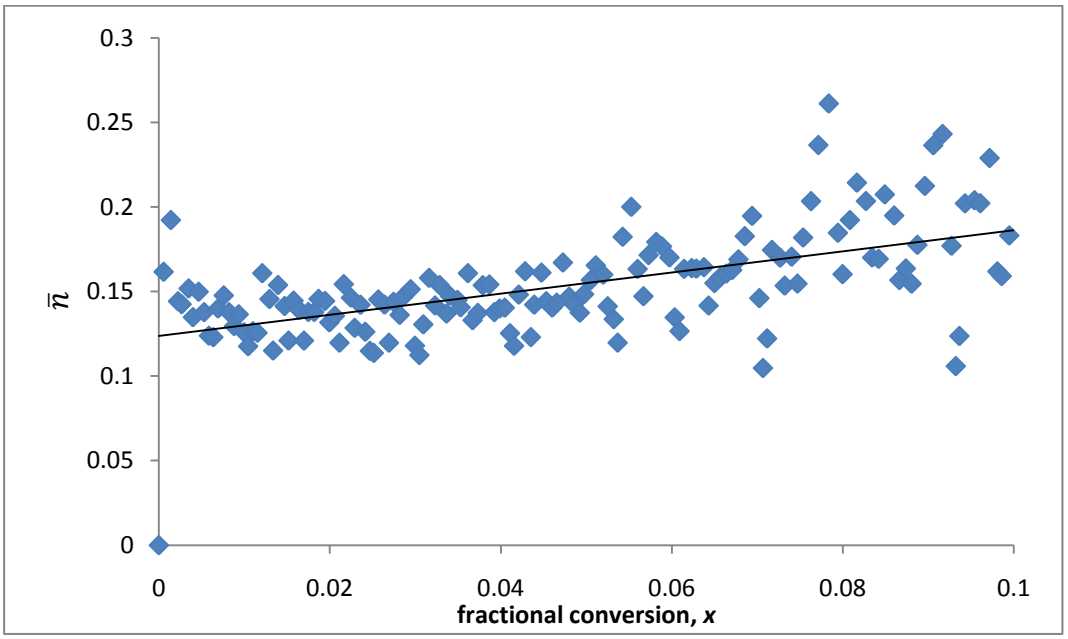

Figure 6.6. Typical $\bar{n}$ conversion plot from an MMA experiment (M122). Points: experimental results; line: best fit.

Figure 6.7 shows the conversion versus time data for the same experiment shown in figures 6.5. It shows a major increase in the reaction rate at around the middle of time

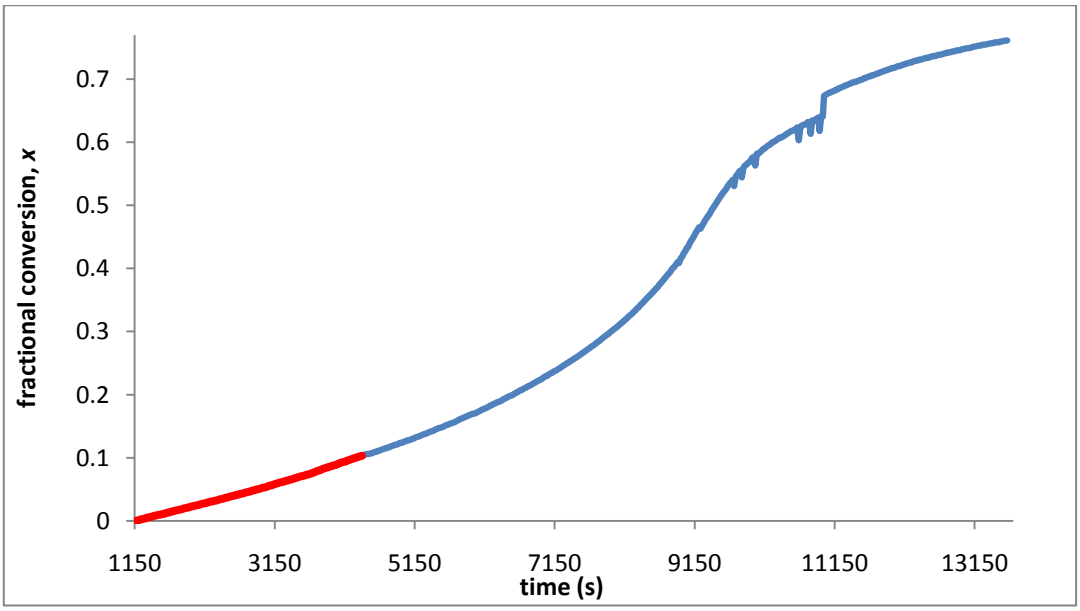

Figure 6.7. Typical conversion versus time plot for a seeded emulsion polymerization experiment for MMA (M122) during both interval II (red) and interval III (blue).

period during which the polymerization was run. Both at the beginning and the end the rate of increase of the reaction rate is comparatively smaller, which is similar to results obtained in previous work.[8]

6.4.3 Effect of CD on chemically initiated MMA polymerization

The reason most commonly agreed upon for the increase of polymerization rate with CD is that CD increases the aqueous phase solubility of monomers, which results in aiding the monomer transport to polymerization loci, which is the particles[28,29]. Another opinion suggests that the impact of CD on polymer properties, like average particle size, is because of the interaction between CD, colloids, buffers, surfactants… and other aqueous phase solutes present within the reaction medium.[30]

It will be seen from the results of chemically initiated emulsion polymerization of MMA that the above mentioned interactions impact also the reaction rate. As CD was not found to affect the aqueous phase solubility of the monomer, it still plays a major role in determining the reaction kinetics.

Experiments were run with five different initiator concentrations, 0.03, 0.1, 0.3, 1 and 3 mmol/L. Summary of results of these experiments is in table 6.2. A major difference between emulsion polymerization of styrene and MMA is that $\bar{n}$ changes with time. Consequently, all variables which involve the use of $\bar{n}$ in their calculation, like ρ_{thermal} and F will keep changing over the course of the reaction.

Results are included in two tables. Table 6.2a presents the values of $\bar{n}_0$, $\rho_{\text{initiator}}$ and F at the beginning of interval II, while table 6.2b presents the values of $\bar{n}_{\text{end}}$, $\rho_{\text{initiator}}$ and F at the end of interval II. For calculations of table 6.2, the value of $k_t = 2.36 \times 10^4$ L/mol.s was used, and $\rho_{\text{thermal}} = 2.54 \times 10^{-5}$ s^{-1} was assumed to remain constant with no change, even with different CD concentrations.

Experiment	N_c x 10^{16}	[KPS] x L/mmol	$\bar{n}_0$	$\rho_{initiator}$ x 10^4 s	F	%CD
M108	1.698	0.036	0.0422	4.675	0.0166	0
M110	1.685	0.036	0.0348	2.367	0.0084	2%
M111	1.689	0.036	0.0286	0.776	0.0027	4%
M112	1.708	0.107	0.0312	1.405	0.0017	0
M113	1.712	0.107	0.0308	1.305	0.0016	2%
M114	1.716	0.107	0.0333	1.954	0.0024	4%
M116	1.694	0.369	0.0629	13.486	0.0047	0
M117	1.660	0.369	0.0701	17.364	0.0059	2%
M118	1.666	0.369	0.1056	42.624	0.0145	4%
M119	1.692	1.086	0.1073	44.090	0.0052	2%
M121	1.659	1.086	0.0465	6.220	0.0007	0
M122	1.617	3.258	0.1267	62.475	0.0023	0
M123	1.559	3.258	0.1027	40.178	0.0015	2%
M124	1.562	3.258	0.0803	23.577	0.0009	4%

Table 6.2a. Summary of results for all chemically initiated experiments done using latex MMA01. Variables presented are calculated as per the conditions at the start of interval II.

Experiment	N_c x 10^{16}	[KPS] x L/mmol	$\bar{n}_{end}$	$\rho_{initiator}$ x 10^4 s	F	%CD
M108	1.698	0.036	0.0381	1.230	0.0044	0
M110	1.685	0.036	0.0362	0.806	0.0028	2%
M111	1.689	0.036	0.0369	0.919	0.0033	4%
M112	1.708	0.107	0.0475	3.480	0.0042	0
M113	1.712	0.107	0.0504	3.594	0.0043	2%
M114	1.716	0.107	0.0466	3.352	0.0041	4%
M116	1.694	0.369	0.1032	23.976	0.0083	0
M117	1.660	0.369	0.1192	35.880	0.0122	2%
M118	1.666	0.369	0.1323	41.798	0.0142	4%
M119	1.692	1.086	0.1728	65.750	0.0077	2%
M120	1.706	1.086	0.1269	38.188	0.0045	4%
M122	1.617	3.258	0.1866	86.623	0.0032	0

Experiment	N_c x 10^{16}	[KPS] x L/mmol	$\bar{n}_{end}$	$\rho_{initiator}$ x 10^4 s	F	%CD
M123	1.559	3.258	0.1496	55.481	0.0020	2%
M124	1.562	3.258	0.1269	38.995	0.0014	4%

Table 6.2b. Summary of results for all chemically initiated experiments done using latex MMA01. Variables presented are calculated as per the conditions at the end of interval II.

It was found throughout the γ-relaxation experiments that $\rho_{thermal}$ increases with CD. As mentioned in section 5.4.5., there are two possibilities, whether $\rho_{thermal}$ remain constant or it changes with different CD concentrations. Experiments done throughout the course of this work did not include any MMA thermal polymerization experiments done with CD. Consequently, current experimental results do not favour one choice over the other.

The increase in the value of $\rho_{thermal}$ will be considered to be exactly at the same rate of its increase, as shown in table 5.8. Consequently, with 2% CD $\rho_{thermal}$ = 5.85 x 10^{-5} s^{-1}, and with 4% CD $\rho_{thermal}$ = 7.28 x 10^{-5} s^{-1}. Following the same method of presenting different kinetic parameters at the beginning and the end of interval II, table 6.3 shows the results for 2% CD experiments, and table 6.4 shows the results for 4% CD experiments.

Experiment	N_c x 10^{16}	[KPS] x L/mmol	$\bar{n}_0$	$\rho_{initiator}$ x 10^4 s	F
M110	1.685	0.036	0.0348	-0.095	-
M113	1.712	0.107	0.0308	-0.201	-
M117	1.660	0.369	0.0701	1.405	0.0048
M119	1.692	1.086	0.1073	4.078	0.0048
M123	1.559	3.258	0.1027	3.686	0.0013

Table 6.3a. Summary of results for chemically initiated experiments done using latex MMA01 with 2% CD concentration. Variables presented are calculated as per the conditions at the start of interval II. Values not mentioned are considered wrong, as it is not possible to have a negative value for entry efficiency.

It is seen from tables 6.3 and 6.4 that, although assuming an increased value for $\rho_{thermal}$ might appear logical, it is actually found that it leads to negative values for $\rho_{initiator}$ and

Experiment	N_c x 10^{16}	[KPS] x L/mmol	$\bar{n}_{end}$	$\rho_{initiator}$ x 10^4 s	F
M110	1.685	0.036	0.0362	-0.251	-
M113	1.712	0.107	0.0504	0.028	3.38E-04
M117	1.660	0.369	0.1192	3.257	1.11E-02
M119	1.692	1.086	0.1728	6.244	7.34E-03
M123	1.559	3.258	0.1496	5.217	1.88E-03

Table 6.3b. Summary of results for chemically initiated experiments done using latex MMA01 with 2% CD concentration. Variables presented are calculated as per the conditions at the end of interval II. Values not mentioned are considered wrong, as it is not possible to have a negative value for entry efficiency.

Experiment	N_c x 10^{16}	[KPS] x L/mmol	$\bar{n}_0$	$\rho_{initiator}$ x 10^4 s	F
M111	1.689	0.036	0.0286	-0.397	-
M114	1.716	0.107	0.0333	-0.279	-
M118	1.666	0.369	0.1056	3.788	0.0129
M124	1.562	3.258	0.0803	1.883	0.0007

Table 6.4a. Summary of results for chemically initiated experiments done using latex MMA01 with 4% CD concentration. Variables presented are calculated as per the conditions at the start of interval II. Values not mentioned are considered wrong, as it is not possible to have a negative value for entry efficiency.

Experiment	N_c x 10^{16}	[KPS] x L/mmol	$\bar{n}_{end}$	$\rho_{initiator}$ x 10^4 s	F
M111	1.689	0.036	0.0369	-0.383	-
M114	1.716	0.107	0.0466	-0.139	-
M118	1.666	0.369	0.1323	3.705	0.0126
M124	1.562	3.258	0.1269	3.425	0.0012

Table 6.4b. Summary of results for chemically initiated experiments done using latex MMA01 with 4% CD concentration. Variables presented are calculated as per the conditions at the end of interval II. Values not mentioned are considered wrong, as it is not possible to have a negative value for entry efficiency.

so for *F*. Such results put some doubt about the assumption of increased $\rho_{thermal}$ value with increasing the amount of CD.

It goes against the expectations to find similarity between experiments with the lowest and highest initiator concentrations used.

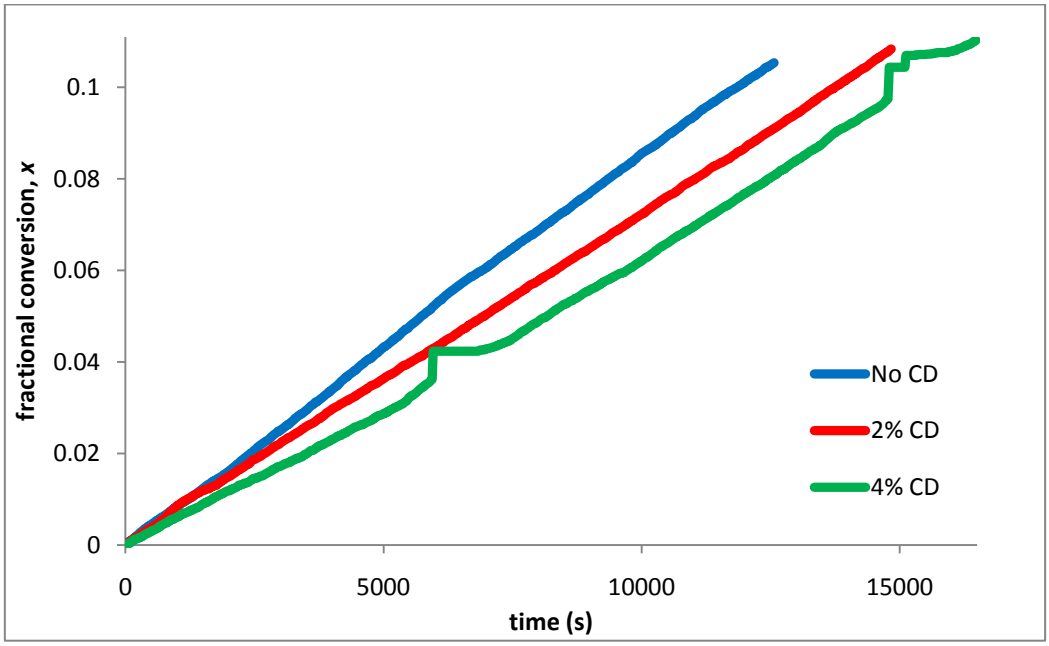

Figure 6.8. Effect of CD on reaction rate at KPS concentration of 0.03 mmol/L. Curves are for experiments M108 (no CD), M110 (2% CD) and M111 (4% CD).

Figure 6.8 shows the effect of CD on reaction rate at the lowest initiator concentration used. It is clear from the figure that at this initiator concentration CD has a negative effect on the reaction rate. Moreover, the more the CD concentration is, the more the reaction is slowed down. Figure 6.9 gives a similar plot.

The main difference between figures 6.8 and 6.9 is that the curve curvature has increased. This is the direct result of increasing the initiator concentration. But both curves show an agreement on the fact that CD slows down the reaction rate.

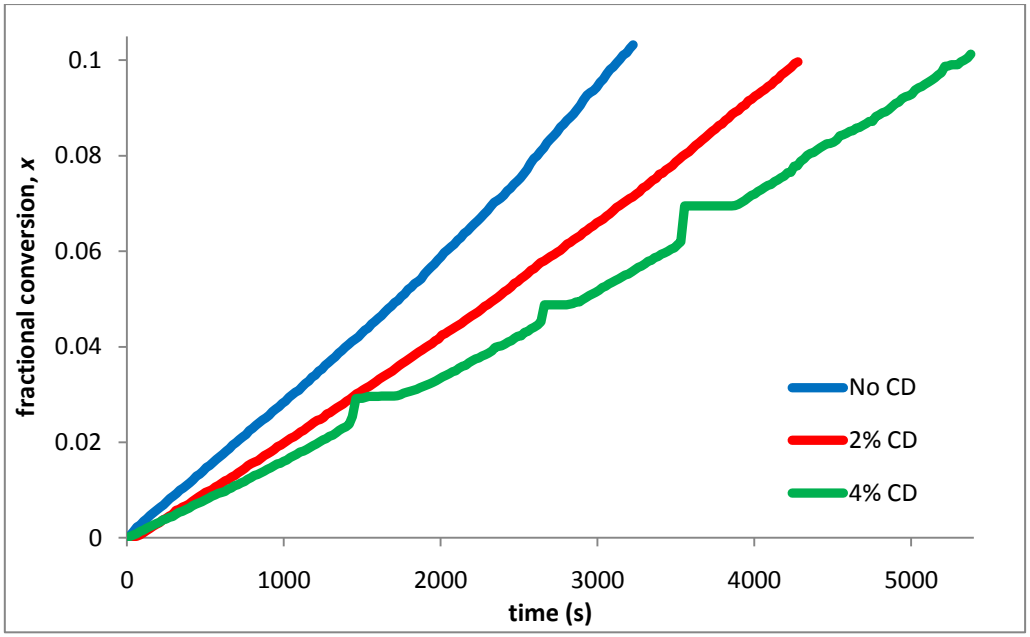

Figure 6.9. Effect of CD on reaction rate at KPS concentration of 3 mmol/L. Curves are for experiments M122 (no CD), M123 (2% CD) and M124 (4% CD).

Experiments run with initiator concentrations between the minimum and maximum initiator concentrations used, CD either has a negligible effect on the reaction rate, which is the case with 0.1 mmol/L KPS, or has a positive impact on the reaction rates, which is the case with 0.3 and 1 mmol/L.

In the case of negligible effect of CD, it can be seen from figure 6.10 that the presence of CD is relatively ineffective in the case of 4% CD concentration. Figure 6.10 is actually very similar to figure 4.3, where the effect of CD on reaction rate was shown to be minor between no CD and 4% CD, and with 2% CD it has a negative impact.

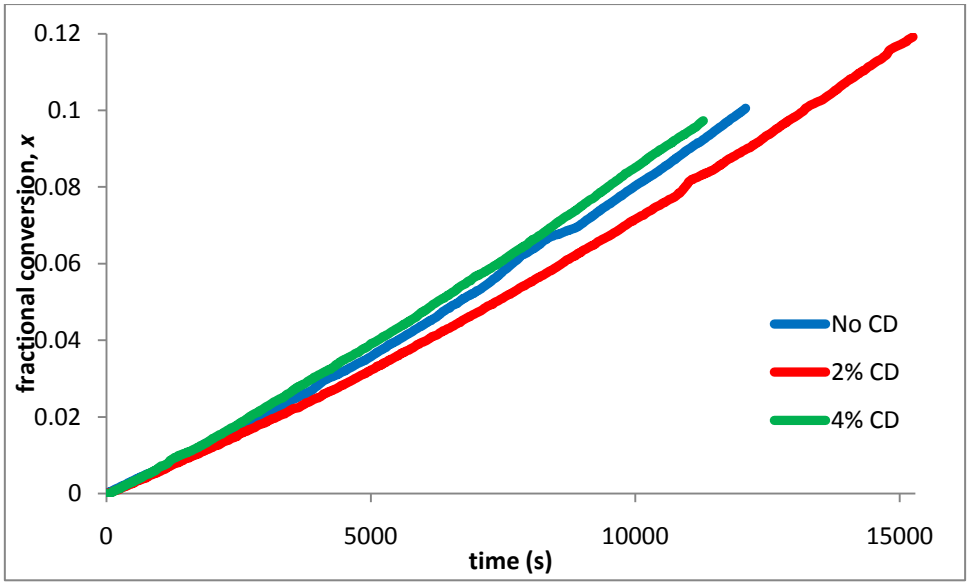

Figure 6.10. Effect of CD on reaction rate at KPS concentration of 0.1 mmol/L. Curves are for experiments M112 (no CD), M113 (2% CD) and M114 (4% CD)

For the case of positive effect of CD on reaction rate, as can be seen in figures 6.11 and figure 6.12, CD has actually increased the reaction rate to a considerable extent. Furthermore, increasing the amount of CD results in an increase in the reaction rate. The case of 2% CD in figure 6.12 can just be considered an experimental error resulting in such a high rate, which might have been caused by any experimental error (what highlights the error is the high acceleration of 1.9 for this experiment).

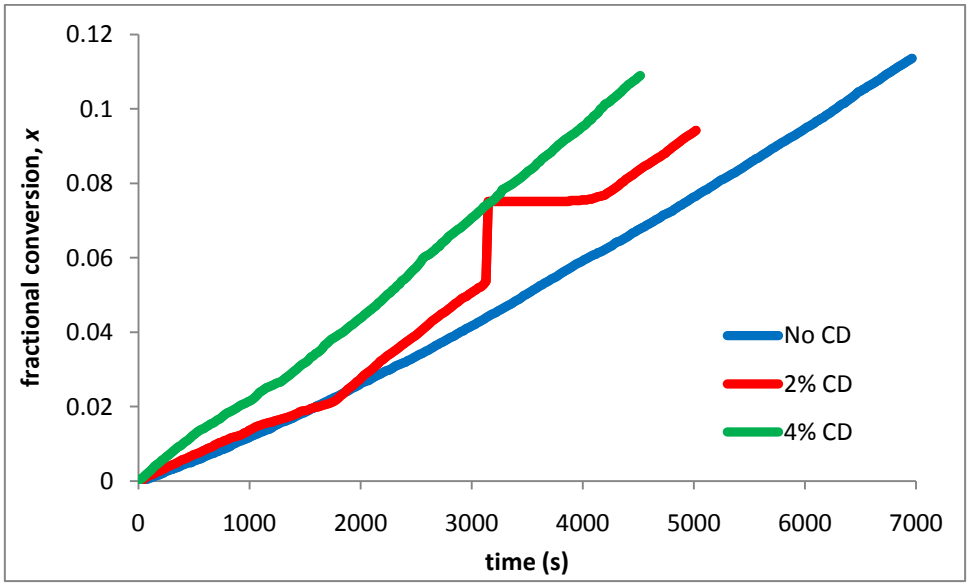

Figure 6.11. Effect of CD on reaction rate at KPS concentration of 0.3 mmol/L

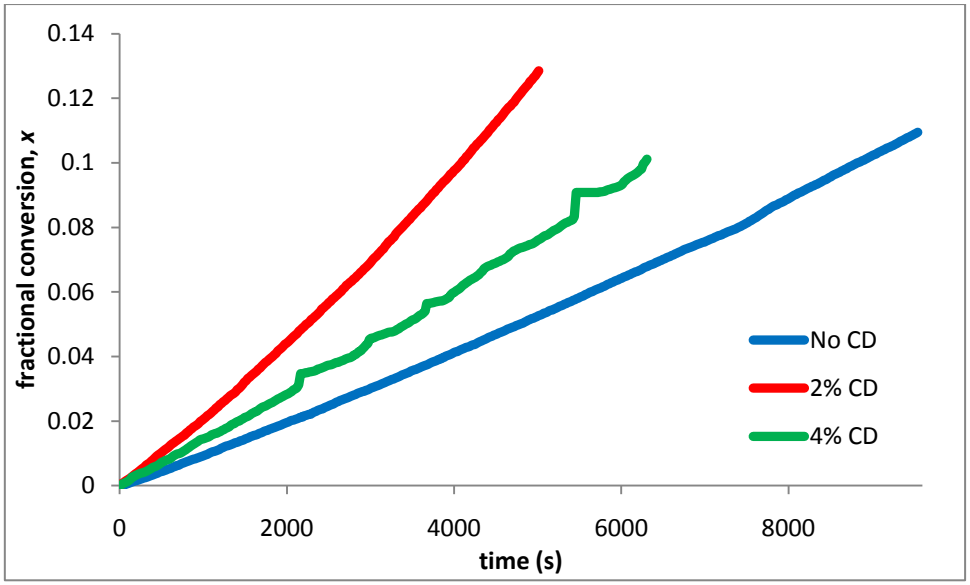

Figure 6.12. Effect of CD on reaction rate at KPS concentration of 1 mmol/L. Curves are for experiments M116 (no CD), M117 (2% CD) and M118 (4% CD).

The results shown in figures 6.8 to 6.12 highlight a few facts. First, the effect of CD in the system MMA/KPS emulsified using AMA-80 is not always positive, this can be explained by the fact of monomer/surfactant competition.[31,32] Although such explanation was for styrene systems, it can be assumed to be applied also for MMA as well. What strengthens this assumption is that same surfactant and initiator were used with both anionic lattices for MMA and styrene.

But this analysis, in the case of MMA, still requires some deeper understanding of the polymerization mechanism.

As surfactant is one of the competitors for CD cavities, then it is better to refer to the sensitivity of reaction rate and acceleration to minor changes in surfactant concentration. Table 5.6 has shown that the wrong surfactant concentrations can lead to negative $\mathrm{d}x/\mathrm{d}t$ and so negative accelerations. In case surfactant and monomer compete for CD cavities, the negative effect of surfactant is more obvious here. This explains why, even at the lowest KPS concentrations, CD did not have a positive effect on the reaction rate as was the case with styrene.

In the case of the highest initiator concentration, CD also has a negative effect. A similar situation has been faced with styrene before (section 4.4.5), For both styrene and MMA

cases, A thermodynamic equilibrium is assumed to exist between the monomer and the free radical. Both components are in equilibrium according to the following equations

$$I—I \xrightarrow{k_d} 2I^{\bullet} \quad (6.25)$$

$$I^{\bullet} + M \xrightarrow{k_{pi}} IM^{\bullet} \quad (6.26)$$

The thermodynamic equilibrium is based on the assumption that both M and $IM^{\bullet}$ exist together in the aqueous phase of the medium, and that they are similar but not exactly the same.

Based on section 5.4.7, the thermal polymerization of MMA in an aqueous phase process, which means that the initiated monomer molecules remain dissolved in water. Consequently, all components present within the aqueous phase, including the initiated monomer molecules, dissolved monomer and surfactant compete for CD cavities. In this case, Le Chatelier's principle can be easily applied. At the highest initiator concentration, the increased amount of $IM^{\bullet}$ present within the aqueous phase, in addition to the M already there compete for the CD cavities. Adding to this the sensitivity of the reaction rate towards surfactant concentration, the dynamic competition between the three components slows down the reaction rate.

The previous explanation can be used for both styrene and MMA, but in the case of MMA it is even more valid, as it explains clearly why at the highest KPS concentration even a greater amount of CD did not have a positive impact on the reaction rate.

This analysis is strengthened by the fact that at 0.1 mmol/L KPS, CD effect was similar to its effect at 1.5 mmol/L KPS with the styrene AN02 latex system. It is clear that at both cases the competition between the monomer, the free radical and the surfactant resulted in the reduced rate at 2% CD, but this negative effect was overcome at the 4% CD, because there was a higher chance for styrene monomer molecules to be complexed within the CD. The higher solubility of MMA enabled CD to play this role at 0.1 mmol/L KPS, while the lower styrene solubility required 1.5 mmol/L KPS to obtain the same CD effect. With higher initiator concentration, the negative effect of CD was totally overcome.

As was found, the main role of CD is mainly affected by the thermodynamic equilibrium between the monomer, concentration of initiated monomer molecules and the surfactant. Such conclusions lead to the preference of using CD in surfactant-free emulsion polymerization mixtures, as has been suggested by previous researchers.[28,33] Another use of CD in which it can improve the reaction rate without having the competition between monomer and surfactant molecules for CD cavities, is to use it with surfactants like DTAB, which do not compete with the monomer for CD.

Another effect of CD which should also be studied is its effect on F and $\bar{a}$. As can be seen in figure 6.12, entry efficiency decreases with higher KPS concentrations. As per the CD effect, with the exception of the lowest and highest KPS concentrations used, the entry efficiency increases in presence of CD. Furthermore, increasing the amount of CD results in an increase in entry efficiency, except in the case of 1 mmol/L, where the results might have been affected by some kind of error.

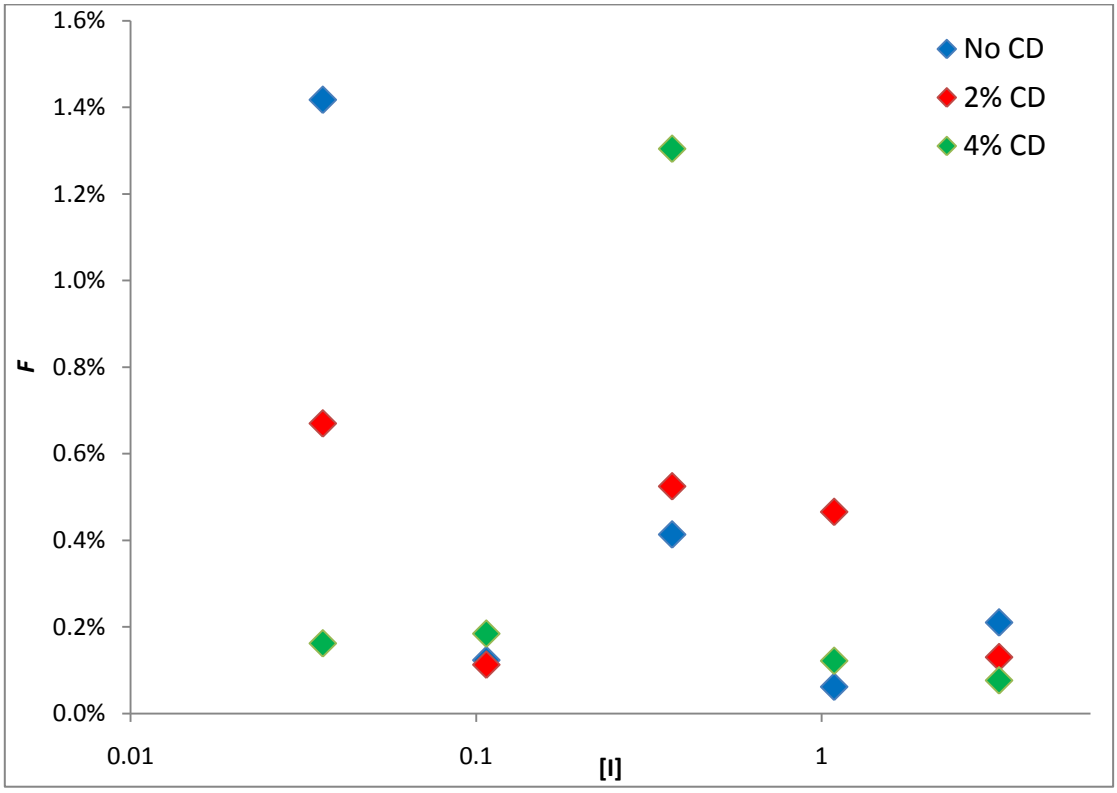

Figure 6.12. Effect of CD on entry efficiency. Calculated values for F are based on the assumption that $\rho_{thermal}$ is constant and does not change with CD concentration.

On the other hand, at lowest and highest KPS concentrations (0.03 and 3 mmol/L), CD

has exactly the opposite effect. CD presence generally results in a decrease of entry efficiency. The higher the CD concentration is, the lower the entry efficiency becomes.

Those results confirm the results obtained earlier, that CD generally improves the polymerization rate for MMA, and so the entry efficiency also improves.

Finally, how does CD affect the acceleration? This is an important question, as its answer determines the practicality of using CD to speed up the rate of emulsion polymerization processes, either on laboratory scale or industrially.

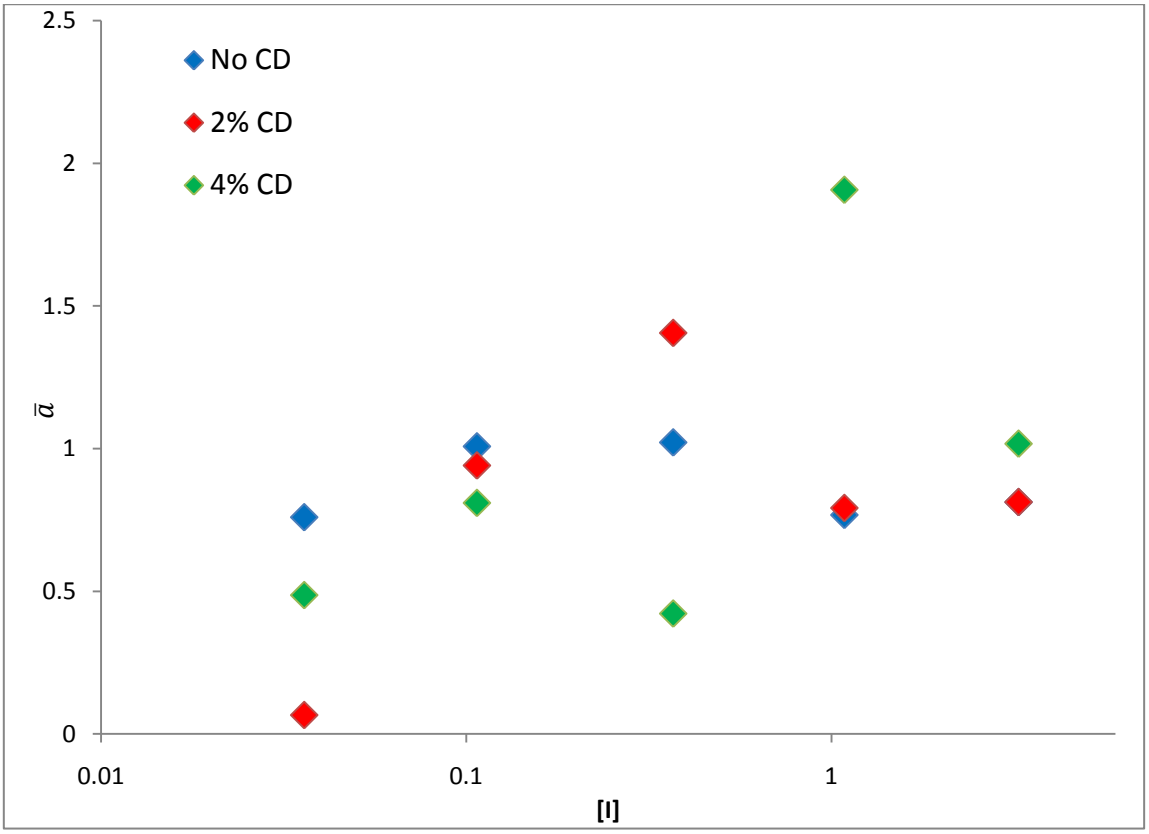

Figure 6.13. Effect of CD on $\bar{a}$.

The answer to this question is in figure 6.13, where it is shown clearly that, although $\bar{a}$ should be theoretically constant, it is affected by the initiator concentration (as was found earlier[6,8]) and also by other factors affecting the reaction rate, CD presence in the current case.

In general, acceleration is slowed down by CD. This can be explained by the fact that CD

presence in emulsion polymerization of MMA results in an increased reaction rate and decreased particle size,[13] which means CD acted in a way similar to that of increased surfactant.[16] There is no clear reason why the acceleration is reduced, but one possible explanation is that, in presence of monomers having relatively high solubility in water, CD acts in a way similar to that of surfactant, which has already been proven earlier.[28] As already shown in table 5.6, an increased amount of surfactant reduces the acceleration. Similarly with CD, increasing the amount of CD reduces the acceleration as well.

Finally, the effect of CD on exit rate coefficient *k*. As was discussed in section 3.5.4, the presence of CD for the styrene/KPS/AN05 system reduced the exit rate coefficient with increasing the amount of CD. This is because of the competition between surfactant and monomer for CD cavities which results in lower monomer concentration within the aqueous phase. In section 6.4.1 it was concluded that CD does not change the MMA solubility in water. As there have been no specific experiments done to determine the effect of CD on *k* for MMA emulsion polymerization, it can be concluded that *k* does not change with presence of CD. In case there is any change, then its value can be reduced because of the competition between monomer and surfactant. Whether the reality is this or that case, termination is still the rate determining step for the exit/termination process for MMA. Consequently, even if *k* changed with MMA this should not affect the accuracy of the results obtained throughout this work.

6.5 Conclusions

Chemically initiated seeded emulsion polymerization experiments were performed using MMA latex stabilized with an anionic surfactant, with and without CD. The effect of CD at different initiator concentrations was thoroughly studied.

Although there was no certain increase in MMA solubility in water in presence of styrene, CD was found to affect the reaction rate either positively or negatively, according to the amount of initiator used. For most cases CD played a catalytic role for the reaction, which was noticed by an increase in both the reaction rate and the entry efficiency.

As per its effect on acceleration, CD was found to act in a way similar to that of a surfactant; CD decreased the acceleration of polymerization during interval II.

Appendix 6.1. Recipes for all MMA solubility measurement experiments with UV-Vis spectroscopy.

Component			Absorbance
MMA	CD	AMA-80	
3.25			0.441
3.35		0.168	0.433
3.02	0.0609		0.378
3.08	0.0621	0.157	0.352
3.07	0.1223		0.380
3.02	0.1285	0.152	0.365

Appendix 6.2. Recipes for all MMA chemically initiated experiments

Experiment	Component				Vessel
	latex	monomer	AMA-80	CD	volume
M108	3.64	3.42	0.16		57.13
M109	3.84	3.49	0.15		57.04
M110	3.61	3.45	0.15	0.0692	57.13
M111	3.61	3.48	0.15	0.1415	57.04
M112	3.66	3.35	0.15		57.04
M113	3.65	3.67	0.15	0.0715	57.13
M114	3.68	3.31	0.15	0.1361	57.04
M115	3.62	3.55	0.15		57.13
M116	3.58	3.34	0.17	0.1334	57.04
M117	3.56	3.33	0.15	0.0703	57.04
M118	3.57	3.44	0.15	0.1376	57.13
M119	3.59	3.82	0.16	0.079	57.04
M120	3.55	3.43	0.15		57.04
M121	3.64	3.55	0.16	0.1414	57.04
M122	3.47	3.29	0.15		57.04
M123	3.33	3.63	0.15	0.0663	57.13
M124	3.33	3.63	0.15	0.1385	57.04

References

(1) El-Aasser, M. and Sudol, E., *Features of Emulsion Polymerization,* El-Aasser, M. and Lovell, P., *Emulsion Polymerization and Emulsion Polymers*, **1997**, John Wiley and sons, New York.

(2) Moad, G. and Solomon, D., *The chemistry of radical polymerization 2nd fully revised edition,* **2006**, Elsevier.

(3) Morrison , R., *An Economic Analysis of Electron Accelerators and Cobalt-60 for Irradiating food*, **1989**, U.S. Department of Agriculture.

(4) Lieser, K., *Nuclear and Radiochemistry Fundamentals and Applications*, **1996**, VCH Verlagsgesellschaft, Germany

(5) Maxwell, I., Morrison, B., Napper, D. and Gilbert, R., *Macromolecules*, **1991**, 24, 1629.

(6) Ballard, M., Napper, D., and Gilbert R., *J. Polym. Sci., Polym. Chem. Ed.*, **1984**, 22, 3225.

(7) van Berkel, K., Russell, G. and Gilbert, R., *Macromolecules*, **2005**, 38, 3214.

(8) van Berkel, K., *Entry and the Kinetics of Emulsion polymerization*, a PhD thesis, University of Canterbury, 2004

(9) Lau, W., *Macromol. Symp.*, **2002**, 182, 283.

(10) Loftsson, T. and Duchêne, D., *Int. J. Pharm.*, **2007**, 329, 1

(11) Ritter, R. and Storsberg, J., *Macromol. Rapid Commun.*, **2000**, 21, 236.

(12) Ritter, H., Steffens, C. and Storsberg, J., *e-polymers*, **2005**, 34, 1.

(13) Hu, J., Li, S., Wang, D., Li, H., Liu, B. and Liao, X., *Polymer*, **2004**, 45, 1511.

(14) W.D. Harkins, *J. Chem. Phys.*, **1947**, 69, 1428

(15) Maxwell, I., Morrison, B., Napper, D. and Gilbert, R., *Macromolecules*, **1991**, 24, 1629.

(16) Gilbert, Robert G., *Emulsion polymerisation, a mechanistic approach*, **1995**, Academic Press, London.

(17) W.V. Smith and R.H. Ewart, *J. Chem. Phys.*,**1948**, 16,592

(18) Ballard, M., Gilbert R. and Napper, D., *J.Polym. Sci., Polym. Letters Ed.*, **1981**, 19, 533.

(19) Ritter, H., Glöckner, P. and Metz, N., *Macromolecules*, **2000**, 33, 4288.

(20) Storsberg, J., Hartenstein, M., Müller, A. and Ritter, H., *Macromol. Rapid. Commun.*, 21, 1342.

(21) Szejtli, J., *Chemistry, Physical and Biological Properties of Cyclodextrins*, in Szejtli, J. and Osa, T., *Volume 3: Cyclodextrins*, in Lehn, J. *at al.* (Editor), *Comprehensive Supramolecular Chemistry*, **1996**, Pergamon, UK

(22) Szejtli, J., *Chem. Rev.*, **1998**, 98, 1743

(23) Lau, W., US Patent Number 5521266.

(24) Szente, L., *Analytical Methods for Cyclodextrins, Cyclodextrin derivatives and Cyclodextrin Complexes*, in Szejtli, J. and Osa, T., *Volume 3: Cyclodextrins*, in Lehn, J. *at al.* (Editor), *Comprehensive Supramolecular Chemistry*, **1996**, Pergamon, UK

(25) Clark, B., Frost, T. and Russellm M., *UV spectroscopy Techniques, instrumentation, data handling*, **1993**, Chapman and Hall, London

(26) Perkampus, H., *UV-Vis spectroscopy and its applications*, **1992**, Springer-Verlag, Berlin

(27) Norrish R.G.W., Smith R.R., *Nature*, **1942**, 150, 336

(28) Madison, P., and Long, T., *Biomacromolecules*, **2000**, 1, 615

(29) Bernhardt, S., Glöckner, P., Theis, A. and Ritter, H., *Macromolecules*, **2001**, 34, 1647

(30) Ritter, H., Storsberg, J., van Aert, H. and Roost, C., *Macromolecules*, **2003**, 36, 50.

(31) Hu, J., Li., Y., Ji, H. and Chen, Z., *Gaofenzi Xuebao*, **2007**, 3, 246

(32) Hu, J., Li, S. and Liu, B, *Journal of Polymer Material*, **2005**, 22, 213.

(33) Hu., J., Huang, R., Cao, S. and Hua, Y., *e-polymers*, **2008**, 171.

Chapter VII
Conclusions and future work

7.1 Conclusions

The aim of this work, as stated in chapter I, was to carry out a mechanistic study with the aim of understanding how exactly cyclodextrins can improve the reaction rate of emulsion polymerisation, as had already been found in various studies. These studies all involved *ab initio* systems, and thus the measured reaction rate reflected both the effects of CD on particle formation and on kinetic parameters once particle formation had ceased. In order to disentangle these effects for the first time, this work carried out only seeded emulsion polymerisations, so that CD could not influence the rate via particle formation processes.

When studying the effect of CD on the seeded emulsion polymerization of styrene, a few misconceptions have already been accepted to be true. One of them was that, in order for CD to have a positive impact on the reaction kinetics, it has to be used in surfactant free emulsion polymerization environment, or an amount of CD used which is big enough to turn the emulsion polymerization process into a solution polymerization. A conclusion of the γ-radiolysis experiments (chapter III) is that this is not true, as CD was found to increase the exit rate coefficient of styrene while running the experiment with surfactant in the medium. This lead to the conclusion that CD and surfactant can, under specific conditions, co-operate to improve the reaction kinetics.

Another conclusion is that the effect of the surfactant present with the CD in the reaction medium depends on its chemistry. Furthermore, having noticed no change of thermal entry rate coefficient with and without CD lead to the conclusion that thermal entry for styrene is possibly not an aqueous phase process.

The most important conclusion is that the exit rate coefficient in presence of CD increased from its value without CD. The ratio between the two values was the same ratio between aqueous phase solubilities of styrene with and without CD. This is as predicted

by the prevailing theory for exit rate coefficients. This confirms the accuracy of the model used to predict the exit rate coefficient, and confirms the assumption that increase in monomer solubility is the main reason for the catalyzing effect of CD.

But the most important conclusion was that CD improves the reaction kinetics as it improves the aqueous phase solubility of styrene (chapter IV). By choosing a suitable surfactant with styrene, its solubility in water almost doubled, though the amount of surfactant and CD used was minor, relative to the amount of monomer.

This does not completely negate conclusions reached earlier, as it was also found that using the wrong surfactant with CD will not nullify its effect, but will also have a negative impact on the overall reaction kinetics.

When the effect of CD on the emulsion polymerization of a monomer with higher aqueous phase solubility, MMA, was studied, a different set of conclusions was reached.

First, through studying the effect of CD on termination (chapter V), CD presence was found to have no effect on the termination rate. This confirms the already established hypothesis that MMA is a pseudo-bulk system, whereradical loss is not affected by many serious changes in the aqueous phase. Furthermore, the thermal entry rate coefficient of MMA was found to follow a completely different mechanism than that of styrene. It was concluded that the thermal polymerization of MMA is an aqueous phase process, where the presence of CD has increased the rate of thermal polymerization.

The mechanism and effect of CD on the emulsion polymerization of MMA was found to be different to that in the case of styrene. There is actually no specific trend through which increasing the amount of CD can directly give an indication whether the reaction rate will increase or decrease (chapter VI). Again, this can be a result of choosing a wrong surfactant with CD. Furthermore, changing the amount of surfactant and CD had only minor impact on MMA solubility. This can lead to a very important conclusion, which is that the mechanism through which CD changes the reaction rate for MMA is not by increasing solubility, but through changing other parameters which still remain unknown. An alternative conclusion is simply that CD does not have a major effect on the emulsion

polymerization kinetics of hydrophilic monomers, but rather is only gainfully employed for highly hydrophobic monomers.

7.2 Future work, having a better understanding on CD role in emulsion polymerization

The conclusions reached above can be considered just hypotheses, as up until the time by which this current work was done, very little has been known about the mechanism of CD within emulsion polymerization.

The first thing is to carry out a deeper study on the reasons for the minor effect of CD on MMA chemically initiated system. This can be done through running similar experiments with a cationically stabilized latex. This will be the only way through which the results of this work, regarding the effect of CD on the emulsion polymerization of MMA can be verified. It was the intention to carry out such studies in this work, but unfortunately the apparatus for automated dilatometry broke down, and could not be repaired for further experiments to be carried out.

It is also important to carry out more advanced research on the relationship between surfactant and CD in the presence of monomer. This might be done using X-ray crystallography on systems which are similar to those used during the course of this work. Running such X-ray tests will be one way to confirm the assumption that some types of surfactant and CD can nullify the effect of each other when present together.

A very important study in the future can be to run a similar study to the current one but having a main change in the preparation of latices. This can be done by preparing the latices without using any surfactant, but replacing it with CD, then running the seeded emulsion polymerization experiments with CD as the surfactant. This study can lead to a better understanding on the effect of CD alone on the emulsion polymerization. Furthermore, results of such study can be used industrially, as a more environmentally friendly technique than the current emulsion polymerization techniques which depend mainly on surfactants, providing less environmentally friendly by-products.

Probably the two major ways in which to extend the current work are as follows:

1. As already mentioned, this work involved only seeded EPs, and thus it did not probe particle formation. It would be highly desirable to carry out a study of the effect of CD on particle formation, as this is possibly the primary way in which CD facilities EP: by enabling particle formationt to occur far more readily where the monomer is highly hydrophobic. It is suggested that such studies commence with surfactant-free investigations, as particle formation is relativey simply in such systems, and really is just a function of aqueous-phase monomer solublity. Once such systems are understood, one could then progress to seeking to understand the effect of CD on particle formation in systems with surfactant.

2. Styrene and MMA were selected for study in this thesis because their kinetics are so well characterized. However commercial applications for CD will more likely involve highly hydrophobic monomers, such as long-chain methacrylates (e.g. dodecyl and stearyl). Now that the effect of CD on styrene and MMA are better understood, it would be logical to carry out seeded EP studies on systems such as butyl, dodecyl and stearyl (meth)acrylate, in order to gain an understanding of CD affects particle-growth kinetics in such systems.

Finally, the work done and presented through this thesis has shed some light on the mechanism of CD on emulsion polymerization, and has provided some hypotheses of how and why CD plays a role in manipulating the reaction kinetics. There is still a lot to be uncovered, but it is hoped that this work has opened some gates for future researchers to go through, in order to obtain a more complete understanding on CD and its role in emulsion polymerization.